

INAUGURAL DISSERTATION

Submitted to the Combined Faculties for the Natural Sciences and Mathematics of the Ruperto-Carola University of Heidelberg, Germany,
for the degree of Doctor of Natural Sciences

Presented by

M.S. Umar Khalid

Born in Gujrat, Pakistan

Date of Oral Examination: July 13th, 2021

Screen of Compounds to Target Tumor Cells with Chromothripsy

Referees: Prof. Dr. Thomas Höfer

Prof. Dr. Peter Licher

Declaration

I hereby declare that I have written the submitted dissertation "Screen of Compounds to Target Tumor Cells with Chromothripsy" myself and in this process have not used any other sources than those expressly indicated.

I hereby declare that I have not applied to be examined at any other institution, nor have I used the dissertation in this or any other form at any other institution as an examination paper, nor submitted it to any other faculty as a dissertation.



Umar Khalid

Contents

1. Introduction	1
1.1 Chromothripsis	1
1.1.1 Factors linked to chromothripsis.....	3
1.2 Chromothripsis in cancer.....	5
1.2.1 Prevalence across different tumor entities, link with poor prognosis and lack of therapeutic options	5
1.3 Synthetic lethality.....	5
1.3.1 Targeting DNA repair defects in cancer therapy using PARP inhibitors.....	5
1.3.2 Mechanism of action of the PARP enzyme	7
1.3.3 Synergistic approach used for cancer therapies	8
1.4 Synergy between drugs.....	10
1.4.1 Definition.....	10
1.4.2 Models to evaluate drug interactions.....	10
1.5 Aim of the study.....	12
2. Materials and Methods	13
2.1 Materials	13
2.1.1 Drugs and Reagents.....	13
2.1.2 Cell Culture Reagents and Materials.....	14
2.1.3 In vivo Reagents and Materials	15
2.1.4 Mice	15
2.1.5 Cell Lines and PDX Spheroid Models	15
2.1.6 Equipment	16
2.1.7 Other Materials	16
2.1.8 Software and R Packages	17
2.2 Methods	18
2.2.1 Cell Culture Conditions.....	18
2.2.2 Molecular Characterization of the Cell Lines and PDX Models.....	19
2.2.3 Primary Screen	19
2.2.4 Analysis of the Primary Screen Data.....	20
2.2.5 Secondary Screen	20
2.2.6 Cell Cycle Analysis	20
2.2.7 Apoptosis	21
2.2.8 Doubling Time	21
2.2.9 <i>In vivo</i> Studies and Chemotherapy	21
2.2.10 Acetyl- α -tubulin and phospho-histone 3 immunostaining	22

CONTENTS

2.2.11	Gene Expression Analysis.....	22
2.2.12	Analysis of Expression Data and GSEA.....	22
2.2.13	Statistical Analysis	23
3.	Results	24
3.1	Cell cycle analysis of spheroid cultures.....	24
3.2	Selection of a PARP inhibitor	24
3.3	Primary screen.....	25
3.3.1	Primary screen set-up	25
3.3.2	Libraries	26
3.3.3	Characterization of the cell lines included in the primary screen	27
3.3.4	Analysis of the primary screen data	28
3.4	Secondary screen.....	41
3.4.1	Secondary screen set-up.....	41
3.4.2	Analysis of the secondary screen data.....	42
3.5	Reduction in Spheroid Growth.....	47
3.6	Functional Assays	49
3.6.1	Synergy effect and relationship to the <i>TP53</i> status.....	49
3.6.2	Cell cycle arrest and apoptosis in DAOY cells	52
3.6.3	Visualization of the mitotic cells.....	54
3.7	Gene expression Data.....	55
3.7.1	Experimental set-up.....	55
3.7.2	GSEA analysis.....	56
3.7.3	Analysis of differentially expressed genes	57
3.8	Molecular analyses of the role of MYC in the combination treatment.....	58
3.8.1	MYC immunohistochemistry on SHH medulloblastoma PDX tissues	58
3.8.2	Validation of the <i>MYC</i> ON/OFF system.....	58
3.8.3	Matrix experiments using the <i>MYC</i> ON/OFF system	59
3.8.4	IC50 curves for the C646 inhibitor	60
3.8.5	Effect of the inhibition of PARP acetylation on the additivity between romidepsin and BGB290	61
3.9	<i>In vivo</i> validation	62
3.9.1	Romidepsin treatment in PDX models	62
3.9.2	Haematoxylin & Eosin (H & E) and Ki67 immunohistochemistry	62
3.9.3	Cleaved caspase 3 immunostaining.....	63
4.	Discussion.....	65
4.1	Romidepsin	65
4.2	Factors affecting the synergistic interaction between romidepsin and BGB290	65

CONTENTS

4.3	Future Perspectives.....	68
5.	References	71
6.	Publications	78
7.	Appendix.....	79
8.	Acknowledgements.....	259

Table of Figures

Figure 1: Schematic representation of chromothripsis	1
Figure 2: An overview of DNA double strand break repair pathways	2
Figure 3: Chromothripsis is linked to HR and cNHEJ repair deficiency	3
Figure 4: Chromothripsis is linked to p53 deficiency	4
Figure 5: Chromothripsis is linked to BRCAnezz	4
Figure 6: High prevalence of chromothripsis in different cancer types. Figure taken from Voronina et al, 2020 [20].....	5
Figure 7: Schematic representation of synthetic lethality and PARP inhibitor treatment.....	6
Figure 8: Mechanism of action of the PARP enzyme.....	8
Figure 9: Synergistic interaction between NAMPT- and PARP inhibitors	9
Figure 10: Graphical representation of synergistic, additive and antagonistic drug interaction	10
Figure 11: Graphical representation of Loewe additivity model of synergy (A) and Bliss independence (B). Figure taken from Chang et al, 2017 [51].....	11
Figure 12: Cell cycle analysis of spheroid cultures	24
Figure 13: PARP trapping assay	25
Figure 14: Primary screen set-up	26
Figure 15: Classification of the library drugs on the basis of their target or mode of action	26
Figure 16: Characterization of the cell types and tumor entities included in the primary screen	27
Figure 17: Determination of chromothripsis status in SJSA-1 osteosarcoma cell line.....	28
Figure 18: t-distributed stochastic neighbor embedding (t-SNE) plot based on the primary screen data	29
Figure 19: Raw ATPlite readout values of a representative 96-well plate from the primary screen with negative controls on the left and positive controls on the right of the plate	29
Figure 20: Scatter plots of the inhibition of the metabolic activity values (percentage of the DMSO controls) for CUDC-907 (a) and entinostat (b), which were present in both drug libraries utilized for the screen	31
Figure 21: Scatter plots of the inhibition of the metabolic activity values (percentage of the DMSO controls) for UWB1.289 (a) and UWB1.289 + BRCA1 (b).....	32
Figure 22: Cluster dendrogram of all the cell lines and spheroid models included in the primary screen	33
Figure 23: Doubling time (hours) of all cell lines included in the primary screen plotted against the percentage inhibition of the metabolic activity data from the primary screen for romidepsin, nanaomycin A and Dp44mT	34
Figure 24: Scatter plots of the inhibition of the metabolic activity values (percentage of the DMSO controls) from the primary screen.....	35
Figure 25: Analysis of the primary screen data	39

Figure 26: Heat-map showing the percentage inhibition of the metabolic activity from the primary screen for romidepsin.....	40
Figure 27: IC50 curves of nanaomycin A for cell lines and spheroid models in the primary screen	41
Figure 28: Schematic representation of the secondary screen strategy	42
Figure 29: Loewe surface plots generated using the combenefit software showing synergistic and antagonistic drug interactions.....	47
Figure 30: Bright-field images of spheroid model LFS_MB_P (Sonic Hedgehog medulloblastoma model, primary tumor) after 24 hours of drug treatment	48
Figure 31: Bright-field images of spheroid model LFS_MB_1R (Sonic Hedgehog medulloblastoma model, first relapse) after 24 hours of drug treatment.....	49
Figure 32: Cell cycle arrest of RPE1 WT and RPE1 TP53 KO cells upon combination treatment with romidepsin and BGB290	52
Figure 33: Cell cycle arrest and apoptosis of DAOY cells upon combination treatment with romidepsin and BGB290	54
Figure 34: Acetyl- α -tubulin and phospho-histone 3 immunostaining of DAOY cells treated with either vehicle control, 6.25 μ M BGB290, 1.7 nM romidepsin or 6.25 μ M BGB290 with 1.7 nM romidepsin for 48 hours.....	55
Figure 35: Schematic representation of the transcriptome experiment	56
Figure 36: Top signatures from GSEA analysis from single treatment compared to control (top, romidepsin versus control) and double treatment compared to single treatment (bottom).....	56
Figure 37: MYC immunohistochemistry on SHH medulloblastoma PDX tissues	58
Figure 38: MYC immunostaining of ONS76 (MYC ON/OFF) cells with and without doxycycline induction	59
Figure 39: Romidepsin and BGB290 synergistic effects are linked to MYC expression	60
Figure 40: IC50 curves for the C646 inhibitor for ONS76 (MYC ON/OFF) cells with and without doxycycline induction	61
Figure 41: Antagonistic effect of romidepsin and BGB290 in the presence of C646	61
Figure 42: <i>In vivo</i> validation in patient-derived xenografts	62
Figure 43: H & E (top 3 panels) and Ki67 immunohistochemistry (bottom 3 panels) of xenograft tumors isolated from the flanks of mice belonging to control, romidepsin alone and romidepsin with BGB290 treatment groups	63
Figure 44: Cleaved caspase 3 and DAPI staining of xenograft tumors isolated from the flanks of mice belonging to control, romidepsin alone and romidepsin with BGB290 treatment groups	64
Figure 45: Graphical representation of the four-factor theory	69
Supplementary figure 46 : Molecular characterization of in vitro models included in the screen	83

Summary

Chromothripsy is a form of genomic instability that begins with a shattering event leading to clustered chromosomal aberrations. Chromothriptic cells acquire multiple genomic alterations in confined genomic regions restricted to one or a few chromosomes. Due to the very high prevalence of chromothripsy in different types of cancers especially Sonic Hedgehog medulloblastomas, osteosarcomas and neuroblastomas and due to the link between chromothripsy and poor prognosis for cancer patients, finding therapeutic options to specifically target tumor cells with chromothripsy is highly relevant. Chromothripsy is linked to homologous recombination (HR) repair deficiency in a number of tumor types. Therefore, synthetic lethality may potentially be used, whereby HR repair deficiencies of cancer cells are exploited by applying a PARP inhibitor, which spares repair-proficient normal cells. In the primary screen, I searched for potential additive or synergistic partners of a PARP inhibitor (BGB290) and also searched for drugs that are potent as single agents. The analysis of the primary screen done in 15 cell lines identified romidepsin and nanaomycin A as promising candidates to eliminate tumor cells with chromothripsy. To confirm the potential additivity or synergism of these drugs with the PARP inhibitor, a secondary screen was done where drugs were titrated against each other in 8×8 matrix settings. The secondary screen revealed a strong synergistic interaction between BGB290 and romidepsin in chromothriptic Sonic Hedgehog (SHH) medulloblastoma patient derived xenograft spheroid models but antagonism in non-chromothriptic control cells. Functional assays revealed that the synergistic effect between BGB290 and romidepsin was not *TP53* dependent. Romidepsin and BGB290 combination treatment caused G2 cell cycle arrest and apoptosis in chromothriptic DAOY cells. The mitotic rate was decreased by romidepsin and BGB290 combination treatment in DAOY cells as shown by acetyl- α -tubulin and phospho-histone H3 immunostaining. Gene expression analysis revealed that the romidepsin and BGB290 combination treatment was associated to the regulation of *MYC* target genes. To further analyze the link between *MYC* expression and the effects of the combination treatment, I used an inducible *MYC* ON / OFF system. When *MYC* was overexpressed, romidepsin and BGB290 showed additivity, while in the *MYC* OFF state the additive effect was replaced by antagonism. This indicates that *MYC* overexpression plays a role in the interaction between BGB290 and romidepsin. Lastly, the *in vivo* efficacy of BGB290 and romidepsin combination treatment was confirmed in patient-derived xenograft mouse models.

Zusammenfassung

Chromothripsis ist eine Form der genomischen Instabilität, bei der es durch ein einmaliges Ereignis zu einer Anhäufung von Umlagerungen in Chromosomen kommt. Chromothriptische Zellen weisen mehrere genomische Veränderungen in bestimmten genomischen Abschnitten auf, die auf ein oder mehrere Chromosomen beschränkt sind. Aufgrund der sehr hohen Prävalenz von Chromothripsis in verschiedenen Tumorentitäten insbesondere Sonic Hedgehog medulloblastomas, osteosarcomas and neuroblastomas, sowie des Zusammenhangs zwischen Chromothripsis und einer schlechten Prognose für Krebspatienten ist es daher von besonderer Notwendigkeit, therapeutische Ansätze zu entwickeln, die sich gezielt gegen Tumorzellen mit Chromothripsis richten. Bei einigen Tumorentitäten ist Chromothripsis mit einer fehlerhaften Reparatur bei der homologen Rekombination (HR) verbunden. Aus diesem Grund kann möglicherweise synthetische Letalität verwendet werden, wobei die fehlerhafte HR-Reparatur von Krebszellen genutzt wird, indem diese mit einem PARP-Inhibitor behandelt werden, wobei normale Zellen mit intakter Reparaturaktivität geschont werden. In einem Primärscreen wurden nach möglichen Inhibitoren gesucht, die eine additive oder synergistische Wirkung zu einem PARP-Inhibitor (BGB290) haben, sowie nach Inhibitoren, die auch als Einzelwirkstoffe wirksam sind. Die Analyse des primären Screens, welches in 15 Zelllinien durchgeführt wurde, brachte Romidepsin und Nanaomycin A als vielversprechende Kandidaten hervor. Um eine mögliche Additivität oder einen Synergismus mit dem PARP-Inhibitor zu bestätigen, wurde ein sekundärer Screen durchgeführt, bei dem die Inhibitoren in einer 8x8-Konzentrationsmatrix gegeneinander titriert wurden. Dieses sekundäre Screening zeigte eine starke synergistische Wechselwirkung zwischen BGB290 und Romidepsin in Sphäroidmodellen, die aus chromothriptischen Sonic Hedgehog (SHH) Medulloblastom-Patienten stammenden Xenotransplantaten (PDX) hergestellt wurden, jedoch einen Antagonismus in Kontrollzellen ohne Chromothripsis. Des Weiteren konnten mit Hilfe von funktionellen Assays gezeigt werden, dass der synergistische Effekt zwischen BGB290 und Romidepsin TP53-unabhängig war. Die kombinierte Behandlung mit Romidepsin und BGB290 bewirkte einen Zellzyklus-Arrest in G2 und Apoptose in chromothriptischen DAOY-Zellen. Acetyl- α -Tubulin- und Phospho-Histon-H3-Immunfärbung zeigten, dass die Mitoserate von DAOY-Zellen durch die Romidepsin- und BGB290-Kombinationsbehandlung reduziert wurde. Genexpressionsanalysen zeigten, dass die Kombinationsbehandlung mit Romidepsin und BGB290 mit der Regulation von MYC-Zielgenen verbunden ist. Um den Zusammenhang zwischen der MYC-Expression und den Auswirkungen der Kombinationsbehandlung weiter zu analysieren, verwendete ich ein induzierbares MYC^{ON/OFF}-System. Während bei einer Überexpression von MYC Romidepsin und BGB290 Additivität zeigten, ist im MYC^{OFF}-Zustand der additive Effekt durch Antagonismus ersetzt worden. Dies weist darauf hin, dass die Überexpression von MYC eine Rolle bei der Wechselwirkung zwischen BGB290 und Romidepsin spielt. Abschließend wurde die *in vivo* Wirksamkeit der Kombinationsbehandlung mit BGB290 und Romidepsin in PDX-Mausmodellen bestätigt.

Abbreviations

7AAD	7-aminoactinomycin
ACESeq	Allele specific copy number estimation sequencing
AD	Auto modification domain
Alt-EJ	Alternative end joining
ANOVA	Analysis of variance
ATP	Adenosine triphosphate
BBB	Blood brain barrier
BFB	Breakage fusion bridge
BRCA	Breast cancer gene
CBP	CREB-binding protein
CDK	Cyclin dependent kinase
CNV	Copy number variant
CSF	Cerebrospinal fluid
CTCL	Cutaneous T-cell lymphoma
DAPI	4',6-diamidino-2-phenylindole
DBD	DNA binding domain
DEA	Differential gene expression analysis
DMEM	Dulbecco's modified eagle medium
DMSO	Dimethyl sulphoxide
DNA	Deoxyribonucleic Acid
DSB	Double strand break
E2F1	E2F transcription factor 1
EDTA	Ethylendiaminetetraacetate
EGF	Epidermal growth factor
EMBL	European molecular biology laboratory
FACS	Fluorescence-activated cell sorting
FCS	Fetal calf serum
FDA	Food and drug administration
FDR	False discovery rate
FGF	Fibroblast growth factor
FITC	Fluorescein isothiocyanate
GEO	Gene expression omnibus
GSEA	Gene set enrichment analysis
H & E	Haematoxylin & Eosin
HDAC	Histone deacetylase

HGG	High grade gliomas
HR	Homologous recombination
HRP	Horse reddish peroxide
i. p.	Intraperitoneal
IC20	Inhibitory concentration 20
IC40	Inhibitory concentration 40
IC50	Half maximal inhibitory concentration
KO	Knock out
KRAS	Kirsten rat sarcoma viral oncogene homolog
LIF	Leukemia inhibitory factor
MB	Medulloblastoma
MEGM	Mammary epithelial cell growth medium
MEM	Minimal essential medium eagle
MSigDB	Molecular Signatures Database
MYC	v-Myc avian myelocytomatosis viral oncogene homolog
NAD	Nicotinamide adenine dinucleotide
NAMPT	Nicotinamide phosphoribosyl transferase
NEAA	Non-essential amino acids
NHEJ	Non-homologous end joining
NIH	National institute of health
NMF	Nonnegative matrix factorization
ns	Non-significant
p.o.	Per os
<i>p21</i>	CDK-interacting protein 1
PALB2	Partner And Localizer Of BRCA2
PAR	Poly ADP-ribose
PARG	Poly(ADP-ribose) glycohydrolase
PARP	Poly-ADP ribose polymerase
PBS	Phosphate buffered saline
PCR	Polymerase chain reaction
PDX	Patient derived xenograft
PFA	Paraformaldehyde
<i>PGBD5</i>	PiggyBac transposable element derived 5
PI	Propidium iodide
PI3K	Phosphoinositide 3-kinase
<i>PTEN</i>	Phosphatase and tensin homolog
RF	Replication fork

ABBREVIATIONS

RIPA	Radioimmunoprecipitation assay
RNA	Ribonucleic Acid
RPE1	Retinal pigment epithelium 1
RT	Room temperature
SDS	Sodium dodecyl sulfate
SEM	Standard error of mean
SHH	Sonic Hedgehog
SSA	Single strand annealing
SSB	Single strand break
TP53	Tumour protein P53
TRIS	Tris-(hydroxymethyl)-aminomethan
t-SNE	t-distributed stochastic neighbour embedding
UHRF1	Ubiquitin-like, containing PHD and RING finger domains, 1
US	United states
UV	Ultraviolet
WT	Wild type

1. Introduction

1.1 Chromothripsis

Chromothripsis is a potentially one-off catastrophic phenomenon that leads to clustered chromosomal rearrangements and to the simultaneous acquisition of multiple genomic aberrations in confined chromosomal regions (Figure 1)[1-3]. Chromothriptic events are restricted to one or a few chromosomes. After the chromosomal shattering event has taken place, tens to hundreds of DNA fragments are formed due to DNA double strand breaks. These breaks are then repaired by error prone DNA repair processes such as non-homologous end joining (NHEJ) and alternative end joining (Alt-EJ) (Figure 2)[4]. This leads to the formation of double minute chromosomes, deletion of DNA fragments and chromosomal rearrangements. When cells that have undergone chromothripsis are subjected to whole genome sequencing, oscillating copy number states are observed, which is indicative of chromothripsis. One of the criteria for chromothripsis scoring is to detect at least 10 copy number switches between two or more copy number states within 50 mega bases. [5].

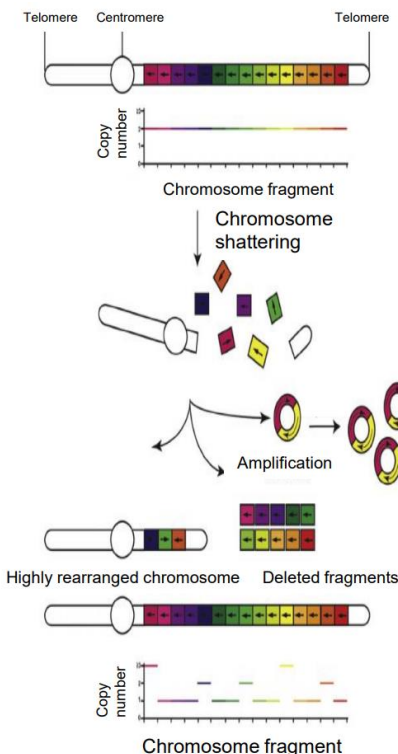


Figure 1: Schematic representation of chromothripsis

A shattering event leading to tens or hundreds of DNA double stranded breaks. The resulting DNA fragments are repaired by error prone processes leading to the formation of double minute chromosomes, deletions and rearrangements. Chromothriptic chromosomes show oscillating copy number profiles. Figure taken from Luijten et al, 2018 [3].

INTRODUCTION

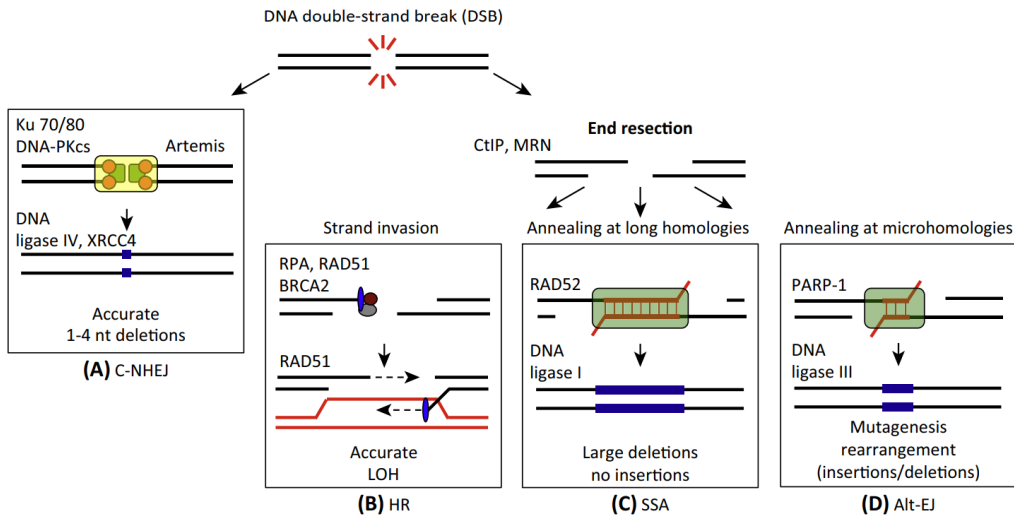


Figure 2: An overview of DNA double strand break repair pathways

(a) Canonical non-homologous end joining (C-NHEJ), leading to 1-4 nucleotide deletions, is more accurate as compared to other pathways, except for homologous recombination (HR). (b) The HR repair pathway is the most accurate pathway in terms of DNA repair. However, loss of heterozygosity can occur. (c) The Single strand annealing (SSA) repair pathway makes use of long homologies at double strand break sites and causes large deletions. (d) The alternative end joining (Alt- EJ) pathway is the least accurate as compared to other pathways. It makes use of micro homologies at double strand break sites and causes rearrangements, insertions and deletions. Figure taken from Ceccaldi et al, 2016 [4].

Possible mechanisms leading to chromothripsis

There are many mechanisms that potentially explain the occurrence of chromothripsis. One such mechanism is micronuclei formation. Micronuclei are nuclear structures outside the main nucleus containing one or a few chromosomes. These structures can be formed by multiple ways, such as centromere inactivation, chromosomal missegregation or lagging chromosomes during mitosis or defects in the nuclear envelope assembly [6, 7]. Chromosomes in micronuclei are particularly vulnerable to DNA damage leading to double strand breaks [8, 9]. In subsequent cell divisions, the DNA fragments from the micronuclei can be deleted, amplified or reintegrate into the genome [9]. Such cells, when sequenced, show oscillating copy number patterns typical of chromothripsis. The micronuclei model of chromothripsis has the potential to explain why genomic rearrangements and alterations are limited to one or a few chromosomes.

The second model that could potentially explain rearrangements caused by chromothripsis is telomere dysfunction. In this model, telomeric regions are lost due to inactivity of the telomerase enzyme or to telomeric lesions [10]. Dysfunctional telomeres ligate, leading to breakage fusion bridge (BFB) cycles in subsequent mitotic events. The dicentric chromosomes formed due to ligation of dysfunctional telomeres are pulled towards opposite poles of the spindle during anaphase, ultimately leading to shattering of the chromosomes and genomic instability [11-13].

Further models for the induction of chromothripsis include the accumulation of double strand breaks by physical agents like ionizing radiations or high energy UV light or chemical agents like doxorubicin [14-16].

1.1.1 Factors linked to chromothripsis

Previous studies have shown a strong link between chromothripsis and homologous recombination (HR) repair deficiency [17]. In one study, factors involved in HR repair and c-NHEJ repair were inactivated in neural progenitor cells from p53 deficient mice. These mice developed high grade gliomas (HGG) or medulloblastomas. Analyzing these tumors revealed a high prevalence of shattering events and genomic instability (Figure 3). This study also showed a strong link between chromothriptic events and MYC/MYCN amplification [18].

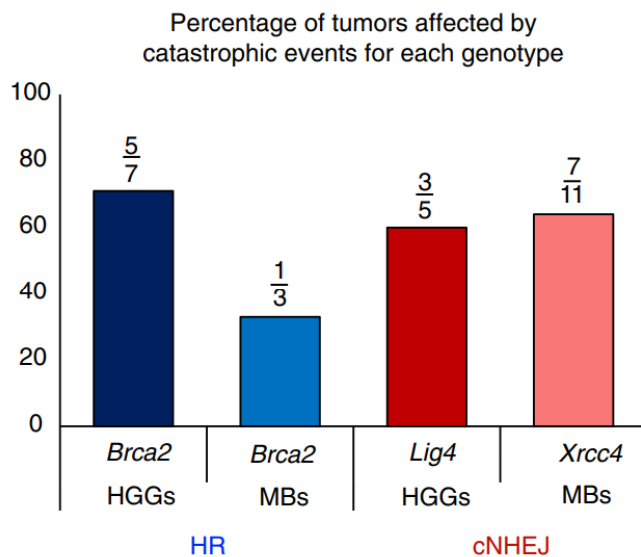


Figure 3: Chromothripsis is linked to HR and cNHEJ repair deficiency

Bar graph showing the ratio of tumors affected by DNA shattering events upon inactivation of factors involved in HR or cNHEJ DNA repair in p53 deficient mice developing high grade gliomas or medulloblastomas. Figure taken from Ratnaparkhe et al, 2018 [18].

In another study, 961 childhood tumors from 24 molecular types were screened for factors linked to genomic instability and large-scale genomic aberrations. The results showed that chromothripsis is strongly linked to p53 deficiency (Figure 4) and BRCAneSS signature (Figure 5)[19].

INTRODUCTION

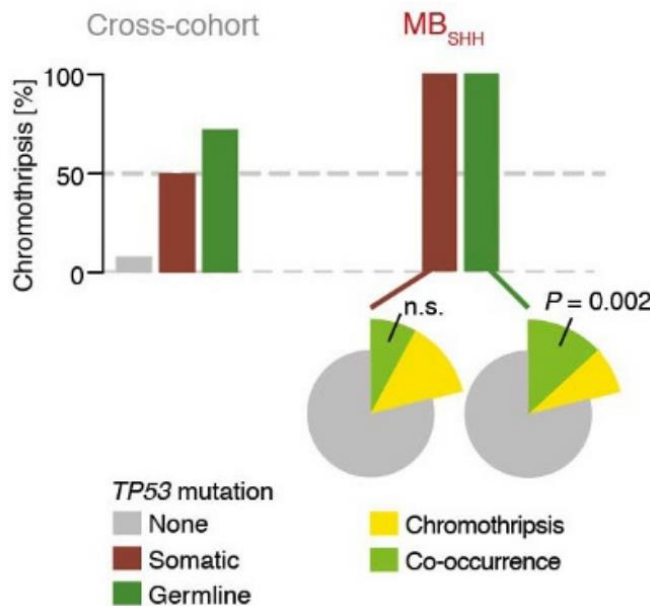


Figure 4: Chromothripsis is linked to p53 deficiency

Prevalence of chromothripsis in a cohort of 961 tumors depending on the *TP53* status – pan-cancer analysis on the left and Sonic Hedgehog medulloblastoma (MB_{SHH}) on the right of the bar graph. Figure taken from Grobner et al, 2018 [19].

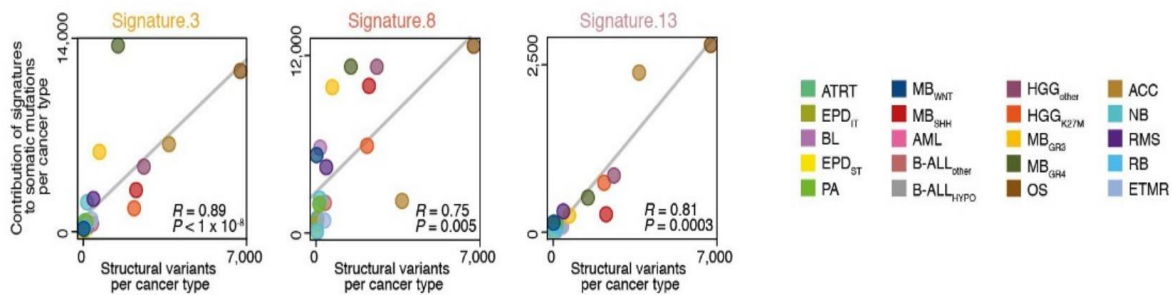


Figure 5: Chromothripsis is linked to BRCAness

Graphs show a high correlation between mutational signature 3 (signature linked with the BRCAness phenotype, left panel), signature 8 (signature linked to *PALB2* or *BRCA2* mutations, middle panel) and signature 13 (signature linked to p53 deficiency and chromothripsis, right panel) with genomic instability in different tumor entities. Figure taken from Grobner et al, 2018 [19].

1.2 Chromothripsy in cancer

1.2.1 Prevalence across different tumor entities, link with poor prognosis and lack of therapeutic options

The prevalence of chromothripsy has recently been found to be above 20% across different tumor entities (Figure 6)[20]. In particular, Sonic Hedgehog medulloblastomas, neuroblastomas and osteosarcomas have extremely high prevalence of chromothripsy [1, 20-22]. Chromothripsy causes large scale genomic aberrations that potentially confer selection advantages to chromothriptic tumor cells as compared to non-chromothriptic cells, by the amplification of oncogenes, deletion of tumor suppressor genes or enhancer hijacking [23]. In addition, chromothripsy has also been linked to poor prognosis in cancer patients [22, 24-26]. Therefore, there is an urgent need for therapeutic options to target tumor cells with chromothripsy.

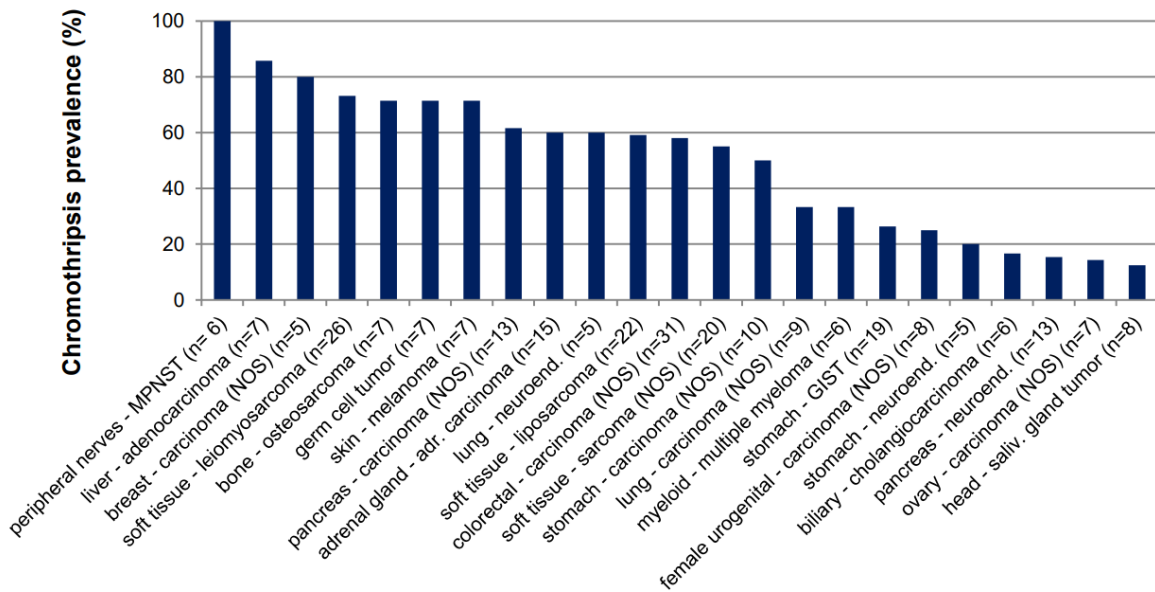


Figure 6: High prevalence of chromothripsy in different cancer types. Figure taken from Voronina et al, 2020 [20]

1.3 Synthetic lethality

1.3.1 Targeting DNA repair defects in cancer therapy using PARP inhibitors

BRCA1 and BRCA2 are key proteins in the HR repair pathway [27, 28] and loss of function of either of these proteins have been linked to genomic instability [29, 30]. In many tumor types, especially breast and ovarian cancers, *BRCA1* and *BRCA2* mutations are frequent and play a key role in tumor

INTRODUCTION

development and progression [31-35]. Therapeutic approaches that cause cell death due to combination of deficiencies in the expression of two or more genes while sparing cells that have only one of the two deficiencies are called synthetic lethality. One such approach is the use of PARP inhibitors in HR deficient tumor cells, which has been found to be extremely successful in the context of breast and ovarian cancer [36].

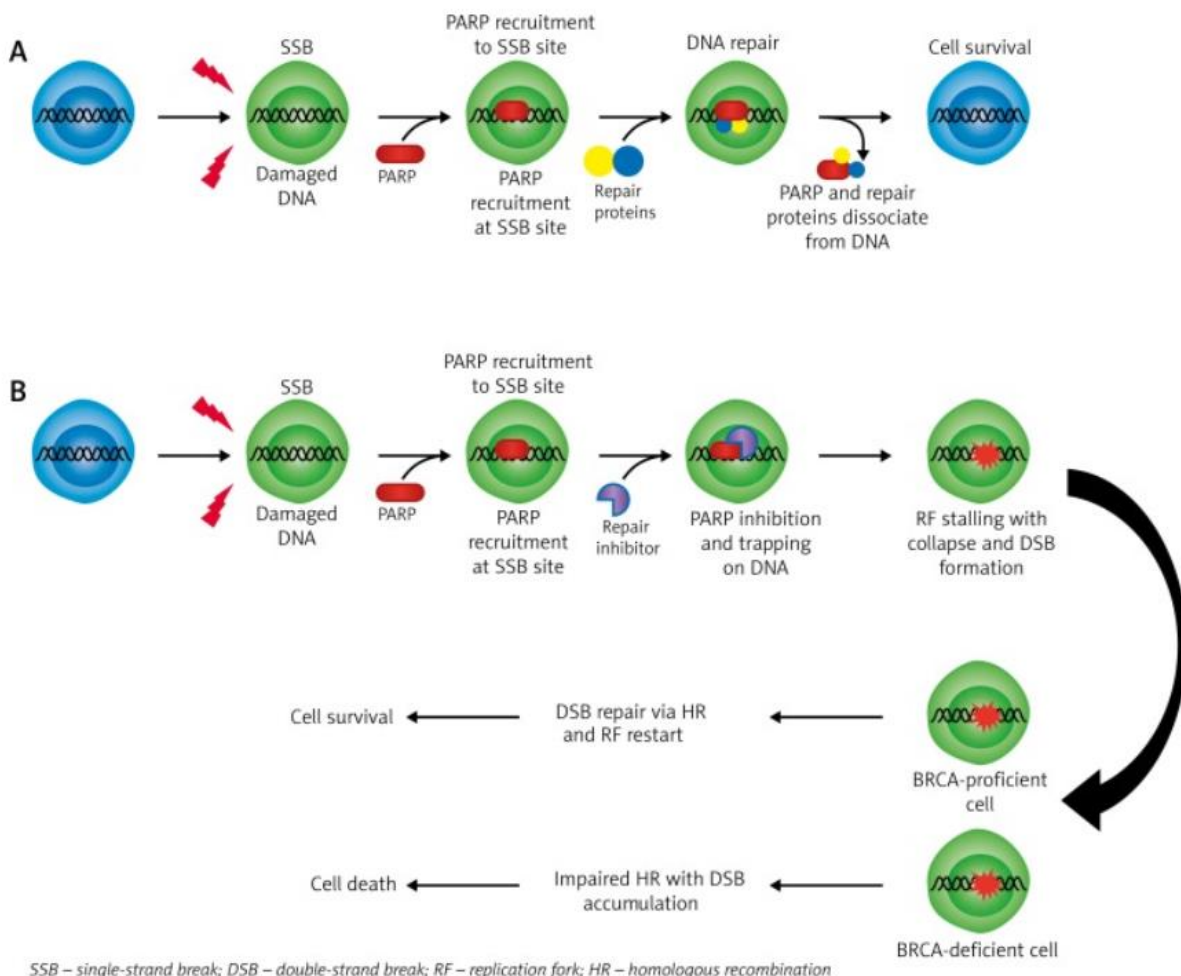


Figure 7: Schematic representation of synthetic lethality and PARP inhibitor treatment

A) Upon DNA damage, PARP is recruited to the site of damage which along with other DNA repair proteins repairs the damaged DNA. (B) In the presence of a PARP inhibitor, PARP activity is inhibited and PARP is trapped at the site of DNA damage. When such a cell undergoes mitosis, the replication fork (RF) is stalled because of trapped PARP leading to further DNA damage. When HR is intact, the DNA is repaired by the HR repair pathway and the RF restarts. But if HR is impaired then DNA damage accumulates, ultimately leading to cell death. Figure taken from Dziadkowiec et al, 2016 [37].

BRCA2 mutant cells were reported to be specifically killed by PARP inhibitor treatment because of their inability to repair double stranded breaks [38]. In a phase II clinical trial on *BRCA1* or *BRCA2* mutant breast and ovarian cancer patients resistant to platinum-based drugs, treatment with olaparib (a PARP

inhibitor) showed encouraging results in terms of tumor response and increased overall survival [39]. As the benefit of using PARP inhibitors became evident, the treatment was successfully extended to other tumor types including lung, pancreas, skin, and bone cancer with BRCAⁿess phenotype [40].

1.3.2 Mechanism of action of the PARP enzyme

Poly(ADP-ribose) polymerases (PARPs) represent a large family of proteins with 18 members [41]. Typically, a PARP enzyme has three domains namely a DNA binding domain (DBD), an auto modification domain (AD) and a catalytic domain. The DBD has three zinc finger domains that help the enzyme to find the site of single or double strand DNA break. The function of auto modification domain is to poly(ADP-ribosyl)ate itself while the function of the catalytic domain is to transfer ADP-ribose subunits from NAD⁺ to protein acceptors producing poly ADP-ribose (PAR) chains. This is an energy consuming step as it requires the use of ATP. This is why over activation of the PARP enzyme is deleterious to the cell. These chains act as signals to recruit additional DNA damage repair proteins to the site of DNA damage. As the negative charge on PARP increases due to autoribosylation, its affinity to the DNA decreases. PARP detaches from the DNA and leaves the site of damage, which is necessary for DNA damage repair. If PARP is trapped at the site of DNA damage by PARP inhibitors, then it cannot leave the site of DNA damage and hinders not only repair of DNA damage but also causes the replication fork to stall, ultimately leading to more DNA damage and cell death. After PARP leaves the site of DNA damage, an enzyme called poly(ADP-ribose) glycohydrolase (PARG) cleaves the PAR chains and restores the PARP ability to bind to the DNA again for the next round of DNA repair (Figure 8)[42].

INTRODUCTION

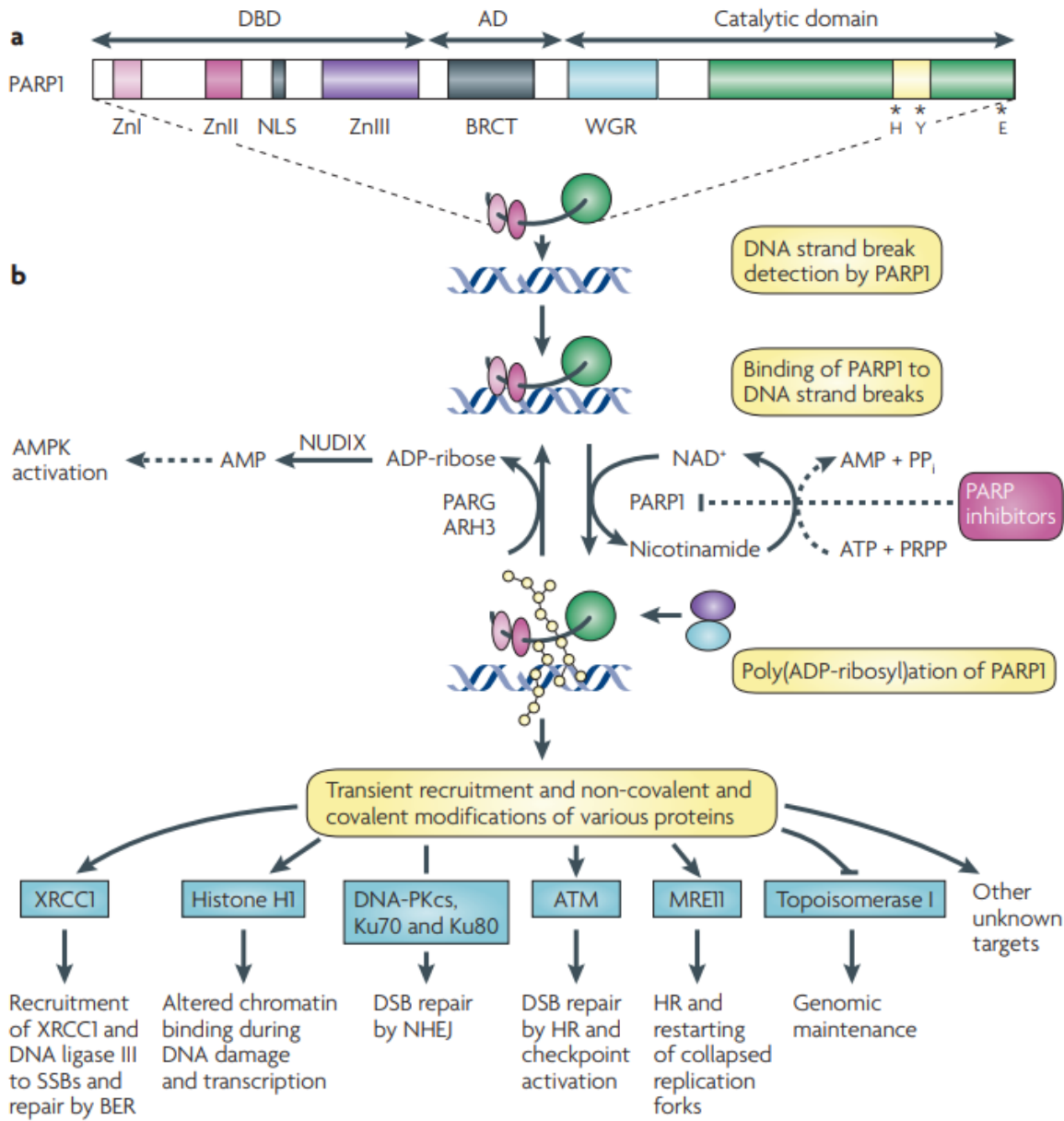


Figure 8: Mechanism of action of the PARP enzyme

(a) Three main domains of the PARP enzyme are the DNA binding domain (DBD), the auto modification domain (AD) and the catalytic domain. (b) Upon DNA damage, the PARP enzyme binds to the DNA and produces PAR chains which recruit more proteins involved in DNA repair to the site of DNA damage. PARP leaves the site of DNA damage and the DNA damage is repaired. Figure taken from Rouleau et al, 2010 [42].

1.3.3 Synergistic approach used for cancer therapies

Although the use of PARP inhibitors was beneficial for certain cancer types, many studies showed that combinational therapy is more effective as compared to monotherapy [43, 44]. In one such study, Ewing sarcoma which was non-responsive to PARP inhibition in clinical trials was found to respond to

combinational treatment with PARP inhibitor. Ewing sarcoma cell lines were used in a matrix screen to identify synergistic partners of PARP inhibitors. An *in vitro* matrix drug screen identified nicotinamide phosphoribosyl transferase (NAMPT) inhibitors (GNE-618, daporinad, GMX-1778) as synergistic partners of PARP inhibitors (niraparib, olaparib, rucaparib) (Figure 9). Combinational treatment with NAMPT- and PARP inhibitors not only inhibited cell growth *in vitro*, but also increased overall survival and decreased tumor growth and progression in *in vivo* Ewing sarcoma mouse models [45].

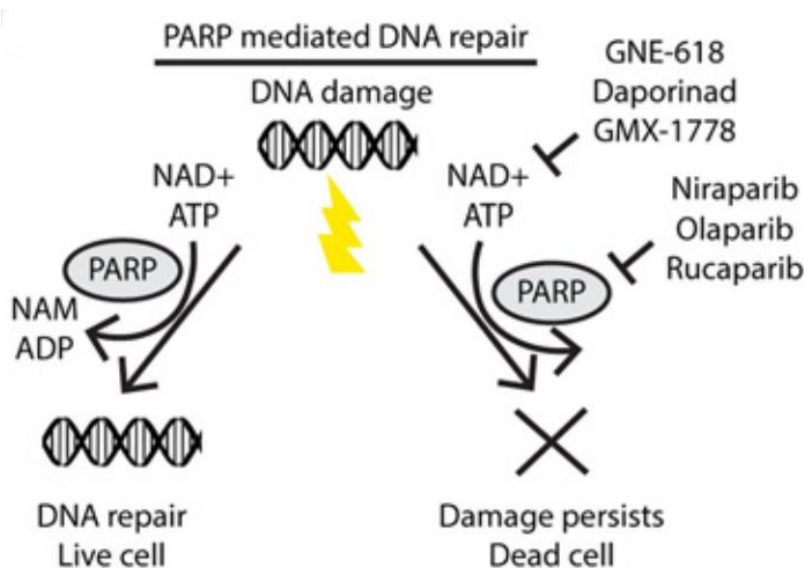


Figure 9: Synergistic interaction between NAMPT- and PARP inhibitors

When DNA damage occurs in the cells, PARP is activated, which leads to DNA repair and cell survival (left side). However, upon DNA damage, if the activity of the PARP enzyme is inhibited by PARP inhibitors (niraparib, olaparib, rucaparib) and the activity of NAMPT is inhibited by NAMPT inhibitors (GNE-618, daporinad, GMX-1778), this leads to decreased PAR levels in the cell, driving the cells to apoptotic cell death. Figure taken from Ryall et al, 2015 [45].

In another study, it was shown that in *PGBD5*-expressing childhood solid tumors including neuroblastoma, medulloblastomas and Ewing sarcomas, AZD6738 treatment is potent to eliminate the tumor cells but spares the normal cells. AZD6738 treatment in combination with cisplatin significantly decreased tumor growth in *PGBD5* expressing primary neuroblastoma patient derived xenograft (PDX) mice models [46].

INTRODUCTION

1.4 Synergy between drugs

1.4.1 Definition

For decades the definition of synergy between drugs has been discussed and argued upon. There are many definitions of synergy, depending upon the null hypothesis on which the specific model of synergy is based. Assumptions such as whether the two drugs under observation are considered to be non-interacting further complicate the debate, as in most of the cases the exact modes of action of the drugs are not known. However, as long as biologically logical rationale about the non-interacting nature of the drugs are given (e.g. the two drugs target different cellular pathways), the assumptions are justified. The basic concept, however, to measure synergy is to determine the difference of effect of a combination treatment as compared to the expected effects of single agents under the null hypothesis.

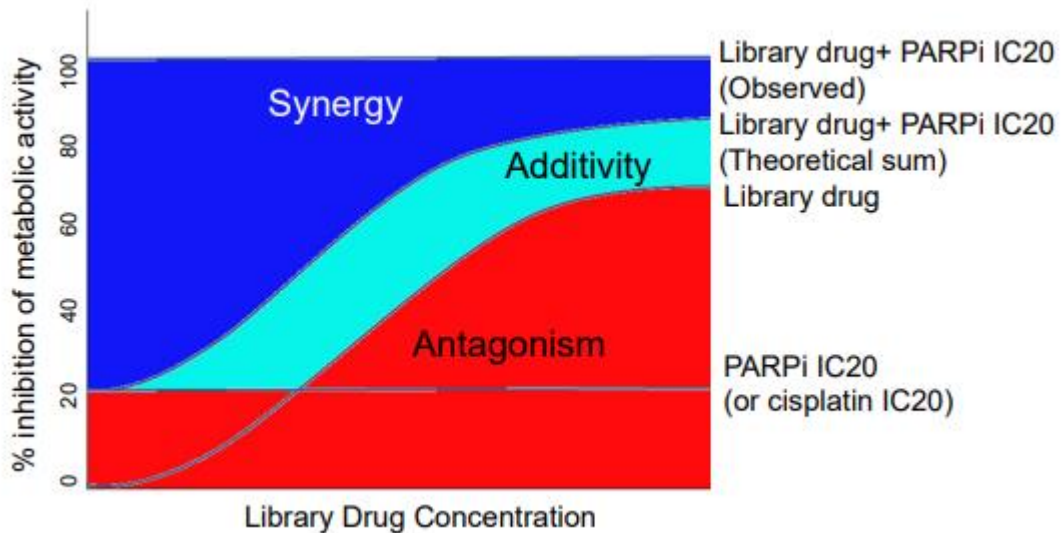


Figure 10: Graphical representation of synergistic, additive and antagonistic drug interaction

PARP inhibitor IC20 or cisplatin IC20 library drug alone inhibits 20% of the metabolic activity of the cells. The library drug at four different concentrations makes a curve with regards to the percentage of inhibition of the metabolic activity. When used in combination, the library drug and PARP inhibitor IC20 (or cisplatin IC20), if the % inhibition of metabolic activity is higher than the effect of the single drugs but stays within the range of the theoretical sum of the individual effects of the two drugs, then the effect is additive. If it exceeds this effect, then it is called synergism. On the other hand, if the % inhibition of the metabolic activity is less than the effect of the single drugs, then it is called antagonism.

1.4.2 Models to evaluate drug interactions

Two main models of synergy (constructed based on the null hypothesis that the two drugs under investigation are non-interacting) include Loewe additivity and bliss independence [47]. The two models have been differentiated from each other based on mechanistic interpretations. Loewe additivity is expected to be more accurate for calculating synergy between non-interacting drugs that target the same

or biologically interconnected pathways [48]. On the other hand, if the two drugs target two unrelated biological pathways, then the Bliss independence model of synergy is expected to be more accurate in determining synergistic interactions between the two non-interacting drugs [49]. In 1992, the Saariselkä agreement, in an attempt to resolve the confusion about different models of synergy, provided a solution on which the scientific community has agreed [50]. As the assumption underlying both models are justifiable and biologically logical, the agreement concluded that either of the models can be used by scientists with only one condition, namely that the specific model used to calculate synergy and antagonism in a study must be explicitly mentioned in published articles. Moreover, it was made clear that the synergistic models are not designed to be selected based on known mechanistic insights about the drug combinations. They are rather intended to be used to determine synergistic or antagonistic interactions between drugs under investigation followed by mechanistic studies to determine the mode of action of the drugs. In my study, I used the Loewe additivity models of synergy as the targeted pathways were interconnected.

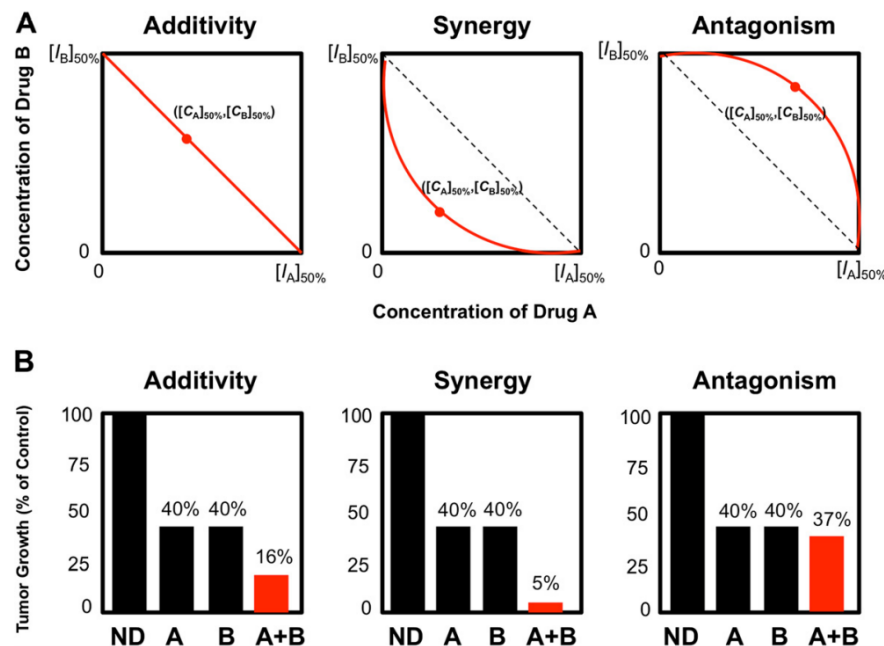


Figure 11: Graphical representation of Loewe additivity model of synergy (A) and Bliss independence (B). Figure taken from Chang et al, 2017 [51]

INTRODUCTION

1.5 Aim of the study

The extremely high prevalence of chromothripsis across different tumor entities and the link between chromothripsis and poor prognosis for cancer patients emphasizes the need for new therapeutic options to treat tumors with chromothripsis. Despite recent advances in understanding the mechanisms that lead to chromothripsis, no therapeutic approach has been taken to target tumor cells with chromothripsis. In this study, a synthetic lethality approach using a PARP inhibitor was taken to exploit homologous recombination (HR) repair deficiency, which is pronounced in chromothriptic tumor cells. The aim of the drug screen was to identify potent drugs that can kill chromothriptic cancer cells either as single agents or as synergistic partners of a PARP inhibitor. The aim of the mechanistic studies was to investigate the molecular link between the PARP inhibitor and its synergistic partner. Finally, the *in vivo* efficacy of the synergistic drug combination was evaluated with the aim of providing evidence that the drug combination inhibits tumor growth in preclinical models and shows potential to be evaluated further in clinical trials.

2. Materials and Methods

2.1 Materials

2.1.1 Drugs and Reagents

Substance	Company
BGB290 (HY-104044)	MedChemExpress
Cisplatin (HY-17394)	MedChemExpress
TargetMol library (L3900)	TargetMol
DiscoveryProbe library (L1033)	ApexBio
ATPlite assay kit (6016947)	Perkin Elmer
Romidepsin (HY-15149)	MedChemExpress
Nanaomycin A (A8191)	Biotrend
Propidium iodide (sc-3541A)	Santa Cruz
DNase-free RNase (10109169001)	Sigma-Aldrich
Annexin buffer (556454)	BD Biosciences
FITC annexin V (556419)	BD Biosciences
7AAD (559925)	BD Biosciences
RNeasy mini kit (74104)	Qiagen
1X annexin buffer (556454)	BD Biosciences
anti-Acetyl- α -Tubulin (5335)	Cell Signalling
anti-Phospho-Histone 3 (9706)	Cell Signalling
Anti-Goat, HRP coupled	Santa Cruz Biotech
Anti-rabbit, HRP coupled	Cell Signalling
Ethanol	Merck Millipore
Ethylenediaminetetraacetate (EDTA) (25 mM)	Thermo Fischer Scientific
Glycerol	Carl Roth
Nuclease-free water	Ambion
Paraformaldehyde (PFA)	Sigma-Aldrich
RIPA-lysis buffer	Sigma-Aldrich
Sodium dodecyl sulfate (SDS)	Sigma-Aldrich
Tris-(hydroxymethyl)-aminomethan (TRIS)	Carl Roth
Triton X-100	Sigma-Aldrich
Tween-20	Sigma-Aldrich
Whole milk powder	Carl Roth

MATERIALS AND METHODS

RNeasy® Mini kit	Qiagen
PARPtrap™ Assay Kit	BPS Bioscience

2.1.2 Cell Culture Reagents and Materials

Article	Company
NeuroCult™ NS-A Proliferation Kit (05751)	STEMCELL Technologies
Neurobasal™-A Medium (10888022)	Invitrogen
DMEM/F-12 (11330057)	Invitrogen
MEM Non-Essential Amino Acids Solution (100X) (11140050)	Invitrogen
Sodium Pyruvate (100 mM) (11360070)	Invitrogen
Hepes buffer (1M) (15630080)	Invitrogen
GlutaMAX™ Supplement (35050061)	Invitrogen
Penicillin-Streptomycin (15140122)	Invitrogen
B-27™ Supplement minus vitamin A (50X) (12587001)	Invitrogen
Heparin (H3149-10KU)	Sigma-Aldrich
Human FGF rec 154aa (GMP100-18 B)	Peprotech
EGF (E 4127)	Sigma-Aldrich
LIF (LIF1010)	Millipore
DMEM high glucose (41965-039)	Gibco
RPMI Medium 1640 (21875-034)	Gibco
MEGM media (CC-3150)	Lonza
Roti®-CELL McCoy's 5A (9111.1)	Carl Roth
Astrocyte media (1801)	ScienCell
poly-L-lysine (P1399)	Sigma-Aldrich
DMEM/F-12 1:1 Medium (11320-074)	Gibco
Cryo tubes	Nunc
Doxycycline	Sigma-Aldrich
Fetal calf serum (FCS)	Merck Millipore
L-Glutamine	Thermo Fischer Scientific
Phosphate buffer saline (PBS)	Thermo Fischer Scientific
Penicillin/Streptomycin (100 µg/ml)	Thermo Fischer Scientific
Reservoir	Corning
Syringe filters (0.45 µm)	Merck Millipore
Trypsin EDTA solution	Sigma-Aldrich

2.1.3 In vivo Reagents and Materials

Article	Company
Matrigel (356234)	Corning
BGB290 (HY-104044)	MedChemExpress
Romidepsin (HY-15149)	MedChemExpress
Insulin syringe with needles	BD Biosciences
Isoflurane	Abbott

2.1.4 Mice

Strain	Source
NSG (NOD.Cg-PrkdcscidIl2rgtm1Wjl)	In-house breeding facility of the DKFZ
NRGS (NOD/RAG1 ^{2-/-} IL2Rγ ^{1-/-} -SGM3)	In-house breeding facility of the DKFZ

2.1.5 Cell Lines and PDX Spheroid Models

Cell Line/PDX spheroid model	Origin
UWB1.289	Ovarian carcinoma
UWB1.289+BRCA1	Ovarian carcinoma
MDA-MB-436	Breast carcinoma
HD-MB03	Group 3 medulloblastoma
HD-N33	Neuroblastoma
SaOS-2	Osteosarcoma
KHOS-240S	Osteosarcoma
SJSA-1	Osteosarcoma
DAOY	Medulloblastoma
ONS-76 (MYC ON/OFF)	Medulloblastoma
RPE1 WT	Retina epithelial cells
RPE1 TP53 KO	Retina epithelial cells
Normal human astrocytes	Healthy human cells
LFS_MB_P (primary tumor)	Sonic hedgehog medulloblastoma PDX spheroids
LFS_MB_1R (first relapse)	Sonic hedgehog medulloblastoma PDX spheroids
LFS_MB_2R (second relapse)	Sonic hedgehog medulloblastoma PDX spheroids
RCMB18	Sonic hedgehog medulloblastoma PDX spheroids
BT084	Sonic hedgehog medulloblastoma PDX spheroids
ICB984	Sonic hedgehog medulloblastoma PDX spheroids

MATERIALS AND METHODS

2.1.6 Equipment

Equipment	Company
Vi-CELL XR 2.03 cell counter	Beckman Coulter
96-well plates for adherent cells (6005689)	Perkin Elmer
96-well plates for spheroids (236105)	Thermo Scientific
25 cm ² flasks (690195)	Greiner
Tissue culture dishes (353004)	Corning
Fortessa flow cytometer	BD Biosciences
Counting slides (145-0011)	Bio Rad
Automated cell counter (TC20)	Bio Rad
Axio Zeiss Imager.M2 microscope	Zeiss
Mithras LB 940 plate reader	Berthold Technologies
NanoDrop® ND-1000 spectrometer	NanoDrop
Water bath B-480	Büchi
Janus integrator (automated platform)	PerkinElmer
MultiDrop Combi cell dispenser	ThermoFisher
EnVision™ HTS plate reader	PerkinElmer
FlexDrop™ IV EXi reagent dispenser	PerkinElmer
MultiProbe® II Plus Ex 4-Channel Pipettor	PerkinElmer

2.1.7 Other Materials

Article	Company
EPIC methylation arrays	Illumina
450K methylation arrays	Illumina
Affymetrix Clariom S arrays	Thermo Fisher scientific
Cover slips (10 mm round)	Thermo Fischer Scientific
Cover slips (26 x 76 mm)	Thermo Fischer Scientific
FACS tubes	BD Bioscience
Falcon® tubes(15 ml and 30 ml)	BD Bioscience
Glass slides	Sigma Aldrich
Glass vials	Mikrolab Aarhus
PCR tubes (0.2 ml)	Molecular BioProducts

Filtered pipette tips (10 µl, 20 µl, 100 µl, 200 µl, 1000 µl)	Eppendorf
Reaction tubes (1.5 ml and 2 ml)	Eppendorf

2.1.8 Software and R Packages

Software / R package

Bioconductor package conumee

Combenefit freeware software

Ward.D linkage and Pearson's correlation distance

NMF package

ComplexHeatmap package

R plotly package

FACSDiva software

Bioconductor package 'oligo'

Limma package

GraphPad PRISM 5

MATERIALS AND METHODS

2.2 Methods

The text of the following section on methods has been taken from Khalid et al (submitted for publication) and the material and methods section of the manuscript was originally written by myself.

2.2.1 Cell Culture Conditions

Preparation of Spheroid Cultures

Spheroid cultures from patient-derived xenograft models were prepared by homogenizing the freshly isolated tumors from mice brains by pipetting in NeuroCult™ NS-A Proliferation Kit (STEMCELL Technologies, 05751). Homogenized tissue was then filtered to get single cell suspension. Cells were then centrifuged at 1000 rpm for 5 minutes and pellets were resuspended to get 0.5 million cells per 10 ml growth medium. Growth medium was comprised of 46.75 ml Neurobasal™-A Medium (Invitrogen, 10888022) with 46.75 ml DMEM/F-12 (Invitrogen, 11330057), 1 ml MEM Non-Essential Amino Acids Solution (100X) (Invitrogen, 11140050), 1 ml Sodium Pyruvate (100 mM) (Invitrogen, 11360070), 2.5 ml Hepes buffer (1M) (Invitrogen, 15630080), 1 ml GlutaMAX™ Supplement (Invitrogen, 35050061), 1 ml Penicillin-Streptomycin (Invitrogen, 15140122), 2 ml B-27™ Supplement minus vitamin A (50X) (Invitrogen, 12587001), 40 µl Heparin (50 mg/ml stock) (Sigma, H3149-10KU), 20ng/ml Human FGF rec 154aa (Peprotech, GMP100-18 B), 10 ng/ml EGF (Sigma, E 4127) and 100 µl LIF(Millipore, LIF1010). Spheroids were cultured for 3 weeks in 25 cm² flasks (Greiner, 690195) and passaged by trypsinization with 0.05% Trypsin/EDTA once a week. All adherent cells were passaged by trypsinization with 0.25% Trypsin/EDTA. Astrocytes and spheroids were passaged by trypsinization with 0.05% Trypsin/EDTA.

Formulations of Culture Media for Cell Lines Used in This Study:

For DAOY, BJ wild-type (WT) and BJ *TP53* KO cells, 1X DMEM high glucose (Gibco, 41965-039) with 10% fetal calf serum (FCS) and 1% L-glutamine. For UWB1.289 and UWB1.289+BRCA1 cells, 48.5 % RPMI Medium 1640 (Gibco, 21875-034) and 48.5% MEGM media (Lonza, CC-3150) (Supplements were provided with the kit) with 3% FCS. For UWB1.289+BRCA1, G418 was added to a final concentration of 200 µg/ml. For MDA-MB-436 cells, 1X DMEM high glucose (Gibco, 41965-039) with 10% FCS. For KHOS-240S cells, 1X DMEM high glucose (Gibco, 41965-039) with 10% FCS, 1% L-glutamine and 1% MEM Non-essential amino acids (MEM NEAA) (Gibco, 11140-050). For SaOS-2 cells, Roti®-CELL McCoy's 5A (Carl Roth, 9111.1) with 15 % FCS and 1% L-glutamine. For SJSA-1 cells, RPMI Medium 1640 (Gibco, 21875-034) with 10% FCS and 1% L-glutamine. For HD-MB-03 cells, RPMI Medium 1640 (Gibco, 21875-034) with 10% Heat inactivated FCS, 1% L-glutamine and 1% MEM NEAA (Gibco, 11140-050). For HD-N33 cells, RPMI Medium 1640 (Gibco, 21875-034) with 10 % FCS and 1% L-glutamine. For normal Astrocytes, astrocyte media (ScienCell, 1801) (Supplements were provided with the kit).

Culture flasks and 96 well plates were coated with poly-L-lysine (Sigma, P1399). For RPE1 WT and RPE1 *TP53* KO, DMEM/F-12 1:1 Medium (Gibco, 11320-074) with 10% FCS and 1% L-glutamine.

Cell Number and Viability Measurements

Before seeding cells for experiments, the viability and absolute number of cells was determined using a Vi-CELL XR 2.03 cell counter. Automatic trypan blue staining allowed the total number of viable cells per ml to be determined. Only cell suspensions with a minimum viability of 90 % were used for experiments and were generally seeded at a density of 50000 per ml, unless otherwise indicated in the respective method section.

2.2.2 Molecular Characterization of the Cell Lines and PDX Models

Copy number states from EPIC and 450K methylation arrays were assessed using the Bioconductor package conumee. For EPIC methylation arrays and 450K methylation arrays, references were taken from the GEO database with accession numbers GSE147740 and GSE68777 respectively. Copy number states were computed per candidate gene by comparing the cell lines with references. Copy number changes were reported for genes with more than 0.15 in log2 fold change. For whole genome sequencing data, copy number analysis was performed using ACESeq. Copy number calls from ACESeq were used to determine the copy number states.

2.2.3 Primary Screen

For each cell line included in the screen (UWB1.289, UWB1.289+BRCA1, MDA-MB-436, HD-MB03, HD-N33, normal human astrocytes, SaOS-2, KHOS-240S, SJS-A-1, LFS_MB_P (primary tumor), LFS_MB_1R (first relapse), LFS_MB_2R (second relapse), RCMB18, BT084 and ICB984) the IC20 and IC40 values of BGB290 (Pamiparib, MedChemExpress, HY-104044) and cisplatin (MedChemExpress, HY-17394) were determined. The 375 compounds from 2 drug libraries, namely TargetMol (Catalog No. L3900) and DiscoveryProbe (ApexBio, L1033) were diluted in 96-well plates (Perkin Elmer, 6005689 for adherent cells and Thermo Scientific, 236105 for spheroids) to achieve final concentrations of 5 μ M, 0.5 μ M, 0.05 μ M and 0.005 μ M. Cells were then seeded at optimized densities. Each cell line was treated with its respective IC20 concentration of BGB290 or cisplatin. Spheroids from patient-derived xenograft models were treated with both IC20 and IC40 of BGB290. Cells were incubated at 37 °C for 96 hours. The metabolic activity was measured after 96 hours with the ATPlite assay (Perkin Elmer, 6016947). Values from the blank measurements were subtracted from the treatment wells and normalized to the vehicle controls. 10% DMSO treatment was used as positive control as measure of 100% metabolic inhibition. Vehicle DMSO concentration was used as negative control as measure of 0% metabolic inhibition. The effect of single treatments was compared to the combination treatments to identify drugs

MATERIALS AND METHODS

that have potential additive or synergistic effects with BGB290 or cisplatin or both. Data from the primary screen were analyzed using a shiny app developed for this purpose.

2.2.4 Analysis of the Primary Screen Data

A custom R/Shiny app [52, 53] was developed for the interactive visualization and analysis of the high-throughput drug screening data. For each cell model, drug-sensitivity profiles were calculated across replicate experiments by averaging the percentage of drug-induced inhibition compared to controls as measured by the metabolic activity of the cells. Hierarchical clustering with ward.D linkage and Pearson's correlation distance was performed to group 15 cell models (independently for single agent or combination treatments) according to their drug-sensitivity profiles and the resulting cluster was represented as dendrogram. Based on the sensitivity profiles across 15 cell models under single agent or combination treatments, drugs with similar profiles were visualized using t-distributed stochastic neighbour embedding (t-SNE)[54] with the parameters theta=0, max_iter=20000 and perplexity=10. R packages 'NMF'[55] and 'ComplexHeatmap' in R/Shiny[56] were utilized to create heatmaps of drug-sensitivity profiles. Interactive scatter plots were generated with the R 'plotly' package[57].

2.2.5 Secondary Screen

Romidepsin (medchemexpress, HY-15149) and nanaomycin A (Biotrend, A8191) were candidate hits selected from the analysis of the primary screen data to be subjected to a secondary screen. Spheroids from 5 patient-derived xenograft models (LFS_MB_P, LFS_MB_1R, RCMB18, BT084, ICB984) and HD-MB03 cells were seeded in 96-well plates (Perkin Elmer, 6005689 for adherent cells and Thermo Scientific, 236105 for spheroids). Cells were then treated with romidepsin or nanaomycin A in combination with BGB290 or cisplatin in an 8x8 matrix. Drug concentration ranges for each cell line were selected to cover 80 % to 0% metabolic inhibition. Cells were incubated at 37 °C for 96 hours. The metabolic activity was measured after 96 hours with the ATPlite assay (Perkin Elmer, 6016947). Values from the blank measurements were subtracted from the treatment wells and normalized to the vehicle controls (as described above). The effect of single treatments was compared to the combination treatments to determine additivity or synergy using the Loewe additivity model. Data from the secondary screen were analyzed using the Combbenefit freeware software.

2.2.6 Cell Cycle Analysis

Cells were seeded in tissue culture dishes (Corning, 353004) and incubated at 37 °C for 24 hours. Cells were then treated with vehicle control, BGB290, romidepsin or BGB290 with romidepsin at the indicated concentrations. Cells were incubated for 48 hours at 37 °C. Supernatant was collected in 50 ml falcon tubes. Cells were trypsinized using 0.25 % trypsin and collected. Cells were centrifuged at 1000 rpm for 5 minutes at room temperature. Supernatant was removed carefully. Pellets were washed once with

sterile 1X PBS. Pellets were resuspended in chilled 70% ethanol and incubated at 4 °C for 2 hours. Cells were centrifuged at 420 g for 10 minutes at room temperature. Supernatant was removed carefully. Pellets were resuspended in cell cycle staining solution made of 2.5% propidium iodide (Santa Cruz, sc-3541A), 2% DNase-free RNase (Sigma, 10109169001) and 0.1% Triton X-100 in PBS. Cell cycle staining solution permeabilizes the cells and stains the DNA. Cells were incubated at 4 °C for 30 minutes. The DNA content was measured using a FACS Fortessa and the data were quantified using the FACSDiva software.

2.2.7 Apoptosis

Cells were seeded in tissue culture dishes (Corning, 353004) and were incubated at 37 °C for 24 hours. Cells were then treated with vehicle control, BGB290, romidepsin or BGB290 with romidepsin. Cells were incubated for 48 hours at 37 °C. Supernatant was collected in 50 ml falcon tubes. Cells were trypsinized using 0.25% trypsin and collected. Cells were centrifuged at 1000 rpm for 5 minutes at room temperature. Supernatant was removed carefully. Pellets were washed once with sterile 1X PBS. Pellets were dissolved in 1X annexin buffer (BD Biosciences, 556454). Suspended cells were distributed in FACS tubes. Cells were then incubated with FITC annexin V (BD Biosciences, 556419), 7AAD (BD Biosciences, 559925), no stain control or FITC annexin V with 7AAD. Cells were incubated at 4 °C for 15 minutes in the dark. Live, early apoptotic and late apoptotic or necrotic cells were quantified using a FACS Fortessa and data were analyzed using the FACSDiva software.

2.2.8 Doubling Time

Cells were seeded in tissue culture dishes (Corning, 353004) at low confluence. Cells were incubated at 37 °C. After 24 hours, cells were trypsinized using 0.25% trypsin. Cells were then treated with 50% trypan blue (Sigma, T8154). Cells were pipetted into counting slides (Bio Rad, 145-0011) and living cells were quantified using an automated cell counter (Bio Rad-TC20). To estimate the average doubling time, exponential linear regression was applied on the doubling time data.

2.2.9 *In vivo* Studies and Chemotherapy

Freshly isolated cells from orthotopic patient-derived xenograft mouse model (LFS_MB_1R, first relapse) were injected into the right flanks of six to 10-week-old female immune-compromised mice (NSG, NOD.Cg-PrkdcscidIl2rgtm1Wjl) with 50% matrigel (Corning, 356234). Twice a week, flank tumor volumes were measured using digital caliper and calculated. Once the tumor volumes reached 100 mm³, the mice were randomized and subjected to either treatment group, vehicle control, romidepsin single treatment or BGB290 with romidepsin combination treatment. In the romidepsin single treatment group, mice were treated with 2 mg/kg of romidepsin administered i.p. (in saline) twice a week. In the BGB290 with romidepsin combination treatment group, mice were treated with 2 mg/kg of romidepsin

MATERIALS AND METHODS

administered i.p. (in saline) twice a week and 6 mg/kg of BGB290 administered p.o. (in 0.5% methylcellulose) twice a day. All animal experiments were performed in accordance with ethical and legal regulations for animal welfare and approved by the governmental council (Regierungspräsidium Karlsruhe, Germany).

2.2.10 Acetyl- α -tubulin and phospho-histone 3 immunostaining

DAOY cells were seeded onto coverslips. After 24 hours the media in each well was replaced with fresh media containing the drug corresponding to the drug treatment group, DMSO control, 6.25 μ M BGB290, 1.7 nM romidepsin and 6.25 μ M BGB290 + 1.7 nM romidepsin. Cells were then incubated for 48 hours. The coverslips were then fixed for 20 minutes with 4% PFA. Next, a blocking buffer (1x PBS, 5% normal goat serum, 0.3% Triton X-100) was prepared and added to the coverslips for 1 hour at room temperature. The blocking buffer was then aspirated and anti-Acetyl- α -Tubulin and anti-Phospho-Histone 3 primary antibodies were diluted to 1:400 and 1:200 respectively in antibody dilution buffer (1x PBS, 1% BSA, 0.3% Triton X-100) and both were added simultaneously to each coverslip. Coverslips were incubated with the primary antibody overnight at 4 °C. Then coverslips were washed thrice for 5 minutes in 1X PBS. Subsequently goat anti-mouse and anti-rabbit secondary antibodies were diluted to 1:500 in antibody dilution buffer and both were added simultaneously to each coverslip. Coverslips were incubated for 2 hours in the dark at room temperature with the secondary antibody and were then washed thrice for 5 minutes in 1X PBS. Then they were rinsed in double distilled H₂O followed by 100% ethanol and left to air dry. Coverslips were then mounted onto microscope slides using DAPI fluoromount and left for 1 hour in the dark before imaging. Imaging was performed on the Axio Zeiss Imager.M2 microscope. Determination of the percentage of mitotic cells per treatment group was done using a macro designed at the DKFZ Light Microscopy Facility.

2.2.11 Gene Expression Analysis

Cells from 3 PDX spheroid models (LFS_MB_P, primary tumor, LFS_MB_1R, first relapse and RCMB18) were seeded in suspension culture flask (Greiner Bio-One, 690195) and treated with either vehicle control, BGB290 (IC20), romidepsin (IC20) or BGB290 (IC20) with romidepsin (IC20) for 24 hours. Pictures were taken using a bright-field microscope to determine the effect of the treatment on the spheroid growth. RNA was then isolated using the RNeasy mini kit (Qiagen, 74104). Expression data were generated using Affymetrix Clariom S arrays.

2.2.12 Analysis of Expression Data and GSEA

Expression analysis and normalization of Affymetrix Clariom S arrays was performed using the Bioconductor package 'oligo'[58]. Sample to sample correlation was illustrated by a heatmap, using the Pearson correlation of the top 1000 variable genes. Cell lines treated with the combination treatment

were compared with both the romidepsin treated cell lines, BGB290 treated cell lines, and the normal human astrocytes. Likewise, romidepsin treated cell lines and BGB290 treated cell lines were compared with the normal human astrocytes. Differential expression analysis was performed by limma [59]. The False Discovery Rate (FDR) adjustment of p-values were performed by the Benjamini-Hochberg method. The Gene Set Enrichment Analysis (GSEA) was performed using gene-sets from MSigDB5. Enrichment test on Oncogenic signature gene sets (C6) from MSigDB was performed using the signed t-statistic from the differential expression analysis. Gene-sets with False Discovery Rate (FDR) smaller than 5% were considered as significant.

2.2.13 Statistical Analysis

Statistical analyses and visualizations were performed using R, shiny app, Combenefit software [60] and GraphPad PRISM 5.

RESULTS

3. Results

Most figures in the result section have been taken from Khalid et al (submitted for publication).

The drug screen was conducted on Sonic Hedgehog (SHH) medulloblastoma PDX spheroid models and cell lines from osteosarcoma, neuroblastoma and ovarian carcinoma tumor entities (Figure 16). Some preliminary experiments were performed before initiating the screen. These experiments included cell cycle analysis of spheroid cultures (3.1) to confirm growth of spheroids in *in vitro* settings and PARP trapping assay (3.2) to determine the type of PARP inhibitor to use for the drug screen.

3.1 Cell cycle analysis of spheroid cultures

As the read-out of the drug screen was inhibition of the metabolic activity, the first point to verify was whether the SHH medulloblastoma PDX cells grow and duplicate in *in vitro* cell culture settings. In order to confirm the spheroid growth, cells isolated from PDX tumors from mice brains were grown for a week in culture flasks and then subjected to propidium iodide staining. FACS analysis of these cells was then performed. This analysis identified a fraction of cells in the S and G2 phases of the cell cycle, which indicates that spheroids grow and duplicate in *in vitro* cell culture settings (Figure 12).

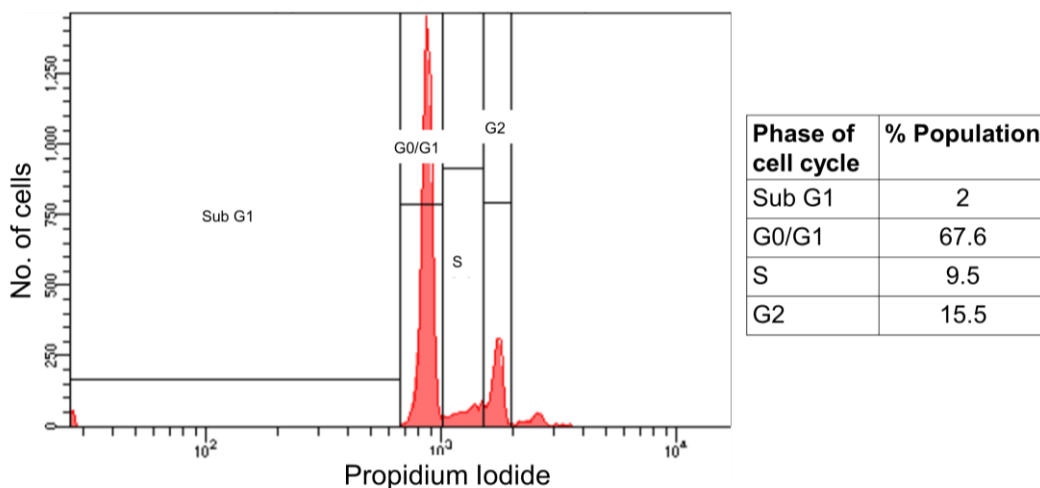


Figure 12: Cell cycle analysis of spheroid cultures

One representative experiment from three independent biological replicates. Number of cells (linear scale) on y-axis plotted against propidium iodide stain intensity (log scale) on x-axis.

3.2 Selection of a PARP inhibitor

PARP inhibitors vary in their ability to trap PARP to the damaged DNA and to cross the blood brain barrier. The PARP trapping abilities of three PARP inhibitors were compared by PARP trapping assays

to select a PARP inhibitor for the screen. The results showed that talazoparib has the highest PARP trapping ability followed by BGB290 and veliparib, respectively (Figure 13). From the literature it is known that talazoparib cannot cross the blood brain barrier well [61]. In the screen, one of the goals was to treat Sonic Hedgehog (SHH) medulloblastomas with chromothripsis. For this reason, we selected BGB290 for the screen, as it can cross the blood brain barrier [62].

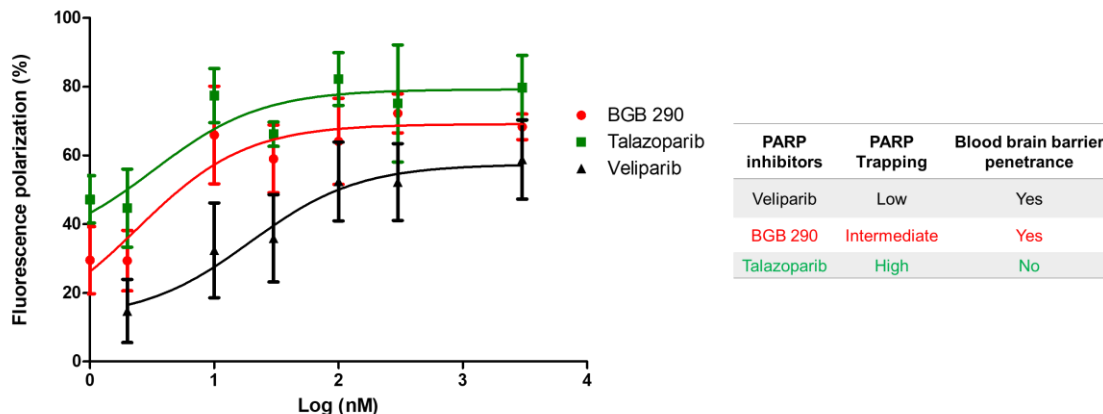


Figure 13: PARP trapping assay

Percentage of fluorescence polarization plotted against increasing concentrations of drugs to compare the relative PARP trapping ability of the PARP inhibitors. The greater the percentage of fluorescence polarization, the greater the PARP trapping ability of the PARP inhibitor is. Error bars represent SEM, n = 5 biological replicates.

3.3 Primary screen

3.3.1 Primary screen set-up

Two libraries containing a total of 375 compounds were diluted in 96 well plates to obtain final concentration of 5 μ M, 0.5 μ M, 0.05 μ M and 0.005 μ M by using the automated platform at the EMBL screening facility. Cells from different tumor entities and cell lines (Figure 16 below) were seeded in the wells of these plates at such a concentration that five days after seeding, wells would show a 90-95 % confluence. IC₂₀s of PARP inhibitor and cisplatin already calculated for each cell line and spheroid culture were added to the designated plates. Three types of sets were obtained: library drugs with PARP inhibitor, library drugs with cisplatin and library drugs alone. After five days of incubation, the ATP substrate solution was added to the wells and the metabolic inhibition values relative to DMSO controls were calculated. The data were then evaluated by quality controls and analyzed.

RESULTS

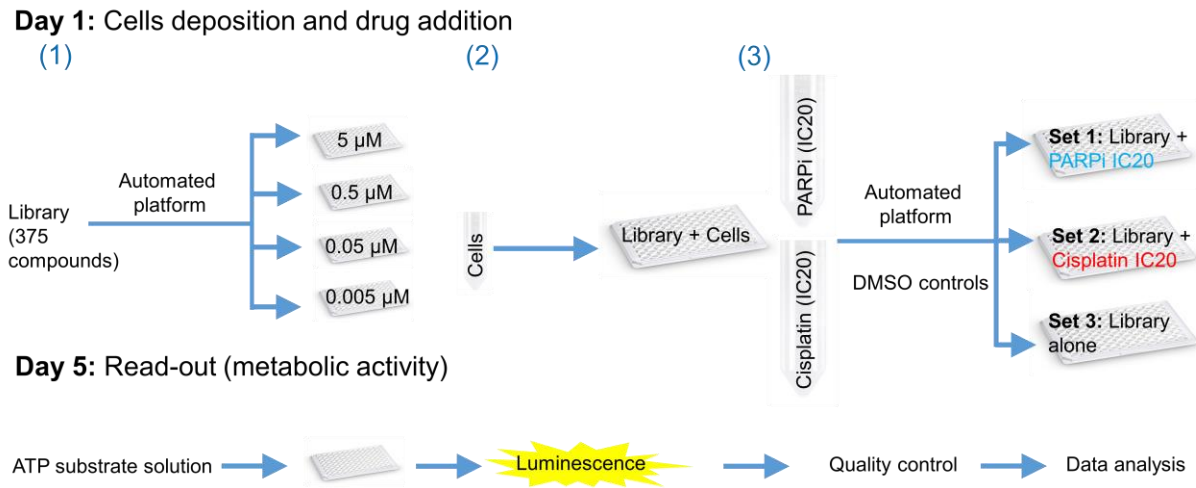


Figure 14: Primary screen set-up

Schematic representation of the primary screen strategy.

3.3.2 Libraries

Two libraries, namely TargetMol and DiscoveryProbe were used for the primary screen. These libraries altogether contained 375 compounds focusing on DNA damage and repair. The compounds in the libraries were classified based on their mode of action (Figure 15).

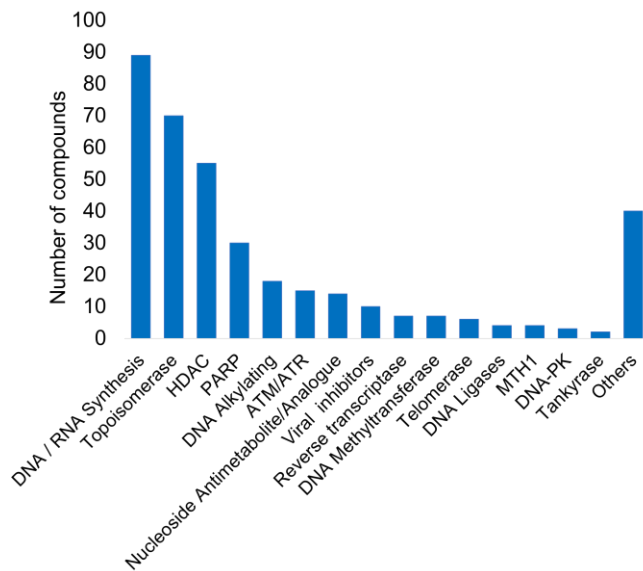


Figure 15: Classification of the library drugs on the basis of their target or mode of action

3.3.3 Characterization of the cell lines included in the primary screen

The cell lines and spheroid cultures included in the primary screen were characterized to access their chromothripsis status and their *TP53* status (Figure 16). In order to determine the chromothripsis status, cells were subjected to EPIC methylation array, 450 K methylation array or whole genome sequencing. Copy number variant (CNV) plots were generated by John K.L Wong (Division of Molecular Genetics) and Martin Sill (Division of Pediatric Neuro-oncology) and cell lines were scored as chromothripsis positive or negative (Figure 17).

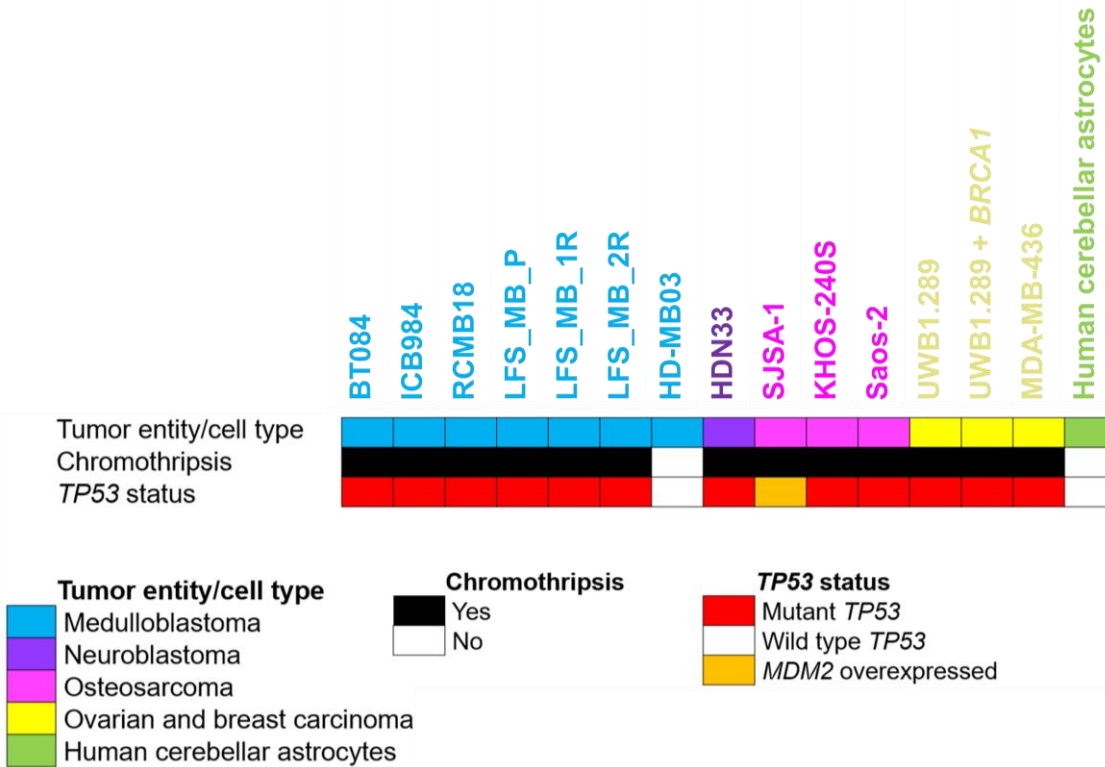


Figure 16: Characterization of the cell types and tumor entities included in the primary screen

RESULTS

SJSA-1 (Osteosarcoma cell line)

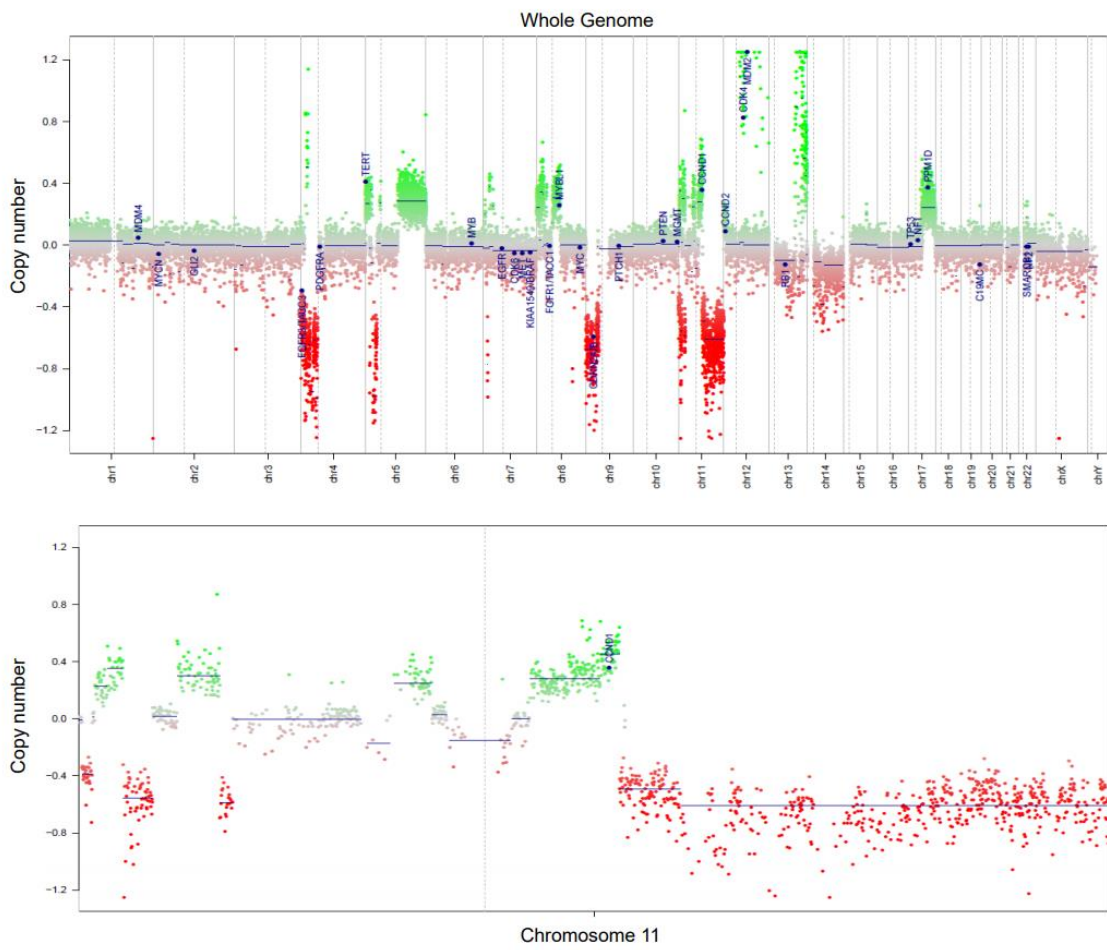


Figure 17: Determination of chromothripsis status in SJSA-1 osteosarcoma cell line

One representative copy number variant (CNV) plot shown for the SJSA-1 cell line included in the primary screen generated using EPIC methylation arrays. Chromothripsis was confirmed on chromosome 11. CNV plots of all other cell lines and spheroid models included in the primary screen are shown in Supplementary figure 46.

3.3.4 Analysis of the primary screen data

t-SNE analysis

Data from the primary screen were subjected to a t-SNE analysis (done by Murat Iskar, Division of Molecular Genetics). The results showed that drugs with similar modes of action cluster together, indicating that the inhibition of the metabolic activity of the cells is potentially due to on-target effects (Figure 18).

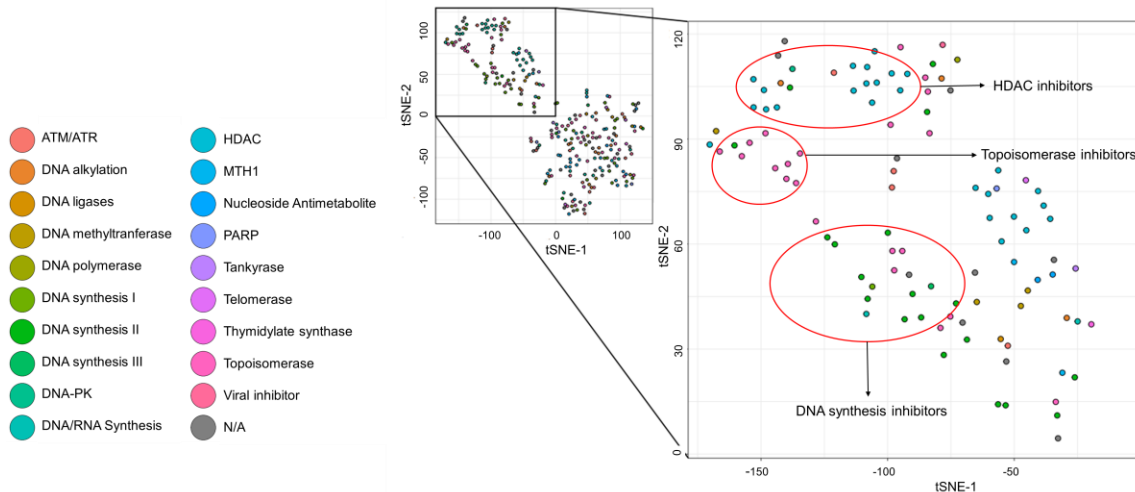


Figure 18: t-distributed stochastic neighbor embedding (t-SNE) plot based on the primary screen data

Drugs with a similar mode of action cluster together. HDAC inhibitors cluster together. Similarly, topoisomerase inhibitors cluster with each other and DNA synthesis inhibitors cluster together.

Quality check analysis of the primary screen data

Negative and positive controls

Negative and positive controls were placed on the 8 wells of each side of the 96 well plates. Negative control wells with 100% metabolic activity showed high and consistent metabolic activity across plates. Similarly, positive control wells set to 0% metabolic activity showed low and consistent metabolic activity across plates, showing that the screen worked (Figure 19).

UWB1.289

4450480	4475720	646640	4161560	4677920	4655440	1851080	4733520	4410200	3581240	4465960	65840
4855760	4830120	5083000	4424640	848160	4753440	4633120	4471520	5267840	4884320	4697200	98600
4200160	1569640	3725600	4710000	4490440	4377320	4160880	2016680	4248040	2187400	4319720	90480
5017840	4650320	4788240	4537600	1129720	5361000	4511760	4154120	4039880	4968480	4500440	99920
3962400	4246600	3966120	3789520	2744960	3941040	1983480	3870800	4185160	4062120	3931760	71200
4640360	3993480	3772640	3923640	2376480	3809800	4152640	851600	4290000	4068800	2237000	60680
3951680	4156640	4053400	4029400	4232200	4009720	3986120	3419240	3021240	472040	1802960	82560
4439440	4549760	4433400	4600280	4467200	4119120	4455840	4543160	4423160	4349720	4477840	83640

Negative control

Positive control

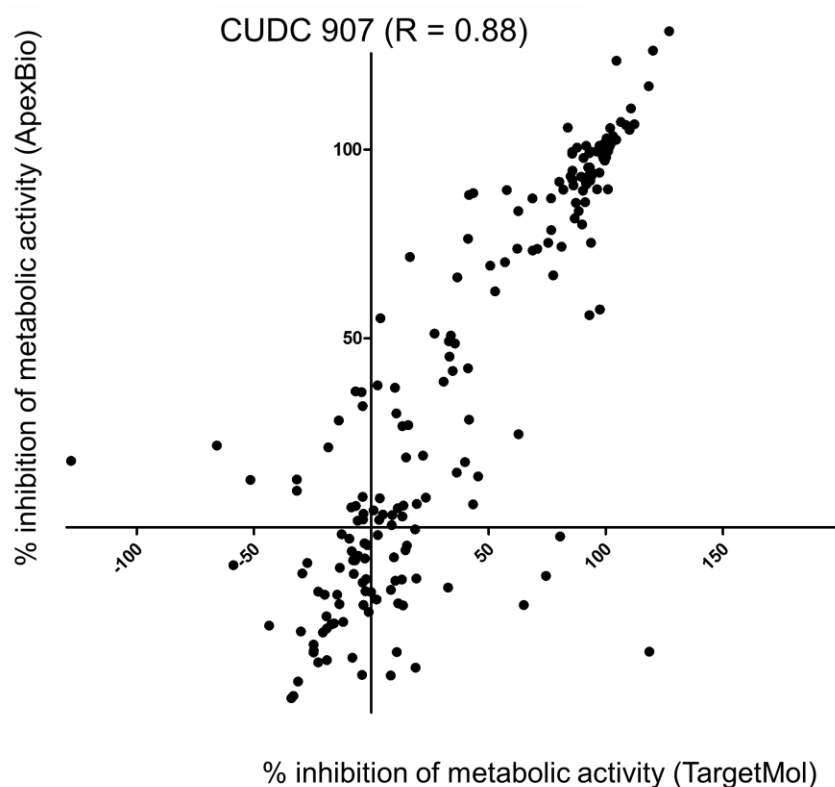
Figure 19: Raw ATPlite readout values of a representative 96-well plate from the primary screen with negative controls on the left and positive controls on the right of the plate

RESULTS

Drugs present in both libraries (Correlation coefficient values)

A subset of drugs (e.g. CUDC907, entinostat) that were part of both libraries; TargetMol and DiscoveryProbe. The percentage of inhibition of the metabolic activity values for such drugs were compared with each other and correlation coefficients were calculated. The results showed a high correlation between the percentage inhibition of metabolic activity values for drugs present in both libraries (Figure 20).

a.



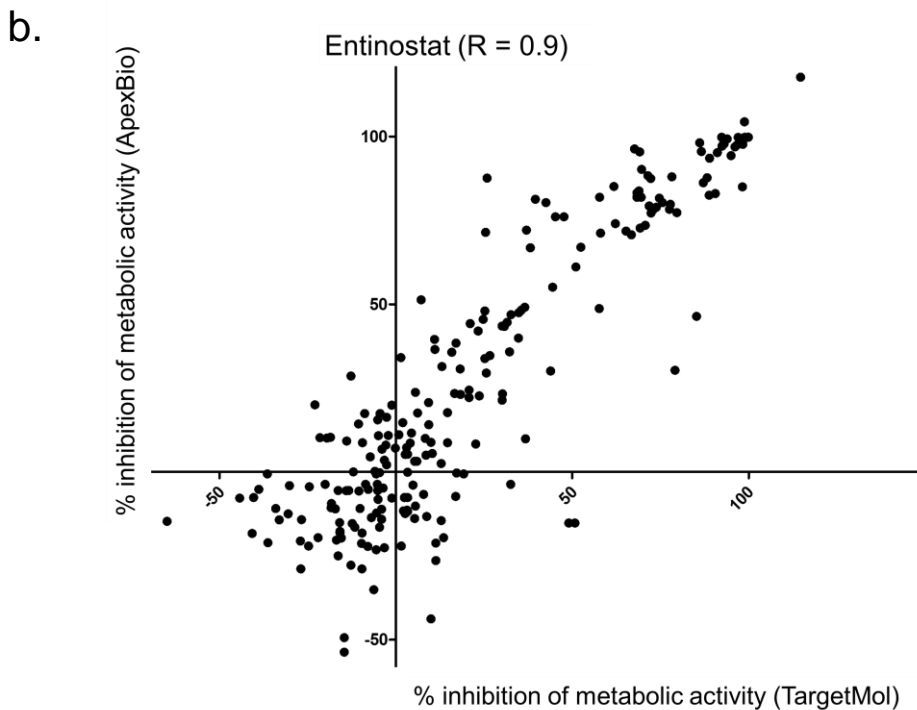


Figure 20: Scatter plots of the inhibition of the metabolic activity values (percentage of the DMSO controls) for CUDC-907 (a) and entinostat (b), which were present in both drug libraries utilized for the screen

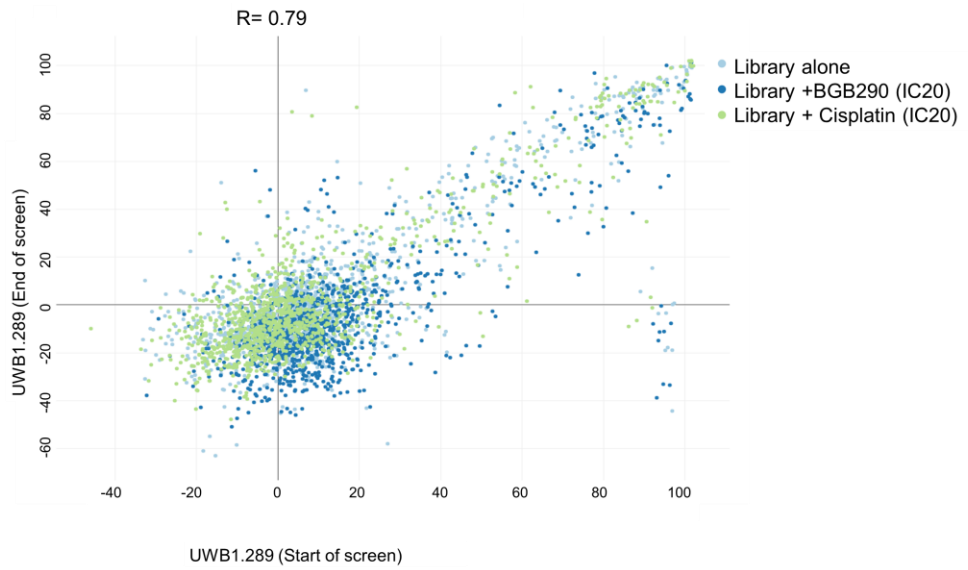
The plot was generated using the percentage of the metabolic inhibition values of the drug in the TargetMol library on the X-axis versus the ApexBio library on the Y-axis.

Comparison between the data generated at the start and at the end of the screen

In order to control for the loss of activity of the drugs over time, two ovarian carcinoma cell lines (UWB1.289 and UWB1.289+ BRCA1) were screened twice; once at the start and once at the end of the primary screen. The percentage inhibition of the metabolic activity values at the start and at the end of the primary screen were compared with each other and correlation coefficients were calculated. The results showed a very high correlation between the percentage inhibition of metabolic activity values at the start and end of the primary screen, indicating minimal to no loss of metabolic activity for the majority of the drugs (Figure 21).

RESULTS

a.



b.

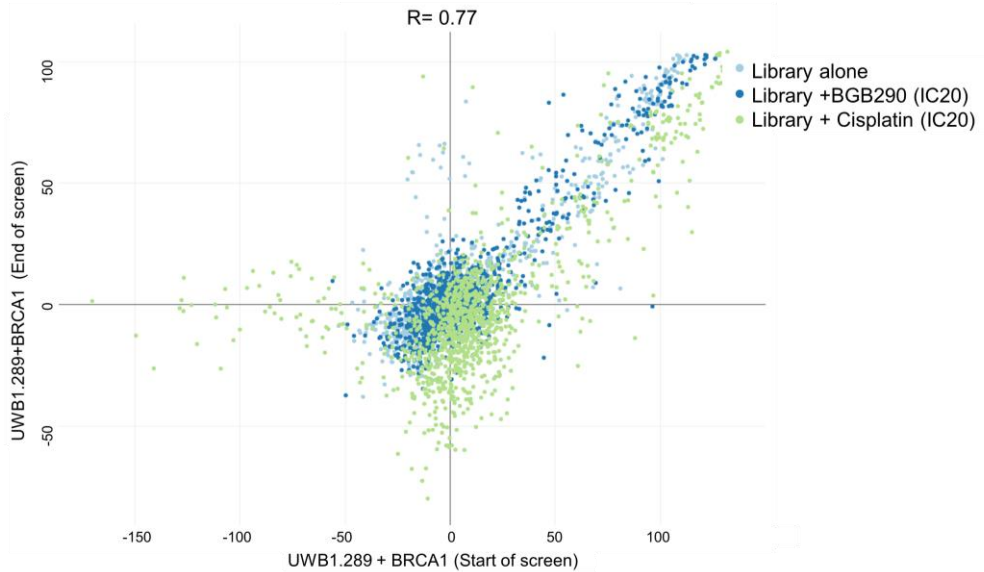


Figure 21: Scatter plots of the inhibition of the metabolic activity values (percentage of the DMSO controls) for UWB1.289 (a) and UWB1.289 + BRCA1 (b).

The plot was generated using the percentage of the metabolic inhibition values at the start of the primary screen on the X-axis versus at the end of the primary screen on the Y-axis.

Cluster dendrogram

A cluster dendrogram was generated from the primary screen data by Murat Iskar (Division of Molecular Genetics). The results showed that cells from the same tumor entities or cell types with similar characteristics clustered together, suggesting a similar response to the drugs (Figure 22).

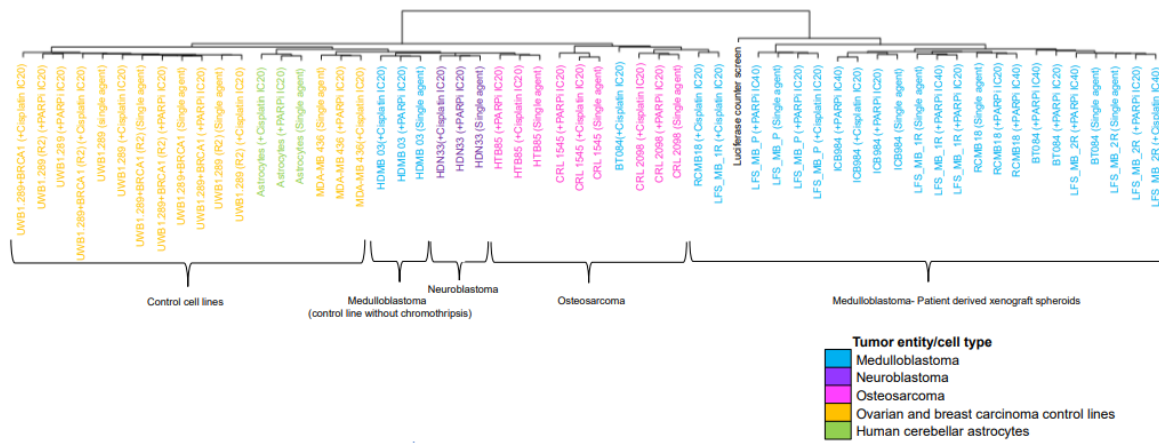


Figure 22: Cluster dendrogram of all the cell lines and spheroid models included in the primary screen

Similar response to the drugs for a given cell type or tumor entity, as shown by the cluster dendrogram constructed based on the percentage inhibition of the metabolic activity data from the primary screen.

Doubling time versus drug response

The doubling time was calculated for each cell line included in the primary screen. The doubling time was plotted against the average of the percentage inhibition of the metabolic activity to determine the doubling time dependency of the observed inhibition (Figure 23). It is important to control for this aspect when comparing the extent of the percentage inhibition of the metabolic activity between cell lines having different doubling times.

RESULTS

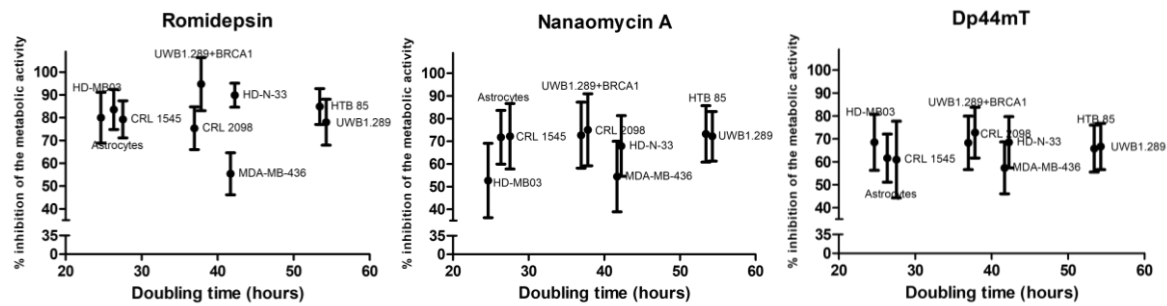


Figure 23: Doubling time (hours) of all cell lines included in the primary screen plotted against the percentage inhibition of the metabolic activity data from the primary screen for romidepsin, nanaomycin A and Dp44mT

Error bars represent SEM, n = 3 biological replicates.

Criteria to select the hits from the primary screen

Stringent thresholds were set to classify a drug as a potent hit in the primary screen. For a drug to be classified as a potent drug as a single agent, it must inhibit 50 % of the metabolic activity at a 0.5 μ M concentration. For a drug to be classified as a potential synergistic partner of either BGB290 or cisplatin, there were two criteria. First, it must show synergism with either BGB290 or cisplatin at two different concentrations. Second, it must show synergism at 0.005 μ M if at higher concentrations the single agent inhibits 100% of the metabolic activity. A shiny app was developed by Murat Iskar to analyze the data from the primary screen bioinformatically. Manual analysis and bioinformatics analysis done in parallel with the above-mentioned thresholds identified 26 drugs either potent as single drugs or potential synergistic partners of either BGB290 or cisplatin or both. Scatter plots were generated by using the shiny app to visually identify potential synergistic partners of either cisplatin or BGB290 (Figure 24).

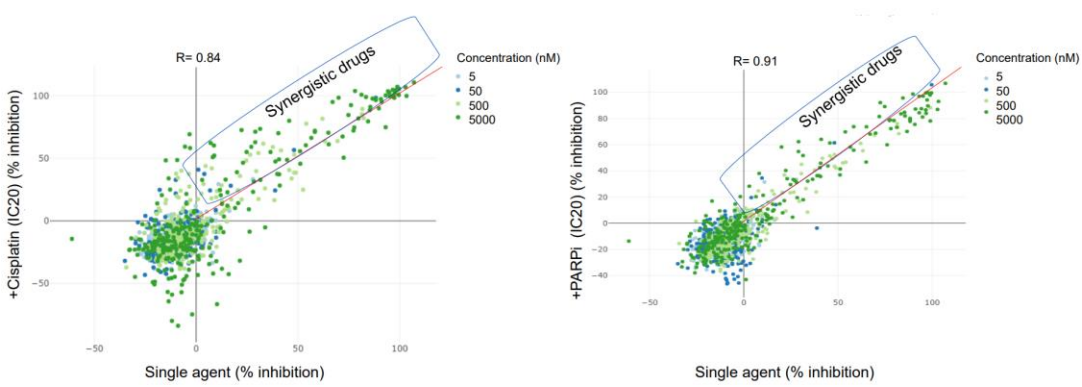


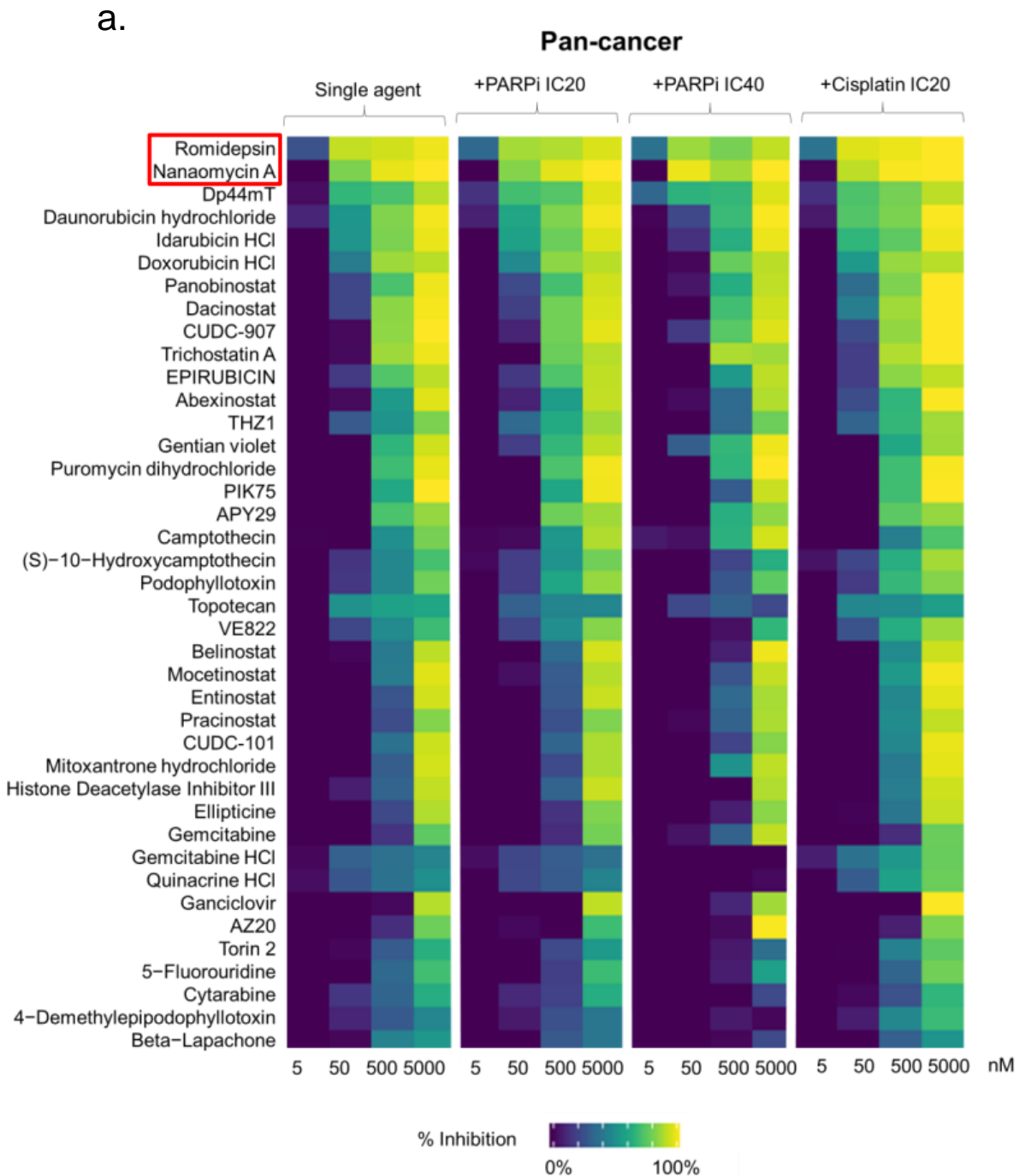
Figure 24: Scatter plots of the inhibition of the metabolic activity values (percentage of the DMSO controls) from the primary screen

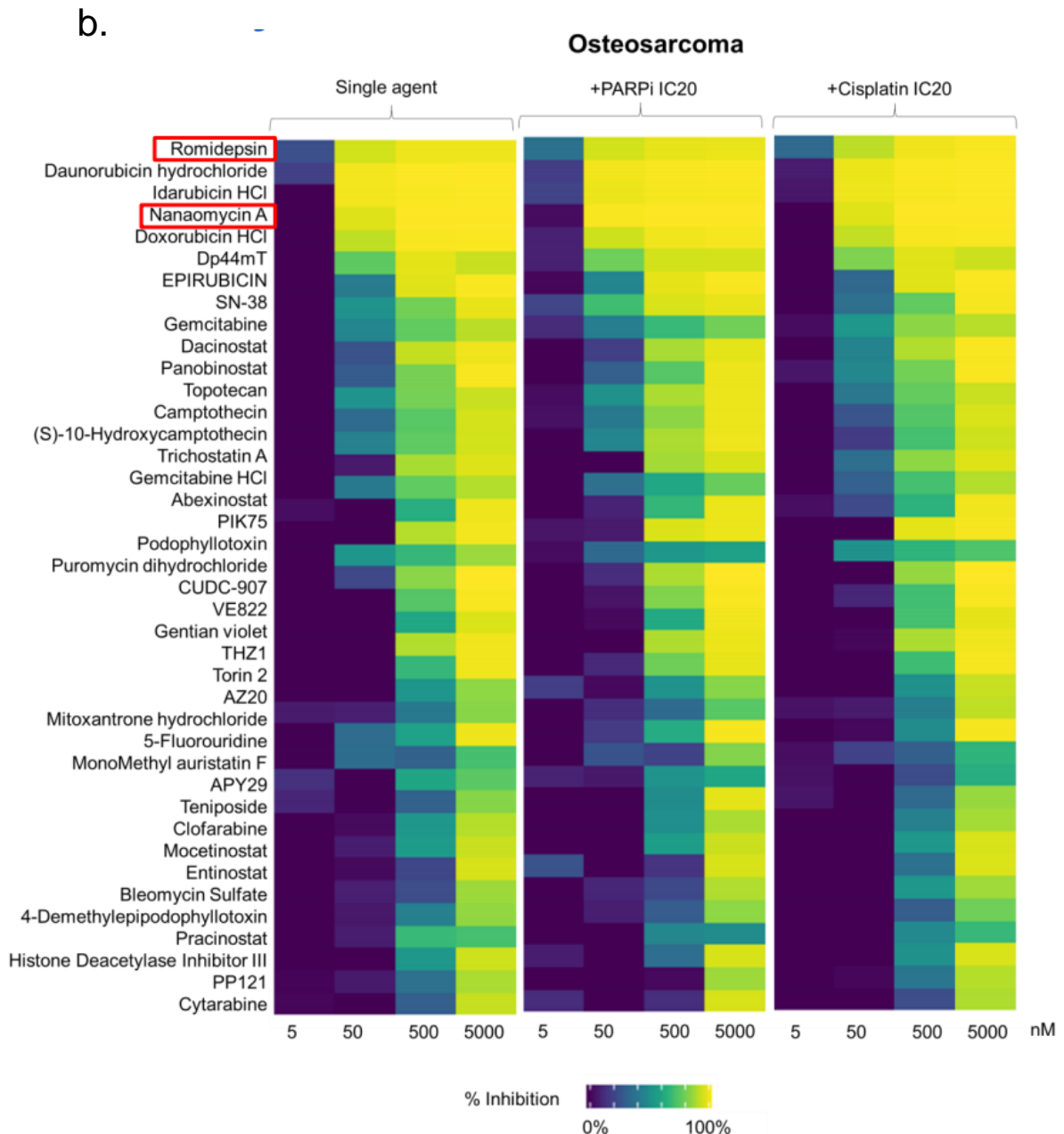
The plots were generated using the percentage of the metabolic inhibition values of the single agents on the X-axis versus the same agent with cisplatin (IC20) double treatment (left plot) or the same agent with BGB290 (IC20) double treatment (right plot) on the Y-axis.

Heat-maps from the shiny app

By using the shiny app, heat-maps were generated by selecting different criteria in order to rank drugs from the most potent to the least potent (Figure 25). On the basis of this detailed analysis of the primary screen, two drugs namely romidepsin and nanaomycin A were identified as extremely potent as single agents and also as potential synergistic partners of BGB290 or cisplatin.

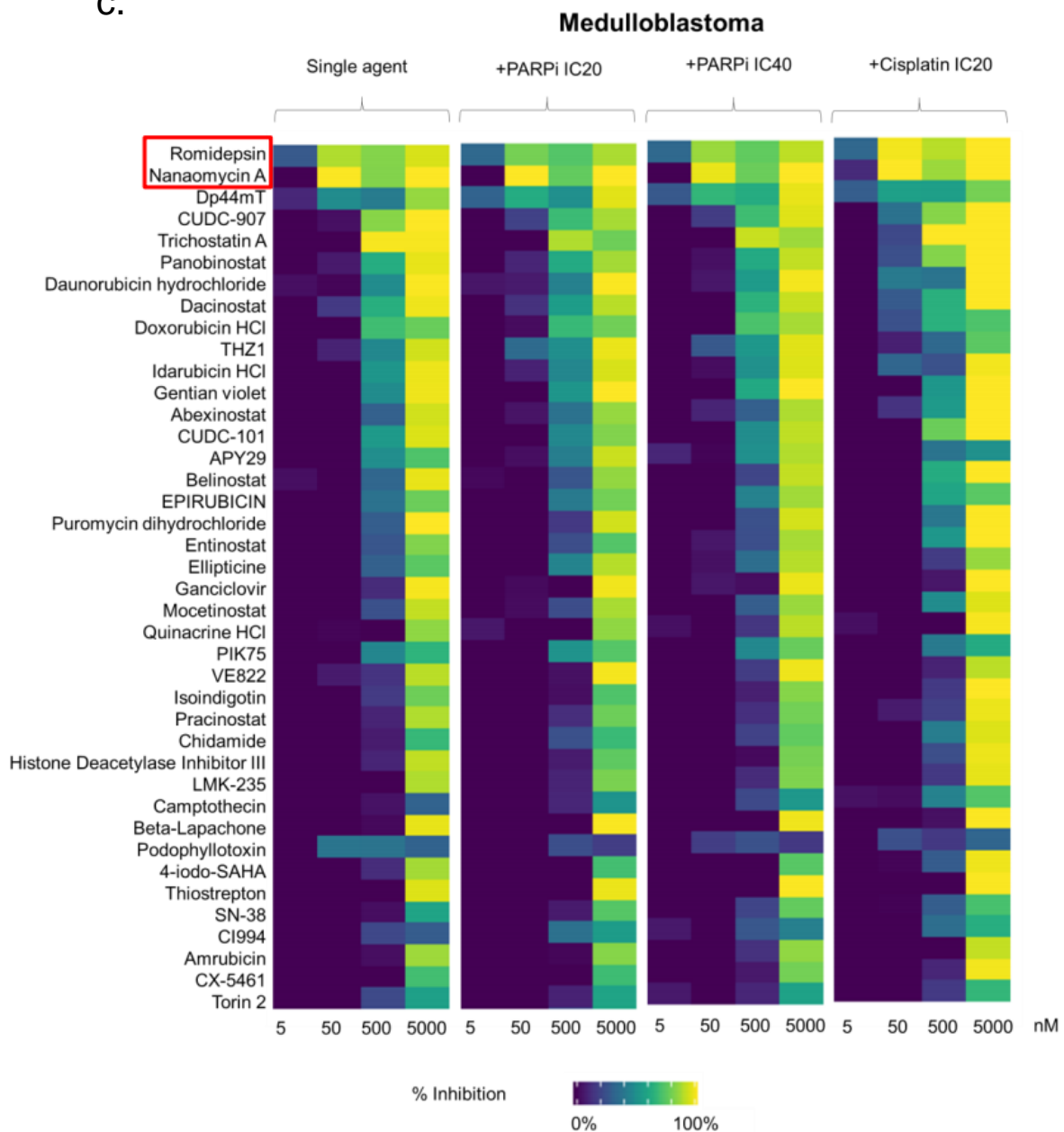
RESULTS





RESULTS

C.



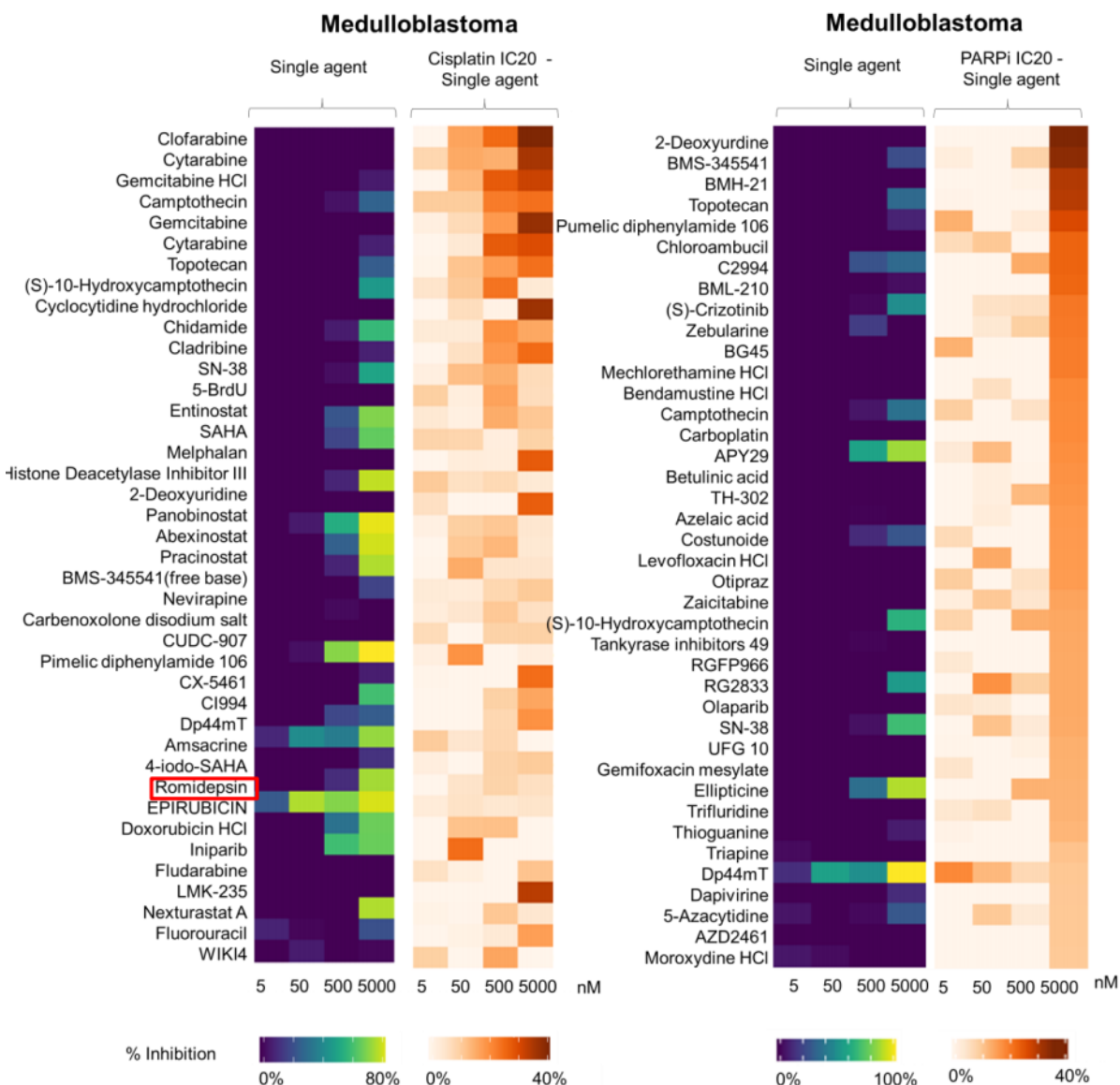


Figure 25: Analysis of the primary screen data

Heat-maps showing the top 40 hits based on the following criteria (a) Maximum overall potency using all tumor lines included in the primary screen ($n = 14$ lines, non-tumor cells were excluded). (b) Maximum overall potency focusing on osteosarcoma cell lines; KHOS-240S, SJS-1 and SaOS-2. (c) Maximum overall potency focusing on Sonic Hedgehog medulloblastoma patient-derived xenograft spheroid models ($n = 4$ lines, for the LFS_MB model only the primary tumor was included here). (a - c) Data are shown as percentages of inhibition of the metabolic activity as compared to the DMSO controls. (d) Synergy with cisplatin IC20 and synergy with BGB290 IC20 focusing on Sonic Hedgehog medulloblastoma patient-derived xenograft spheroid models.

RESULTS

Individual heat-map for romidepsin

All values for the percentage inhibition of the metabolic activity for romidepsin from the primary screen were plotted as a heat-map by Murat Iskar (Figure 26). The heat-map gives an overview for one representative candidate hit from the primary screen.

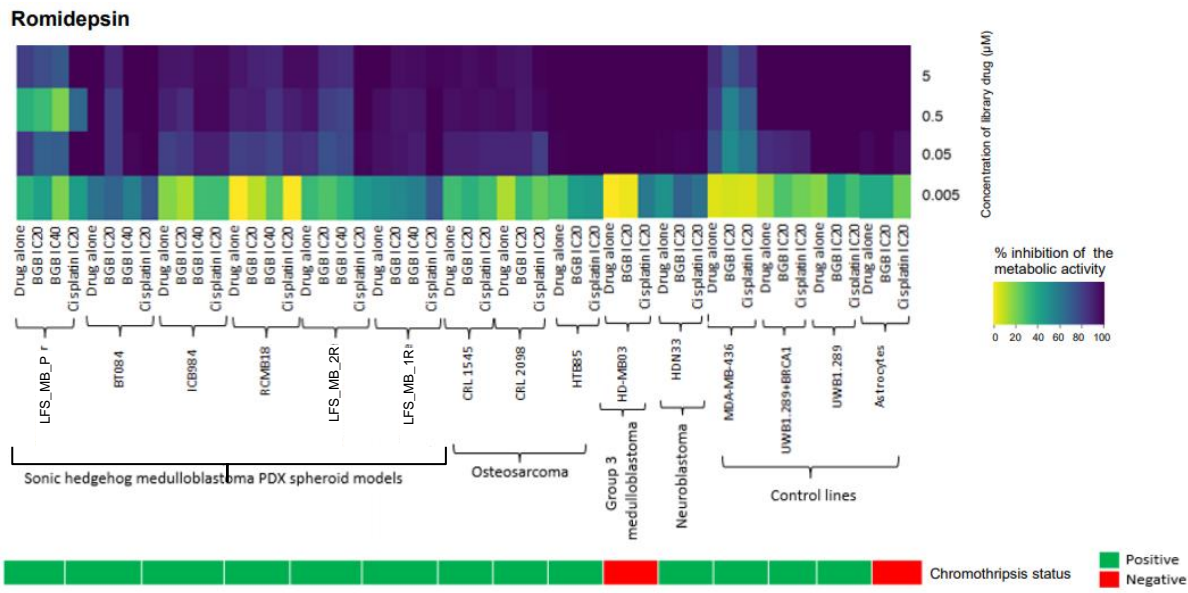


Figure 26: Heat-map showing the percentage inhibition of the metabolic activity from the primary screen for romidepsin

IC50 curves for nanaomycin A

Using the shiny app, IC50 curves for nanaomycin A were generated to compare the relative sensitivity of different cell lines and spheroid cultures towards nanaomycin A. The results showed that SHH medulloblastoma PDX models were more sensitive to nanaomycin A treatment as compared to non-SHH medulloblastoma cell lines and healthy human astrocyte control cells (Figure 27).

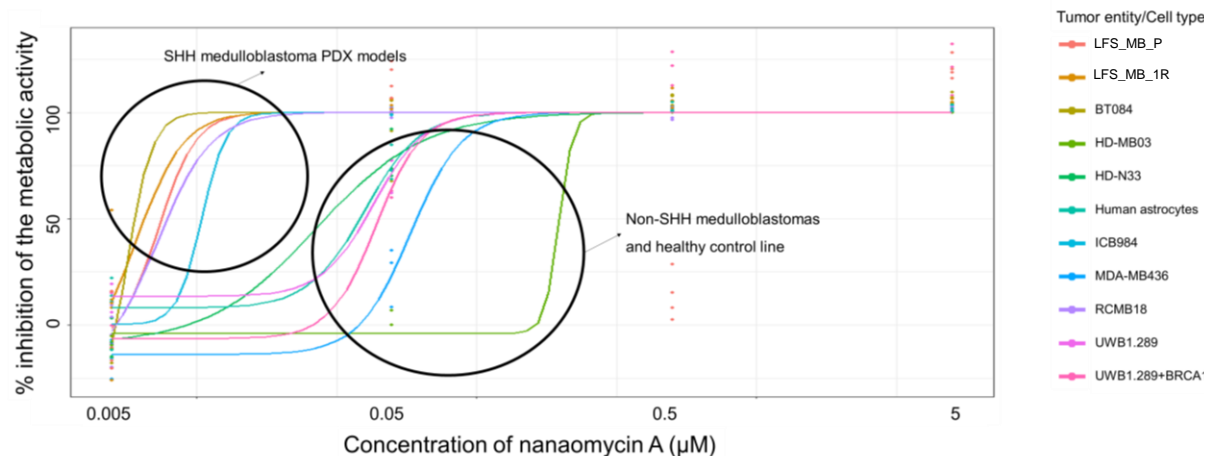


Figure 27: IC50 curves of nanaomycin A for cell lines and spheroid models in the primary screen

SHH medulloblastoma PDX models are more sensitive to nanaomycin A treatment in comparison to non-SHH medulloblastoma and healthy control lines. This suggests a potential tumor entity specific inhibition of metabolic activity for nanaomycin A.

3.4 Secondary screen

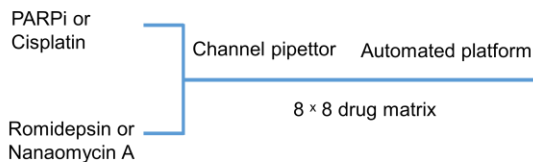
3.4.1 Secondary screen set-up

The top two hits from the primary screen, romidepsin and nanaomycin A, were selected for the secondary screen. The purpose of the secondary screen was to confirm the additive or synergistic interaction of romidepsin or nanaomycin A with BGB290 or cisplatin. For this purpose, 8 different concentrations of all four drugs were selected for each cell line or spheroid model based on the IC50 data. The criteria were that the highest concentration should inhibit 80% of the metabolic activity of a specific cell line or spheroid model while the lowest concentration could be ineffective as a single drug, to identify additive or synergistic effects. Two or three intermediate concentrations within the range of 0% to 80% of inhibition of the metabolic activity were also included when possible. Once concentrations were selected, 8×8 matrices of BGB290 or cisplatin with romidepsin or nanaomycin A were prepared in 96 well plates by using the automated platform at the EMBL screening facility. We achieved four types of sets; BGB290 with romidepsin, BGB290 with nanaomycin A, cisplatin with romidepsin and cisplatin with nanaomycin A. Cells from different tumor entities and spheroid models were seeded in the wells of these plates at such a concentration that five days after seeding, wells would reach a 90-95 % confluence. After five days of incubation, the ATP substrate solution was added to the wells and the metabolic inhibition values relative to DMSO controls were calculated. Data were then evaluated through quality control inspections and analyzed.

RESULTS

Day 1: Cells deposition and drug addition

(1)



Set 1: PARPi +
Romidepsin

(2)

Set 2: PARPi +
Nanaomycin A

Set 3: Cisplatin +
Romidepsin

Set 4: Cisplatin +
Nanaomycin A

Day 5: Read-out (metabolic activity)

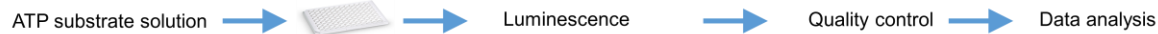
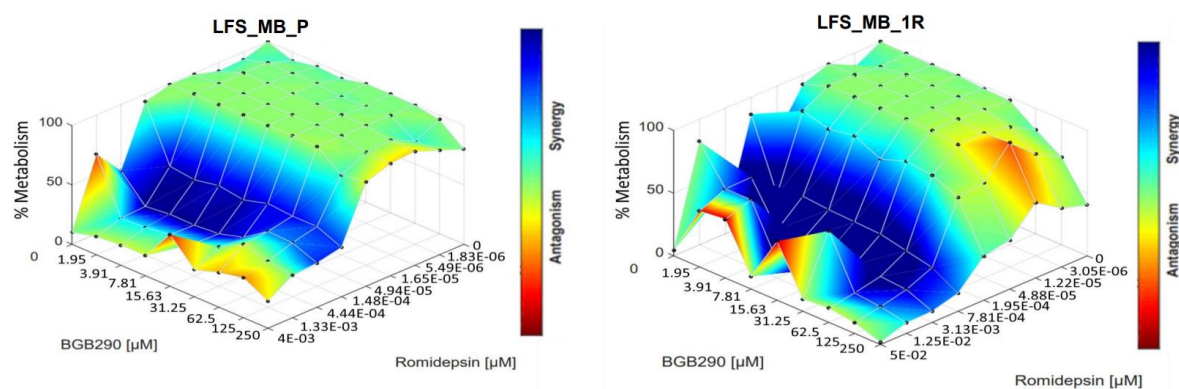


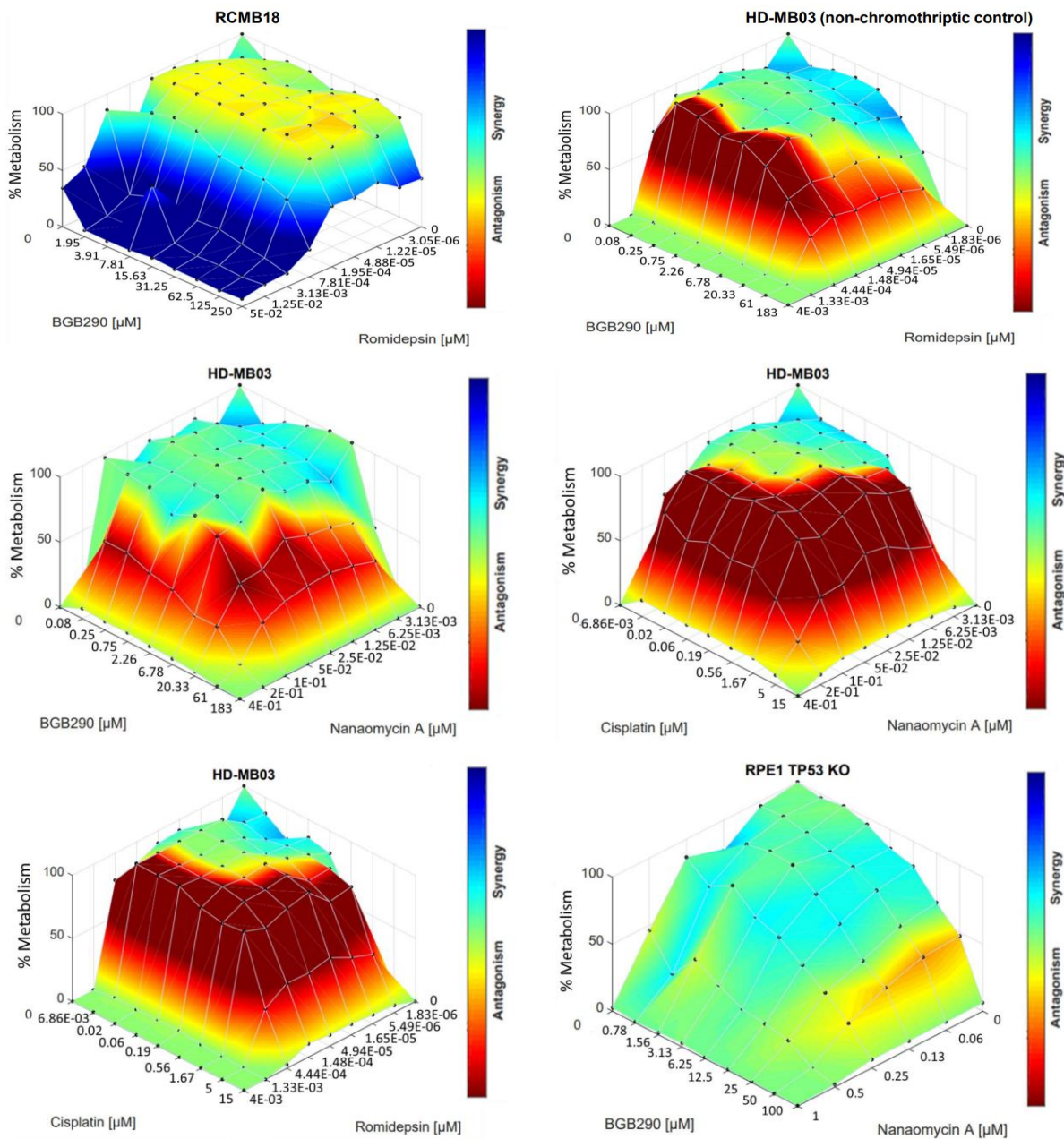
Figure 28: Schematic representation of the secondary screen strategy

PARP inhibitor or cisplatin titrated against romidepsin or nanaomycin A in an 8 x 8 matrix experiment followed by cells seeding in 96 well plates. 96 hours after cell seeding, the read-out for the metabolic activity of the cells was done, followed by quality control and data analysis.

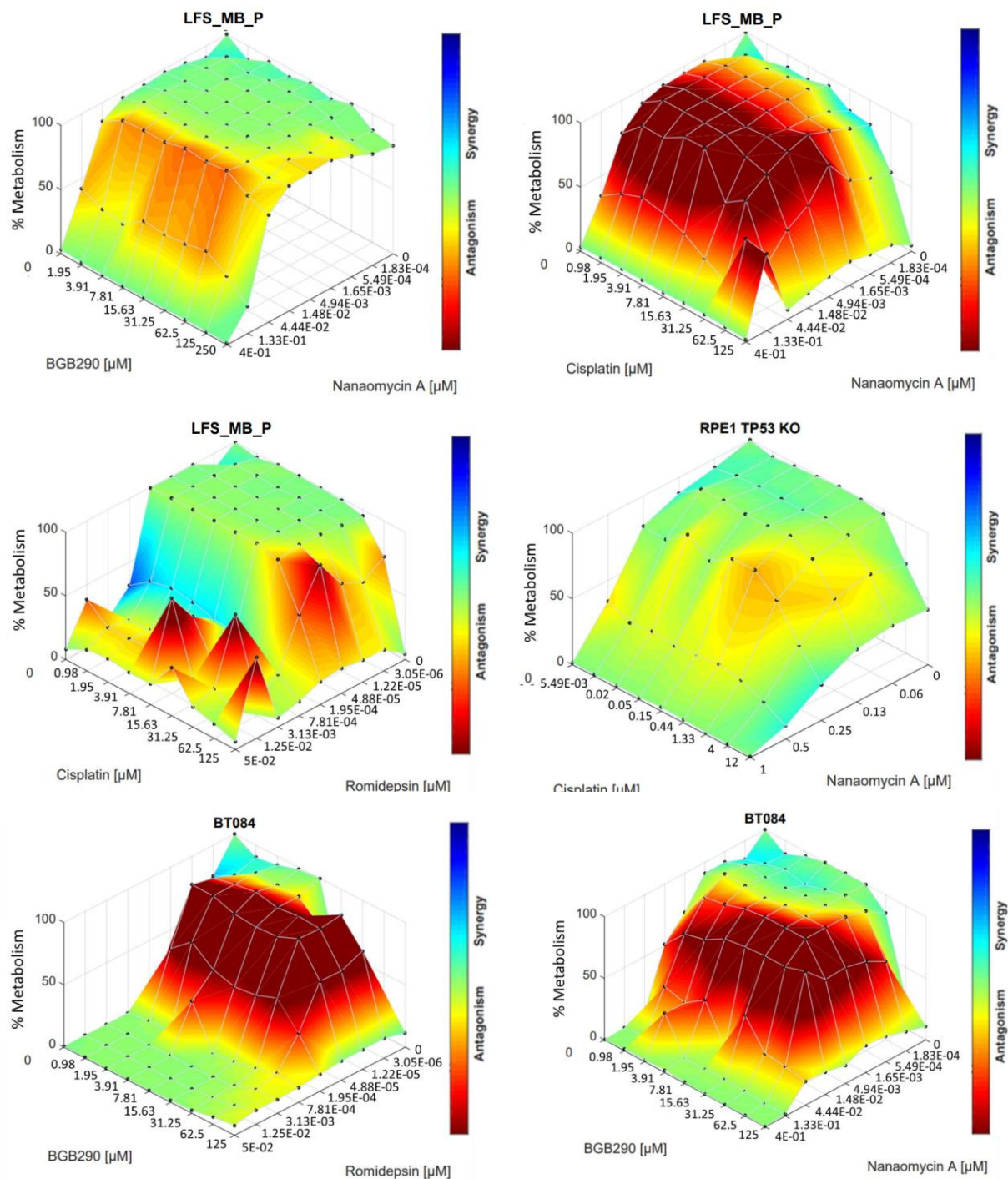
3.4.2 Analysis of the secondary screen data

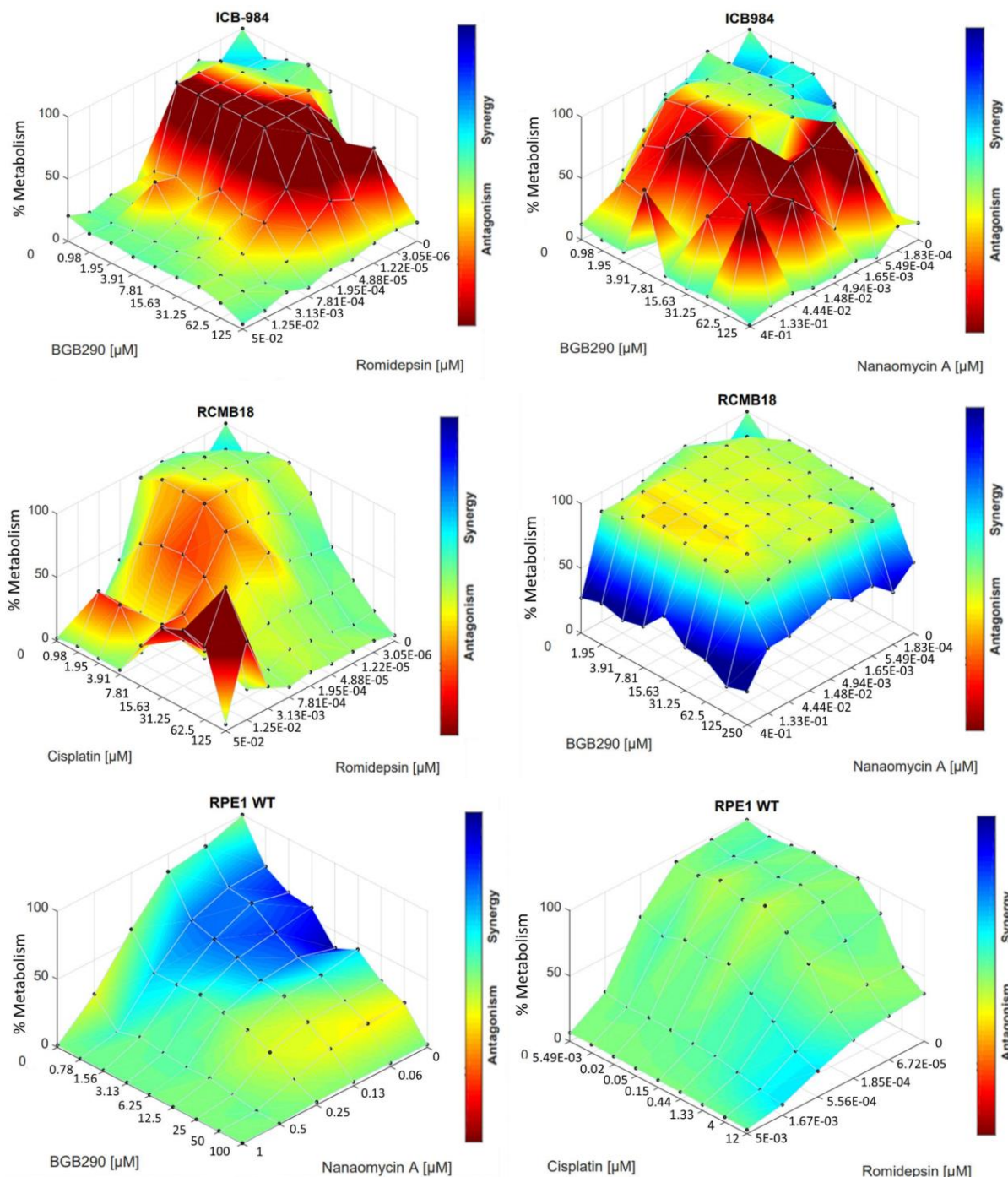
Secondary screen data were analyzed using the combenefit software. The results revealed a strong synergistic interaction between romidepsin and BGB290 in three SHH medulloblastoma spheroid models with chromothripsis (LFS_MB_P, LFS_MB_1R and RCMB18). In contrast, romidepsin and BGB290 combination treatment resulted into an antagonistic interaction in the HD-MB03 non-chromothriptic control cell line. All other combinations showed antagonism except for BGB290 and nanaomycin A displaying additive or synergistic effects for DAOY, RPE1 WT and RPE1 TP53KO cell lines and a synergistic interaction at only highest concentrations of both drugs for RCMB18 (Figure 29).



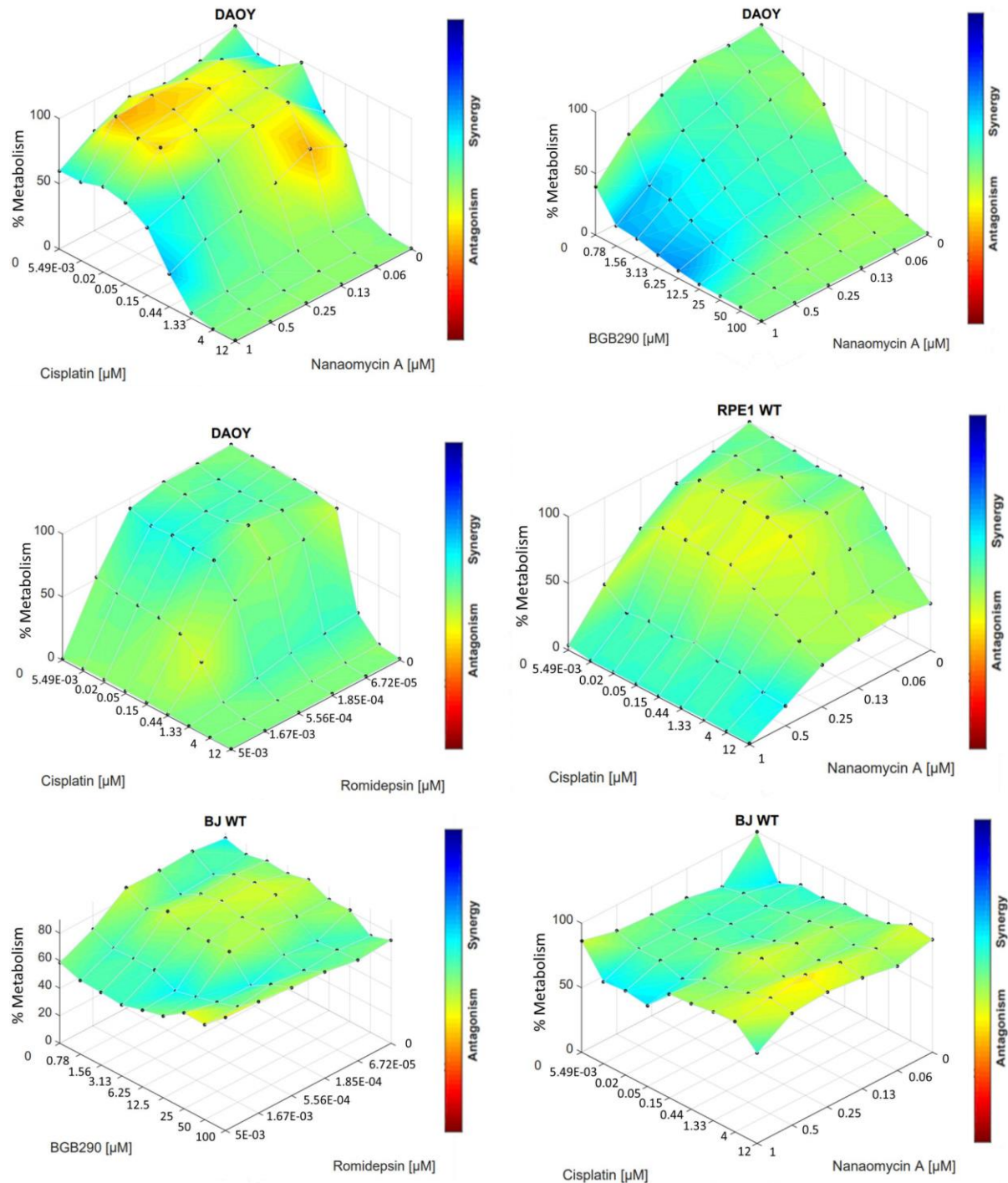


RESULTS





RESULTS



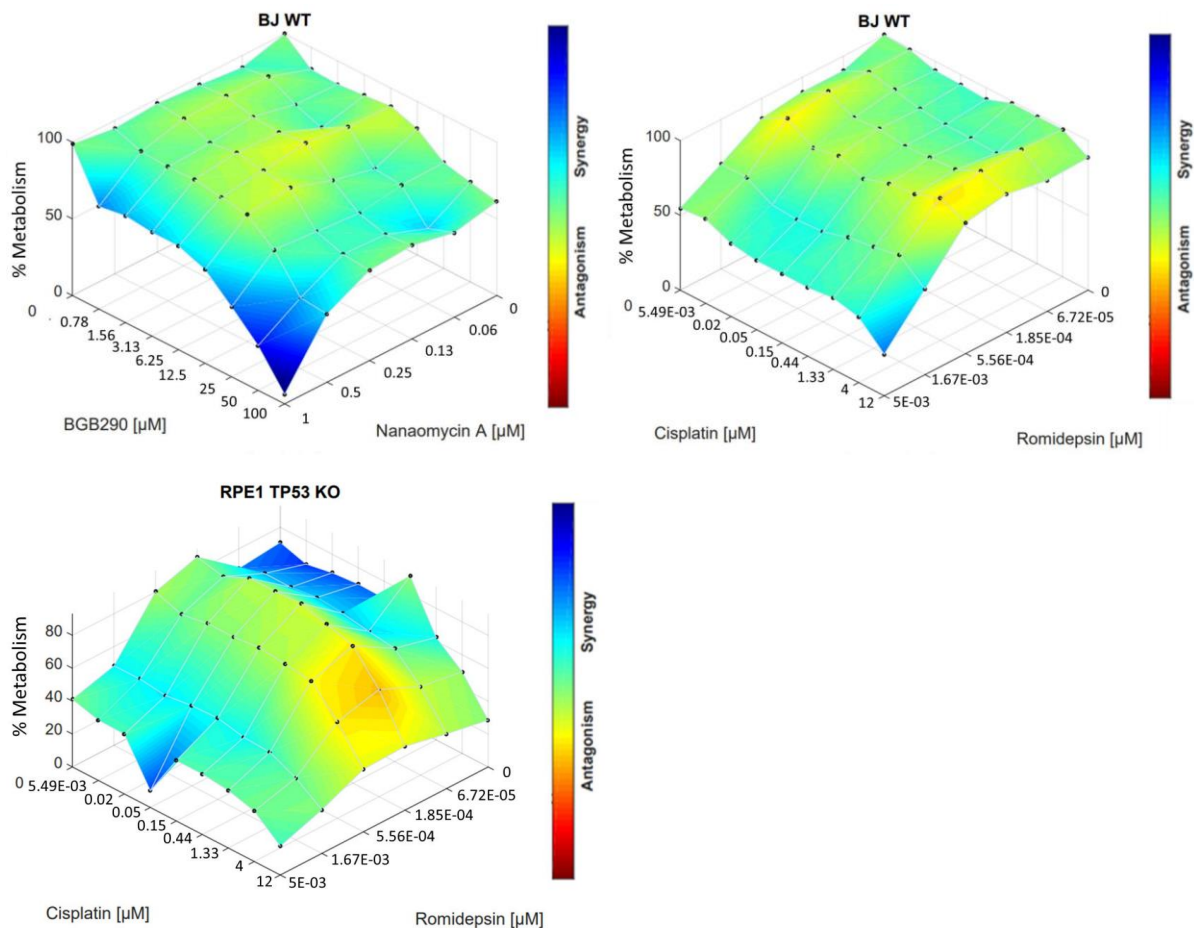


Figure 29: Loewe surface plots generated using the combenefit software showing synergistic and antagonistic drug interactions

Synergy and antagonism are mapped to dose response curves using the average of the percentage of the metabolic activity values of 3 replicates per data point. Technical replicates for patient derived xenograft spheroid models and HD-MB03 cell line. Biological replicates for all other cell models.

3.5 Reduction in Spheroid Growth

To phenotypically confirm the findings of the secondary screen, the effect of romidepsin and BGB290 combinatorial treatment on the spheroid growth were observed under the brightfield microscope for LFS_MB_P (Figure 30) and LFS_MB_1R (Figure 31) spheroid models. The results confirmed the findings from the metabolic activity measurements, with spheroid growth adversely affected by combinatorial treatment as compared to control and single drug treatments.

RESULTS

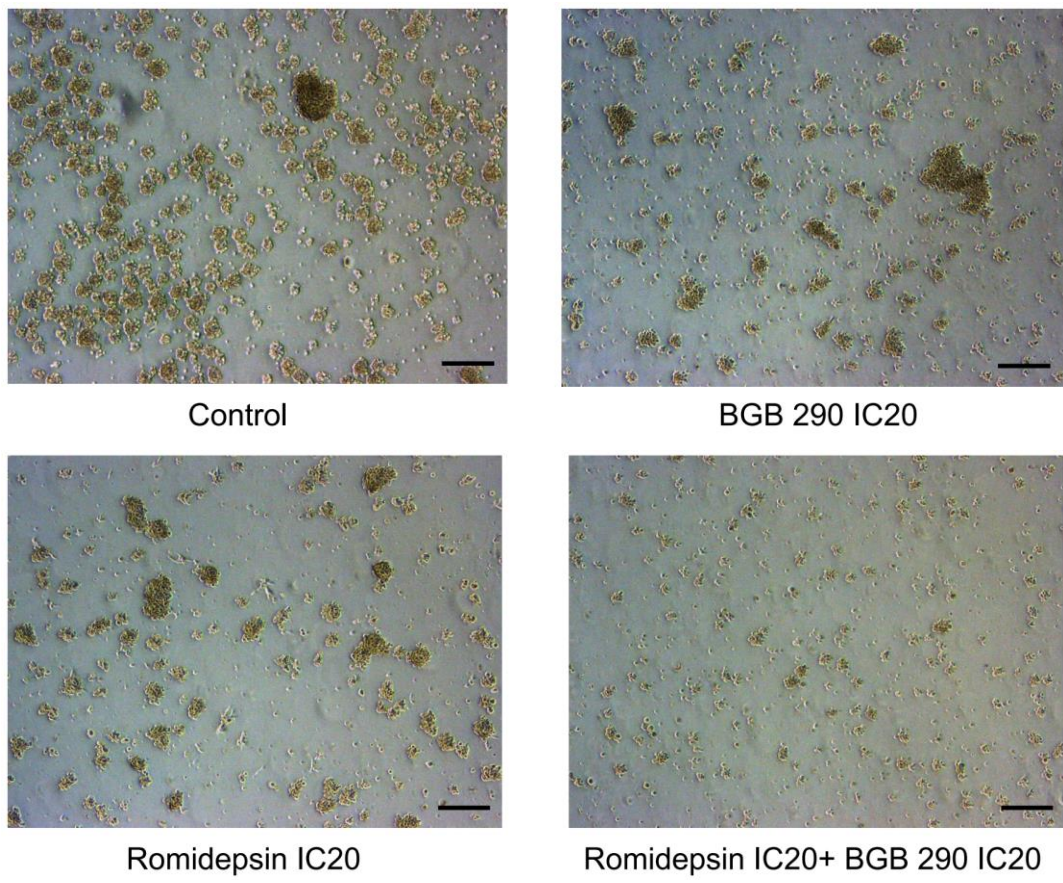
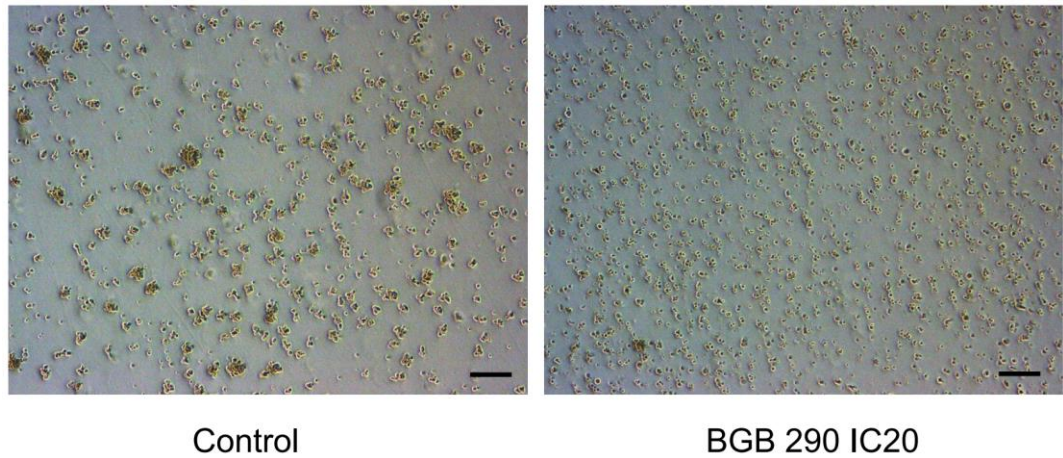


Figure 30: Bright-field images of spheroid model LFS_MB_P (Sonic Hedgehog medulloblastoma model, primary tumor) after 24 hours of drug treatment

Scale bar in each panel: 100 μm .



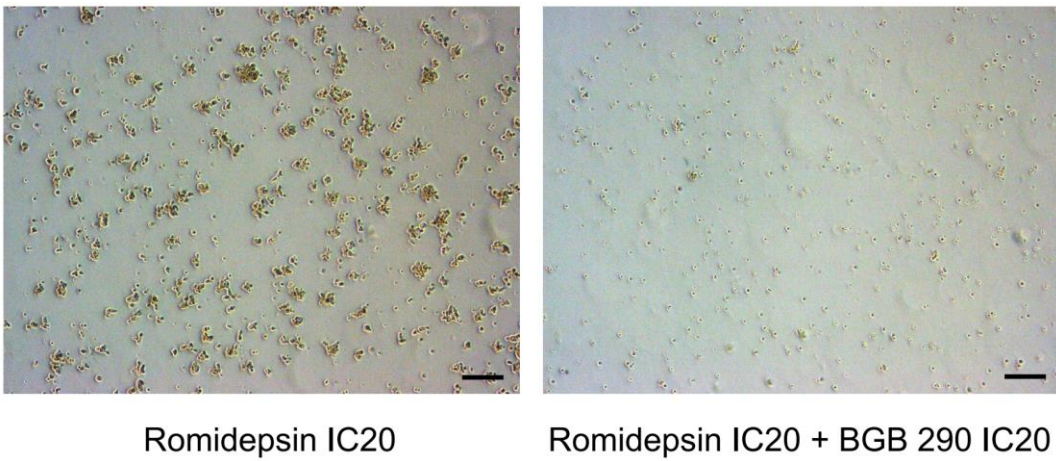


Figure 31: Bright-field images of spheroid model LFS_MB_1R (Sonic Hedgehog medulloblastoma model, first relapse) after 24 hours of drug treatment

Scale bar in each panel: 100 μ m.

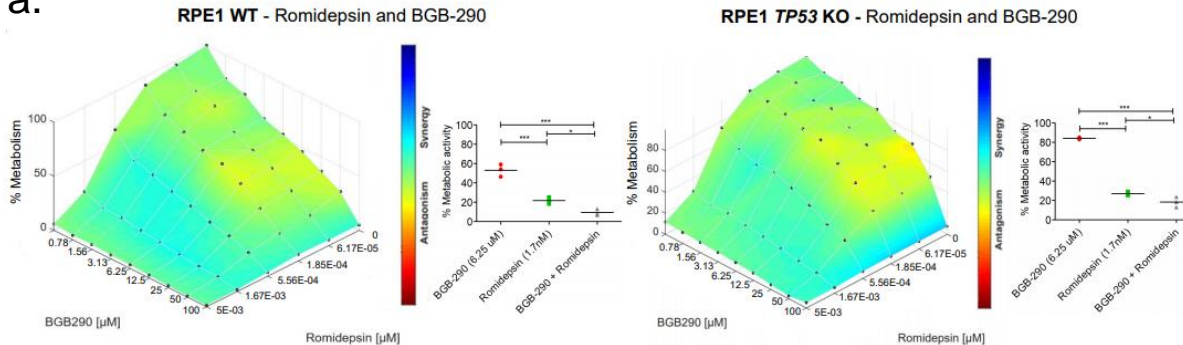
3.6 Functional Assays

3.6.1 Synergy effect and relationship to the *TP53* status

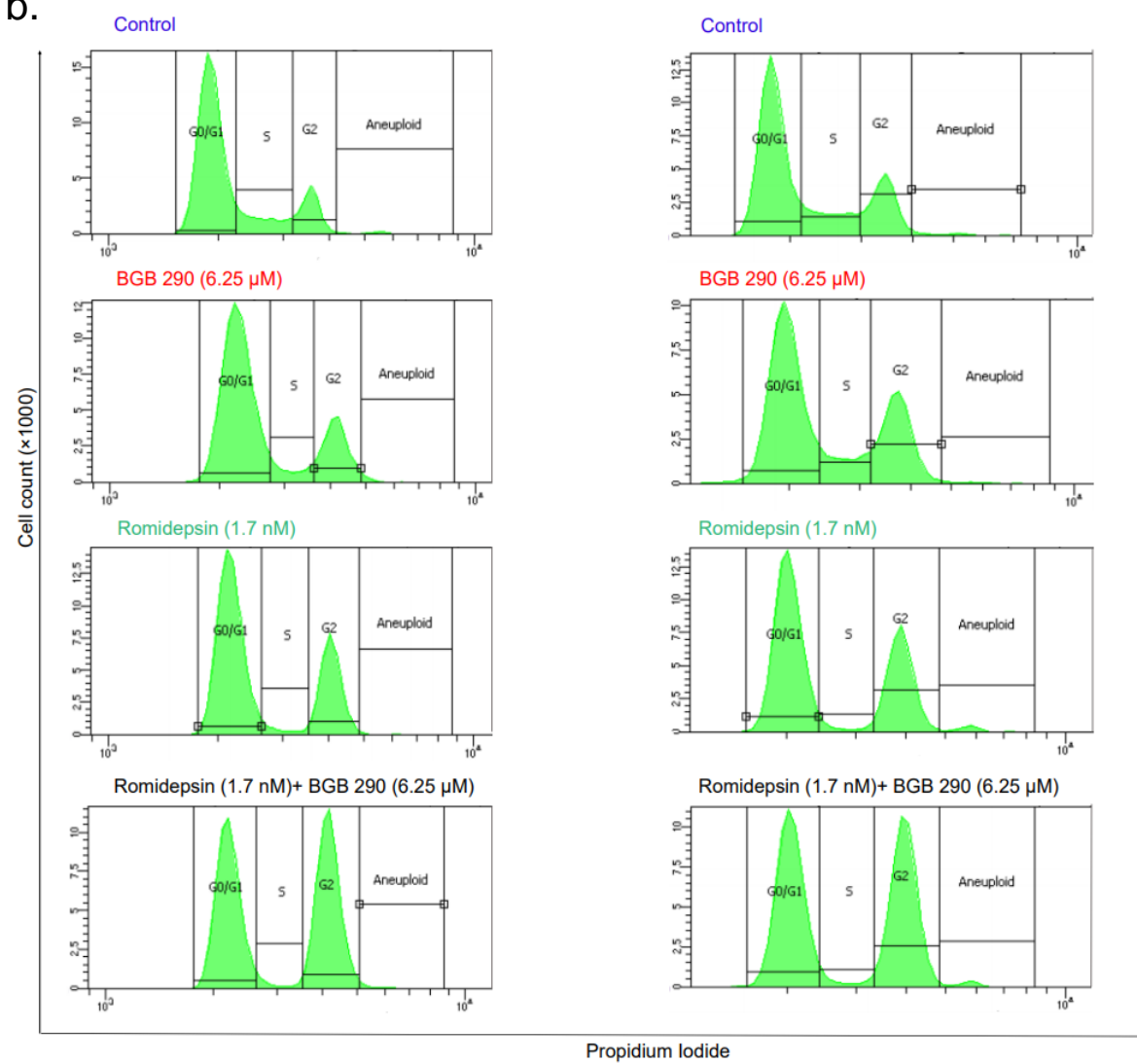
As chromothripsis is known to be highly associated with *TP53* loss of function [19], the dependency of romidepsin and BGB290 synergistic or additive effect on the *TP53* status was determined. For this purpose, two cell lines, namely Retina Pigmented Epithelium 1 (RPE1) cells with wild type *TP53* (RPE1 WT) and RPE1 with *TP53* knock out (RPE1 *TP53* KO) were used. The two cell lines were subjected to 8×5 matrix experiments which revealed an additive effect between romidepsin and BGB290. RPE1 WT and RPE1 *TP53* KO cell lines were then subjected to cell cycle analysis and apoptosis experiments. Cell cycle analysis experiments revealed a strong G2 arrest in both cell lines upon romidepsin and BGB290 combination treatment, which significantly differed from control or single drug treatment. The G2 phase cell fractions of the RPE1 WT and RPE1 *TP53* KO cell lines were compared. The results revealed a *TP53* independent effect of the romidepsin and BGB290 combinatorial treatment. Furthermore, the results of the apoptosis experiment revealed that RPE1 WT and RPE1 *TP53* KO cell lines do not undergo apoptosis at the tested drug concentrations either alone or in combination (Figure 32).

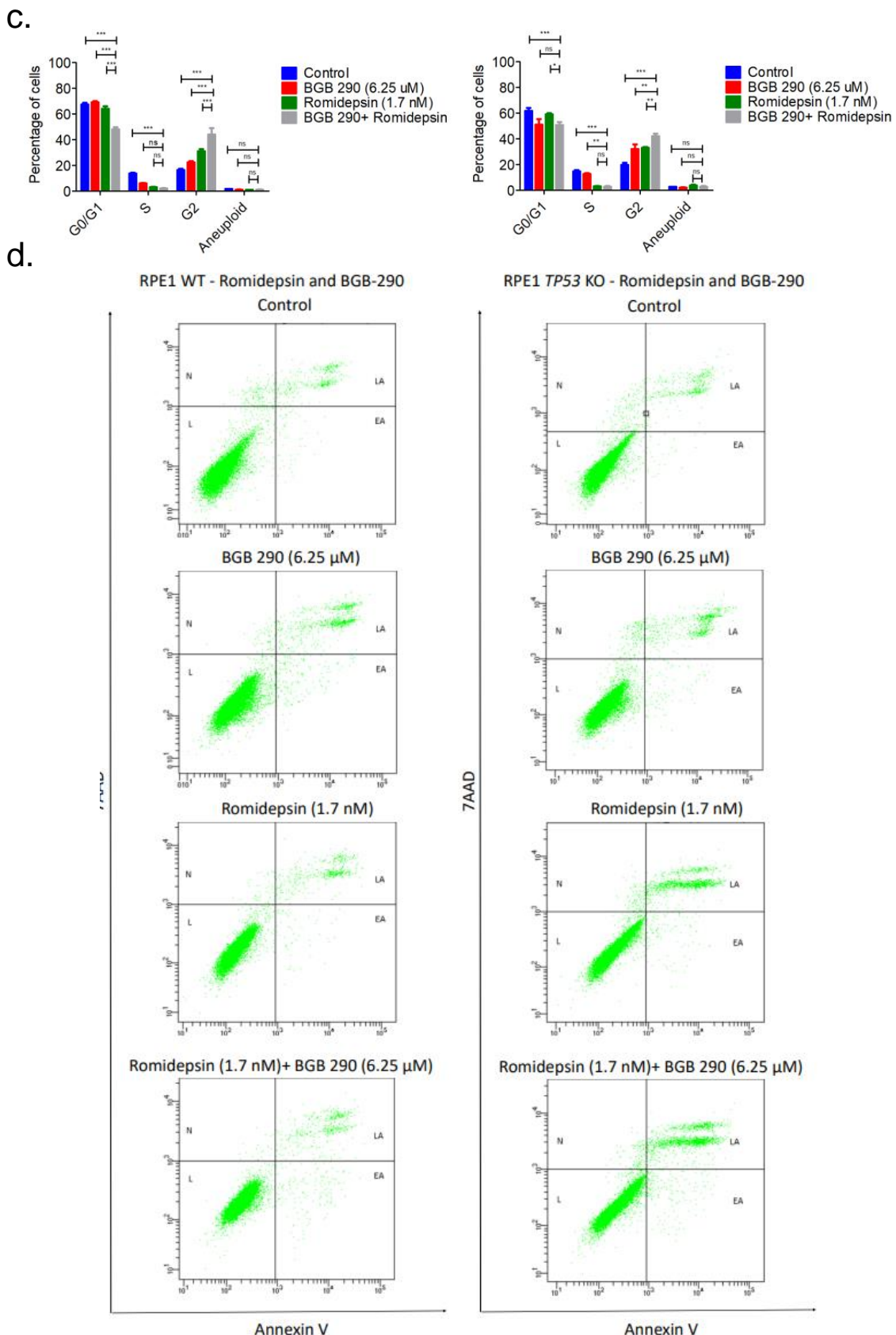
RESULTS

a.



b.





RESULTS

e.

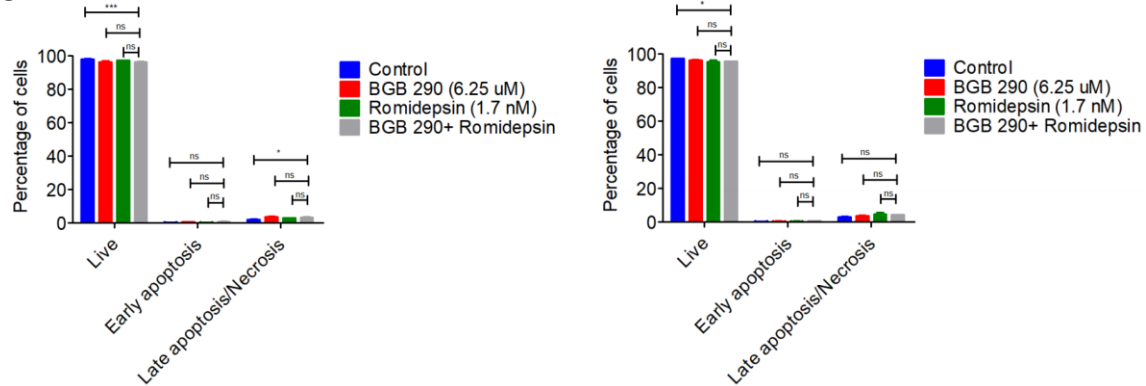
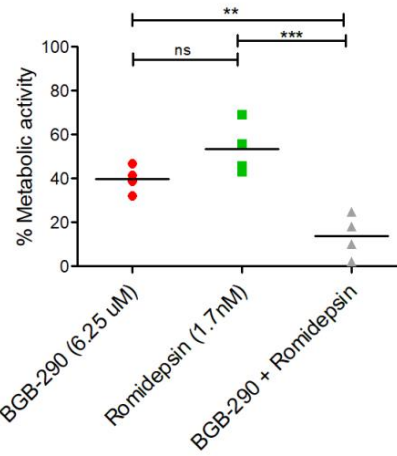
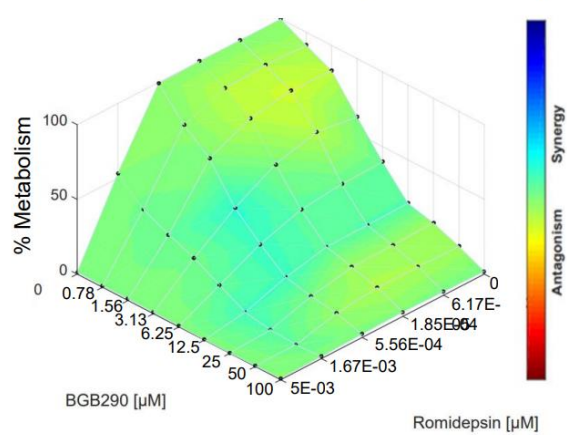
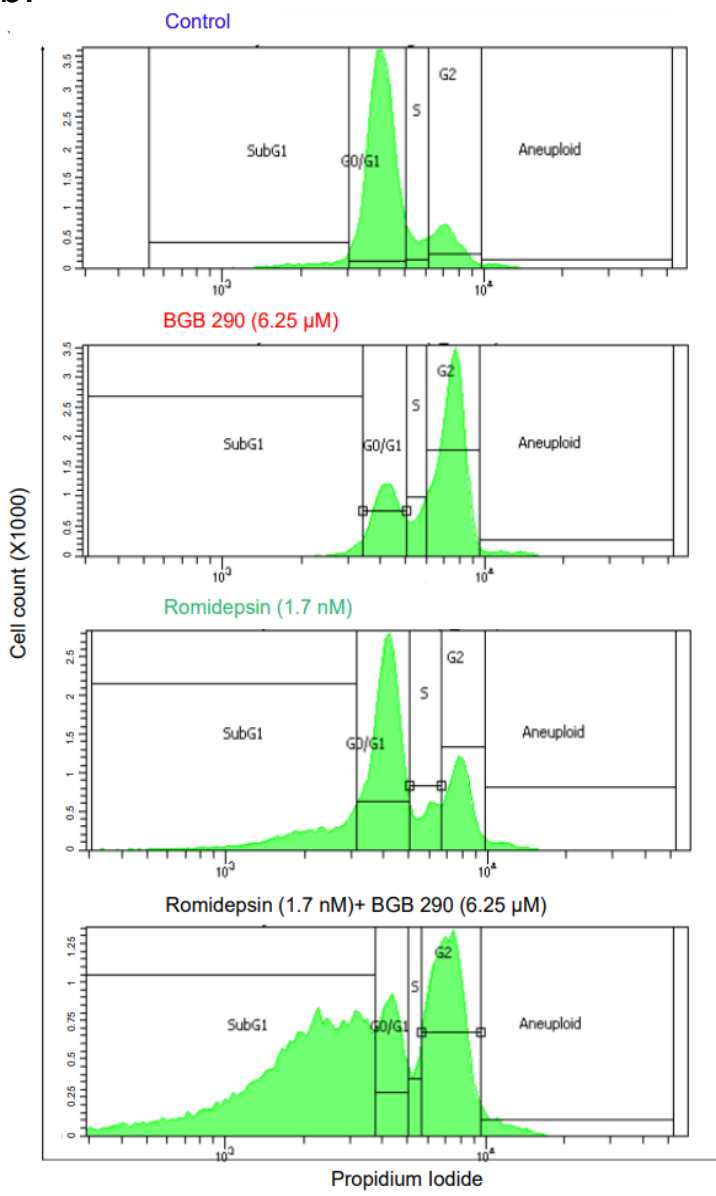
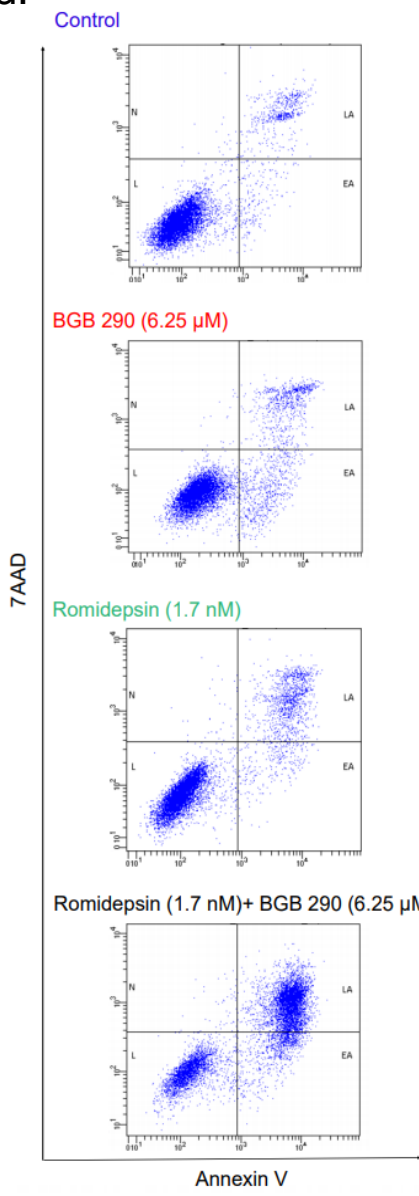


Figure 32: Cell cycle arrest of RPE1 WT and RPE1 TP53 KO cells upon combination treatment with romidepsin and BGB290

(a) Loewe surface plot for RPE1 WT cells (on the left) and TP53 KO RPE1 cells (on the right). Plots were generated using the combbenefit software. Synergy and antagonism are plotted on the dose-response values using the average percentages of the metabolic activity values for 3 biological replicates per data point. Dot plots on the right of each Loewe surface plot show the metabolic activity values (as percentages of the DMSO controls) for 3 biological replicates. Statistical significance was tested by one-way ANOVA followed by Tukey's Multiple Comparison Test (*, p < 0.05). Horizontal lines represent the means, n=3 biological replicates. (b) Cell cycle analysis of RPE1 WT cells (on the left) and RPE1 TP53 KO cells (on the right) using propidium iodide. Cells were treated with drugs at the indicated concentrations for 48 hours before the flow cytometry analysis. Histograms are representative of three biological replicates. (c) Bar graphs showing the quantitative distribution of RPE1 WT cells (on the left) and TP53 KO RPE1 cells (on the right) in the different cell cycle phases. Statistical significance was tested using two-way ANOVA followed by Bonferroni post-test, *** p < 0.001, ** p < 0.01, * p < 0.05, non-significant (ns) p > 0.05. Error bars represent SEM, n = 3 biological replicates. (d) RPE1 WT cells (on the left) and TP53 KO RPE1 cells (on the right) were stained by FITC-annexin V and 7AAD to quantify apoptotic fractions. Cells were treated with drugs at the indicated concentrations for 48 hours and subjected to flow cytometry analysis. Dot plots are representative of three biological replicates. (e) Bar graph showing the quantitative distribution of RPE1 WT cells (on the left) and TP53 KO RPE1 cells (on the right) as living, early apoptotic and late apoptotic/ necrotic. Statistical significance was tested by two-way ANOVA followed by Bonferroni post-test, *** p<0.001, ** p<0.01, * p<0.05, ns p>0.05. Error bars represent SEM, n = 3 biological replicates.

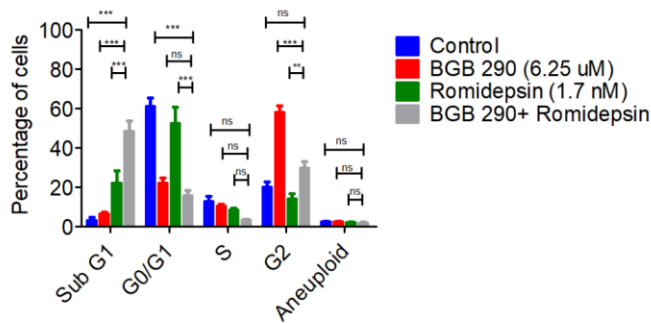
3.6.2 Cell cycle arrest and apoptosis in DAOY cells

Functional assays were performed on the DAOY cell line which is a medulloblastoma chromothriptic cell line. DAOY cells subjected to 8 × 5 matrix experiments revealed an additive effect between romidepsin and BGB290. DAOY cells were then subjected to cell cycle analysis and apoptosis experiments. Cell cycle analysis experiments revealed a strong G2 phase arrest along with a SubG1 population in DAOY cells upon romidepsin and BGB290 combination treatment, which significantly differed from control or single drug treatment. Quantification of cells in the different phases of the cell cycle confirmed a strong G2 phase arrest and induction of a SubG1 population. The results of the apoptosis experiment confirmed the cell cycle analysis experiment. These results revealed the induction of apoptosis upon romidepsin and BGB290 combination treatment (Figure 33).

a. DAOY - Romidepsin and BGB-290**b.****d.**

RESULTS

C.



e.

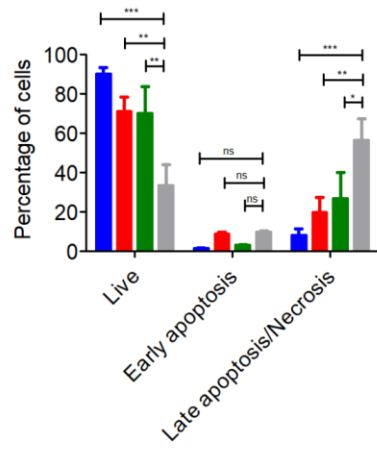


Figure 33: Cell cycle arrest and apoptosis of DAOY cells upon combination treatment with romidepsin and BGB290

(a) Loewe surface plot for DAOY cells. The plot was generated using the combbenefit software. Synergy and antagonism are plotted on the dose-response values using the average of the metabolic activity values (as percentages of the DMSO controls) for 3 biological replicates per data point. Dot plot on the right of the Loewe surface plot shows the metabolic activity for 3 biological replicates at the indicated drug concentrations. Statistical significance was tested by one-way ANOVA followed by Tukey's Multiple Comparison Test (*, p < 0.05). Horizontal lines represent the means, n = 3 biological replicates. (b) Cell cycle analysis of DAOY cells using propidium iodide. Cells were treated with drugs at the indicated concentrations for 48 hours and subjected to flow cytometry analysis. Histograms are representative of three biological replicates. (c) Bar graph showing the quantitative distribution of DAOY cells in the different cell cycle phases. Statistical significance was tested by two-way ANOVA followed by Bonferroni post-test, *** p<0.001, ** p<0.01, * p<0.05, ns p>0.05. Error bars represent SEM, n=3 biological replicates (ns = non-significant). (d) Apoptotic fractions in DAOY cells were analyzed by FITC-annexin V and 7AAD stains. Cells were treated with drugs at the indicated concentrations for 48 hours and subjected to flow cytometry analysis. Dot plots are representative of three biological replicates. (e) Bar graph showing the quantitative distribution of DAOY cells as living, early apoptotic and late apoptotic/ necrotic. Statistical significance was tested by two-way ANOVA followed by Bonferroni post-test, *** p<0.001, ** p<0.01, * p<0.05, ns p>0.05. Error bars represent SEM, n = 3 biological replicates.

3.6.3 Visualization of the mitotic cells

The effect of the romidepsin and BGB290 combination treatment on the mitotic activity of DAOY cells was visualized by acetyl- α -tubulin and phospho H3 immunostaining done by Rithu Kumar. Quantification of the data revealed that the number of mitotic cells upon romidepsin and BGB290 combination treatment was significantly lower than in the control cells, suggesting an adverse effect of the combination treatment on mitosis (Figure 34).

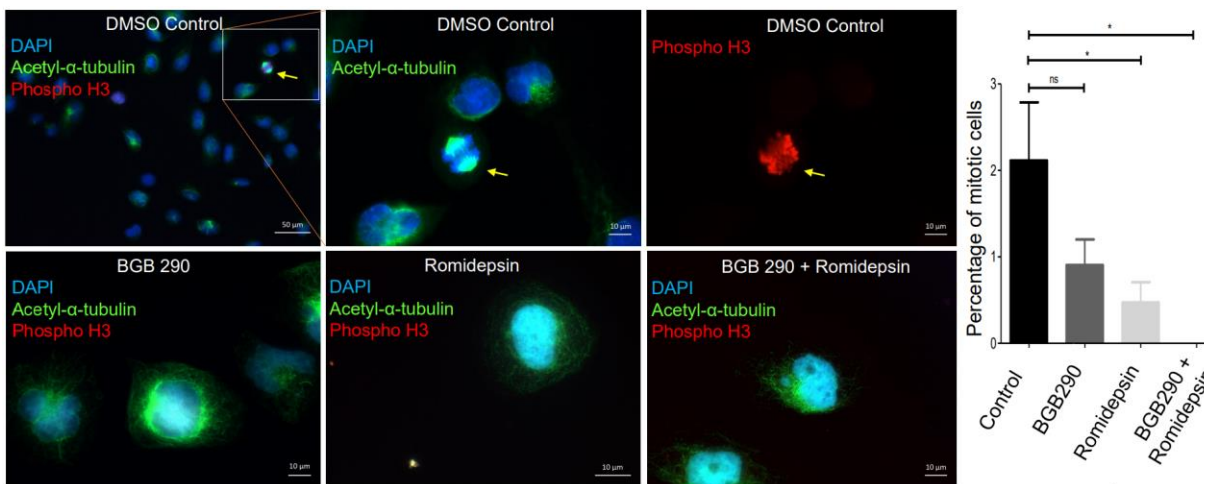


Figure 34: Acetyl- α -tubulin and phospho-histone 3 immunostaining of DAOY cells treated with either vehicle control, 6.25 μ M BGB290, 1.7 nM romidepsin or 6.25 μ M BGB290 with 1.7 nM romidepsin for 48 hours

Scale bar in top left panel: 50 μ m. Scale bar in all other panels: 10 μ m. Bar graph showing the percentage of mitotic cells in each treatment group. Statistical significance was tested by one-way ANOVA followed by Dunnett's Multiple Comparison Test, * $p < 0.05$, ns $p > 0.05$. Error bars represent the SEM, $n= 3$ biological replicates. A minimum of 250 cells were counted for each group in each replicate.

3.7 Gene expression Data

3.7.1 Experimental set-up

In order to investigate the molecular link underlying the combination treatment with romidepsin (HDAC inhibitor) and BGB290 (PARP inhibitor), three SHH medulloblastoma PDX spheroid models namely LFS_MB_P, LFS_MB_1R and RCMB18 were grown *in vitro*. Spheroids were treated with IC20s of romidepsin and BGB290 for each spheroid model (single drug and combination treatments). After 24 hours of treatment, RNA was isolated and subjected to expression arrays. Data were then used to perform gene set enrichment analysis (GSEA) and differential gene expression analysis (DEA) done by John K.L. Wong (Figure 35).

RESULTS

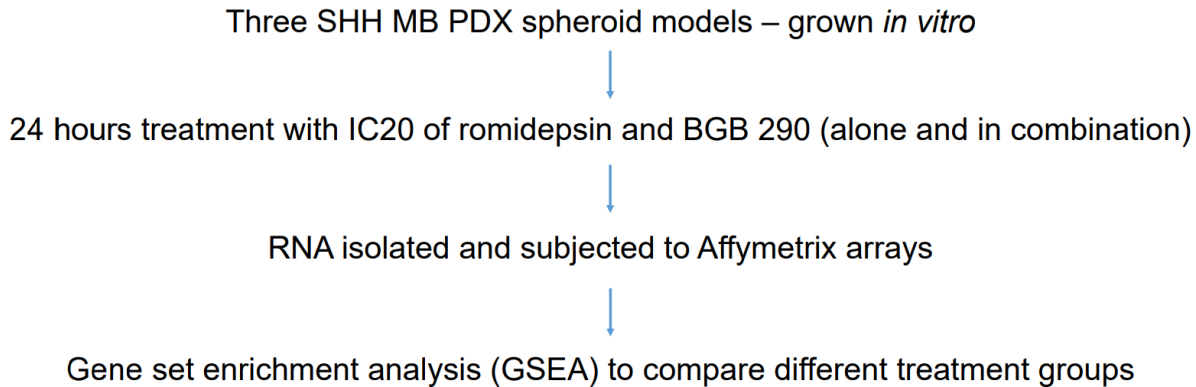


Figure 35: Schematic representation of the transcriptome experiment

3.7.2 GSEA analysis

GSEA analysis was done to compare initially single treatment to control, which revealed that upon romidepsin single treatment, the HDAC target gene signature was significantly enriched. This confirmed the efficacy of the romidepsin treatment. Data were also used to compare the double treatment (romidepsin and BGB290 combinational treatment) to the single treatment (romidepsin single treatment and BGB290 single treatment) groups. The most significantly enriched signature included *MYC* target genes, *KRAS*, *cyclin D1* and *E2F1* related genes. *Cyclin D1* and *E2F1* related gene sets enrichment potentially explains the G2 phase arrest that was observed in the cell cycle analysis experiments (Figure 36).

Single treatment vs control



Double treatment vs single treatment



Figure 36: Top signatures from GSEA analysis from single treatment compared to control (top, romidepsin versus control) and double treatment compared to single treatment (bottom)

3.7.3 Analysis of differentially expressed genes

Differential expression analysis done on the transcriptional data revealed 125 differentially expressed genes for double treatment versus single treatment (Supplementary Table 2), 1076 differentially expressed genes for double treatment versus control (Supplementary Table 3), 288 differentially expressed genes for BGB290 single treatment versus control (Supplementary Table 4) and 1495 differentially expressed genes for romidepsin treatment versus control (Supplementary Table 5) with thresholds of p value < 0.005 and fold change of ≥ 1.5 .

Table 1: Double treatment versus single treatment: differentially expressed genes (Top 12 genes, complete list in appendix)

Probe ID	Symbol	Gene name	P value	Fold change
TC0500007292.hg.1	<i>NIM1K</i>	NIM1 serine/threonine protein kinase	1.05E-04	5.02
HTA2-neg-47424007_st	NA	NA	3.44E-03	4.11
HTA2-pos-3475282_st	NA	NA	3.30E-03	3.24
TC0X00007013.hg.1	<i>MPC1L</i>	mitochondrial pyruvate carrier 1-like	5.22E-03	3.21
TC0200010447.hg.1	<i>CASP8</i>	caspase 8, apoptosis-related cysteine peptidase	3.54E-03	2.46
TC0400008390.hg.1	<i>LRIT3</i>	leucine-rich repeat, immunoglobulin-like and transmembrane domains 3	1.86E-03	2.41
TC1700011905.hg.1	<i>DNAH17</i>	dynein, axonemal, heavy chain 17	1.81E-04	2.40
TC0600012064.hg.1	<i>GCM1</i>	glial cells missing homolog 1 (Drosophila)	2.81E-03	2.39
TC0100015789.hg.1	<i>POGZ</i>	Transcript Identified by AceView, Entrez Gene ID(s) 23126	3.64E-04	2.38
TC1300010039.hg.1	<i>NEK5</i>	NIMA-related kinase 5	3.39E-03	2.36
TC0900008222.hg.1	<i>STX17</i>	syntaxin 17	1.08E-03	2.29

RESULTS

3.8 Molecular analyses of the role of MYC in the combination treatment

3.8.1 MYC immunohistochemistry on SHH medulloblastoma PDX tissues

As *MYC* target genes were significantly enriched in the GSEA, the expression of *MYC* in SHH medulloblastoma PDX tissues was determined by immunohistochemistry (Frauke Devens). The results revealed high expression of *MYC* in SHH medulloblastoma PDX tumor tissues (Figure 37).

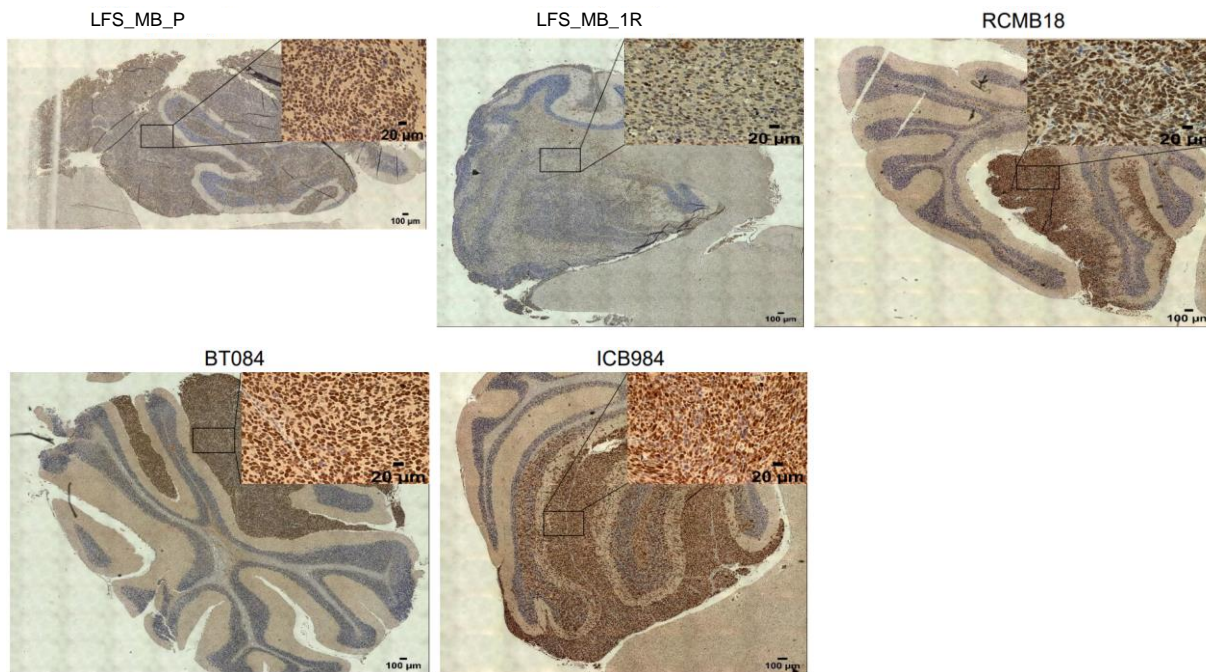


Figure 37: MYC immunohistochemistry on SHH medulloblastoma PDX tissues

Scale bar in zoom in images (top right in each panel): 20 μm . Scale bar in zoom out images (main panels): 100 μm . MYC protein stained in brown (HRP-DAB). Nuclei stained blue due to hematoxylin counterstain.

3.8.2 Validation of the *MYC* ON/OFF system

To investigate the role of *MYC* in the combination treatment, a *MYC* ON/OFF system was kindly provided by Dr. Till Milde's group (DKFZ). In this system, ONS76 medulloblastoma cells were stably transfected with a plasmid for inducible *MYC* expression, which leads to overexpression of *MYC* upon doxycycline induction. The system was validated by immunostaining of ONS76 cells with a *MYC* specific antibody with and without doxycycline induction. Overexpression of *MYC* upon doxycycline induction was confirmed (Figure 38).

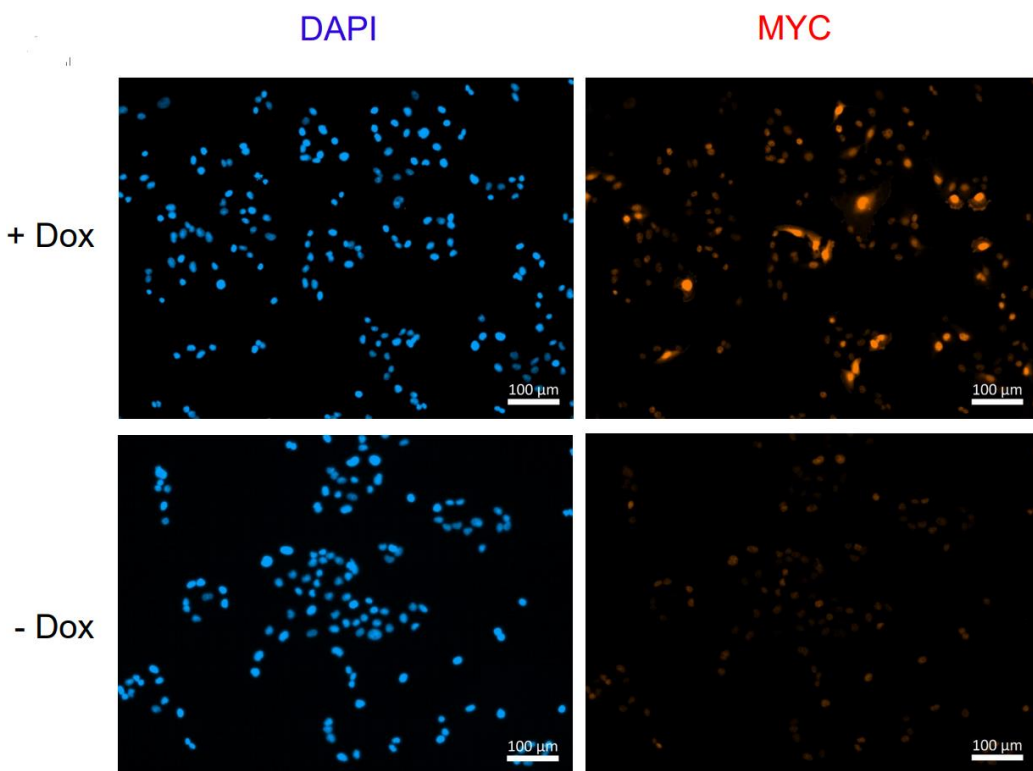


Figure 38: MYC immunostaining of ONS76 (*MYC* ON/OFF) cells with and without doxycycline induction

Scale bar in each panel: 100 μ m.

3.8.3 Matrix experiments using the *MYC* ON/OFF system

In order to confirm the effect of *MYC* overexpression on additivity or synergy between romidepsin and BGB290, ONS76 (*MYC* ON and *MYC* OFF) cells were subjected to 5 \times 8 matrix experiments. ONS76 (*MYC* ON) cells showed additive effects between romidepsin and BGB290. However, the additivity turned into antagonism in ONS76 (*MYC* OFF) cells, confirming that *MYC* overexpression plays a role in romidepsin and BGB290 additive or synergistic interaction (Figure 39).

RESULTS

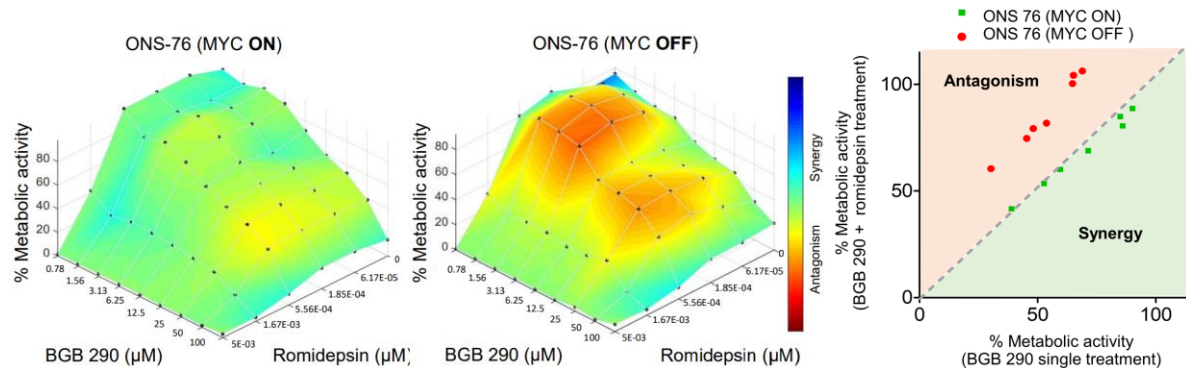


Figure 39: Romidepsin and BGB290 synergistic effects are linked to MYC expression

Loewe surface plot (left and middle) for ONS76 (MYC ON/OFF) cells with and without doxycyclin induction. The plots were generated using the combenefit software. Synergy and antagonism are plotted on the dose-response values using the average of the metabolic activity values (percentage of the DMSO controls) for 3 biological replicates per data point. Scatter plot (right) of the average of the metabolic activity values (percentage of the DMSO controls) for 3 biological replicates per data point for ONS76 (MYC ON/OFF) cells with and without doxycycline induction. The plot was generated with BGB290 single treatment on the X-axis versus BGB290 with romidepsin (0.56 nM) double treatment on the Y-axis.

3.8.4 IC50 curves for the C646 inhibitor

In order to determine the effect of deacetylation of PARP on the additivity between romidepsin and BGB290, cells were treated with the C646 inhibitor prior to romidepsin and BGB290 combinatorial treatment. C646 is a histone acetyltransferase inhibitor that inhibits p300, which in turn acetylates PARP [63]. In order to confirm that the effect was not due to varying sensitivities of ONS76 (MYC ON) and ONS76 (MYC OFF) cells to the C646 inhibitor, IC50 curves were generated for both and the curves were compared. The results confirmed there was no difference in sensitivities of ONS76 (MYC ON) and ONS76 (MYC OFF) cells to the C646 inhibitor (Figure 40).

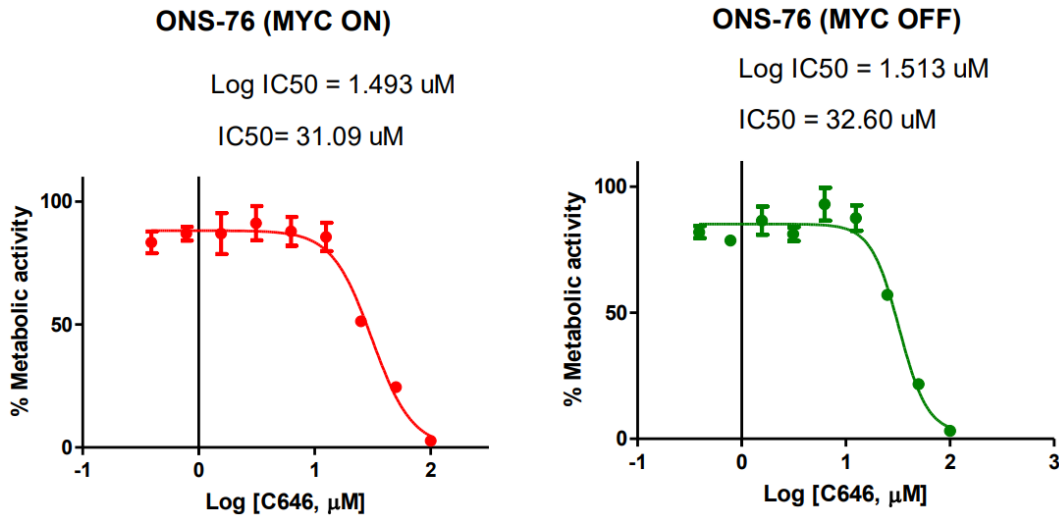


Figure 40: IC₅₀ curves for the C646 inhibitor for ONS76 (MYC ON/OFF) cells with and without doxycycline induction

Error bars represent the SEM, n= 3 technical replicates per data point.

3.8.5 Effect of the inhibition of PARP acetylation on the additivity between romidepsin and BGB290

ONS76 (MYC ON and MYC OFF) cells were subjected to 5 × 8 matrix experiments upon prior treatment with the C646 inhibitor. Both MYC ON and MYC OFF cells were seeded in 96 well plates. At the time of cell seeding, cells were treated with the C646 inhibitor. After 24 hours of treatment with C646, cells were treated with BGB290 and romidepsin. Both MYC ON and MYC OFF cells treated with C646 showed antagonism between romidepsin and BGB290 (Figure 41).

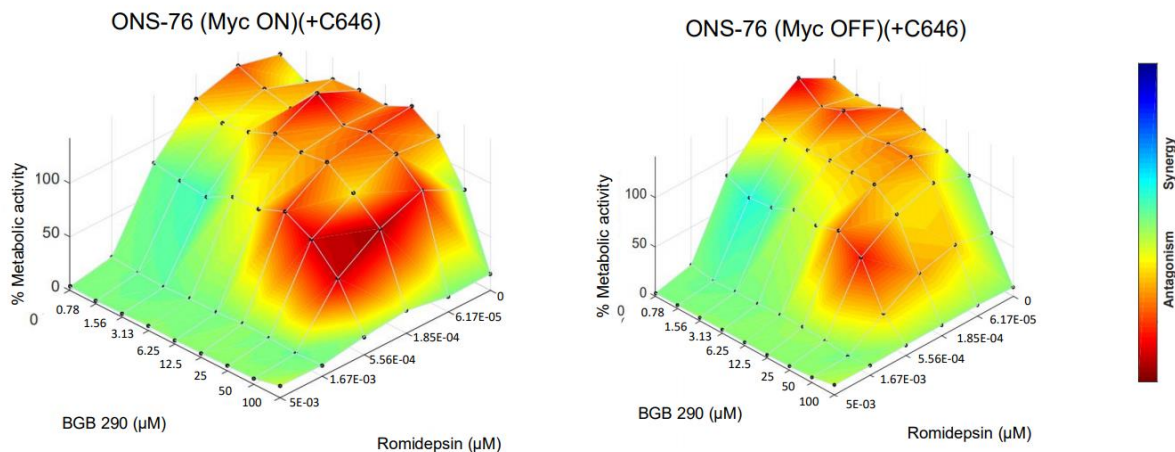


Figure 41: Antagonistic effect of romidepsin and BGB290 in the presence of C646

Loewe surface plot for ONS76 (MYC ON/OFF) cells with and without doxycycline induction with prior C646 treatment. The plots were generated using the combbenefit software. Synergy and antagonism are plotted on the dose-response values using the average of the metabolic activity values (percentage of the DMSO controls) for 3 biological replicates per data point.

RESULTS

3.9 *In vivo validation*

3.9.1 Romidepsin treatment in PDX models

The *in vivo* efficacy of the romidepsin and BGB290 combinational treatment was determined in flank tumors using the LFS_MB_1R PDX model. The results showed a significant reduction in tumor growth in romidepsin and BGB290 combinational treatment group as compared to romidepsin alone treatment and control groups (Figure 42).

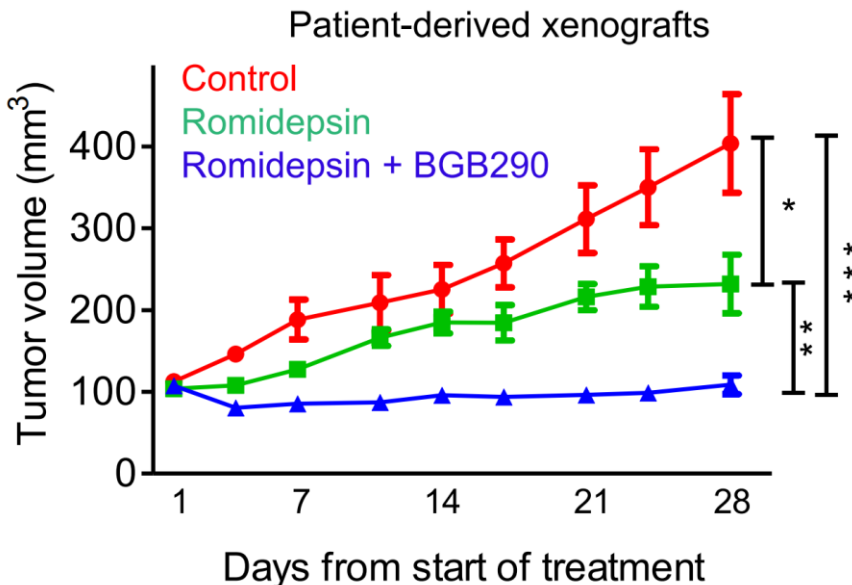


Figure 42: *In vivo validation in patient-derived xenografts*

Line graph showing the evolution of the tumor volume for patient-derived xenografts in immunocompromised mice. The statistical significance was tested by one-way ANOVA followed by Tukey's Multiple Comparison Test (* $p < 0.05$). Error bars represent the SEM, 6 mice per treatment group.

3.9.2 Haematoxylin & Eosin (H & E) and Ki67 immunohistochemistry

Xenograft tumors isolated from the flanks of mice belonging to different treatment groups were subjected to H & E and Ki67 immunohistochemistry. No significant difference was observed between romidepsin and BGB290 combinatorial treatment group as compared to romidepsin single treatment or control groups (Figure 43).

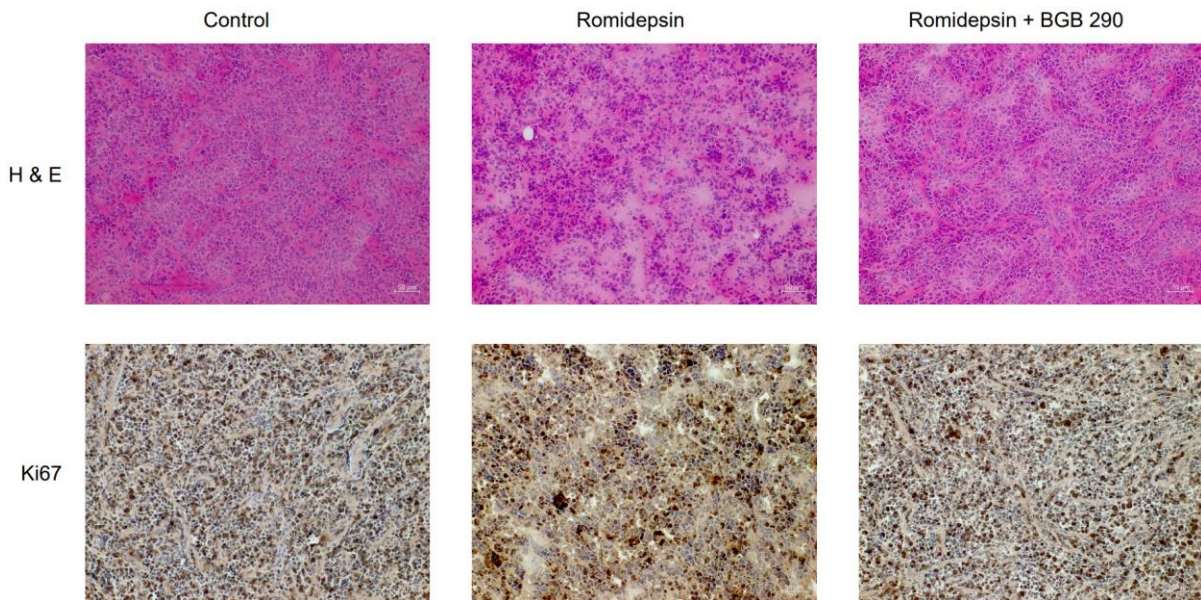


Figure 43: H & E (top 3 panels) and Ki67 immunohistochemistry (bottom 3 panels) of xenograft tumors isolated from the flanks of mice belonging to control, romidepsin alone and romidepsin with BGB290 treatment groups

3.9.3 Cleaved caspase 3 immunostaining

Xenograft tumors isolated from the flanks of mice belonging to different treatment groups were subjected to cleaved caspase 3 immunostaining to determine potential differences in apoptosis between the different treatment groups (staining done by Michaela Herdt). The data were also quantified using a Macro with the imageJ software. A slight difference in the cleaved caspase 3 signal was observed between romidepsin and BGB290 combinatorial treatment group as compared to single romidepsin treatment or to control groups but this difference was not statistically significant (Figure 44).

RESULTS

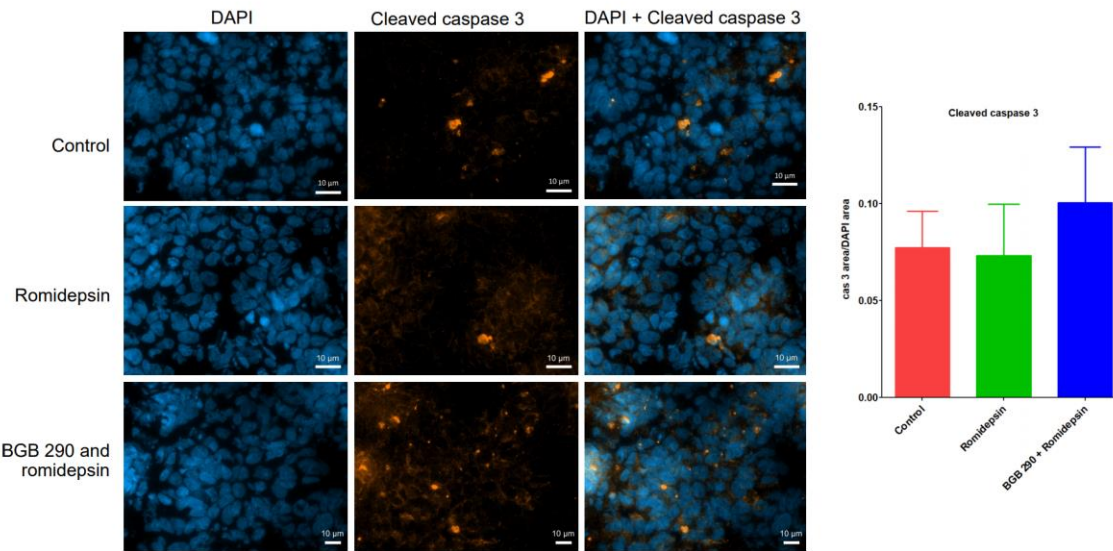


Figure 44: Cleaved caspase 3 and DAPI staining of xenograft tumors isolated from the flanks of mice belonging to control, romidepsin alone and romidepsin with BGB290 treatment groups

Representative images of three independent biological replicates. Bar graph on the right shows the quantification of cleaved caspase 3 fluorescence intensity relative to DAPI background. For each tumor, 2 sections (front and back of the tumor tissue) were stained with a cleaved caspase 3 antibody to quantify apoptosis. Quantification of the cleaved caspase 3 immunofluorescence signal was done using a macro in which the cleaved caspase 3 positive area was divided by the DAPI area. The statistical significance was tested by one-way ANOVA followed by Tukey's Multiple Comparison Test (* p < 0.05). The difference was non-significant. Error bars represent the SEM, 6 mice per treatment group except for romidepsin alone treatment group with 4 mice.

4. Discussion

4.1 Romidepsin

The most potent drug as a single agent in the primary screen was romidepsin. Along with showing extremely strong effects in terms of inhibition of the metabolic activity, romidepsin also showed potential additive or synergistic effects with BGB290. The synergy between romidepsin and BGB290 was then confirmed in the secondary screen. Romidepsin is an FDA approved therapeutic drug that inhibits histone deacetylase (HDAC class I) enzymes [64, 65]. It is approved for cutaneous T-cell lymphoma (CTCL) treatment [66]. Histone deacetylation is a form of epigenetic regulation that alters the gene expression. Histone deacetylases remove acetyl groups from histone proteins, which alters the interactions between DNA and histones. This leads to chromatin remodeling, which causes changes in gene transcription and ultimately protein expression is changed [67].

Class I HDACs comprise four enzymes called HDAC 1, HDAC 2, HDAC 3 and HDAC 8. HDAC 2 has been found to be functionally linked to p53 whereas HDAC 1 and HDAC 3 regulate angiogenesis [68, 69]. In the GSEA analysis, HDAC 2 was enriched as one of the most differentially expressed genes upon treatment with romidepsin alone as well as upon romidepsin and BGB290 combinational treatment.

In the clinical trial database of national institute of health (NIH), US national library of medicine, there are a total of 96 clinical trials listed for romidepsin against cancer. Out of these 96 trials, 43 studies have been completed, 13 are active and recruiting, 15 are not recruiting and 23 studies were either withdrawn, terminated or suspended. A phase 1 clinical trial in children suffering from refractory solid tumors was conducted. These refractory solid tumors also included childhood medulloblastoma, neuroblastoma and osteosarcoma patients. The results of the trial showed an accumulation of acetylated histone 3, which is a target of romidepsin. The doses of romidepsin used in the study were tolerable for the children, with a recommended dose for children of 17 mg/m² [70].

4.2 Factors affecting the synergistic interaction between romidepsin and BGB290

MYC expression

The GSEA analysis of the transcriptome data showed that *MYC* target genes are downregulated upon BGB290 and romidepsin combinational treatment. In order to further investigate this interesting observation, an inducible *MYC* ON / OFF system was used. ONS-76 cells overexpressing *MYC* after doxycycline induction in matrix experiments showed additive effects. In contrast, ONS-76 cells in *MYC* OFF state showed antagonism. This result confirmed the involvement of *MYC* in additive or synergistic interactions between BGB290 and romidepsin. *MYC* and *MYCN* (two members of *MYC* family) have

DISCUSSION

been found to have overlapping downstream targets [71]. In neuroblastoma patients, the expression levels of *MYC* and *MYCN* are inversely correlated and overexpression of either gene is linked with poor prognosis in different neuroblastoma subtypes [72]. In a study on malignant T cells, it was found that the β catenin pathway was downregulated upon romidepsin treatment. The authors also observed a reduction in c-MYC expression in a dose dependent manner [73].

In a study by Sasakawa et al, 2003 [74], *in vivo* regulation of the *c-MYC* and *p21* genes was investigated upon romidepsin treatment. Two xenograft models were used in this study. PC-3 xenografts were sensitive to romidepsin treatment and ACHN xenografts were less sensitive to romidepsin. The mRNA expression levels of *c-MYC* and *p21* were determined before and after treatment by romidepsin *in vivo* and compared. It was found that the sensitivity of the xenografts correlated to the expression of the *c-MYC* and *p21* genes. In PC-3 xenografts, *c-MYC* expression was downregulated and *p21* expression level increased, potentially leading to a decrease in tumor growth. On the other hand, in ACHN xenografts *c-MYC* expression was upregulated and *p21* expression level increased insufficiently, potentially explaining the absence of decrease in the tumor growth in this model [74].

In multiple studies done on group 3 medulloblastoma, which is a *MYC* driven cancer, the co-localization, and protein to protein interactions between class 1 HDAC2 and *MYC* were determined. In one study, the effect of the HDAC2 inhibitor entinostat on transcription regulation in *MYC* amplified cells was also observed [75]. HDAC2 acts as a cofactor of *MYC* and the HDAC2-*MYC* complex was found bound to *MYC* driven genes [76]. Moreover, inhibition of HDAC2 by a class 1 HDAC2 inhibitor disrupts the HDAC2-*MYC* interaction, leading to decreased binding of *MYC* to its target genes. This ultimately leads to transcriptional activation of *MYC* repressed genes and on the other hand causes transcriptional downregulation of *MYC* activating genes [77, 78].

In a high throughput screen to find therapeutic options to treat pediatric *MYC* driven medulloblastoma, researchers revealed HDAC inhibitors as potent drugs. When high throughput screening data were coupled with expression profiles of *MYC* driven medulloblastoma mice models, it was found that HDAC inhibitors when used in combination with another drug class (in this case PI3K inhibitors), inhibit the growth on *MYC* driven medulloblastomas both *in vitro* and *in vivo* [79]. The findings of this study are in line with the findings of my work where the HDAC inhibitor romidepsin synergistically interacts with the PARP inhibitor BGB290 to inhibit medulloblastoma PDX mouse model in a *MYC* dependent manner.

PARP acetylation

Apart from chromothripsis and *MYC*, two factors that potentially affect the synergistic interaction between romidepsin and BGB290 are PARP acetylation and BRCA2 expression. In a study done on leukemia cells, it was found that if PARP expression is decreased by knockdown approaches, it decreases the efficacy of HDAC inhibition [80]. This suggests that PARP expression has a direct role to play in the HDAC inhibitor treatment. It was found that treatment of cells with the HDAC inhibitor trichostatin A

increases the binding of the PARP1 enzyme to DNA double strand breaks due to increased acetylation of PARP1 [81]. Moreover, increasing the treatment time with trichostatin A increases PARP1 localization to damaged DNA and PAPR trapping. The DNA repair defects caused by acetylation of PARP due to the HDAC inhibitor treatment is counteracted by treatment with the C646 inhibitor. C646 inhibits the acetylase enzyme p300/CBP, which acetylates the PARP1 enzyme. In an *in vivo* study, acute myeloid patients were treated with the HDAC inhibitor entinostat. Increased formation of poly ADP- ribose (PAR) chains were found to be co-localized to DNA double strand breaks indicating PARP trapping. When the HDAC inhibitor was combined with talazoparib (a PARP inhibitor), a dose dependent increase in PARP trapping and apoptosis was observed in leukemia cells [80]. In another study done in glioblastoma, it was found that the HDAC inhibitor activates PARP1 and activated PARP is in turn recruited to DNA damage sites [82, 83]. Co-treatment with the PARP inhibitor olaparib leads to impaired cell cycle and checkpoint regulation and ultimately apoptosis [84]. These findings are in line with my results suggesting that the treatment of ONS-76 MYC ON cells with C646 inhibitor may potentially alleviate the additive effect between romidepsin and BGB290 combinatorial treatment.

Expression of HR-related protein

One of the rationales for using a PARP inhibitor in my project was that chromothripsis is linked to HR-repair deficiency. In a previous study conducted on prostate cancer, the HDAC inhibitor SAHA and the PARP inhibitor veliparib showed synergistic interactions in *in vivo* xenograft mouse models, decreasing the growth of xenografts upon combinatorial treatment. It was found that a synergistic interaction between SAHA and veliparib resulted in degradation of the BRCA1 protein due to disruption of BRCA1/UHRF1 complex. This caused an impairment of the HR repair pathway and an increase in DNA damage due to the HDAC- and PARP inhibitor combinatorial treatment, which ultimately lead to cell death and apoptosis [85]. In a study done in glioblastoma, it was found that glioblastoma xenografts treated with the HDAC inhibitor SAHA show a decrease in the expression of HR related proteins including BRCA1 and Rad51, which impaired the HR-repair pathway. It was also found that supplementing the HDAC inhibition with PARP inhibition further increased the suppression of HR- related proteins [84]. This finding is in line with my transcriptomic data, where the HDAC single treatment versus control analysis shows downregulated HR-related genes like *BRCA2*. Moreover, the downregulation of *BRCA2* was also observed upon combinatorial treatment of romidepsin and BGB290.

In another study on prostate cancer, it was found that combinatorial treatment of olaparib and SAHA causes downregulation of Rad51 and BRCA1, which are part of the HR repair pathway [86]. The sensitivity to HDAC- and PARP inhibitors combinatorial treatment on HR-repair pathway impairment can be assessed by the finding that if alone Rad51 is silenced, the prostate cancer cells get sensitized to the treatment [87].

DISCUSSION

In a study done on triple negative breast cancer, sensitization of cells to combinatorial treatment with HDAC- and PARP inhibitor was linked to *PTEN* expression. This finding was demonstrated both *in vitro* and *in vivo* in triple negative breast cancer models [88].

4.3 Future Perspectives

Based on my findings and results from previous studies, I propose a four-factor theory to explain the effects of synergistic interactions between the HDAC inhibitor romidepsin and the PARP inhibitor BGB290. The four factors that potentially play an important role in synergistic interactions between romidepsin and BGB290 are the chromothriptic status (genomic instability), *MYC* expression, HR-repair pathway impairment and PARP acetylation (Figure 45).

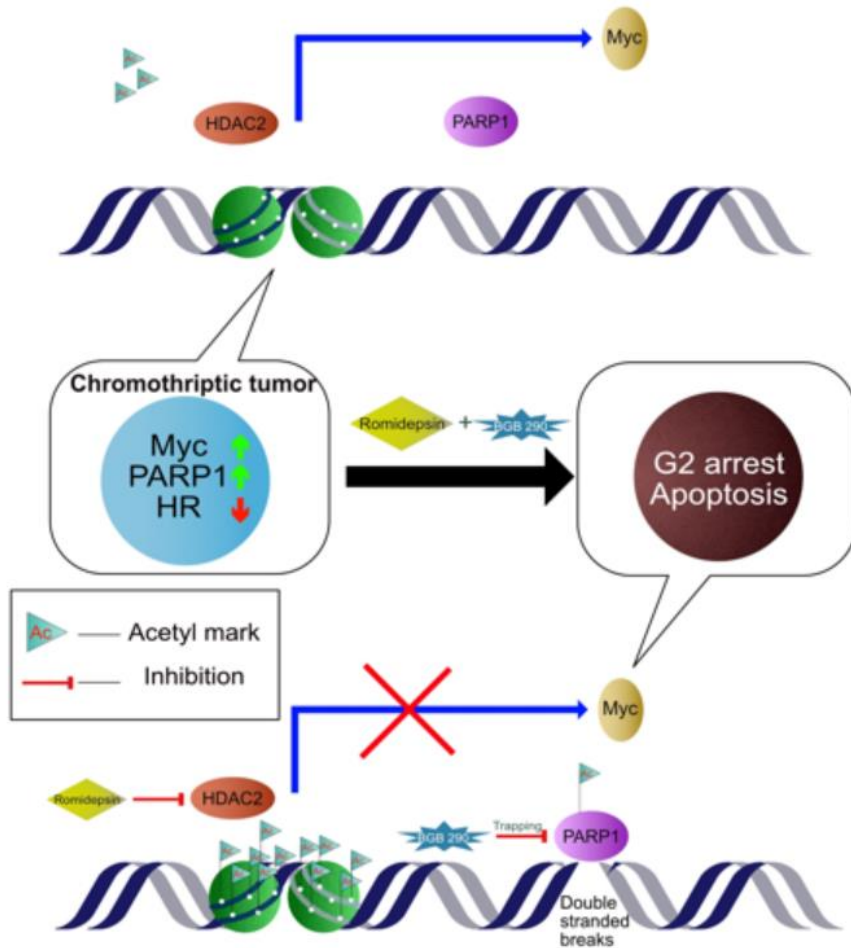


Figure 45: Graphical representation of the four-factor theory

Chromothriptic tumor with HR-repair deficiency and high expression of *MYC* and *PARP1*. *MYC* is deacetylated by HDAC2 and is functionally active. *PARP1* is not trapped at the chromatin. Upon the combinatorial treatment, romidepsin inhibits HDAC2, which causes *MYC* acetylation, leading to functional inactivation as well as downregulation of *MYC*. The combinational treatment causes DNA damage, which activates *PARP1*. *PARP1* is trapped at the DNA damage site due to BGB290 and inhibition of HDAC2 by romidepsin, which causes acetylation of *PARP1*. Ultimately, as DNA damage sites are not repaired due to the dysfunctional HR repair pathway and *PARP* trapping at the site of DNA double strand breaks, *MYC* expressing genomic instable chromothriptic cells undergo G2 phase cell cycle arrest and apoptosis.

In my project, the efficacy of the BGB290 and romidepsin combinatorial treatment has been tested and verified in the LFS_MB_1R PDX model, in which the tumor growth was significantly reduced as compared to romidepsin single treatment and control groups. *In vivo* studies in additional SHH medulloblastoma PDX models with chromothripsy like RCMB18 should be done to confirm the findings observed in the LFS_MB_1R PDX model. Moreover, as romidepsin shows potency against other tumor types included in the screen (e.g. neuroblastoma, osteosarcoma), confirming the synergistic interaction in osteosarcoma and neuroblastoma cell lines and ultimately *in vivo* validation of the efficacy of the combinatory treatment might reveal interesting results.

DISCUSSION

Romidepsin has a poor blood brain barrier (BBB) penetrance, with only 2% of drug in steady plasma state reaching the brain [89]. It has been found that some brain tumors like gliomas have a compromised blood brain barrier, thus facilitating the increased uptake into the brain across the blood brain barrier. Even the 2% drug delivery into the tumor could be sufficient, as the intra-tumor drug concentration will still be higher than the concentration required to kill glioma cells *in vitro* [89]. The need to develop methods to facilitate the crossing of the blood brain barrier by drugs has stimulated the recent development of brain delivery methods and materials. Nearly all the large molecules and more than 98% of small molecule drugs fail to cross the blood brain barrier [90]. The methods that can increase the uptake of drugs into the brain include trans-cranial and trans-nasal delivery. Trans-cranial delivery has been found to have many complications for the patient and has been shown to be ineffective in distributing the drug to the tumor site for a therapeutically relevant period of time [91]. Trans-nasal delivery has the limitation of delivering only the lipid solution molecules into the CSF across the nasal mucosal barrier [92]. As most of the therapeutic drugs are water soluble instead of lipid soluble, this method can be supplemented with disrupting the nasal mucosal barrier via local nasal injury [93]. Another method is to disrupt the blood brain barrier. This can be done in many ways like local ultrasonic irradiation or making drug formulations that include solvents like dimethyl sulfoxide (DMSO), Tween-80, glycerol, sodium dodecyl sulphate (SDS) or ethanol [94, 95]. Another method involves the exploitation of endogenous BBB transporters [96]. Three types of transporters containing a number of candidate receptor and transporter proteins and systems have been investigated in this regard [97]. These three types include receptor mediated transport, carrier mediated transport and active efflux transport [98, 99]. Coating drugs with lipid carriers or lipidization of drugs so that they can cross the BBB is also a method being investigated extensively [100]. Combining treatment of romidepsin and BGB290 with one of the methods described above to enhance the delivery of romidepsin to the tumor site in the brain may be beneficial for the patients suffering from brain cancers.

Further testing of potent drug candidates from the primary screen, first in *in vivo* mouse models and then in clinical trials, has the potential to reveal therapeutically relevant strategies and to improve the therapeutic options available for cancer patients.

5. References

1. Rausch, T., et al., *Genome sequencing of pediatric medulloblastoma links catastrophic DNA rearrangements with TP53 mutations*. Cell, 2012. **148**(1-2): p. 59-71.
2. Stephens, P.J., et al., *Massive genomic rearrangement acquired in a single catastrophic event during cancer development*. Cell, 2011. **144**(1): p. 27-40.
3. Luijten, M.N.H., J.X.T. Lee, and K.C. Crasta, *Mutational game changer: Chromothripsis and its emerging relevance to cancer*. Mutation Research/Reviews in Mutation Research, 2018. **777**: p. 29-51.
4. Ceccaldi, R., B. Rondinelli, and A.D. D'Andrea, *Repair pathway choices and consequences at the double-strand break*. Trends in cell biology, 2016. **26**(1): p. 52-64.
5. Edelmann, J., et al., *High-resolution genomic profiling of chronic lymphocytic leukemia reveals new recurrent genomic alterations*. Blood, The Journal of the American Society of Hematology, 2012. **120**(24): p. 4783-4794.
6. Ford, J.H., A.T. Schultz Cj Fau - Correll, and A.T. Correll, *Chromosome elimination in micronuclei: a common cause of hypoploidy*. 1988(0002-9297 (Print)).
7. Utani, K., N. Okamoto A Fau - Shimizu, and N. Shimizu, *Generation of micronuclei during interphase by coupling between cytoplasmic membrane blebbing and nuclear budding*. 2011(1932-6203 (Electronic)).
8. Maass, K.K., et al., *Altered nuclear envelope structure and proteasome function of micronuclei*. Experimental Cell Research, 2018. **371**(2): p. 353-363.
9. Crasta, K., et al., *DNA breaks and chromosome pulverization from errors in mitosis*. 2012(1476-4687 (Electronic)).
10. Blasco, M.A., *Telomeres and human disease: ageing, cancer and beyond*. Nature Reviews Genetics, 2005. **6**(8): p. 611-622.
11. McClintock, B., *The Stability of Broken Ends of Chromosomes in Zea Mays*. 1941(0016-6731 (Print)).
12. Maciejowski, J., et al., *Chromothripsis and Kataegis Induced by Telomere Crisis*. Cell, 2015. **163**(7): p. 1641-1654.
13. Umbreit, N.T., et al., *Mechanisms generating cancer genome complexity from a single cell division error*. Science (New York, N.Y.), 2020. **368**(6488): p. eaba0712.
14. Morishita, M., et al., *Chromothripsis-like chromosomal rearrangements induced by ionizing radiation using proton microbeam irradiation system*. Oncotarget, 2016. **7**(9): p. 10182-10192.
15. Kolb, T., et al., *A versatile system to introduce clusters of genomic double-strand breaks in large cell populations*. Genes Chromosomes Cancer, 2020. **2020 Jul 31**(1098-2264 (Electronic)).

REFERENCES

16. Mardin, B.R., et al., *A cell-based model system links chromothripsis with hyperploidy*. Molecular systems biology, 2015. **11**(9): p. 828-828.
17. Simovic, M. and A. Ernst. *Chromothripsis, DNA repair and checkpoints defects*. in *Seminars in Cell & Developmental Biology*. 2021. Elsevier.
18. Ratnaparkhe, M., et al., *Defective DNA damage repair leads to frequent catastrophic genomic events in murine and human tumors*. Nat Commun, 2018. **9**(1): p. 4760.
19. Grobner, S.N., et al., *The landscape of genomic alterations across childhood cancers*. Nature, 2018.
20. Voronina, N., et al., *The landscape of chromothripsis across adult cancer types*. Nat Commun, 2020. **11**(1): p. 2320.
21. Cortes-Ciriano, I., et al., *Comprehensive analysis of chromothripsis in 2,658 human cancers using whole-genome sequencing*. Nat Genet, 2020.
22. Takagi, M., et al., *Loss of DNA Damage Response in Neuroblastoma and Utility of a PARP Inhibitor*. J Natl Cancer Inst, 2017. **109**(11).
23. Wyatt, A.W. and C.C. Collins, *In brief: chromothripsis and cancer*. 2013, Wiley Online Library.
24. Waszak, S.M., et al., *Spectrum and prevalence of genetic predisposition in medulloblastoma: a retrospective genetic study and prospective validation in a clinical trial cohort*. Lancet Oncol, 2018. **19**(6): p. 785-798.
25. Molenaar, J.J., et al., *Sequencing of neuroblastoma identifies chromothripsis and defects in neuritogenesis genes*. Nature, 2012. **483**(7391): p. 589-93.
26. Fontana, M.C., et al., *Chromothripsis in acute myeloid leukemia: biological features and impact on survival*. Leukemia, 2018. **32**(7): p. 1609-1620.
27. Moynahan, M.E., et al., *Brca1 controls homology-directed DNA repair*. Molecular cell, 1999. **4**(4): p. 511-518.
28. Moynahan, M.E., A.J. Pierce, and M. Jasin, *BRCA2 is required for homology-directed repair of chromosomal breaks*. Molecular cell, 2001. **7**(2): p. 263-272.
29. Shen, S.-X., et al., *A targeted disruption of the murine Brca1 gene causes γ -irradiation hypersensitivity and genetic instability*. Oncogene, 1998. **17**(24): p. 3115-3124.
30. Tutt, A., et al., *Absence of Brca2 causes genome instability by chromosome breakage and loss associated with centrosome amplification*. Current Biology, 1999. **9**(19): p. 1107-S1.
31. Wooster, R., et al., *Identification of the breast cancer susceptibility gene BRCA2*. Nature, 1995. **378**(6559): p. 789-792.

REFERENCES

32. Tavtigian, S., et al., *The complete BRCA2 gene and mutations in chromosome 13q-linked kindreds*. Nature genetics, 1996. **12**(3): p. 333-337.
33. Futreal, P.A., et al., *BRCA1 mutations in primary breast and ovarian carcinomas*. Science, 1994. **266**(5182): p. 120-122.
34. Miki, Y., et al., *A strong candidate for the breast and ovarian cancer susceptibility gene BRCA1*. Science, 1994. **266**(5182): p. 66-71.
35. Kinzler, K.W. and B. Vogelstein, *Gatekeepers and caretakers*. Nature, 1997. **386**(6627): p. 761-763.
36. Evers, B., T. Helleday, and J. Jonkers, *Targeting homologous recombination repair defects in cancer*. Trends Pharmacol Sci, 2010. **31**(8): p. 372-80.
37. Dziadkowiec, K.N., et al., *PARP inhibitors: review of mechanisms of action and BRCA1/2 mutation targeting*. Przeglad menopauzalny= Menopause review, 2016. **15**(4): p. 215.
38. Bryant, H.E., et al., *Specific killing of BRCA2-deficient tumours with inhibitors of poly(ADP-ribose) polymerase*. Nature, 2005. **434**(7035): p. 913-7.
39. Kaufman, B., et al., *Olaparib monotherapy in patients with advanced cancer and a germline BRCA1/2 mutation*. J Clin Oncol, 2015. **33**(3): p. 244-50.
40. Pilie, P.G., et al., *PARP Inhibitors: Extending Benefit Beyond BRCA-Mutant Cancers*. Clin Cancer Res, 2019. **25**(13): p. 3759-3771.
41. Amé, J.C., C. Spenlehauer, and G. de Murcia, *The PARP superfamily*. Bioessays, 2004. **26**(8): p. 882-893.
42. Rouleau, M., et al., *PARP inhibition: PARP1 and beyond*. Nature reviews cancer, 2010. **10**(4): p. 293-301.
43. Huober, J., et al., *Higher efficacy of letrozole in combination with trastuzumab compared to letrozole monotherapy as first-line treatment in patients with HER2-positive, hormone-receptor-positive metastatic breast cancer—results of the eLEcTRA trial*. The breast, 2012. **21**(1): p. 27-33.
44. Sun, C., et al., *Rational combination therapy with PARP and MEK inhibitors capitalizes on therapeutic liabilities in RAS mutant cancers*. Science translational medicine, 2017. **9**(392).
45. Heske, C.M., et al., *Matrix Screen Identifies Synergistic Combination of PARP Inhibitors and Nicotinamide Phosphoribosyltransferase (NAMPT) Inhibitors in Ewing Sarcoma*. Clin Cancer Res, 2017. **23**(23): p. 7301-7311.
46. Henssen, A.G., et al., *Therapeutic targeting of PGBD5-induced DNA repair dependency in pediatric solid tumors*. Sci Transl Med, 2017. **9**(414).

REFERENCES

47. Lederer, S., T.M. Dijkstra, and T. Heskes, *Additive dose response models: defining synergy*. Frontiers in pharmacology, 2019. **10**: p. 1384.
48. Loewe, S., *The problem of synergism and antagonism of combined drugs*. Arzneimittelforschung, 1953. **3**: p. 285-290.
49. Zhao, W., et al., *A new bliss independence model to analyze drug combination data*. Journal of biomolecular screening, 2014. **19**(5): p. 817-821.
50. Greco, W., et al., *Consensus on concepts and terminology for combined-action assessment: the Saariselkä agreement*. Arch Complex Environ Stud, 1992. **4**(3): p. 65-9.
51. Ryall, K.A. and A.C. Tan, *Systems biology approaches for advancing the discovery of effective drug combinations*. Journal of cheminformatics, 2015. **7**(1): p. 1-15.
52. Team, R.C., *R: A language and environment for statistical computing*. 2013.
53. Chang, W., et al., *Shiny: web application framework for R*. R package version, 2017. **1**(5): p. 2017.
54. van der Maaten, L. and G. Hinton, *Visualizing data using t-SNE*. journal of Machine Learning Research 9. Nov (2008), 2008.
55. Gaujoux, R. and C. Seoighe, *A flexible R package for nonnegative matrix factorization*. BMC bioinformatics, 2010. **11**(1): p. 1-9.
56. Gu, Z., R. Eils, and M. Schlesner, *Complex heatmaps reveal patterns and correlations in multidimensional genomic data*. Bioinformatics, 2016. **32**(18): p. 2847-2849.
57. Sievert, C., *Interactive web-based data visualization with R, plotly, and shiny*. 2020: CRC Press.
58. Carvalho, B.S. and R.A. Irizarry, *A framework for oligonucleotide microarray preprocessing*. Bioinformatics, 2010. **26**(19): p. 2363-7.
59. Ritchie, M.E., et al., *limma powers differential expression analyses for RNA-sequencing and microarray studies*. Nucleic Acids Res, 2015. **43**(7): p. e47.
60. Di Veroli, G.Y., et al., *Combenefit: an interactive platform for the analysis and visualization of drug combinations*. Bioinformatics, 2016. **32**(18): p. 2866-8.
61. Kizilbash, S.H., et al., *Restricted delivery of talazoparib across the blood–brain barrier limits the sensitizing effects of PARP inhibition on temozolomide therapy in glioblastoma*. Molecular cancer therapeutics, 2017. **16**(12): p. 2735-2746.
62. Xiong, Y., et al., *Pamiparib is a potent and selective PARP inhibitor with unique potential for the treatment of brain tumor*. Neoplasia, 2020. **22**(9): p. 431-440.

REFERENCES

63. Wang, Y.-M., et al., *Histone acetyltransferase p300/CBP inhibitor C646 blocks the survival and invasion pathways of gastric cancer cell lines*. International journal of oncology, 2017. **51**(6): p. 1860-1868.
64. Bradner, J.E., et al., *Chemical phylogenetics of histone deacetylases*. Nature chemical biology, 2010. **6**(3): p. 238-243.
65. Furumai, R., et al., *FK228 (depsipeptide) as a natural prodrug that inhibits class I histone deacetylases*. Cancer research, 2002. **62**(17): p. 4916-4921.
66. Whittaker, S.J., et al., *Final results from a multicenter, international, pivotal study of romidepsin in refractory cutaneous T-cell lymphoma*. J Clin Oncol, 2010. **28**(29): p. 4485-4491.
67. Bolden, J.E., M.J. Peart, and R.W. Johnstone, *Anticancer activities of histone deacetylase inhibitors*. Nature reviews Drug discovery, 2006. **5**(9): p. 769-784.
68. Lane, A.A. and B.A. Chabner, *Histone deacetylase inhibitors in cancer therapy*. Journal of clinical oncology, 2009. **27**(32): p. 5459-5468.
69. Thiagalingam, S., et al., *Histone deacetylases: unique players in shaping the epigenetic histone code*. Annals of the New York Academy of Sciences, 2003. **983**(1): p. 84-100.
70. Fouladi, M., et al., *Phase I study of depsipeptide in pediatric patients with refractory solid tumors: a Children's Oncology Group report*. Journal of Clinical Oncology, 2006. **24**(22): p. 3678-3685.
71. Gustafson, W. and W. Weiss, *Myc proteins as therapeutic targets*. Oncogene, 2010. **29**(9): p. 1249-1259.
72. Westermann, F., et al., *Distinct transcriptional MYCN/c-MYC activities are associated with spontaneous regression or malignant progression in neuroblastomas*. Genome biology, 2008. **9**(10): p. 1-14.
73. Valdez, B., et al., *Romidepsin targets multiple survival signaling pathways in malignant T cells*. Blood cancer journal, 2015. **5**(10): p. e357-e357.
74. Sasakawa, Y., et al., *Effects of FK228, a novel histone deacetylase inhibitor, on tumor growth and expression of p21 and c-myc genes in vivo*. Cancer letters, 2003. **195**(2): p. 161-168.
75. Tanioka, M., et al., *Identification of Jun loss promotes resistance to histone deacetylase inhibitor entinostat through Myc signaling in luminal breast cancer*. Genome medicine, 2018. **10**(1): p. 1-14.
76. Ecker, J., et al., *Targeting class I histone deacetylase 2 in MYC amplified group 3 medulloblastoma*. Acta neuropathologica communications, 2015. **3**(1): p. 1-14.
77. Ecker, J., et al., *Reduced chromatin binding of MYC is a key effect of HDAC inhibition in MYC amplified medulloblastoma*. Neuro Oncol, 2021. **23**(2): p. 226-239.

REFERENCES

78. Ecker, J., et al., *MB-57 INTERACTION OF HDAC2 AND MYC IN GROUP 3 MEDULLOBLASTOMA-A NOVEL THERAPEUTIC TARGET.* Neuro-Oncology, 2016. **18**(suppl_3): p. iii110-iii110.
79. Pei, Y., et al., *HDAC and PI3K Antagonists Cooperate to Inhibit Growth of MYC-Driven Medulloblastoma.* Cancer Cell, 2016. **29**(3): p. 311-323.
80. Robert, C., et al., *Histone deacetylase inhibitors decrease NHEJ both by acetylation of repair factors and trapping of PARP1 at DNA double-strand breaks in chromatin.* Leukemia research, 2016. **45**: p. 14-23.
81. Hassa, P.O., et al., *Acetylation of poly (ADP-ribose) polymerase-1 by p300/CREB-binding protein regulates coactivation of NF- κ B-dependent transcription.* Journal of biological chemistry, 2005. **280**(49): p. 40450-40464.
82. Di Bernardo, G., et al., *Impact of histone deacetylase inhibitors SAHA and MS-275 on DNA repair pathways in human mesenchymal stem cells.* Journal of cellular physiology, 2010. **225**(2): p. 537-544.
83. Valdez, B.C., et al., *Combination of a hypomethylating agent and inhibitors of PARP and HDAC traps PARP1 and DNMT1 to chromatin, acetylates DNA repair proteins, down-regulates NuRD and induces apoptosis in human leukemia and lymphoma cells.* Oncotarget, 2018. **9**(3): p. 3908.
84. Rasmussen, R.D., et al., *Enhanced efficacy of combined HDAC and PARP targeting in glioblastoma.* Molecular oncology, 2016. **10**(5): p. 751-763.
85. Yin, L., et al., *PARP inhibitor veliparib and HDAC inhibitor SAHA synergistically co-target the UHRF1/BRCA1 DNA damage repair complex in prostate cancer cells.* Journal of Experimental & Clinical Cancer Research, 2018. **37**(1): p. 1-14.
86. Ward, A., K.K. Khanna, and A.P. Wiegmans, *Targeting homologous recombination, new pre-clinical and clinical therapeutic combinations inhibiting RAD51.* Cancer treatment reviews, 2015. **41**(1): p. 35-45.
87. Chao, O.S. and O.B. Goodman, *Synergistic loss of prostate cancer cell viability by coinhibition of HDAC and PARP.* Molecular cancer research, 2014. **12**(12): p. 1755-1766.
88. Min, A., et al., *Histone deacetylase inhibitor, suberoylanilide hydroxamic acid (SAHA), enhances anti-tumor effects of the poly (ADP-ribose) polymerase (PARP) inhibitor olaparib in triple-negative breast cancer cells.* Breast Cancer Research, 2015. **17**(1): p. 1-13.
89. Iwamoto, F.M., et al., *A phase I/II trial of the histone deacetylase inhibitor romidepsin for adults with recurrent malignant glioma: North American Brain Tumor Consortium Study 03-03.* Neuro-oncology, 2011. **13**(5): p. 509-516.
90. Pardridge, W.M., *Blood-brain barrier drug targeting: the future of brain drug development.* Molecular interventions, 2003. **3**(2): p. 90.
91. Bazzett, T.J., J.B. Becker, and R.L. Albin, *A novel device for chronic intracranial drug delivery via microdialysis.* Journal of neuroscience methods, 1991. **40**(1): p. 1-8.

REFERENCES

92. Pardridge, W.M., *Drug targeting to the brain*. Pharmaceutical research, 2007. **24**(9): p. 1733-1744.
93. Merkus, P., et al., *Direct access of drugs to the human brain after intranasal drug administration?* Neurology, 2003. **60**(10): p. 1669-1671.
94. Rubin, P., et al., *Disruption of the blood-brain barrier as the primary effect of CNS irradiation*. Radiotherapy and Oncology, 1994. **31**(1): p. 51-60.
95. Pardridge, W.M., *The blood-brain barrier: bottleneck in brain drug development*. NeuroRx, 2005. **2**(1): p. 3-14.
96. Pardridge, W.M., *Blood-brain barrier genomics and the use of endogenous transporters to cause drug penetration into the brain*. Current Opinion in Drug Discovery and Development, 2003. **6**(5): p. 683-691.
97. Sanchez-Covarrubias, L., et al., *Transporters at CNS barrier sites: obstacles or opportunities for drug delivery?* Current pharmaceutical design, 2014. **20**(10): p. 1422-1449.
98. Nau, R., F. Sörgel, and H. Eiffert, *Penetration of drugs through the blood-cerebrospinal fluid/blood-brain barrier for treatment of central nervous system infections*. Clinical microbiology reviews, 2010. **23**(4): p. 858-883.
99. Pardridge, W.M., *Blood-brain barrier delivery*. Drug discovery today, 2007. **12**(1-2): p. 54-61.
100. Pardridge, W.M., *Drug and gene delivery to the brain: the vascular route*. Neuron, 2002. **36**(4): p. 555-558.

6. Publications

A synergistic interaction between HDAC- and PARP inhibitors in childhood tumors with chromothripsis.

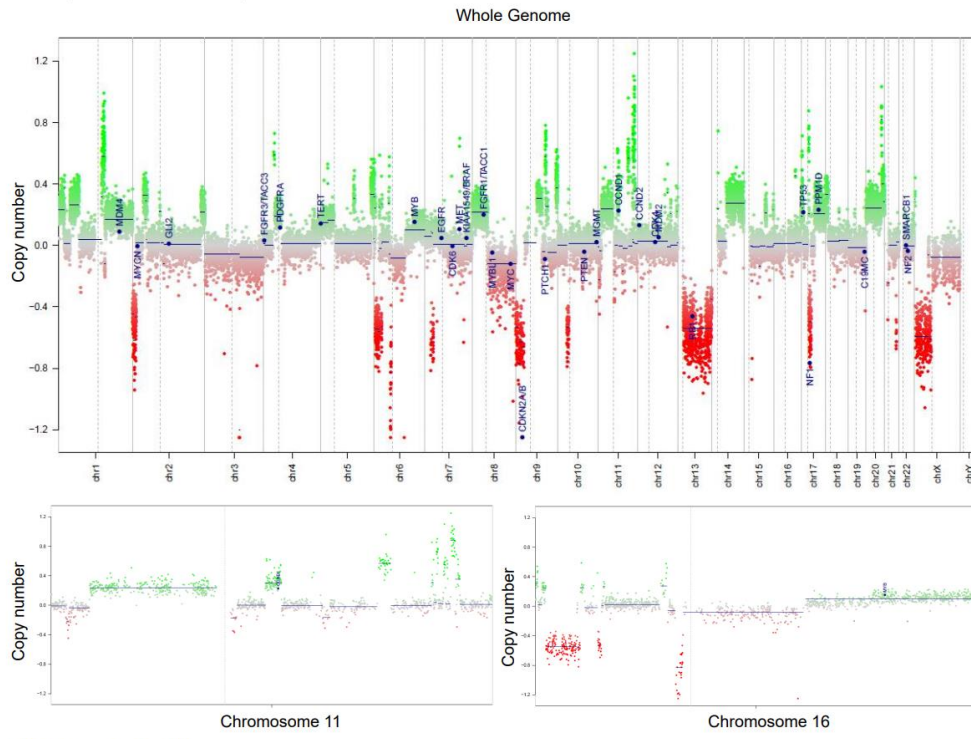
Umar Khalid, Milena Simovic, Murat Iskar, John KL Wong, Rithu Kumar, Manfred Jugold, Martin Sill, Michiel Bolkestein, Thorsten Kolb, Michaela Hergt, Frauke Devens, Jonas Ecker, Marcel Kool, Till Milde, Frank Westermann, Joe Lewis, Sascha Dietrich, Stefan M Pfister, Peter Lichter, Marc Zapatka, Aurélie Ernst. *Submitted for publication.*

A versatile system to introduce clusters of genomic double-strand breaks in large cell populations. Kolb, T., **Khalid, U.**, Simović, M., Ratnaparkhe, M., Wong, J., Jauch, A., Schmezer, P., Rode, A., Sebban, S., Haag, D. and Hergt, M., 2021. Genes, Chromosomes and Cancer, 60(5), pp.303-313.

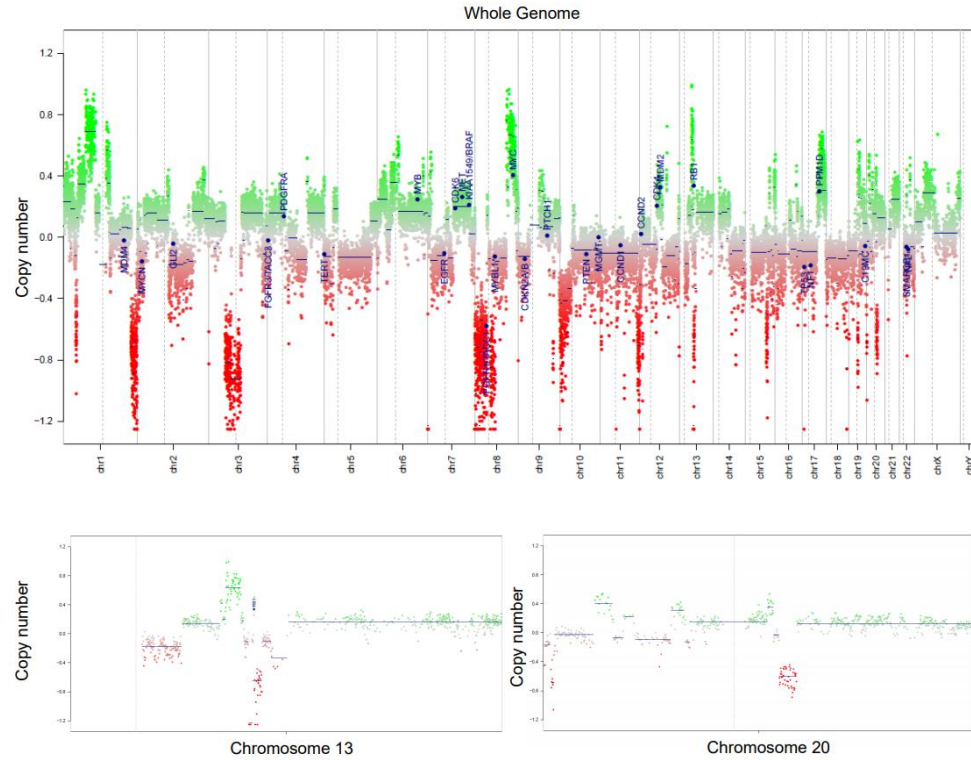
Carbon ion radiotherapy eradicates medulloblastomas with chromothripsis in an orthotopic Li-Fraumeni patient-derived mouse model. Milena Simovic, Michiel Bolkestein, Mahmoud Moustafa, John K.L. Wong, Verena Körber, Sarah Benedetto, **Umar Khalid**, Hannah Sophia Schreiber, Manfred Jugold, Andrey Korshunov, Daniel Hübschmann, Norman Mack, Stephan Brons, Pei-Chi Wei, Michael Breckwoldt, Sabine Heiland, Martin Bendszus, Jürgen Debus, Thomas Höfer, Marc Zapatka, Marcel Kool, Stefan M. Pfister, Amir Abdollahi, Aurélie Ernst. Neuro-oncology, 2021, *under review*

7. Appendix

KHOS-240S (Osteosarcoma cell line)

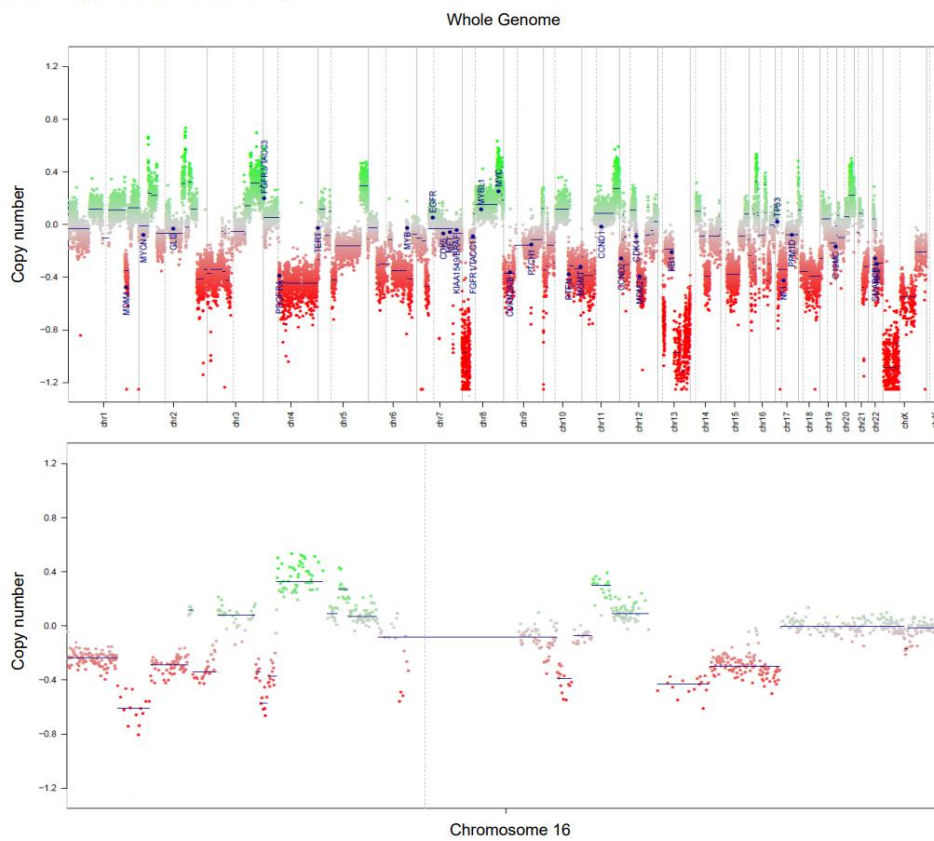


Saos-2 (Osteosarcoma cell line)

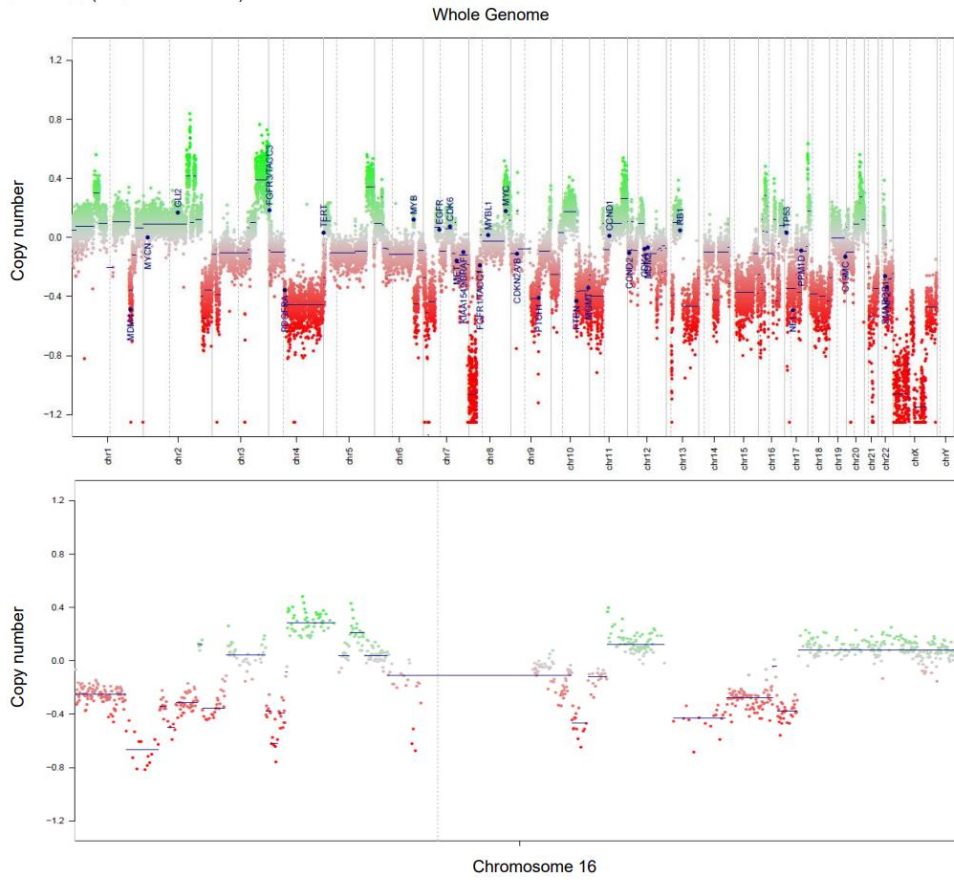


APPENDIX

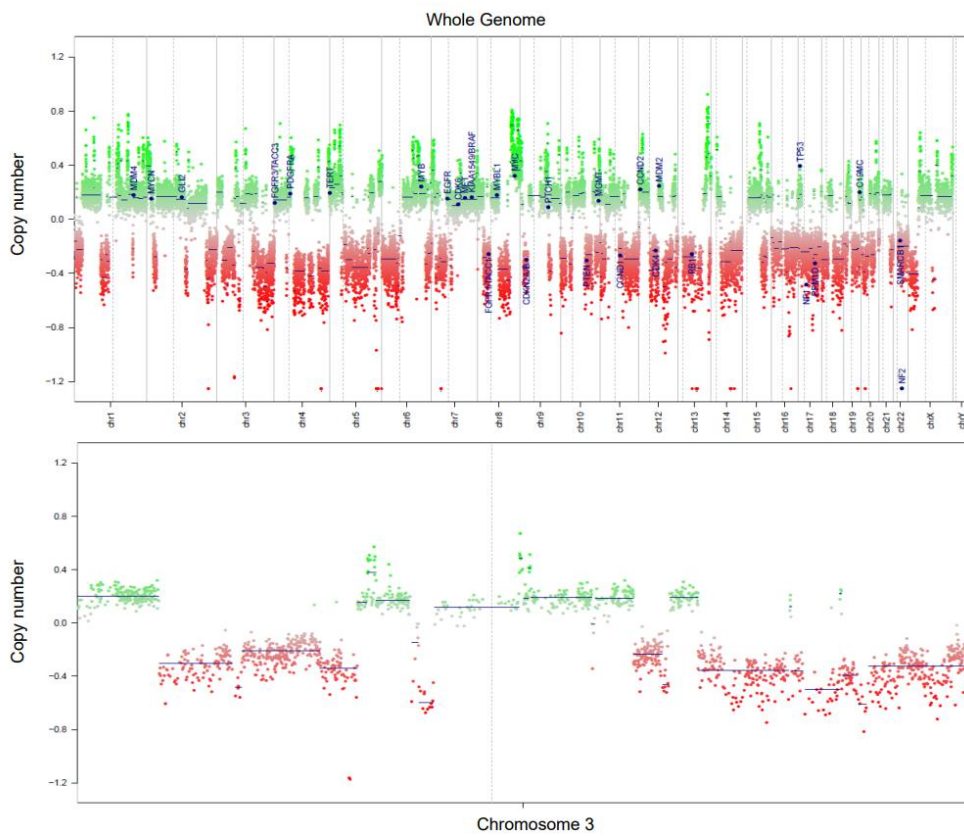
UWB1.289 (*BRCA1* mutant control line)



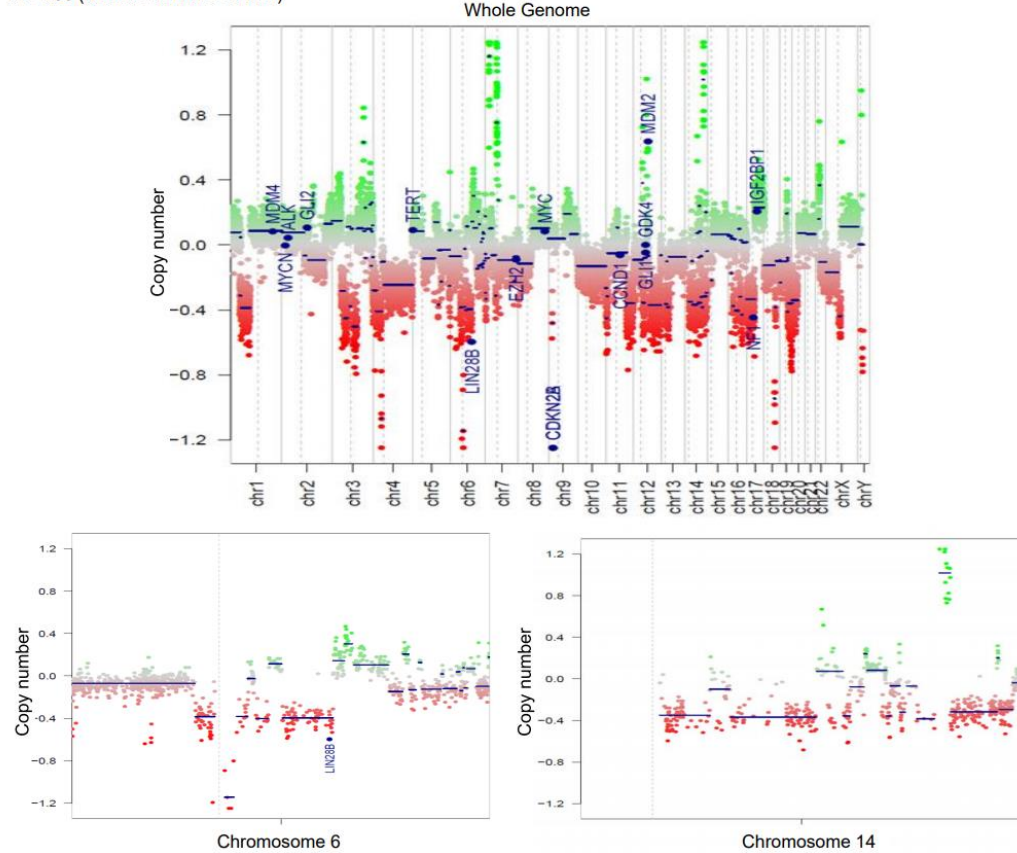
UWB1.289 (*BRCA1* rescue line)



MDA-MB-436 (BRCA 1 mutant line)

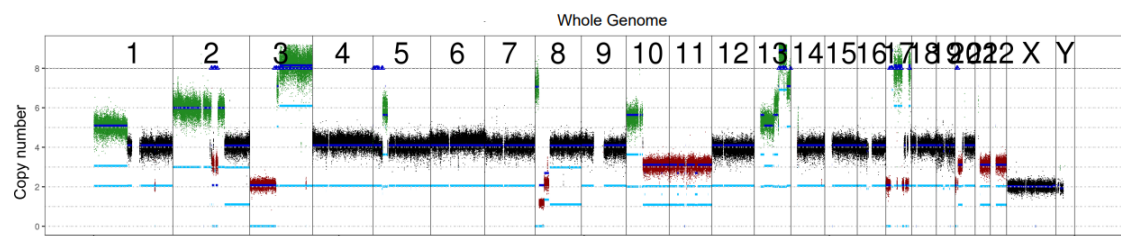


HD-N33 (Neuroblastoma cell line)

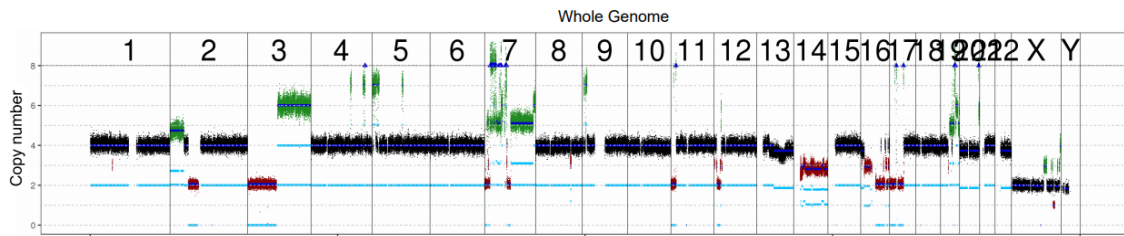


APPENDIX

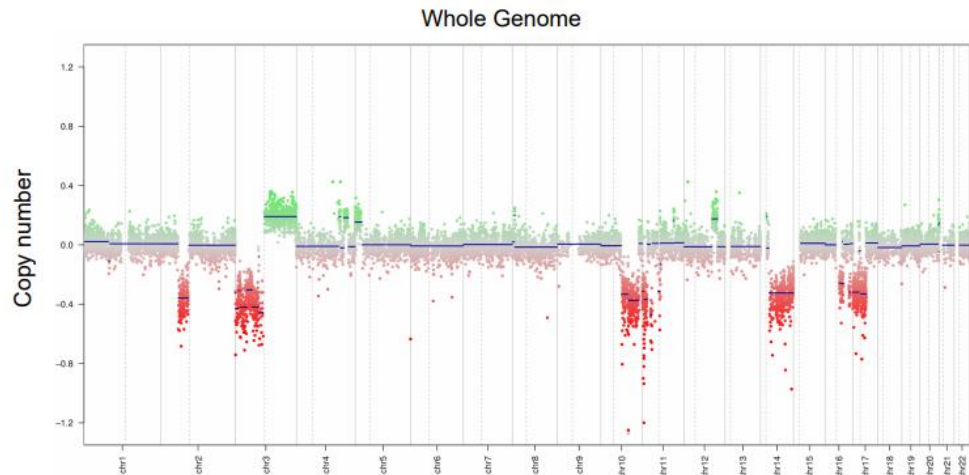
MB145 (medulloblastoma from which patient-derived xenograft model BT084 was established)



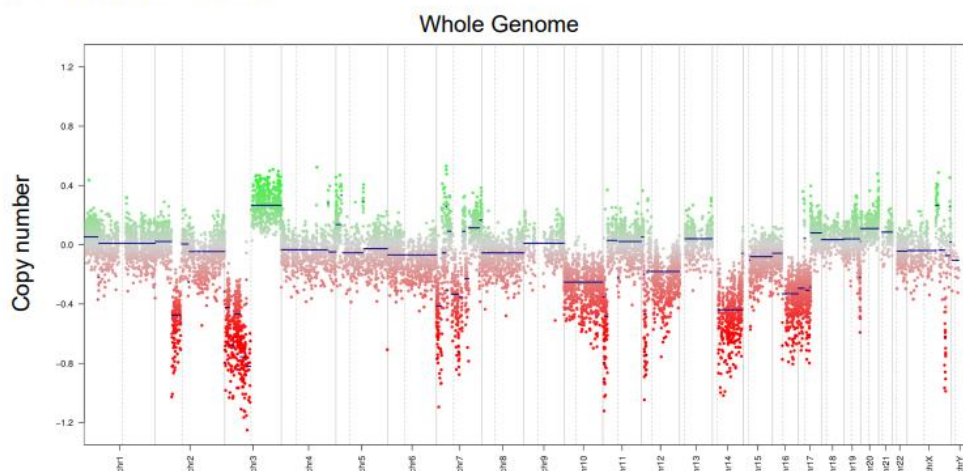
LFS_MB_P (medulloblastoma)



LFS_MB_1R (medulloblastoma)



LFS_MB_2R (medulloblastoma)

**Supplementary figure 46 : Molecular characterization of in vitro models included in the screen**

Copy number variant (CNV) plots of cell lines included in the screen generated using 450 K methylation array, EPIC methylation arrays or whole-genome sequencing.

Supplementary Table 2: Double treatment versus single treatment: Differentially expressed genes (Complete list)

Probe ID	Symbol	Gene name	P value	Fold change
TC0500007292.hg.1	<i>NIM1K</i>	NIM1 serine/threonine protein kinase	1.05E-04	5.02
HTA2-neg-47424007_st	NA	NA	3.44E-03	4.11
HTA2-pos-3475282_st	NA	NA	3.30E-03	3.24
TC0X00007013.hg.1	<i>MPC1L</i>	mitochondrial pyruvate carrier 1-like	5.22E-03	3.21
TC0200010447.hg.1	<i>CASP8</i>	caspase 8, apoptosis-related cysteine peptidase	3.54E-03	2.46
TC0400008390.hg.1	<i>LRIT3</i>	leucine-rich repeat, immunoglobulin-like and transmembrane domains 3	1.86E-03	2.41
TC1700011905.hg.1	<i>DNAH17</i>	dynein, axonemal, heavy chain 17	1.81E-04	2.40
TC0600012064.hg.1	<i>GCM1</i>	glial cells missing homolog 1 (Drosophila)	2.81E-03	2.39

APPENDIX

TC0100015789.hg.1	<i>POGZ</i>	Transcript Identified by AceView, Entrez Gene ID(s) 23126	3.64E-04	2.38
TC1300010039.hg.1	<i>NEK5</i>	NIMA-related kinase 5	3.39E-03	2.36
TC0900008222.hg.1	<i>STX17</i>	syntaxin 17	1.08E-03	2.29
TC1700012355.hg.1	<i>KRBA2</i>	KRAB-A domain containing 2	5.98E-03	2.28
HTA2-neg-47424044_st	NA	NA	5.94E-03	2.24
HTA2-neg-47424360_st	NA	NA	2.12E-03	2.22
TC0800010802.hg.1	<i>C8orf89</i>	chromosome 8 open reading frame 89	6.51E-04	2.20
TC1500010745.hg.1	<i>POLR2M</i>	polymerase (RNA) II (DNA directed) polypeptide M	5.19E-03	2.20
TC1500007409.hg.1	<i>GCNT3</i>	glucosaminyl (N-acetyl) transferase 3, mucin type	6.48E-03	2.17
TC2200007132.hg.1	<i>RFPL3</i>	ret finger protein-like 3	5.91E-05	2.17
HTA2-neg-47424024_st	NA	NA	2.45E-03	2.16
TC0200010474.hg.1	<i>KIAA2012</i>	KIAA2012	5.20E-03	2.16
TC1100007216.hg.1	<i>PRRG4</i>	proline rich Gla (G-carboxyglutamic acid) 4 (transmembrane)	7.43E-03	2.15
TC0400012977.hg.1	<i>SH3D19</i>	SH3 domain containing 19	3.74E-03	2.09
HTA2-neg-47422090_st	NA	NA	1.57E-03	2.09
TC2200008513.hg.1	<i>RFPL3S</i>	RFPL3 antisense	2.62E-04	2.07
HTA2-neg-47420194_st	NA	NA	2.88E-03	2.06

TC0600007262.hg.1	<i>HIST1H3A</i>	histone cluster 1, H3a	3.81E-03	2.05
TC0600007293.hg.1	<i>HIST1H2BI</i>	histone cluster 1, H2bi	1.27E-03	2.03
TC0200011129.hg.1	SAG	S-antigen; retina and pineal gland (arrestin)	1.62E-03	2.02
TC0200007038.hg.1	<i>DRC1</i>	dynein regulatory complex subunit 1	3.77E-04	2.02
TC1700006813.hg.1	<i>ODF4</i>	outer dense fiber of sperm tails 4	3.75E-03	2.02
TC0300012771.hg.1	<i>TM4SF18</i>	Transcript Identified by AceView, Entrez Gene ID(s) 116441	3.33E-03	2.01
HTA2-neg-47422060_st	NA	NA	2.74E-03	2.00
TC1700007871.hg.1	<i>HSPB9</i>	heat shock protein, alpha-crystallin-related, B9	1.95E-03	1.99
TC0300009772.hg.1	<i>AHSG</i>	alpha-2-HS-glycoprotein	2.72E-03	1.98
TC1500009998.hg.1	<i>GOLGA6A</i>	golgin A6 family, member A	7.39E-04	1.98
TC0800012350.hg.1	<i>MTBP</i>	MDM2 binding protein	1.41E-03	1.96
TC1400010637.hg.1	<i>C14orf178</i>	chromosome 14 open reading frame 178	3.01E-03	1.95
23067837	NA	NA	1.30E-03	1.95
TC0200007418.hg.1	<i>SLC3A1</i>	solute carrier family 3 (amino acid transporter heavy chain), member 1	1.95E-04	1.94
TC1100010044.hg.1	<i>ST5</i>	Transcript Identified by AceView, Entrez Gene ID(s) 6764	1.83E-04	1.94
TC1400010749.hg.1	<i>LINC01599</i>	long intergenic non-protein coding RNA 1599	8.21E-03	1.92

APPENDIX

TC0200016417.hg.1	<i>CENPA</i>	centromere protein A	9.44E-05	1.88
TC1700010550.hg.1	<i>C17orf98</i>	chromosome 17 open reading frame 98	4.62E-03	1.86
HTA2-neg-47424023_st	NA	NA	3.33E-03	1.86
HTA2-neg-47420912_st	NA	NA	3.54E-03	1.84
TC0900007069.hg.1	<i>C9orf131</i>	chromosome 9 open reading frame 131	6.88E-03	1.81
TC0200008268.hg.1	<i>GNLY</i>	granulysin	3.47E-03	1.79
TC0100015586.hg.1	<i>PDZK1</i>	PDZ domain containing 1	2.56E-04	1.79
TC0100008773.hg.1	<i>MSH4</i>	mutS homolog 4	1.47E-03	1.78
HTA2-neg-47423805_st	NA	NA	3.64E-03	1.78
HTA2-neg-47422085_st	NA	NA	1.72E-03	1.78
TC1500010769.hg.1	<i>GOLGA6C</i>	golgin A6 family, member C	9.92E-03	1.77
TC0600014246.hg.1	<i>C6orf229</i>	chromosome 6 open reading frame 229	2.39E-03	1.77
TC1700011117.hg.1	<i>LINC00483</i>	long intergenic non-protein coding RNA 483	6.29E-04	1.77
TC1100012352.hg.1	<i>TMPRSS5</i>	transmembrane protease, serine 5	2.28E-03	1.76
TC0900010370.hg.1	<i>TRPM3</i>	transient receptor potential cation channel, subfamily M, member 3	8.33E-03	1.76
TC0700013525.hg.1	<i>FAM126A</i>	family with sequence similarity 126, member A	8.76E-04	1.76
TC0200010445.hg.1	<i>CASP10</i>	caspase 10	4.70E-03	1.75
TC0100009913.hg.1	<i>ADAMTSL4</i>	ADAMTS like 4	4.73E-03	1.74

TC0300011997.hg.1	<i>BTLA</i>	B and T lymphocyte associated	5.15E-03	1.74
TC1200012660.hg.1	<i>SLC35E3</i>	solute carrier family 35, member E3	8.44E-03	1.73
HTA2-neg-47424704_st	<i>NA</i>	NA	8.15E-03	1.72
TC0500008654.hg.1	<i>LEAP2</i>	liver expressed antimicrobial peptide 2	2.06E-04	1.72
TC1600007189.hg.1	<i>VWA3A</i>	von Willebrand factor A domain containing 3A	9.81E-04	1.71
TC0100010526.hg.1	<i>TBX19</i>	T-box 19	3.99E-03	1.71
TC1200009547.hg.1	<i>SLC6A13</i>	solute carrier family 6 (neurotransmitter transporter), member 13	1.03E-03	1.71
TC0100018360.hg.1	<i>DISC1</i>	disrupted in schizophrenia 1	1.60E-03	1.70
HTA2-neg-47424705_st	<i>NA</i>	NA	2.69E-03	1.69
TC0500011296.hg.1	<i>ACOT12</i>	acyl-CoA thioesterase 12	1.68E-04	1.69
TC1200009220.hg.1	<i>CCDC62</i>	coiled-coil domain containing 62	8.64E-03	1.69
TC0100009936.hg.1	<i>BNIPL</i>	BCL2/adenovirus E1B 19kD interacting protein like	5.80E-03	1.69
TC1200008223.hg.1	<i>GLIPR1L2</i>	GLI pathogenesis-related 1 like 2	9.30E-03	1.68
TC1100013093.hg.1	<i>BCO2</i>	beta-carotene oxygenase 2	8.52E-03	1.67
TC0200016751.hg.1	<i>LOC100130691</i>	uncharacterized LOC100130691	5.53E-03	1.66
TC0200016661.hg.1	<i>C2orf61</i>	chromosome 2 open reading frame 61	1.51E-03	1.66
TC0200012071.hg.1	<i>UCN</i>	urocortin	4.36E-04	1.65

APPENDIX

HTA2-neg-47422095_st	NA	NA	8.42E-04	1.65
TC1700012241.hg.1	<i>TBC1D3L</i>	TBC1 domain family, member 3L	4.77E-03	1.65
TSUnmapped00000145.hg.1	<i>SAG</i>	S-antigen; retina and pineal gland (arrestin)	1.00E-04	1.64
TC0X00009089.hg.1	<i>FAM9C</i>	family with sequence similarity 9, member C	9.64E-03	1.64
TC0600009623.hg.1	<i>ECT2L</i>	epithelial cell transforming 2 like	9.77E-03	1.63
TC0X00007562.hg.1	<i>ITGB1BP2</i>	integrin beta 1 binding protein (melusin) 2	5.30E-04	1.63
TC1900006602.hg.1	<i>ZNF555</i>	zinc finger protein 555	8.88E-03	1.63
TC0200010837.hg.1	<i>ANKZF1</i>	ankyrin repeat and zinc finger domain containing 1	8.90E-03	1.61
TC1500010712.hg.1	<i>GOLGA8N</i>	golgin A8 family, member N	9.53E-03	1.61
HTA2-neg-47419220_st	NA	NA	5.60E-04	1.59
TC1200012744.hg.1	<i>C1R</i>	complement component 1, r subcomponent	5.41E-03	1.59
TC0100016445.hg.1	<i>SERPINC1</i>	serpin peptidase inhibitor, clade C (antithrombin), member 1	5.03E-03	1.58
TC1100010733.hg.1	<i>SPI1</i>	Spi-1 proto-oncogene	2.27E-04	1.58
TC0700012228.hg.1	<i>LAMB4</i>	laminin, beta 4	3.01E-03	1.58
TC0300013941.hg.1	<i>MKRN2OS</i>	MKRN2 opposite strand	4.53E-04	1.58
AFFX-r2-Ec-bioB-5_at	NA	NA	6.75E-03	1.58
TC0900007163.hg.1	<i>FRMPD1</i>	FERM and PDZ domain containing 1	4.72E-03	1.57

TC1700009746.hg.1	<i>MYH3</i>	myosin, heavy chain 3, skeletal muscle, embryonic	7.83E-03	1.56
AFFX-r2-Ec-bioB-3_at	NA	NA	7.40E-03	1.56
TC1100011029.hg.1	<i>VWCE</i>	von Willebrand factor C and EGF domains	5.53E-04	1.56
TSUnmapped00000176.hg.1	<i>SAG</i>	S-antigen; retina and pineal gland (arrestin)	8.78E-03	1.56
AFFX-r2-Ec-bioC-3_at	NA	NA	6.90E-03	1.56
TC0500010592.hg.1	<i>C6</i>	complement component 6	2.34E-03	1.56
TC0800008946.hg.1	<i>TG</i>	thyroglobulin	2.32E-03	1.56
TC1000009916.hg.1	<i>CUBN</i>	cubilin (intrinsic factor- cobalamin receptor)	6.40E-03	1.56
TC1500008271.hg.1	<i>WDR93</i>	WD repeat domain 93	4.63E-03	1.55
TSUnmapped00000141.hg.1	<i>HMBS</i>	hydroxymethylbilane synthase	2.92E-03	1.55
TC2200008588.hg.1	<i>APOL3</i>	apolipoprotein L, 3	5.59E-03	1.55
TC1600009192.hg.1	<i>MTRNR2L4</i>	MT-RNR2-like 4	7.88E-03	1.55
TC0600010071.hg.1	<i>SLC22A1</i>	solute carrier family 22 (organic cation transporter), member 1	1.50E-03	1.55
23075460	NA	NA	1.69E-04	1.55
HTA2-pos- PSR0X007730.hg.1	NA	NA	4.51E-03	1.54
TC0900008667.hg.1	<i>OR1N2</i>	olfactory receptor, family 1, subfamily N, member 2	2.34E-03	1.54
TC0600014251.hg.1	<i>ZBED9</i>	zinc finger, BED-type containing 9	2.72E-04	1.54

APPENDIX

HTA2-neg-47422763_st	NA	NA	2.70E-03	1.54
TC0600011805.hg.1	<i>USP49</i>	ubiquitin specific peptidase 49	4.43E-03	1.54
TC0X00011291.hg.1	<i>PAGE2</i>	P antigen family, member 2 (prostate associated)	4.94E-03	1.54
TC0700013471.hg.1	<i>MGAM</i>	maltase-glucoamylase	9.81E-03	1.54
TC1600009545.hg.1	<i>ABCC6</i>	ATP binding cassette subfamily C member 6	7.14E-03	1.52
TC1700008328.hg.1	<i>STXBP4</i>	syntaxin binding protein 4	8.74E-03	1.52
TC0100009274.hg.1	<i>AMY1C</i>	amylase, alpha 1C (salivary)	1.64E-03	1.52
HTA2-neg-47420204_st	NA	NA	7.74E-03	1.52
TC2000007094.hg.1	<i>TTLL9</i>	tubulin tyrosine ligase-like family member 9	8.91E-03	1.52
TC0200006537.hg.1	<i>COLEC11</i>	collectin subfamily member 11	4.33E-03	1.51
HTA2-neg-47420566_st	NA	NA	5.80E-03	1.51
TC0700008063.hg.1	<i>SPDYE5</i>	speedy/RINGO cell cycle regulator family member E5	4.83E-03	1.51
AFFX-BioB-3_at	NA	NA	8.91E-03	1.50
TC1400009924.hg.1	<i>EML5</i>	echinoderm microtubule associated protein like 5	1.01E-03	1.50
TC0X00007371.hg.1	<i>PAGE2B</i>	P antigen family, member 2B	6.90E-03	1.50

Supplementary Table 3: Double treatment versus control: Differentially expressed genes

Probe ID	Symbol	Gene name	P value	Fold change

TC1200011845.hg.1	<i>SELPLG</i>	selectin P ligand	3.20E -05	10.41
TC0500007292.hg.1	<i>NIM1K</i>	NIM1 serine/threonine protein kinase	1.68E -04	7.65
TC1200012643.hg.1	<i>ERBB3</i>	erb-b2 receptor tyrosine kinase 3	2.44E -04	6.27
HTA2-neg-47422282_st	NA	NA	2.93E -05	6.10
HTA2-neg-47424007_st	NA	NA	5.54E -03	5.81
TC1400006697.hg.1	<i>DHRS2</i>	dehydrogenase/reductase (SDR family) member 2	1.08E -03	5.21
TC0X00007013.hg.1	<i>MPC1L</i>	mitochondrial pyruvate carrier 1-like	1.95E -04	5.11
TC0300014032.hg.1	<i>POPDC2</i>	popeye domain containing 2	3.09E -06	5.07
TC0600014190.hg.1	<i>ZC2HC1B</i>	zinc finger, C2HC-type containing 1B	1.75E -03	4.98
23076543	NA	NA	3.55E -05	4.76
HTA2-neg-47424020_st	NA	NA	2.71E -03	4.64
TC0600007262.hg.1	<i>HIST1H3A</i>	histone cluster 1, H3a	1.27E -05	4.35
TC0700013472.hg.1	<i>MGAM</i>	maltase-glucoamylase	4.35E -07	4.35
TC1900006977.hg.1	<i>ICAM1</i>	intercellular adhesion molecule 1	5.47E -04	4.34
HTA2-neg-47424041_st	NA	NA	6.56E -03	4.24
TC0300012007.hg.1	<i>CD200R1</i>	CD200 receptor 1	2.64E -05	4.19
TC1300008048.hg.1	<i>TEX29</i>	testis expressed 29	4.70E -05	4.02
TC1000006911.hg.1	<i>TMEM236</i>	transmembrane protein 236	4.96E -04	4.02

APPENDIX

TC1700008673.hg.1	<i>CACNG5</i>	calcium channel, voltage-dependent, gamma subunit 5	5.13E -03	3.90
TC0400008240.hg.1	<i>DAPP1</i>	dual adaptor of phosphotyrosine and 3-phosphoinositides	1.20E -03	3.79
TC0600012064.hg.1	<i>GCM1</i>	glial cells missing homolog 1 (Drosophila)	9.66E -06	3.76
TC0300014084.hg.1	<i>CRYGS</i>	crystallin gamma S	1.84E -04	3.70
TC1100009075.hg.1	<i>NCAM1</i>	Transcript Identified by AceView, Entrez Gene ID(s) 4684	2.50E -03	3.60
TC1200007053.hg.1	<i>SPX</i>	spexin hormone	1.37E -03	3.57
TC1200008686.hg.1	<i>CHST11</i>	Transcript Identified by AceView, Entrez Gene ID(s) 50515	4.36E -04	3.55
TC0700009411.hg.1	<i>MGAM2</i>	maltase-glucoamylase 2 (putative)	8.58E -06	3.54
TC1600006593.hg.1	<i>RAB26</i>	RAB26, member RAS oncogene family	1.09E -04	3.49
TC1600007147.hg.1	<i>TMEM159</i>	transmembrane protein 159	3.01E -06	3.45
TC0700008495.hg.1	<i>BUD31</i>	Transcript Identified by AceView, Entrez Gene ID(s) 8896	1.86E -06	3.44
TC1300010039.hg.1	<i>NEK5</i>	NIMA-related kinase 5	9.38E -05	3.44
TC1900009240.hg.1	<i>GNG7</i>	guanine nucleotide binding protein (G protein), gamma 7	1.29E -03	3.43
TC1100007216.hg.1	<i>PRRG4</i>	proline rich Gla (G-carboxyglutamic acid) 4 (transmembrane)	5.05E -06	3.43
TC0300009412.hg.1	<i>SERPINI1</i>	serpin peptidase inhibitor, clade I (neuroserpin), member 1	2.50E -04	3.43
23070242	NA	NA	2.16E -05	3.42

TC1100010123.hg.1	<i>DKK3</i>	dickkopf WNT signaling pathway inhibitor 3	1.03E -05	3.40
TC2000009964.hg.1	<i>SDCBP2</i>	syndecan binding protein (syntenin) 2	1.52E -06	3.38
TC0600009597.hg.1	<i>TNFAIP3</i>	tumor necrosis factor, alpha-induced protein 3	2.28E -03	3.38
TC1600008712.hg.1	<i>IRF8</i>	interferon regulatory factor 8	2.21E -04	3.36
TC0600011133.hg.1	<i>HIST1H2BE</i>	Memczak2013 ANTISENSE, CDS, coding, upstream_start, UTR3, UTR5 best transcript NM_003523	2.35E -03	3.32
TC0500007077.hg.1	<i>NPR3</i>	natriuretic peptide receptor 3	2.45E -04	3.31
HTA2-pos-47421925_st	NA	NA	6.55E -04	3.29
HTA2-neg-47422060_st	NA	NA	1.27E -04	3.28
TC2000009905.hg.1	<i>EFCAB8</i>	EF-hand calcium binding domain 8	2.75E -03	3.28
TC0700010899.hg.1	<i>POLR2J4</i>	polymerase (RNA) II (DNA directed) polypeptide J4, pseudogene	1.19E -05	3.25
TC0700008506.hg.1	<i>CYP3A43</i>	cytochrome P450, family 3, subfamily A, polypeptide 43	5.94E -05	3.21
TC1500010745.hg.1	<i>POLR2M</i>	polymerase (RNA) II (DNA directed) polypeptide M	1.38E -04	3.21
TC0900008222.hg.1	<i>STX17</i>	syntaxin 17	5.78E -04	3.21
HTA2-neg-47424360_st	NA	NA	5.25E -03	3.20
TC1900010016.hg.1	<i>ISYNA1</i>	inositol-3-phosphate synthase 1	7.99E -06	3.15
TC0300009916.hg.1	<i>HES1</i>	hes family bHLH transcription factor 1	1.59E -05	3.15

APPENDIX

TC1300008813.hg.1	<i>KCTD4</i>	potassium channel tetramerization domain containing 4	3.33E -04	3.11
TC0X00009025.hg.1	<i>ANOS1</i>	anosmin 1	3.78E -04	3.11
TC0600007263.hg.1	<i>HIST1H4A</i>	histone cluster 1, H4a	3.23E -04	3.10
TC0500012017.hg.1	<i>IRF1</i>	interferon regulatory factor 1	6.72E -03	3.08
TC2100008297.hg.1	<i>SIK1</i>	salt-inducible kinase 1	7.91E -03	3.08
TC1700010550.hg.1	<i>C17orf98</i>	chromosome 17 open reading frame 98	3.17E -05	3.07
TC0600014151.hg.1	<i>SMIM8</i>	small integral membrane protein 8	2.24E -03	3.03
HTA2-neg-47424044_st	NA	NA	1.79E -03	3.02
TC0800010802.hg.1	<i>C8orf89</i>	chromosome 8 open reading frame 89	1.26E -03	3.01
TC0400012977.hg.1	<i>SH3D19</i>	SH3 domain containing 19	6.80E -05	3.00
HTA2-pos-47421982_st	NA	NA	1.39E -04	3.00
HTA2-neg-47421192_st	NA	NA	1.32E -04	2.97
TC0700013525.hg.1	<i>FAM126A</i>	family with sequence similarity 126, member A	1.34E -04	2.97
TC0600007274.hg.1	<i>HIST1H2BD</i>	histone cluster 1, H2bd	1.80E -06	2.96
TC0700013424.hg.1	GS1-259H13.2	transmembrane protein 225-like	7.98E -06	2.96
HTA2-neg-47423838_st	NA	NA	1.24E -04	2.94
HTA2-pos-3475282_st	NA	NA	4.40E -03	2.93
TC1900008931.hg.1	<i>RFPL4A</i>	ret finger protein-like 4A	9.34E -03	2.89

TC0100009442.hg.1	<i>WNT2B</i>	wingless-type MMTV integration site family, member 2B	3.41E -05	2.86
TC0700013587.hg.1	<i>SHFM1</i>	split hand/foot malformation (ectrodactyly) type 1	5.20E -04	2.85
TC1700008635.hg.1	<i>RGS9</i>	regulator of G-protein signaling 9	7.85E -03	2.84
HTA2-pos-47421926_st	NA	NA	5.49E -04	2.83
HTA2-pos-47421981_st	NA	NA	4.89E -04	2.83
TC1300006676.hg.1	<i>RASL11A</i>	RAS-like, family 11, member A	4.69E -04	2.82
TC2200008513.hg.1	<i>RFPL3S</i>	RFPL3 antisense	1.23E -05	2.80
TSUnmapped00000401.hg.1	<i>INPP5D</i>	inositol polyphosphate-5-phosphatase D	4.09E -03	2.80
TC0900008219.hg.1	<i>NR4A3</i>	nuclear receptor subfamily 4, group A, member 3	7.69E -04	2.79
HTA2-pos-PSR02023992.hg.1	NA	NA	4.80E -04	2.78
TC0100011378.hg.1	<i>RASSF5</i>	Ras association (RaIGDS/AF-6) domain family member 5	4.44E -05	2.76
TC0200009078.hg.1	<i>EPB41L5</i>	erythrocyte membrane protein band 4.1 like 5	4.98E -04	2.76
TC0600007293.hg.1	<i>HIST1H2BI</i>	histone cluster 1, H2bi	5.82E -04	2.76
TC0X00008747.hg.1	<i>GABRQ</i>	gamma-aminobutyric acid (GABA) A receptor, theta	7.57E -05	2.69
TC1900006588.hg.1	<i>GADD45B</i>	growth arrest and DNA-damage-inducible, beta	5.25E -05	2.67
TC1000007895.hg.1	<i>TSPAN15</i>	tetraspanin 15	9.53E -04	2.67
TC0200016661.hg.1	<i>C2orf61</i>	chromosome 2 open reading frame 61	3.31E -04	2.67

APPENDIX

TC0700013442.hg.1	<i>LSMEM1</i>	leucine-rich single-pass membrane protein 1	1.54E -04	2.66
HTA2-neg-47423602_st	NA	NA	2.51E -03	2.66
TC2000007202.hg.1	<i>ACSS2</i>	acyl-CoA synthetase short-chain family member 2	6.92E -03	2.64
TC1900010782.hg.1	<i>ATP1A3</i>	ATPase, Na+/K+ transporting, alpha 3 polypeptide	6.50E -06	2.64
HTA2-pos-2960249_st	NA	NA	1.40E -04	2.64
TC0600010797.hg.1	<i>MAK</i>	male germ cell-associated kinase	2.98E -04	2.63
TC0700013601.hg.1	<i>RASA4B</i>	RAS p21 protein activator 4B	1.38E -04	2.63
TC0700013603.hg.1	<i>RASA4</i>	RAS p21 protein activator 4	3.72E -04	2.61
TC0900012173.hg.1	<i>GARNL3</i>	GTPase activating Rap/RanGAP domain-like 3	7.49E -05	2.61
TC0100009913.hg.1	<i>ADAMTSL4</i>	ADAMTS like 4	9.37E -05	2.60
TC2200007132.hg.1	<i>RFPL3</i>	ret finger protein-like 3	7.23E -04	2.60
TC0600012502.hg.1	<i>GJB7</i>	gap junction protein beta 7	2.05E -05	2.59
TC1600008661.hg.1	<i>CRISPLD2</i>	cysteine-rich secretory protein LCCL domain containing 2	1.11E -04	2.59
TC1400010749.hg.1	<i>LINC01599</i>	long intergenic non-protein coding RNA 1599	4.26E -04	2.58
TC0400008389.hg.1	<i>RRH</i>	retinal pigment epithelium-derived rhodopsin homolog	4.16E -05	2.57
TC1900011817.hg.1	<i>ZNF773</i>	zinc finger protein 773	6.35E -06	2.57
TC0500007050.hg.1	<i>PDZD2</i>	PDZ domain containing 2	2.18E -05	2.57

TC0100018207.hg.1	<i>TSSK3</i>	testis-specific serine kinase 3	6.36E -04	2.55
TC0200007458.hg.1	<i>EPAS1</i>	endothelial PAS domain protein 1	1.13E -03	2.55
HTA2-neg-47424241_st	NA	NA	1.99E -03	2.55
TC0400008390.hg.1	<i>LRIT3</i>	leucine-rich repeat, immunoglobulin-like and transmembrane domains 3	5.28E -05	2.55
TC0100014191.hg.1	<i>RAB3B</i>	RAB3B, member RAS oncogene family	3.08E -04	2.51
TSUnmapped00000108.hg.1	<i>RPS6KA1</i>	ribosomal protein S6 kinase, 90kDa, polypeptide 1	3.97E -05	2.50
TC0300012771.hg.1	<i>TM4SF18</i>	Transcript Identified by AceView, Entrez Gene ID(s) 116441	2.76E -03	2.50
TC1700011905.hg.1	<i>DNAH17</i>	dynein, axonemal, heavy chain 17	2.70E -03	2.50
TC2000009886.hg.1	<i>PANK2</i>	pantothenate kinase 2	2.55E -05	2.50
TC0100009936.hg.1	<i>BNIPL</i>	BCL2/adenovirus E1B 19kD interacting protein like	3.58E -05	2.49
TC0300007050.hg.1	<i>C3orf35</i>	chromosome 3 open reading frame 35	6.45E -05	2.49
TC1500010744.hg.1	<i>GCOM1</i>	GRINL1A complex locus 1	6.20E -05	2.48
TC0200013595.hg.1	<i>MGAT4A</i>	mannosyl (alpha-1,3)-glycoprotein beta-1,4-N-acetylglucosaminyltransferase, isozyme A	3.55E -04	2.48
TC0500008785.hg.1	<i>EGR1</i>	early growth response 1	3.38E -04	2.48
TC0400007360.hg.1	<i>DCAF4L1</i>	DDB1 and CUL4 associated factor 4-like 1	1.24E -03	2.46
TC0500008356.hg.1	<i>KCNN2</i>	potassium channel, calcium activated intermediate/small conductance subfamily N alpha, member 2	1.10E -03	2.46

APPENDIX

TC1500009606.hg.1	<i>MYO1E</i>	Transcript Identified by AceView, Entrez Gene ID(s) 4643	1.80E -03	2.46
TC0900007069.hg.1	<i>C9orf131</i>	chromosome 9 open reading frame 131	2.26E -03	2.46
HTA2-pos-47421984_st	NA	NA	1.59E -03	2.45
TC0500013280.hg.1	<i>ZDHHC11B</i>	zinc finger, DHHC-type containing 11B	4.91E -04	2.45
TC1900008826.hg.1	<i>CACNG7</i>	calcium channel, voltage-dependent, gamma subunit 7	2.17E -04	2.45
TC0500007895.hg.1	<i>CMY45</i>	cardiomyopathy associated 5	1.40E -05	2.44
TC1700006763.hg.1	<i>ATP1B2</i>	ATPase, Na+/K+ transporting, beta 2 polypeptide	7.63E -05	2.44
TC1500007409.hg.1	<i>GCNT3</i>	glucosaminyl (N-acetyl) transferase 3, mucin type	8.31E -04	2.44
HTA2-pos-47421983_st	NA	NA	1.04E -03	2.44
TC1000009535.hg.1	<i>IDI2</i>	isopentenyl-diphosphate delta isomerase 2	4.19E -03	2.43
HTA2-neg-47423726_st	NA	NA	2.18E -04	2.42
TC2000008910.hg.1	<i>EIF2S2</i>	Zhang2013 ALT_ACCEPTOR, ALT_DONOR, coding, INTERNAL, intronic best transcript NM_003908	6.47E -03	2.42
TC1500009998.hg.1	<i>GOLGA6A</i>	golgin A6 family, member A	2.79E -04	2.42
TC1400007443.hg.1	<i>HSPA2</i>	heat shock 70kDa protein 2	1.33E -03	2.42
23067837	NA	NA	3.87E -04	2.41
TC0200015869.hg.1	<i>AP1S3</i>	adaptor-related protein complex 1 sigma 3 subunit	4.36E -03	2.41

TC0200006627.hg.1	<i>ID2</i>	inhibitor of DNA binding 2, dominant negative helix-loop-helix protein	2.47E -03	2.41
TC0100008334.hg.1	<i>ZYG11A</i>	zyg-11 family member A, cell cycle regulator	2.69E -03	2.39
TC1400010637.hg.1	<i>C14orf178</i>	chromosome 14 open reading frame 178	4.00E -04	2.39
TC0800010685.hg.1	<i>MYBL1</i>	v-myb avian myeloblastosis viral oncogene homolog-like 1	2.08E -04	2.39
TC0700009472.hg.1	<i>EPHB6</i>	EPH receptor B6	9.75E -04	2.39
TC1100010505.hg.1	<i>ABTB2</i>	ankyrin repeat and BTB (POZ) domain containing 2	2.00E -04	2.38
TC1100007729.hg.1	<i>DTX4</i>	deltex 4, E3 ubiquitin ligase	1.83E -05	2.38
TC0200015226.hg.1	<i>HIBCH</i>	Transcript Identified by AceView, Entrez Gene ID(s) 26275	5.24E -05	2.37
TC0200007048.hg.1	<i>MAPRE3</i>	microtubule-associated protein, RP/EB family, member 3	1.04E -04	2.37
TC0100018485.hg.1	<i>ADAMTSL4-AS1</i>	ADAMTSL4 antisense RNA 1	1.06E -04	2.37
TC0300008853.hg.1	<i>TMEM108</i>	transmembrane protein 108	4.22E -04	2.37
TC1500010369.hg.1	<i>MFGE8</i>	milk fat globule-EGF factor 8 protein	3.05E -05	2.36
TC0500008654.hg.1	<i>LEAP2</i>	liver expressed antimicrobial peptide 2	9.14E -05	2.36
TC0900008793.hg.1	<i>ZBTB34</i>	zinc finger and BTB domain containing 34	1.57E -04	2.36
TC0200015402.hg.1	<i>FAM126B</i>	family with sequence similarity 126, member B	4.93E -05	2.36
TC0200006671.hg.1	<i>GRHL1</i>	grainyhead-like transcription factor 1	1.27E -03	2.35

APPENDIX

TC1000010432.hg.1	<i>RASGEF1A</i>	RasGEF domain family member 1A	7.47E -03	2.35
TC1500007615.hg.1	<i>MAP2K1</i>	Transcript Identified by AceView, Entrez Gene ID(s) 5604	6.38E -05	2.35
TC0500012588.hg.1	<i>HAVCR1</i>	hepatitis A virus cellular receptor 1	8.22E -04	2.35
TC0X00006593.hg.1	<i>CLCN4</i>	chloride channel, voltage-sensitive 4	8.48E -06	2.35
HTA2-neg-47423769_st	NA	NA	6.85E -03	2.35
TC0X00007562.hg.1	<i>ITGB1BP2</i>	integrin beta 1 binding protein (melusin) 2	5.22E -05	2.35
HTA2-neg-47422979_st	NA	NA	7.60E -03	2.34
TC1900007399.hg.1	<i>TMEM59L</i>	transmembrane protein 59-like	7.47E -04	2.33
TC1200012711.hg.1	<i>LINC00173</i>	long intergenic non-protein coding RNA 173	6.26E -04	2.33
TC0200008870.hg.1	<i>BCL2L11</i>	BCL2-like 11 (apoptosis facilitator)	1.18E -04	2.33
TC1200008683.hg.1	<i>CHST11</i>	carbohydrate (chondroitin 4) sulfotransferase 11	2.58E -04	2.33
TC0300009279.hg.1	<i>KCNAB1</i>	potassium channel, voltage gated subfamily A regulatory beta subunit 1	4.83E -04	2.33
TC0600006870.hg.1	<i>SNRNP48</i>	small nuclear ribonucleoprotein, U11/U12 48KDa subunit	3.14E -04	2.33
TC2000007094.hg.1	<i>TTLL9</i>	tubulin tyrosine ligase-like family member 9	3.11E -05	2.33
TC0100017844.hg.1	<i>NID1</i>	nidogen 1	1.98E -03	2.33
TC0700011924.hg.1	<i>TMEM130</i>	transmembrane protein 130	6.06E -03	2.33
TC0400011043.hg.1	<i>CDKL2</i>	cyclin-dependent kinase-like 2 (CDC2-related kinase)	4.82E -04	2.32

TC0300011525.hg.1	<i>RYBP</i>	RING1 and YY1 binding protein	2.65E -03	2.32
TC1400008622.hg.1	<i>OR5AU1</i>	olfactory receptor, family 5, subfamily AU, member 1	3.22E -03	2.32
TC0200008894.hg.1	<i>MERTK</i>	MER proto-oncogene, tyrosine kinase	9.13E -04	2.32
TC1900006602.hg.1	<i>ZNF555</i>	zinc finger protein 555	5.75E -04	2.32
TC0100009341.hg.1	<i>KIAA1324</i>	KIAA1324	1.97E -03	2.32
TC1100009242.hg.1	<i>ABCG4</i>	ATP binding cassette subfamily G member 4	1.40E -04	2.32
TC0500013282.hg.1	<i>ZDHHC11</i>	zinc finger, DHHC-type containing 11	3.27E -04	2.32
TC0600014152.hg.1	<i>LINC01590</i>	long intergenic non-protein coding RNA 1590	5.75E -04	2.31
TC1900010375.hg.1	<i>RHPN2</i>	rhophilin, Rho GTPase binding protein 2	9.80E -03	2.31
TC0400011973.hg.1	<i>CLGN</i>	calmegin	2.06E -04	2.31
TC1400008415.hg.1	<i>ZFYVE21</i>	zinc finger, FYVE domain containing 21	1.27E -05	2.31
HTA2-neg-47422085_st	NA	NA	1.19E -03	2.31
TC0500011296.hg.1	<i>ACOT12</i>	acyl-CoA thioesterase 12	3.29E -05	2.31
TC0100015436.hg.1	<i>SPAG17</i>	sperm associated antigen 17	5.37E -04	2.31
TC1600009944.hg.1	<i>KCTD13</i>	potassium channel tetramerization domain containing 13	6.81E -05	2.29
TC0200008268.hg.1	<i>GNLY</i>	granulysin	1.71E -04	2.29
HTA2-pos-3295162_st	NA	NA	8.25E -03	2.29

APPENDIX

TC2000007177.hg.1	<i>RALY</i>	Jeck2013 ALT_DONOR, coding, INTERNAL, intronic best transcript NM_016732	3.72E -03	2.28
TC1600008638.hg.1	<i>DNAAF1</i>	dynein, axonemal, assembly factor 1	2.92E -03	2.28
TC1700011436.hg.1	<i>ERN1</i>	endoplasmic reticulum to nucleus signaling 1	3.01E -03	2.28
TC0X00011174.hg.1	<i>PDZD4</i>	PDZ domain containing 4	1.18E -03	2.27
TC0100015789.hg.1	<i>POGZ</i>	Transcript Identified by AceView, Entrez Gene ID(s) 23126	2.33E -03	2.27
HTA2-pos-PSR02023993.hg.1	NA	NA	1.05E -03	2.27
TC1200009734.hg.1	<i>VAMP1</i>	vesicle associated membrane protein 1	1.08E -03	2.27
TC0600011234.hg.1	<i>HIST1H4L</i>	histone cluster 1, H4I	4.44E -03	2.27
TC1200012111.hg.1	<i>TAOK3</i>	TAO kinase 3	3.49E -03	2.27
TC0700012099.hg.1	<i>RASA4</i>	Salzman2013 ALT_ACCEPTOR, ALT_DONOR, coding, INTERNAL, intronic best transcript NM_006989	6.29E -04	2.25
TC1500010886.hg.1	<i>CALML4</i>	calmodulin-like 4	4.07E -05	2.24
TC0400007876.hg.1	<i>THAP6</i>	THAP domain containing 6	3.51E -04	2.24
TC2000009945.hg.1	<i>FAM209A</i>	family with sequence similarity 209, member A	8.35E -04	2.24
TC0900010808.hg.1	<i>BICD2</i>	bicaudal D homolog 2 (Drosophila)	8.64E -04	2.24
TC0400010618.hg.1	<i>TEC</i>	tec protein tyrosine kinase	2.31E -04	2.24
TC1700011117.hg.1	<i>LINC00483</i>	long intergenic non-protein coding RNA 483	6.76E -06	2.24

TC1500010157.hg.1	<i>ADAMTS7</i>	ADAM metallopeptidase with thrombospondin type 1 motif 7	1.51E -04	2.23
TC1700009746.hg.1	<i>MYH3</i>	myosin, heavy chain 3, skeletal muscle, embryonic	3.64E -04	2.23
TC1200007359.hg.1	<i>CNTN1</i>	contactin 1	4.86E -03	2.22
TC0100013610.hg.1	<i>FAM229A</i>	family with sequence similarity 229, member A	5.26E -05	2.22
TC0500009984.hg.1	<i>FLJ33360</i>	FLJ33360 protein	2.39E -03	2.22
TC1700009318.hg.1	<i>FAM101B</i>	family with sequence similarity 101, member B	2.16E -03	2.22
TC1900009603.hg.1	<i>OLFM2</i>	olfactomedin 2	2.99E -04	2.21
TC0200010837.hg.1	<i>ANKZF1</i>	ankyrin repeat and zinc finger domain containing 1	1.44E -03	2.21
TC0100018418.hg.1	<i>IFFO2</i>	intermediate filament family orphan 2	3.33E -03	2.20
TC0200010586.hg.1	<i>CPO</i>	carboxypeptidase O	1.32E -03	2.20
TC0600008166.hg.1	<i>SLC25A27</i>	solute carrier family 25, member 27	3.61E -03	2.20
TC1800008281.hg.1	<i>TMEM241</i>	transmembrane protein 241	1.14E -03	2.19
23076546	NA	NA	2.64E -03	2.19
TC0500008541.hg.1	<i>TEX43</i>	testis expressed 43	1.53E -03	2.19
TC0100012465.hg.1	<i>CPSF3L</i>	cleavage and polyadenylation specific factor 3-like	1.27E -04	2.19
TSUnmapped00000109.hg.1	<i>ATG16L1</i>	autophagy related 16-like 1	7.09E -04	2.18
TC0500009521.hg.1	<i>CPEB4</i>	cytoplasmic polyadenylation element binding protein 4	4.18E -04	2.18
TC2100006659.hg.1	<i>CXADR</i>	coxsackie virus and adenovirus receptor	1.83E -04	2.18

APPENDIX

TC0X00009576.hg.1	<i>SYN1</i>	synapsin I	2.07E -03	2.18
TC2100007599.hg.1	<i>SAMSN1</i>	SAM domain, SH3 domain and nuclear localization signals 1	7.36E -04	2.17
TC0100015586.hg.1	<i>PDZK1</i>	PDZ domain containing 1	6.45E -04	2.17
TC1100012352.hg.1	<i>TMPRSS5</i>	transmembrane protease, serine 5	3.00E -03	2.17
TC1100012389.hg.1	<i>CADM1</i>	cell adhesion molecule 1	1.41E -04	2.17
TC0200012071.hg.1	<i>UCN</i>	urocortin	1.71E -05	2.17
HTA2-neg-47423694_st	NA	NA	1.48E -03	2.17
TC1200007108.hg.1	<i>KRAS</i>	Memczak2013 ANTISENSE, coding, INTERNAL, intronic best transcript NM_033360	6.16E -05	2.16
TC1400008615.hg.1	<i>NDRG2</i>	NDRG family member 2	2.52E -03	2.16
TC1100006576.hg.1	<i>CD81</i>	CD81 molecule	8.41E -05	2.16
TC1500010712.hg.1	<i>GOLGA8N</i>	golgin A8 family, member N	1.07E -03	2.16
TC0200012977.hg.1	<i>MXD1</i>	Memczak2013 ANTISENSE, coding, INTERNAL, intronic best transcript NM_001202514	4.22E -03	2.16
TSUnmapped00000141.hg.1	<i>HMBS</i>	hydroxymethylbilane synthase	9.91E -04	2.15
TC0900011501.hg.1	<i>NR6A1</i>	nuclear receptor subfamily 6, group A, member 1	7.18E -04	2.15
TC1300010007.hg.1	<i>TMEM255B</i>	transmembrane protein 255B	4.25E -04	2.14
TC0100013578.hg.1	<i>ADGRB2</i>	adhesion G protein-coupled receptor B2	1.01E -03	2.14

TC2200007525.hg.1	<i>SERHL2</i>	serine hydrolase-like 2	2.06E -04	2.14
HTA2-pos-3145790_st	NA	NA	1.17E -03	2.14
HTA2-pos-47422721_st	NA	NA	1.02E -04	2.14
TC0900008795.hg.1	<i>RALGPS1</i>	Ral GEF with PH domain and SH3 binding motif 1	4.71E -05	2.14
TC0100010609.hg.1	<i>DNM3</i>	dynamin 3	1.99E -03	2.13
TC1500007972.hg.1	<i>CRABP1</i>	cellular retinoic acid binding protein 1	1.07E -04	2.13
TC1700006813.hg.1	<i>ODF4</i>	outer dense fiber of sperm tails 4	9.68E -03	2.13
TC0100008052.hg.1	<i>CFAP57</i>	cilia and flagella associated protein 57	8.39E -04	2.13
TC0600007375.hg.1	<i>HIST1H3H</i>	histone cluster 1, H3h	2.10E -03	2.12
TC1500010769.hg.1	<i>GOLGA6C</i>	golgin A6 family, member C	1.56E -03	2.12
TC1700010198.hg.1	<i>UNC119</i>	unc-119 lipid binding chaperone	2.01E -05	2.12
TC0700012296.hg.1	<i>C7orf60</i>	chromosome 7 open reading frame 60	1.05E -03	2.12
TC0100015271.hg.1	<i>OVGP1</i>	oviductal glycoprotein 1	6.50E -04	2.12
TC0400010519.hg.1	<i>APBB2</i>	amyloid beta (A4) precursor protein-binding, family B, member 2	2.36E -03	2.11
TC0700010644.hg.1	<i>CRHR2</i>	corticotropin releasing hormone receptor 2	2.92E -04	2.11
TC0200007418.hg.1	<i>SLC3A1</i>	solute carrier family 3 (amino acid transporter heavy chain), member 1	7.54E -04	2.11
TC0600007792.hg.1	<i>PPARD</i>	peroxisome proliferator-activated receptor delta	1.33E -03	2.11

APPENDIX

TC0600014246.hg.1	<i>C6orf229</i>	chromosome 6 open reading frame 229	2.20E -03	2.11
TC2000008242.hg.1	<i>RNF24</i>	ring finger protein 24	9.31E -04	2.10
TC1500010770.hg.1	<i>GOLGA6D</i>	golgin A6 family, member D	9.51E -04	2.10
TC0900011660.hg.1	<i>CCBL1</i>	cysteine conjugate-beta lyase, cytoplasmic	5.60E -03	2.10
TC2000007670.hg.1	<i>SNAI1</i>	snail family zinc finger 1	1.36E -04	2.10
TC0500013088.hg.1	<i>MAPK9</i>	mitogen-activated protein kinase 9	8.50E -04	2.10
TC1400009617.hg.1	<i>DPF3</i>	D4, zinc and double PHD fingers, family 3	3.20E -03	2.09
HTA2-neg-47424023_st	NA	NA	1.65E -04	2.09
TC0100012089.hg.1	<i>GPR137B</i>	G protein-coupled receptor 137B	1.63E -03	2.09
TC0600011125.hg.1	<i>HIST1H2AB</i>	histone cluster 1, H2ab	4.98E -03	2.09
TC0400008331.hg.1	<i>NPNT</i>	nephronectin	3.91E -05	2.09
TC0200007746.hg.1	<i>B3GNT2</i>	UDP-GlcNAc:betaGal beta-1,3-N-acetylglucosaminyltransferase 2	3.08E -04	2.08
TC1000012525.hg.1	<i>ACBD7</i>	acyl-CoA binding domain containing 7	5.07E -03	2.08
TC0800011861.hg.1	<i>LRRC6</i>	leucine rich repeat containing 6	2.56E -03	2.08
TC0200011040.hg.1	<i>ITM2C</i>	integral membrane protein 2C	3.91E -04	2.08
TC1200009547.hg.1	<i>SLC6A13</i>	solute carrier family 6 (neurotransmitter transporter), member 13	4.02E -05	2.08
TC0900006559.hg.1	<i>CD274</i>	CD274 molecule	5.66E -03	2.07

TC1500008183.hg.1	<i>GOLGA6L3</i>	golgin A6 family-like 3	1.67E -03	2.07
HTA2-neg-47422090_st	NA	NA	3.20E -03	2.07
TC1900010855.hg.1	<i>CADM4</i>	cell adhesion molecule 4	9.90E -05	2.07
TC0500013260.hg.1	<i>MFAP3</i>	microfibrillar associated protein 3	1.31E -03	2.07
TC0100014127.hg.1	<i>SPATA6</i>	spermatogenesis associated 6	6.65E -04	2.06
TC0100018249.hg.1	<i>AMY2B</i>	amylase, alpha 2B (pancreatic)	1.28E -04	2.06
TC0900012276.hg.1	<i>SCAI</i>	suppressor of cancer cell invasion	4.67E -05	2.06
TC1900011814.hg.1	<i>ZNF17</i>	zinc finger protein 17	4.08E -05	2.06
TC0200009829.hg.1	<i>GCA</i>	grancalcin, EF-hand calcium binding protein	4.39E -04	2.06
TC1100008188.hg.1	<i>PPP6R3</i>	Memczak2013 ALT_ACCEPTOR, ALT_DONOR, coding, INTERNAL, intronic best transcript NM_001164162	5.65E -04	2.05
TC2000008211.hg.1	<i>UBOX5</i>	U-box domain containing 5	1.73E -04	2.05
TC0100018360.hg.1	<i>DISC1</i>	disrupted in schizophrenia 1	1.44E -04	2.05
TC1900009756.hg.1	<i>SYCE2</i>	synaptonemal complex central element protein 2	9.40E -04	2.05
23076544	NA	NA	5.62E -05	2.04
TC1100012382.hg.1	<i>NXPE4</i>	neurexophilin and PC-esterase domain family, member 4	1.26E -03	2.04
TC0200007038.hg.1	<i>DRC1</i>	dynein regulatory complex subunit 1	3.53E -04	2.04

APPENDIX

TC1500010915.hg.1	<i>GOLGA6L5P</i>	golgin A6 family-like 5, pseudogene	1.15E -03	2.04
TC1200009220.hg.1	<i>CCDC62</i>	coiled-coil domain containing 62	6.11E -05	2.03
TC2000008268.hg.1	<i>SLC23A2</i>	solute carrier family 23 (ascorbic acid transporter), member 2	2.50E -03	2.03
TC0500008619.hg.1	<i>IL3</i>	interleukin 3	6.71E -03	2.03
AFFX-DapX-M_st	NA	NA	7.90E -05	2.03
TC0200011450.hg.1	<i>FAM150B</i>	family with sequence similarity 150, member B	2.77E -05	2.03
TC1100011629.hg.1	<i>XRRA1</i>	X-ray radiation resistance associated 1	8.89E -04	2.03
TC0100014910.hg.1	<i>TGFB3R</i>	transforming growth factor beta receptor III	1.19E -03	2.03
TC0800007529.hg.1	<i>SPIDR</i>	scaffolding protein involved in DNA repair	8.52E -04	2.03
TC0100017018.hg.1	<i>ETNK2</i>	ethanolamine kinase 2	9.90E -03	2.02
HTA2-neg-47424705_st	NA	NA	5.11E -04	2.02
TC1600006893.hg.1	<i>CLEC16A</i>	C-type lectin domain family 16, member A	4.47E -05	2.02
TC0700013323.hg.1	<i>SUN1</i>	Sad1 and UNC84 domain containing 1	1.86E -03	2.02
TC1600010000.hg.1	<i>STX1B</i>	syntaxin 1B	1.19E -03	2.01
TC0500007231.hg.1	<i>PTGER4</i>	prostaglandin E receptor 4 (subtype EP4)	5.20E -05	2.01
TC1300008253.hg.1	<i>CRYL1</i>	crystallin lambda 1	1.34E -03	2.01
TC0100018261.hg.1	<i>GSTM4</i>	glutathione S-transferase mu 4	5.69E -04	2.01
AFFX-r2-Bs-dap-3_st	NA	NA	5.12E -05	2.01

TC1900008287.hg.1	<i>PVRL2</i>	poliovirus receptor-related 2 (herpesvirus entry mediator B)	4.73E -04	2.00
TC1200007594.hg.1	<i>ASIC1</i>	acid sensing ion channel 1	5.28E -04	2.00
TC0100018262.hg.1	<i>GSTM2</i>	glutathione S-transferase mu 2 (muscle)	1.37E -03	2.00
AFFX-r2-Bs-phe-3_st	NA	NA	6.06E -04	2.00
TC0700008063.hg.1	<i>SPDYE5</i>	speedy/RINGO cell cycle regulator family member E5	8.93E -04	2.00
TC1200011993.hg.1	<i>SLC8B1</i>	solute carrier family 8 (sodium/lithium/calcium exchanger), member B1	1.18E -03	1.99
TC0200014620.hg.1	<i>CACNB4</i>	calcium channel, voltage-dependent, beta 4 subunit	1.80E -03	1.99
TC1900009584.hg.1	<i>ZNF560</i>	zinc finger protein 560	1.01E -03	1.98
TC0700013604.hg.1	<i>UPK3BL</i>	uroplakin 3B-like	5.35E -05	1.98
TC1900010005.hg.1	<i>RAB3A</i>	RAB3A, member RAS oncogene family	3.74E -04	1.98
TC0100013205.hg.1	<i>ECE1</i>	endothelin converting enzyme 1	3.24E -04	1.98
TC0800012447.hg.1	<i>AZIN1</i>	antizyme inhibitor 1	4.92E -04	1.98
TC2200006827.hg.1	<i>GNAZ</i>	guanine nucleotide binding protein (G protein), alpha z polypeptide	5.38E -03	1.97
23075476	NA	NA	6.01E -04	1.97
TC0200014361.hg.1	<i>LYPD1</i>	LY6/PLAUR domain containing 1	8.58E -03	1.97
HTA2-pos-PSR01002164.hg.1	NA	NA	8.58E -04	1.97
TC0100018210.hg.1	<i>SH3D21</i>	SH3 domain containing 21	4.44E -04	1.97

APPENDIX

TC0800010926.hg.1	<i>PAG1</i>	phosphoprotein membrane anchor with glycosphingolipid microdomains 1	5.04E -04	1.97
TC0800012405.hg.1	<i>FUT10</i>	fucosyltransferase 10 (alpha (1,3) fucosyltransferase)	7.53E -04	1.96
TC0800009853.hg.1	<i>BIN3</i>	bridging integrator 3	1.19E -03	1.96
TC0X00010643.hg.1	<i>44080</i>	septin 6	8.32E -04	1.96
23075475	NA	NA	7.95E -04	1.96
TC0300010821.hg.1	<i>ULK4</i>	unc-51 like kinase 4	1.81E -03	1.95
TC1200012660.hg.1	<i>SLC35E3</i>	solute carrier family 35, member E3	7.54E -03	1.95
TC0700009036.hg.1	<i>LEP</i>	leptin	6.76E -03	1.95
AFFX-DapX-5_st	NA	NA	1.71E -04	1.95
TC0600013165.hg.1	<i>EPB41L2</i>	erythrocyte membrane protein band 4.1-like 2	1.64E -04	1.95
TC0200011504.hg.1	<i>PXDN</i>	Transcript Identified by AceView, Entrez Gene ID(s) 7837	7.39E -03	1.95
TC2000009250.hg.1	<i>PLTP</i>	phospholipid transfer protein	1.11E -04	1.95
TC1500010128.hg.1	<i>TBC1D2B</i>	TBC1 domain family, member 2B	1.59E -03	1.94
TC0X00011275.hg.1	<i>TCEANC</i>	transcription elongation factor A (SII) N-terminal and central domain containing	1.18E -03	1.94
TC1500008086.hg.1	<i>SAXO2</i>	stabilizer of axonemal microtubules 2	1.02E -04	1.94
TC2000006791.hg.1	<i>PCSK2</i>	proprotein convertase subtilisin/kexin type 2	1.80E -03	1.94
TC0100015401.hg.1	<i>IGSF3</i>	immunoglobulin superfamily, member 3	1.13E -03	1.93

TC1900007096.hg.1	<i>JUNB</i>	jun B proto-oncogene	1.20E -04	1.93
TC1700007918.hg.1	<i>AOC2</i>	amine oxidase, copper containing 2 (retina-specific)	1.03E -03	1.93
TC2200008196.hg.1	<i>MIF-AS1</i>	MIF antisense RNA 1	2.11E -03	1.93
TC0500011334.hg.1	<i>TMEM167A</i>	Transcript Identified by AceView, Entrez Gene ID(s) 153339	9.13E -03	1.93
TC2200006643.hg.1	<i>ZDHHC8</i>	zinc finger, DHHC-type containing 8	1.76E -04	1.93
TC0700011477.hg.1	<i>TRIM74</i>	tripartite motif containing 74	4.45E -04	1.93
TC1100010718.hg.1	<i>LRP4</i>	LDL receptor related protein 4	2.43E -03	1.93
TC1400007145.hg.1	<i>FRMD6</i>	FERM domain containing 6	4.80E -03	1.92
TC0800009856.hg.1	<i>EGR3</i>	early growth response 3	4.97E -03	1.92
TC1100009302.hg.1	<i>TECTA</i>	tectorin alpha	5.23E -03	1.92
TC2100007967.hg.1	<i>PAXBP1</i>	PAX3 and PAX7 binding protein 1	4.50E -05	1.92
TSUnmapped00000085.hg.1	<i>CCDC84</i>	coiled-coil domain containing 84	6.48E -04	1.92
HTA2-pos-2985880_st	NA	NA	7.98E -03	1.92
TC0100014502.hg.1	<i>WDR78</i>	WD repeat domain 78	9.66E -05	1.92
TC1100011652.hg.1	<i>GDPD5</i>	glycerophosphodiester phosphodiesterase domain containing 5	6.42E -04	1.92
TC0900010580.hg.1	<i>GKAP1</i>	G kinase anchoring protein 1	1.51E -03	1.92
TC1900009947.hg.1	<i>MYO9B</i>	Memczak2013 ANTISENSE, CDS, coding, INTERNAL best transcript NM_004145	4.21E -04	1.92

APPENDIX

TC1300006919.hg.1	<i>FREM2</i>	FRAS1 related extracellular matrix protein 2	7.09E -05	1.92
TC2000010008.hg.1	<i>NFS1</i>	NFS1 cysteine desulfurase	6.03E -05	1.92
TC1900007888.hg.1	<i>APLP1</i>	amyloid beta (A4) precursor-like protein 1	8.23E -04	1.92
HTA2-neg-47423221_st	NA	NA	4.11E -03	1.92
TC1900011734.hg.1	<i>MIA</i>	melanoma inhibitory activity	6.34E -05	1.92
TC0300012482.hg.1	<i>RAB6B</i>	RAB6B, member RAS oncogene family	4.35E -03	1.91
TC0100010526.hg.1	<i>TBX19</i>	T-box 19	3.14E -04	1.91
TC1900009867.hg.1	<i>AKAP8L</i>	A kinase (PRKA) anchor protein 8-like	8.93E -05	1.91
TC0100010281.hg.1	<i>ATP1A2</i>	ATPase, Na+/K+ transporting, alpha 2 polypeptide	3.58E -03	1.91
23071851	NA	NA	9.36E -04	1.91
23071994	NA	NA	9.36E -04	1.91
TC1500010780.hg.1	<i>GOLGA6L9</i>	golgin A6 family-like 9	1.62E -03	1.91
TC1900009670.hg.1	<i>DOCK6</i>	dedicator of cytokinesis 6	6.12E -04	1.90
TC1100010472.hg.1	<i>CCDC73</i>	coiled-coil domain containing 73	5.13E -03	1.90
TC1000010982.hg.1	<i>ASCC1</i>	Transcript Identified by AceView, Entrez Gene ID(s) 51008	1.55E -03	1.90
AFFX-DapX-3_st	NA	NA	1.21E -04	1.90
TC0100007876.hg.1	<i>RRAGC</i>	Memczak2013 ANTISENSE, coding, INTERNAL, intronic best transcript NM_022157	3.90E -04	1.90

TC0200011107.hg.1	<i>EFHD1</i>	EF-hand domain family member D1	1.68E -03	1.90
TC1900007155.hg.1	<i>MIR1199</i>	microRNA 1199	9.07E -05	1.90
TSUnmapped00000176.hg.1	<i>SAG</i>	S-antigen; retina and pineal gland (arrestin)	5.98E -03	1.90
TC1700006768.hg.1	<i>EFNB3</i>	ephrin-B3	8.22E -03	1.90
TC0100017241.hg.1	<i>TMEM206</i>	transmembrane protein 206	4.03E -03	1.90
TC0900007547.hg.1	<i>C9orf85</i>	chromosome 9 open reading frame 85	3.72E -03	1.90
TC1700007262.hg.1	<i>MAP2K3</i>	mitogen-activated protein kinase kinase 3	9.12E -04	1.90
TC1600010987.hg.1	<i>CMIP</i>	Memczak2013 ANTISENSE, coding, INTERNAL, intronic best transcript NM_198390	6.69E -04	1.90
TC1600009192.hg.1	<i>MTRNR2L4</i>	MT-RNR2-like 4	1.07E -04	1.90
TC0X00006799.hg.1	<i>SAT1</i>	spermidine/spermine N1-acetyltransferase 1	7.70E -04	1.90
TC0600011227.hg.1	<i>HIST1H4K</i>	histone cluster 1, H4k	1.01E -03	1.89
TC0100016121.hg.1	<i>KCNJ10</i>	potassium channel, inwardly rectifying subfamily J, member 10	1.62E -04	1.89
TC0100017445.hg.1	<i>TLR5</i>	toll-like receptor 5	2.44E -03	1.89
TC1000007461.hg.1	<i>RASSF4</i>	Ras association (RalGDS/AF-6) domain family member 4	3.43E -03	1.89
HTA2-pos-2985881_st	NA	NA	8.61E -04	1.89
TC0100017716.hg.1	<i>FAM89A</i>	family with sequence similarity 89, member A	5.98E -04	1.88
TC1900011874.hg.1	<i>ZNF878</i>	zinc finger protein 878	5.15E -03	1.88

APPENDIX

TC0200016571.hg.1	<i>OSBPL6</i>	oxysterol binding protein-like 6	2.36E -03	1.88
TC0100017310.hg.1	<i>ESRRG</i>	estrogen-related receptor gamma	8.65E -04	1.88
TC0700013602.hg.1	<i>POLR2J3</i>	polymerase (RNA) II (DNA directed) polypeptide J3	5.88E -05	1.88
AFFX-r2-Bs-dap-M_st	NA	NA	6.80E -05	1.88
TC1700010560.hg.1	<i>PLXDC1</i>	plexin domain containing 1	9.40E -04	1.88
TC1100010274.hg.1	<i>SPTY2D1</i>	SPT2 chromatin protein domain containing 1	4.24E -04	1.88
TC1700007204.hg.1	<i>SPECC1</i>	sperm antigen with calponin homology and coiled-coil domains 1	5.08E -03	1.88
HTA2-neg-47419415_st	NA	NA	3.01E -04	1.88
TC1700008769.hg.1	<i>KCNJ2</i>	potassium channel, inwardly rectifying subfamily J, member 2	2.89E -04	1.88
TC0800009619.hg.1	<i>CTSB</i>	cathepsin B	8.67E -04	1.88
TC0300008086.hg.1	<i>ARL6</i>	ADP-ribosylation factor like GTPase 6	9.26E -03	1.88
TC1700008016.hg.1	<i>HIGD1B</i>	HIG1 hypoxia inducible domain family, member 1B	6.79E -03	1.88
TC0X00011279.hg.1	<i>TSPAN7</i>	tetraspanin 7	2.35E -03	1.88
TC1900007127.hg.1	<i>IER2</i>	immediate early response 2	2.58E -04	1.88
23067838	NA	NA	8.96E -04	1.87
TC1400008058.hg.1	<i>PPP4R4</i>	protein phosphatase 4, regulatory subunit 4	8.96E -04	1.87
TC1600011442.hg.1	<i>MAP1LC3B</i>	microtubule-associated protein 1 light chain 3 beta	1.55E -03	1.87

HTA2-neg-47422232_st	NA	NA	3.21E -03	1.87
TC1900009158.hg.1	<i>RPS15</i>	Memczak2013 ANTISENSE, coding, INTERNAL, intronic best transcript NM_001018	8.78E -04	1.87
TC1600010801.hg.1	<i>PKD1L3</i>	polycystic kidney disease 1- like 3	1.09E -03	1.87
TC0100006861.hg.1	<i>FBXO44</i>	F-box protein 44	1.47E -04	1.87
TC0200011419.hg.1	<i>ATG4B</i>	autophagy related 4B, cysteine peptidase	1.88E -03	1.87
TC0600007613.hg.1	<i>HSPA1A</i>	heat shock 70kDa protein 1A	9.31E -05	1.87
TC1600007448.hg.1	<i>CORO1A</i>	coronin, actin binding protein, 1A	5.30E -03	1.87
TC1000012433.hg.1	<i>SPAG6</i>	sperm associated antigen 6	2.58E -03	1.86
TC0600008255.hg.1	<i>EFHC1</i>	EF-hand domain (C-terminal) containing 1	2.11E -03	1.86
TC1400010754.hg.1	<i>C14orf37</i>	chromosome 14 open reading frame 37	3.31E -04	1.86
TC0700013421.hg.1	<i>ZNF789</i>	zinc finger protein 789	5.26E -04	1.86
HTA2-pos-PSR0X007730.hg.1	NA	NA	9.11E -04	1.86
TC1800008677.hg.1	<i>CFAP53</i>	cilia and flagella associated protein 53	5.31E -03	1.86
TC0200015424.hg.1	<i>ALS2CR12</i>	amyotrophic lateral sclerosis 2 chromosome region candidate 12	4.16E -03	1.86
TC1900011879.hg.1	<i>ZNF44</i>	zinc finger protein 44	6.64E -03	1.86
TC0200016464.hg.1	<i>APLF</i>	aprataxin and PNKP like factor	2.29E -04	1.86
TC1200007653.hg.1	<i>NR4A1</i>	nuclear receptor subfamily 4, group A, member 1	6.86E -03	1.86

APPENDIX

TC0900011669.hg.1	<i>SH3GLB2</i>	SH3-domain GRB2-like endophilin B2	2.40E -03	1.86
TC1000011567.hg.1	<i>CRTAC1</i>	cartilage acidic protein 1	1.78E -03	1.85
23076588	NA	NA	1.17E -03	1.85
TC0800009212.hg.1	<i>MAPK15</i>	mitogen-activated protein kinase 15	1.17E -03	1.85
HTA2-neg-47422095_st	NA	NA	1.45E -03	1.85
TC0X00011236.hg.1	<i>RAB39B</i>	Transcript Identified by AceView, Entrez Gene ID(s) 116442	4.09E -03	1.85
TC1900011816.hg.1	<i>ZNF419</i>	zinc finger protein 419	8.08E -05	1.85
HTA2-pos-JUC01000985.hg.1	NA	NA	8.13E -05	1.85
HTA2-pos-JUC13008384.hg.1	NA	NA	8.13E -05	1.85
HTA2-pos-JUC19003067.hg.1	NA	NA	8.13E -05	1.85
TSUnmapped00000608.hg.1	<i>ZNF35</i>	zinc finger protein 35	1.07E -03	1.85
TC2100007952.hg.1	<i>URB1</i>	URB1 ribosome biogenesis 1 homolog (S. cerevisiae)	1.57E -03	1.85
TC0600014371.hg.1	<i>RNASET2</i>	ribonuclease T2	7.99E -03	1.85
TC0300011264.hg.1	<i>IL17RD</i>	interleukin 17 receptor D	1.83E -03	1.85
TC1100010041.hg.1	<i>ST5</i>	Transcript Identified by AceView, Entrez Gene ID(s) 6764	9.67E -03	1.85
TC0200015776.hg.1	<i>RESP18</i>	regulated endocrine-specific protein 18	1.69E -04	1.84
TC1600009351.hg.1	<i>GRIN2A</i>	Transcript Identified by AceView, Entrez Gene ID(s) 2903	7.26E -05	1.84

TC0200006703.hg.1	<i>ATP6V1C2</i>	ATPase, H ⁺ transporting, lysosomal 42kDa, V1 subunit C2	2.98E-03	1.84
TC0800011597.hg.1	<i>EXT1</i>	Jeck2013 ALT_ACCEPTOR, ALT_DONOR, coding, INTERNAL, intronic best transcript NM_000127	1.81E-03	1.84
TC1700008328.hg.1	<i>STXBP4</i>	syntaxin binding protein 4	5.78E-04	1.84
TC0600011821.hg.1	<i>GUCA1B</i>	guanylate cyclase activator 1B (retina)	9.59E-04	1.84
TC1600007240.hg.1	<i>PRKCB</i>	protein kinase C, beta	1.24E-03	1.84
TC2100008534.hg.1	<i>PCBP3</i>	poly(rC) binding protein 3	8.57E-04	1.84
TC1500009200.hg.1	<i>TTBK2</i>	tau tubulin kinase 2	1.93E-03	1.84
TC0300009696.hg.1	<i>VWA5B2</i>	von Willebrand factor A domain containing 5B2	6.36E-03	1.84
TC0200014728.hg.1	<i>LY75-CD302</i>	LY75-CD302 readthrough	4.65E-04	1.84
TC0100018464.hg.1	<i>PPM1J</i>	protein phosphatase, Mg ²⁺ /Mn ²⁺ dependent, 1J	1.70E-03	1.84
TC0800012351.hg.1	<i>WDYHV1</i>	WDYHV motif containing 1	1.88E-03	1.84
TC0100015701.hg.1	<i>HIST2H3A</i>	histone cluster 2, H3a	4.97E-04	1.84
TC0800009194.hg.1	<i>RHPN1</i>	rhopophilin, Rho GTPase binding protein 1	2.83E-03	1.84
TC0200010745.hg.1	<i>IGFBP2</i>	insulin like growth factor binding protein 2	1.27E-03	1.84
TC1300006690.hg.1	<i>POLR1D</i>	polymerase (RNA) I polypeptide D	6.14E-05	1.83
TC2200007903.hg.1	<i>LOC101929372</i>	uncharacterized LOC101929372	6.86E-04	1.83

APPENDIX

TC0200008536.hg.1	<i>ANKRD36</i>	Transcript Identified by AceView, Entrez Gene ID(s) 375248	6.70E -04	1.83
TC1900008259.hg.1	<i>ZNF233</i>	zinc finger protein 233	4.95E -04	1.83
TC0100008773.hg.1	<i>MSH4</i>	mutS homolog 4	3.81E -03	1.83
TC0900007163.hg.1	<i>FRMPD1</i>	FERM and PDZ domain containing 1	9.84E -04	1.83
TC1100012519.hg.1	<i>CBL</i>	Memczak2013 ANTISENSE, coding, INTERNAL, UTR3 best transcript NM_005188	4.98E -03	1.83
TC1100011101.hg.1	<i>NXF1</i>	nuclear RNA export factor 1	3.24E -03	1.83
TC1600009620.hg.1	<i>SMG1</i>	SMG1 phosphatidylinositol 3-kinase-related kinase	5.65E -04	1.83
HTA2-pos-JUC09010881.hg.1	NA	NA	4.98E -03	1.82
TC0800011334.hg.1	<i>KLF10</i>	Kruppel-like factor 10	2.37E -04	1.82
TC1800009203.hg.1	<i>PQLC1</i>	PQ loop repeat containing 1	2.22E -03	1.82
TC1900011653.hg.1	<i>MCOLN1</i>	mucolipin 1	8.82E -04	1.82
TC0800010234.hg.1	<i>SFRP1</i>	secreted frizzled-related protein 1	9.22E -05	1.82
TC1900009269.hg.1	<i>TLE2</i>	transducin-like enhancer of split 2	7.46E -03	1.82
TC1900008860.hg.1	<i>LENG8</i>	leukocyte receptor cluster (LRC) member 8	1.44E -03	1.82
23076569	NA	NA	2.70E -04	1.82
TC1500010841.hg.1	<i>CHRFAM7A</i>	CHRNA7 (cholinergic receptor, nicotinic, alpha 7, exons 5-10) and FAM7A (family with sequence similarity 7A, exons A-E) fusion	3.19E -03	1.81

TC0100009746.hg.1	<i>NUDT17</i>	nudix hydrolase 17	2.11E -03	1.81
23069220	NA	NA	2.42E -04	1.81
TSUnmapped00000145.hg.1	<i>SAG</i>	S-antigen; retina and pineal gland (arrestin)	1.62E -04	1.81
TC0700013388.hg.1	<i>STAG3L1</i>	stromal antigen 3-like 1 (pseudogene)	2.66E -04	1.81
TC1500010709.hg.1	<i>ARHGAP11B</i>	Rho GTPase activating protein 11B	5.45E -03	1.81
TC0500011752.hg.1	<i>FEM1C</i>	Jeck2013 ALT_ACCEPTOR, ALT_DONOR, coding, INTERNAL, intronic best transcript NM_020177	8.95E -03	1.81
TC0X00007116.hg.1	<i>RP2</i>	retinitis pigmentosa 2 (X-linked recessive)	1.62E -03	1.81
TC1100010044.hg.1	<i>ST5</i>	Transcript Identified by AceView, Entrez Gene ID(s) 6764	2.21E -03	1.81
TC0100016649.hg.1	<i>NMNAT2</i>	nicotinamide nucleotide adenyllyltransferase 2	9.09E -03	1.81
TC1800007218.hg.1	<i>C18orf25</i>	chromosome 18 open reading frame 25	2.41E -03	1.80
TC0700010162.hg.1	<i>FBXL18</i>	F-box and leucine-rich repeat protein 18	2.80E -04	1.80
23072532	NA	NA	1.41E -03	1.80
TC1600007189.hg.1	<i>VWA3A</i>	von Willebrand factor A domain containing 3A	7.04E -04	1.80
TC0700012163.hg.1	<i>EFCAB10</i>	EF-hand calcium binding domain 10	4.82E -04	1.80
TC0800011713.hg.1	<i>MTSS1</i>	metastasis suppressor 1	5.09E -03	1.80
TC0300011834.hg.1	<i>FILIP1L</i>	filamin A interacting protein 1-like	9.33E -05	1.80
TC0700013401.hg.1	AC007566.10	---	5.19E -03	1.80

APPENDIX

TC1500007805.hg.1	<i>BBS4</i>	Memczak2013 ALT_ACCEPTOR, ALT_DONOR, coding, INTERNAL, intronic best transcript NM_033028	5.19E -03	1.80
TC0200016734.hg.1	<i>MAP3K19</i>	mitogen-activated protein kinase kinase kinase 19	2.53E -04	1.80
TC0X00009117.hg.1	<i>FANCB</i>	Fanconi anemia complementation group B	1.23E -03	1.80
TC2200007909.hg.1	<i>MICAL3</i>	microtubule associated monooxygenase, calponin and LIM domain containing 3	1.37E -04	1.80
TC1000011040.hg.1	<i>CAMK2G</i>	calcium/calmodulin- dependent protein kinase II gamma	3.94E -03	1.80
TC0900010737.hg.1	<i>DIRAS2</i>	DIRAS family, GTP-binding RAS-like 2	2.30E -03	1.79
TC0100009274.hg.1	<i>AMY1C</i>	amylase, alpha 1C (salivary)	6.44E -04	1.79
TC1300006658.hg.1	<i>WASF3</i>	WAS protein family, member 3	4.35E -03	1.79
TC1900011765.hg.1	<i>PPP1R37</i>	protein phosphatase 1, regulatory subunit 37	2.45E -04	1.79
TC1500008135.hg.1	<i>UBE2Q2L</i>	ubiquitin conjugating enzyme E2Q family member 2-like	5.37E -04	1.79
TC1200009076.hg.1	<i>SUDS3</i>	SDS3 homolog, SIN3A corepressor complex component	2.34E -03	1.79
TC0200014717.hg.1	<i>WDSUB1</i>	WD repeat, sterile alpha motif and U-box domain containing 1	3.97E -03	1.79
TC0200008263.hg.1	<i>USP39</i>	ubiquitin specific peptidase 39	2.81E -04	1.79
TC0100015180.hg.1	<i>WDR47</i>	WD repeat domain 47	8.51E -03	1.79
TC2000008587.hg.1	<i>RALGAPA2</i>	Ral GTPase activating protein, alpha subunit 2 (catalytic)	2.12E -04	1.79

AFFX-r2-Bs-phe-M_st	NA	NA	2.98E -04	1.79
TC1700011795.hg.1	<i>PRPSAP1</i>	phosphoribosyl pyrophosphate synthetase- associated protein 1	1.66E -04	1.78
TSUnmapped00000149.hg.1	<i>ZNF35</i>	zinc finger protein 35	1.36E -03	1.78
TC0700013586.hg.1	<i>C7orf76</i>	chromosome 7 open reading frame 76	9.00E -04	1.78
TC2000009966.hg.1	<i>FKBP1A-</i> <i>SDCBP2</i>	FKBP1A-SDCBP2 readthrough (NMD candidate)	2.71E -04	1.78
TC0100013763.hg.1	<i>POU3F1</i>	POU class 3 homeobox 1	2.95E -03	1.78
TC1100013020.hg.1	<i>PPP1R32</i>	protein phosphatase 1, regulatory subunit 32	7.72E -03	1.78
TC0200012412.hg.1	<i>C1GALT1C1L</i>	C1GALT1-specific chaperone 1 like	1.19E -03	1.78
TC0400008384.hg.1	<i>PLA2G12A</i>	Memczak2013 ANTISENSE, CDS, coding, INTERNAL best transcript NM_030821	5.40E -03	1.78
TC1500010845.hg.1	<i>OTUD7A</i>	OTU deubiquitinase 7A	9.60E -04	1.78
TC0700012080.hg.1	<i>SPDYE6</i>	speedy/RINGO cell cycle regulator family member E6	9.98E -04	1.78
TC1300006770.hg.1	<i>ALOX5AP</i>	arachidonate 5-lipoxygenase- activating protein	3.81E -04	1.78
TC0800010450.hg.1	<i>ATP6V1H</i>	ATPase, H ⁺ transporting, lysosomal 50/57kDa, V1 subunit H	5.08E -03	1.78
TC0300013763.hg.1	<i>RUBCN</i>	RUN domain and cysteine- rich domain containing, Beclin 1-interacting protein	3.54E -03	1.78
HTA2-neg-47420204_st	NA	NA	4.40E -03	1.78
TC0700013457.hg.1	<i>FSCN3</i>	fascin actin-bundling protein 3, testicular	8.69E -04	1.78

APPENDIX

TC1100012712.hg.1	<i>ACRV1</i>	acrosomal vesicle protein 1	1.96E -03	1.78
TC0500009824.hg.1	<i>ZDHHC11</i>	Transcript Identified by AceView, Entrez Gene ID(s) 79844	4.52E -03	1.78
TC1900011819.hg.1	<i>ZNF211</i>	zinc finger protein 211	7.66E -05	1.78
TC0400012882.hg.1	<i>ZNF732</i>	zinc finger protein 732	5.06E -04	1.78
HTA2-pos-2960237_st	NA	NA	8.76E -03	1.78
TC1500008139.hg.1	<i>GOLGA6L4</i>	Homo sapiens golgin A6 family-like 4 (GOLGA6L4), mRNA.	1.73E -03	1.77
TC1600011047.hg.1	<i>HSDL1</i>	hydroxysteroid dehydrogenase like 1	5.01E -04	1.77
HTA2-pos-47422722_st	NA	NA	1.95E -04	1.77
HTA2-pos-PSR02023970.hg.1	NA	NA	9.13E -04	1.77
TC1200012700.hg.1	<i>C12orf75</i>	chromosome 12 open reading frame 75	8.51E -03	1.77
TC0900008865.hg.1	<i>CERCAM</i>	cerebral endothelial cell adhesion molecule	1.93E -03	1.77
TSUnmapped00000262.hg.1	<i>MLXIP</i>	MLX interacting protein	4.01E -04	1.77
TC0700008639.hg.1	<i>SPDYE2</i>	speedy/RINGO cell cycle regulator family member E2	4.03E -04	1.77
TC0700008647.hg.1	<i>SPDYE2B</i>	speedy/RINGO cell cycle regulator family member E2B	4.03E -04	1.77
TC0700008000.hg.1	<i>LAT2</i>	linker for activation of T-cells family member 2	8.10E -04	1.77
TC1500010291.hg.1	<i>NMB</i>	neuromedin B	2.99E -03	1.77
TC0300013687.hg.1	<i>TFRC</i>	Transcript Identified by AceView, Entrez Gene ID(s) 7037	4.98E -03	1.77

23076565	NA	NA	2.60E -03	1.76
AFFX-PheX-3_st	NA	NA	2.02E -04	1.76
23075412	NA	NA	9.95E -03	1.76
TC0300009974.hg.1	<i>MUC20</i>	mucin 20, cell surface associated	9.95E -03	1.76
TC0700013119.hg.1	<i>XRCC2</i>	X-ray repair complementing defective repair in Chinese hamster cells 2	2.26E -03	1.76
TC0400011180.hg.1	<i>SCD5</i>	stearoyl-CoA desaturase 5	9.76E -04	1.76
TC2000009014.hg.1	<i>NDRG3</i>	NDRG family member 3	2.49E -04	1.76
TC1400008583.hg.1	<i>CCNB1IP1</i>	cyclin B1 interacting protein 1, E3 ubiquitin protein ligase	2.47E -03	1.76
TC0700007364.hg.1	<i>SPDYE1</i>	speedy/RINGO cell cycle regulator family member E1	1.15E -03	1.76
TC0700012998.hg.1	<i>ZNF767P</i>	zinc finger family member 767, pseudogene	8.42E -04	1.76
TC1200010108.hg.1	<i>GYS2</i>	glycogen synthase 2 (liver)	7.28E -03	1.76
TSUnmapped00000268.hg.1	<i>CCDC84</i>	coiled-coil domain containing 84	5.70E -04	1.76
TC0100011325.hg.1	<i>TMCC2</i>	transmembrane and coiled-coil domain family 2	6.30E -03	1.76
TC1000009152.hg.1	<i>HTRA1</i>	HtrA serine peptidase 1	2.11E -03	1.76
TC0100010284.hg.1	<i>PEA15</i>	phosphoprotein enriched in astrocytes 15	9.02E -05	1.76
TC0800009326.hg.1	<i>TDRP</i>	testis development related protein	6.58E -03	1.76
TC1100013053.hg.1	<i>RAD9A</i>	RAD9 checkpoint clamp component A	2.44E -04	1.76
23068514	NA	NA	7.12E -03	1.76

APPENDIX

TC0800007311.hg.1	<i>ADGRA2</i>	adhesion G protein-coupled receptor A2	2.86E -03	1.75
TC0700013575.hg.1	<i>STAG3L3</i>	stromal antigen 3-like 3 (pseudogene)	4.20E -04	1.75
TC1500010909.hg.1	<i>STARD5</i>	StAR-related lipid transfer domain containing 5	3.70E -03	1.75
TC0200015434.hg.1	<i>ALS2</i>	ALS2, alsin Rho guanine nucleotide exchange factor	1.02E -03	1.75
23075635	NA	NA	3.33E -04	1.75
TC1400010632.hg.1	<i>GPATCH2L</i>	G-patch domain containing 2 like	1.21E -04	1.75
TC1700011919.hg.1	<i>CEP295NL</i>	CEP295 N-terminal like	1.76E -03	1.75
TC0400011053.hg.1	<i>CXCL10</i>	chemokine (C-X-C motif) ligand 10	4.62E -03	1.75
TC0100007184.hg.1	<i>OTUD3</i>	OTU deubiquitinase 3	3.81E -04	1.75
TC0100013349.hg.1	<i>RSRP1</i>	arginine/serine-rich protein 1	3.00E -03	1.75
23068498	NA	NA	3.13E -03	1.75
TC0200008734.hg.1	<i>C2orf49</i>	chromosome 2 open reading frame 49	5.91E -04	1.75
TC0200015514.hg.1	<i>GPR1</i>	G protein-coupled receptor 1	1.46E -03	1.74
TC1700011815.hg.1	<i>MXRA7</i>	matrix-remodelling associated 7	6.89E -04	1.74
TC0100015698.hg.1	<i>HIST2H3D</i>	histone cluster 2, H3d	1.10E -03	1.74
TC1400009710.hg.1	<i>ACYP1</i>	acylphosphatase 1, erythrocyte (common) type	5.30E -03	1.74
TC1100012994.hg.1	<i>CRY2</i>	cryptochrome circadian clock 2	1.15E -03	1.74
TC0300009310.hg.1	<i>MLF1</i>	myeloid leukemia factor 1	1.57E -03	1.74

TC1500010906.hg.1	<i>RP11-351M8.2</i>	---	2.17E-03	1.74
TC0700012086.hg.1	<i>POLR2J</i>	polymerase (RNA) II (DNA directed) polypeptide J, 13.3kDa	1.73E-04	1.74
TC0900008684.hg.1	<i>GPR21</i>	G protein-coupled receptor 21	2.87E-04	1.74
TC1200006905.hg.1	<i>FAM234B</i>	family with sequence similarity 234, member B	1.17E-03	1.74
HTA2-neg-47420908_st	NA	NA	5.28E-03	1.74
TC0100009877.hg.1	<i>HIST2H3A</i>	histone cluster 2, H3a	1.99E-03	1.74
HTA2-neg-47420639_st	NA	NA	1.52E-03	1.74
TC0700011519.hg.1	<i>STAG3L2</i>	stromal antigen 3-like 2 (pseudogene)	7.78E-04	1.74
TC2200008346.hg.1	<i>MN1</i>	meningioma (disrupted in balanced translocation) 1	1.03E-04	1.74
TC0100018248.hg.1	<i>RNPC3</i>	RNA binding region (RNP1, RRM) containing 3	5.06E-04	1.74
TC2000007083.hg.1	<i>ID1</i>	inhibitor of DNA binding 1, dominant negative helix-loop-helix protein	7.09E-03	1.73
TC0300007610.hg.1	<i>PXK</i>	PX domain containing serine/threonine kinase	1.77E-04	1.73
TC0600010331.hg.1	<i>FAM120B</i>	family with sequence similarity 120B	6.21E-03	1.73
TC1600008454.hg.1	<i>GABARAPL2</i>	GABA(A) receptor-associated protein like 2	3.94E-04	1.73
TC0200014694.hg.1	<i>ACVR1C</i>	activin A receptor type IC	2.79E-03	1.73
TC1100008038.hg.1	<i>SNX32</i>	sorting nexin 32	3.47E-03	1.73
TC0400012964.hg.1	<i>SCLT1</i>	sodium channel and clathrin linker 1	1.07E-03	1.73

APPENDIX

TC1600007957.hg.1	<i>MT2A</i>	metallothionein 2A	5.30E -03	1.73
TC0200014204.hg.1	<i>HS6ST1</i>	heparan sulfate 6-O-sulfotransferase 1	5.17E -03	1.73
TC1900007040.hg.1	<i>CNN1</i>	calponin 1, basic, smooth muscle	7.38E -03	1.73
TC0100013747.hg.1	<i>SNIP1</i>	Smad nuclear interacting protein 1	2.02E -03	1.73
TC0200013616.hg.1	<i>AFF3</i>	AF4/FMR2 family, member 3	8.05E -03	1.73
TC1000008927.hg.1	<i>VT1A</i>	vesicle transport through interaction with t-SNAREs 1A	4.44E -04	1.73
HTA2-neg-47423802_st	NA	NA	4.33E -03	1.73
TC1200011991.hg.1	<i>IQCD</i>	IQ motif containing D	3.57E -03	1.73
TC0700011050.hg.1	<i>FIGNL1</i>	fidgetin-like 1	3.24E -03	1.73
TC0500013425.hg.1	<i>C5orf45</i>	chromosome 5 open reading frame 45	2.93E -03	1.73
TC0200010165.hg.1	<i>PPP1R1C</i>	protein phosphatase 1, regulatory (inhibitor) subunit 1C	4.23E -03	1.72
TC0100009215.hg.1	<i>CDC14A</i>	cell division cycle 14A	3.63E -04	1.72
TC0800009726.hg.1	<i>MTMR7</i>	myotubularin related protein 7	2.60E -04	1.72
TC1500010755.hg.1	<i>ANKDD1A</i>	ankyrin repeat and death domain containing 1A	3.08E -04	1.72
TC1100009122.hg.1	<i>NXPE2</i>	neurexophilin and PC-esterase domain family, member 2	5.48E -03	1.72
TC0700011977.hg.1	<i>GAL3ST4</i>	galactose-3-O-sulfotransferase 4	6.07E -03	1.72
TC0400011188.hg.1	<i>LIN54</i>	lin-54 DREAM MuvB core complex component	2.97E -03	1.72

TC0200016417.hg.1	<i>CENPA</i>	centromere protein A	8.45E -04	1.72
TC2000009813.hg.1	<i>EEF1A2</i>	eukaryotic translation elongation factor 1 alpha 2	1.10E -03	1.72
TC0600013193.hg.1	<i>STX7</i>	syntaxin 7	1.80E -03	1.72
TC2200008920.hg.1	<i>SULT4A1</i>	sulfotransferase family 4A member 1	1.98E -03	1.72
TC0900012222.hg.1	<i>APTX</i>	aprataxin	1.02E -03	1.72
TC1300008834.hg.1	<i>SIAH3</i>	siah E3 ubiquitin protein ligase family member 3	3.21E -03	1.72
TC0700006977.hg.1	<i>NFE2L3</i>	nuclear factor, erythroid 2-like 3	1.01E -03	1.72
TC0900012167.hg.1	<i>GSN</i>	gelsolin	6.44E -03	1.72
TC1100009521.hg.1	<i>APLP2</i>	amyloid beta (A4) precursor-like protein 2	2.27E -03	1.72
TC0700012728.hg.1	<i>PTN</i>	pleiotrophin	4.50E -04	1.72
TC1900006819.hg.1	<i>TRIP10</i>	thyroid hormone receptor interactor 10	9.69E -04	1.72
TC1200006771.hg.1	<i>CLEC2D</i>	C-type lectin domain family 2, member D	1.27E -03	1.71
23071946	NA	NA	9.31E -03	1.71
TC0900011705.hg.1	<i>ASB6</i>	ankyrin repeat and SOCS box containing 6	8.72E -04	1.71
TC1200006670.hg.1	<i>CLSTN3</i>	calsyntenin 3	8.89E -04	1.71
TC0800008916.hg.1	<i>EFR3A</i>	EFR3 homolog A	1.40E -03	1.71
TC1700008844.hg.1	<i>TTYH2</i>	tweety family member 2	6.13E -04	1.71
TC0900011423.hg.1	<i>TTLL11</i>	tubulin tyrosine ligase-like family member 11	6.98E -04	1.71

APPENDIX

TC0500011049.hg.1	<i>NAIP</i>	NLR family, apoptosis inhibitory protein	4.92E -04	1.71
TC1600009252.hg.1	<i>PPL</i>	periplakin	9.36E -03	1.71
23075636	<i>NA</i>	NA	4.07E -03	1.71
23076269	<i>NA</i>	NA	4.07E -03	1.71
TC0200008534.hg.1	<i>ANKRD36</i>	ankyrin repeat domain 36	5.18E -03	1.71
TC0200014775.hg.1	<i>KCNH7</i>	potassium channel, voltage gated eag related subfamily H, member 7	8.82E -03	1.71
TC1100012528.hg.1	<i>THY1</i>	Thy-1 cell surface antigen	6.33E -04	1.71
23066337	<i>NA</i>	NA	1.18E -03	1.70
TC1600009545.hg.1	<i>ABCC6</i>	ATP binding cassette subfamily C member 6	7.30E -04	1.70
TC0500009488.hg.1	<i>CREBRF</i>	CREB3 regulatory factor	4.44E -03	1.70
TC1100012052.hg.1	<i>CCDC82</i>	coiled-coil domain containing 82	2.97E -03	1.70
TC2000008267.hg.1	<i>RASSF2</i>	Ras association (RalGDS/AF-6) domain family member 2	6.30E -04	1.70
TC2200007987.hg.1	<i>CLDN5</i>	claudin 5	5.99E -03	1.70
TC0800007439.hg.1	<i>POLB</i>	polymerase (DNA directed), beta	4.13E -03	1.70
TC0200014790.hg.1	<i>GRB14</i>	growth factor receptor bound protein 14	2.32E -03	1.70
TC0700009240.hg.1	<i>AGBL3</i>	ATP/GTP binding protein-like 3	4.48E -03	1.70
TC1200009550.hg.1	<i>KDM5A</i>	lysine (K)-specific demethylase 5A	6.02E -04	1.70

TC0700013224.hg.1	<i>LMBR1</i>	Transcript Identified by AceView, Entrez Gene ID(s) 64327	5.46E -03	1.70
TC0100015795.hg.1	<i>POGZ</i>	Transcript Identified by AceView, Entrez Gene ID(s) 23126	1.56E -03	1.70
TC0100016503.hg.1	<i>ASTN1</i>	astrotactin 1	9.62E -03	1.70
TC1600006525.hg.1	<i>CACNA1H</i>	calcium channel, voltage-dependent, T type, alpha 1H subunit	3.66E -03	1.70
TC0700006945.hg.1	<i>MPP6</i>	membrane protein, palmitoylated 6	2.69E -03	1.70
TC1500009970.hg.1	<i>HIGD2B</i>	HIG1 hypoxia inducible domain family, member 2B	2.53E -04	1.69
TC1800008235.hg.1	<i>ABHD3</i>	Transcript Identified by AceView, Entrez Gene ID(s) 171586	9.87E -03	1.69
HTA2-pos-2930617_st	NA	NA	1.55E -03	1.69
HTA2-pos-PSR02023951.hg.1	NA	NA	2.52E -04	1.69
TC0600014276.hg.1	<i>HLA-DMB</i>	major histocompatibility complex, class II, DM beta	5.84E -04	1.69
TC1100006906.hg.1	<i>FAR1</i>	fatty acyl CoA reductase 1	4.73E -04	1.69
TC0100011451.hg.1	<i>CAMK1G</i>	calcium/calmodulin-dependent protein kinase IG	3.44E -04	1.69
TC1400007495.hg.1	<i>PLEKHH1</i>	pleckstrin homology domain containing, family H (with MyTH4 domain) member 1	7.26E -03	1.69
TC1700012241.hg.1	<i>TBC1D3L</i>	TBC1 domain family, member 3L	7.64E -04	1.69
TC0500012519.hg.1	<i>SPARC</i>	secreted protein, acidic, cysteine-rich (osteonectin)	4.89E -04	1.69
TC1900008747.hg.1	<i>ZNF765</i>	zinc finger protein 765	9.58E -04	1.69

APPENDIX

TC0500013207.hg.1	<i>LIX1</i>	Memczak2013 ANTISENSE, coding, INTERNAL, intronic best transcript NM_153234	1.03E -03	1.69
TC2000008940.hg.1	<i>PIGU</i>	Salzman2013 ALT_ACCEPTOR, ALT_DONOR, coding, INTERNAL, intronic best transcript NM_080476	6.36E -03	1.69
23075808	<i>NA</i>	NA	1.57E -03	1.69
TSUnmapped00000513.hg.1	<i>DGKD</i>	diacylglycerol kinase, delta 130kDa	8.29E -04	1.69
TC1600010593.hg.1	<i>CMTM4</i>	CKLF-like MARVEL transmembrane domain containing 4	1.47E -03	1.69
TC0800011137.hg.1	<i>RAD54B</i>	RAD54 homolog B (S. cerevisiae)	2.55E -03	1.69
TC0900010370.hg.1	<i>TRPM3</i>	transient receptor potential cation channel, subfamily M, member 3	7.99E -03	1.69
TC1400009579.hg.1	<i>ADAM20</i>	ADAM metallopeptidase domain 20	7.31E -04	1.68
TC1500007034.hg.1	<i>SNAP23</i>	synaptosome associated protein 23kDa	4.62E -03	1.68
TC1800009215.hg.1	<i>ANKRD12</i>	ankyrin repeat domain 12	1.72E -03	1.68
TC0800007065.hg.1	<i>CDCA2</i>	cell division cycle associated 2	2.82E -03	1.68
TC0100006723.hg.1	<i>VAMP3</i>	vesicle associated membrane protein 3	6.00E -03	1.68
TC2200007505.hg.1	44077	septin 3	8.58E -03	1.68
TC1900006766.hg.1	<i>HSD11B1L</i>	hydroxysteroid (11-beta) dehydrogenase 1-like	9.25E -04	1.68
TC1600007317.hg.1	<i>KIAA0556</i>	KIAA0556	3.36E -03	1.68
TC0500006479.hg.1	<i>NKD2</i>	naked cuticle homolog 2 (Drosophila)	1.28E -03	1.68

TC0900011938.hg.1	<i>C9orf116</i>	chromosome 9 open reading frame 116	8.42E -04	1.68
TC0400008329.hg.1	<i>GSTCD</i>	glutathione S-transferase, C-terminal domain containing	2.52E -03	1.68
TC0X00009972.hg.1	<i>SLC7A3</i>	solute carrier family 7 (cationic amino acid transporter, y+ system), member 3	5.36E -03	1.68
TC0100018361.hg.1	<i>TSNAX-DISC1</i>	TSNAX-DISC1 readthrough (NMD candidate)	3.65E -04	1.68
TC2000008107.hg.1	<i>TCEA2</i>	transcription elongation factor A (SII), 2	2.12E -04	1.68
TC0700011982.hg.1	<i>GATS</i>	GATS, stromal antigen 3 opposite strand	9.81E -03	1.67
TC0400009088.hg.1	<i>GUCY1B3</i>	guanylate cyclase 1, soluble, beta 3	2.22E -03	1.67
TC1500008545.hg.1	<i>ASB7</i>	ankyrin repeat and SOCS box containing 7	8.23E -03	1.67
TC0700011784.hg.1	<i>FAM133B</i>	Transcript Identified by AceView, Entrez Gene ID(s) 257415	1.49E -03	1.67
TC1000008743.hg.1	<i>SUFU</i>	Transcript Identified by AceView, Entrez Gene ID(s) 51684	4.13E -04	1.67
TC1200008734.hg.1	<i>RIC8B</i>	RIC8 guanine nucleotide exchange factor B	2.81E -04	1.67
TC2000008666.hg.1	<i>NAPB</i>	N-ethylmaleimide-sensitive factor attachment protein, beta	2.27E -03	1.67
23076268	NA	NA	8.48E -04	1.67
TC0300010035.hg.1	<i>SENP5</i>	SUMO1/sentrin specific peptidase 5	2.88E -04	1.67
TSUnmapped00000410.hg.1	<i>ATG16L1</i>	autophagy related 16-like 1	6.59E -03	1.67
TC1700009049.hg.1	<i>PGS1</i>	phosphatidylglycerophosphate synthase 1	7.47E -04	1.67

APPENDIX

TC0300013520.hg.1	<i>CLDN1</i>	claudin 1	4.69E -03	1.67
TC1700009417.hg.1	<i>SMG6</i>	SMG6 nonsense mediated mRNA decay factor	5.53E -04	1.67
TC1600009580.hg.1	<i>XYLT1</i>	xylosyltransferase I	1.78E -03	1.67
TC1500010236.hg.1	<i>GOLGA6L10</i>	golgin A6 family-like 10	1.04E -03	1.67
TC1200012593.hg.1	<i>CLEC4A</i>	C-type lectin domain family 4, member A	4.14E -04	1.66
TC0500013215.hg.1	<i>LVRN</i>	laeverin	6.04E -03	1.66
TC2200007021.hg.1	<i>RFPL1</i>	ret finger protein-like 1	6.19E -04	1.66
TC0500012285.hg.1	<i>FCHSD1</i>	FCH and double SH3 domains 1	5.45E -03	1.66
23072563	NA	NA	1.96E -04	1.66
TC2000009447.hg.1	<i>DPM1</i>	dolichyl-phosphate mannosyltransferase polypeptide 1, catalytic subunit	2.39E -04	1.66
TC1600008656.hg.1	<i>KLHL36</i>	kelch-like family member 36	2.36E -03	1.66
TC0100018285.hg.1	<i>NBPF19</i>	neuroblastoma breakpoint family, member 19	1.72E -03	1.66
TC0X00011291.hg.1	<i>PAGE2</i>	P antigen family, member 2 (prostate associated)	2.08E -03	1.66
TC1900007043.hg.1	<i>ZNF833P</i>	zinc finger protein 833, pseudogene	4.23E -03	1.66
TC1600010685.hg.1	<i>SMPD3</i>	sphingomyelin phosphodiesterase 3, neutral membrane (neutral sphingomyelinase II)	2.07E -03	1.66
TC1200010865.hg.1	<i>ITGA7</i>	integrin alpha 7	7.30E -03	1.66

TC0700009079.hg.1	<i>TSPAN33</i>	tetraspanin 33	4.43E -04	1.66
23075460	NA	NA	3.20E -04	1.66
TC1500009458.hg.1	<i>ARPP19</i>	cAMP-regulated phosphoprotein 19kDa	4.55E -03	1.66
23070237	NA	NA	3.48E -03	1.66
TC0800008371.hg.1	<i>SPAG1</i>	sperm associated antigen 1	3.49E -03	1.66
TC0300012164.hg.1	<i>POLQ</i>	polymerase (DNA directed), theta	1.73E -03	1.66
TSUnmapped00000105.hg.1	<i>ZNF501</i>	zinc finger protein 501 [Source:HGNC Symbol;Acc:HGNC:23717]	7.60E -03	1.65
TC2200008862.hg.1	<i>CYP2D6</i>	cytochrome P450, family 2, subfamily D, polypeptide 6	2.94E -04	1.65
TC0100015896.hg.1	<i>NUP210L</i>	nucleoporin 210kDa like	8.96E -03	1.65
TC1900011852.hg.1	<i>RFX2</i>	regulatory factor X, 2 (influences HLA class II expression)	5.98E -04	1.65
23075463	NA	NA	8.86E -03	1.65
TC0500010998.hg.1	<i>CCDC125</i>	coiled-coil domain containing 125	8.86E -03	1.65
TC0800012325.hg.1	<i>SLC26A7</i>	solute carrier family 26 (anion exchanger), member 7	3.18E -03	1.65
TC2000006464.hg.1	<i>FAM110A</i>	family with sequence similarity 110, member A	2.53E -03	1.65
TC0300012720.hg.1	<i>PLSCR4</i>	phospholipid scramblase 4	1.71E -03	1.65
TC1000011743.hg.1	<i>CFAP43</i>	cilia and flagella associated protein 43	8.37E -03	1.65
TC0200014703.hg.1	<i>CCDC148</i>	coiled-coil domain containing 148	4.09E -04	1.65

APPENDIX

TC0200016601.hg.1	<i>GIGYF2</i>	GRB10 interacting GYF protein 2	4.09E -03	1.65
TC0700010189.hg.1	<i>CYTH3</i>	cytohesin 3	3.28E -03	1.65
TC2000009178.hg.1	<i>JPH2</i>	junctophilin 2	4.77E -03	1.65
TC1000008891.hg.1	<i>DUSP5</i>	dual specificity phosphatase 5	6.90E -03	1.65
TC0500011495.hg.1	<i>SPATA9</i>	spermatogenesis associated 9	7.35E -03	1.65
TC0100015707.hg.1	<i>HIST2H4A</i>	histone cluster 2, H4a	4.38E -03	1.65
TC0100018208.hg.1	<i>ZBTB8B</i>	zinc finger and BTB domain containing 8B	6.37E -04	1.64
23074047	NA	NA	9.72E -03	1.64
TC1900011892.hg.1	<i>RTBDN</i>	retbindin	4.46E -03	1.64
TC0100006675.hg.1	<i>KCNAB2</i>	potassium channel, voltage gated subfamily A regulatory beta subunit 2	2.02E -03	1.64
TC0600013519.hg.1	<i>ZC3H12D</i>	zinc finger CCCH-type containing 12D	3.27E -04	1.64
TC0600014240.hg.1	<i>LOC100130357</i>	uncharacterized LOC100130357	7.58E -03	1.64
TC2000010007.hg.1	<i>RBM12</i>	RNA binding motif protein 12	1.11E -03	1.64
TC0X00007371.hg.1	<i>PAGE2B</i>	P antigen family, member 2B	6.57E -03	1.64
TC0600007266.hg.1	<i>HIST1H1C</i>	Memczak2013 ANTISENSE, CDS, coding, INTERNAL best transcript NM_005319	1.71E -03	1.64
TC0600007887.hg.1	<i>ZFAND3</i>	zinc finger, AN1-type domain 3	1.22E -03	1.64
TC1100010733.hg.1	<i>SPI1</i>	Spi-1 proto-oncogene	7.84E -04	1.64

TC0100018264.hg.1	<i>GSTM2</i>	glutathione S-transferase mu 2 (muscle)	5.64E -03	1.64
TC0600007869.hg.1	<i>CMTR1</i>	cap methyltransferase 1	4.46E -03	1.64
TC1100011029.hg.1	<i>VWCE</i>	von Willebrand factor C and EGF domains	7.74E -04	1.64
TC1400010331.hg.1	<i>XRCC3</i>	X-ray repair complementing defective repair in Chinese hamster cells 3	4.48E -03	1.63
AFFX-PheX-M_st	NA	NA	3.34E -03	1.63
TC0200009687.hg.1	<i>ARL6IP6</i>	ADP-ribosylation factor like GTPase 6 interacting protein 6	4.62E -03	1.63
TC0800008946.hg.1	<i>TG</i>	thyroglobulin	1.89E -03	1.63
TC0100011219.hg.1	<i>PPP1R12B</i>	protein phosphatase 1, regulatory subunit 12B	7.58E -04	1.63
TC0900009076.hg.1	<i>STKLD1</i>	serine/threonine kinase-like domain containing 1	6.59E -03	1.63
TC1600011560.hg.1	<i>MTSS1L</i>	metastasis suppressor 1-like	2.06E -03	1.63
TC1000007678.hg.1	<i>MTRNR2L5</i>	MT-RNR2-like 5	4.87E -03	1.63
TC1400008056.hg.1	<i>IFI27</i>	interferon, alpha-inducible protein 27	6.45E -04	1.63
TC1900009302.hg.1	<i>PIP5K1C</i>	phosphatidylinositol-4-phosphate 5-kinase, type I, gamma	6.93E -03	1.63
TC0600009623.hg.1	<i>ECT2L</i>	epithelial cell transforming 2 like	8.03E -03	1.63
TC0600008515.hg.1	<i>KCNQ5</i>	Jeck2013 ALT_ACCEPTOR, ALT_DONOR, coding, INTERNAL, intronic best transcript NM_001160133	8.25E -03	1.63
TC1900011891.hg.1	<i>HOOK2</i>	hook microtubule-tethering protein 2	7.60E -04	1.63

APPENDIX

TC0300006618.hg.1	<i>SYN2</i>	synapsin II	7.70E -03	1.63
TC1500010319.hg.1	<i>KLHL25</i>	kelch-like family member 25	9.90E -03	1.63
TC0100015102.hg.1	<i>COL11A1</i>	collagen, type XI, alpha 1	4.27E -03	1.63
TC0100013634.hg.1	<i>TMEM54</i>	transmembrane protein 54	1.21E -03	1.62
HTA2-pos-PSR02004962.hg.1	NA	NA	1.16E -03	1.62
TC0200011890.hg.1	<i>LAPTM4A</i>	Memczak2013 ALT_ACCEPTOR, ALT_DONOR, coding, INTERNAL, intronic best transcript NM_014713	7.18E -03	1.62
TC1100013061.hg.1	<i>NADSYN1</i>	NAD synthetase 1	5.61E -03	1.62
TC0700013526.hg.1	<i>FAM126A</i>	family with sequence similarity 126, member A	5.43E -04	1.62
TC1700010515.hg.1	<i>TBC1D3</i>	TBC1 domain family, member 3	7.04E -04	1.62
23074024	NA	NA	9.14E -03	1.62
TC0100007638.hg.1	<i>SERINC2</i>	serine incorporator 2	1.46E -03	1.62
23068496	NA	NA	1.82E -03	1.62
TC0100009897.hg.1	<i>CA14</i>	carbonic anhydrase XIV	8.51E -03	1.62
TC0800007414.hg.1	<i>GOLGA7</i>	golgin A7	6.33E -04	1.62
TC1700008539.hg.1	<i>MRC2</i>	mannose receptor, C type 2	8.96E -04	1.62
TC2000007476.hg.1	<i>STK4</i>	serine/threonine kinase 4	6.38E -04	1.62

TC0700010355.hg.1	<i>AGR2</i>	anterior gradient 2, protein disulphide isomerase family member	9.06E -04	1.62
TC0500011408.hg.1	<i>TMEM161B</i>	transmembrane protein 161B	7.29E -04	1.62
TC0X00006477.hg.1	<i>CD99</i>	CD99 molecule	8.11E -04	1.62
TC0700012547.hg.1	<i>OPN1SW</i>	opsin 1 (cone pigments), short-wave-sensitive	7.17E -04	1.62
TC0500009580.hg.1	<i>SIMC1</i>	SUMO-interacting motifs containing 1	2.02E -03	1.62
TC1200009464.hg.1	<i>EP400NL</i>	EP400 N-terminal like	5.43E -03	1.62
HTA2-neg-47420566_st	NA	NA	4.93E -03	1.62
TC1300006966.hg.1	<i>WBP4</i>	Transcript Identified by AceView, Entrez Gene ID(s) 11193	5.59E -04	1.61
HTA2-neg-47422462_st	NA	NA	1.30E -03	1.61
TC1900010067.hg.1	<i>PBX4</i>	pre-B-cell leukemia homeobox 4	6.22E -04	1.61
TC0800012306.hg.1	<i>MTFR1</i>	mitochondrial fission regulator 1	7.88E -03	1.61
TC0200016454.hg.1	<i>KIAA1841</i>	KIAA1841	8.37E -03	1.61
TC1900008999.hg.1	<i>ZNF549</i>	zinc finger protein 549	4.74E -03	1.61
23070220	NA	NA	8.77E -03	1.61
TC0700009770.hg.1	<i>DPP6</i>	dipeptidyl-peptidase 6	7.32E -03	1.61
TC0700012228.hg.1	<i>LAMB4</i>	laminin, beta 4	5.00E -03	1.61
TC1900011766.hg.1	<i>MARK4</i>	MAP/microtubule affinity-regulating kinase 4	1.40E -03	1.61

APPENDIX

TC1600008869.hg.1	<i>ZNF778</i>	zinc finger protein 778	4.89E -03	1.61
TC0500012980.hg.1	<i>FAM193B</i>	family with sequence similarity 193, member B	1.39E -03	1.61
TC0X00008836.hg.1	<i>PLXNA3</i>	plexin A3	2.87E -03	1.61
TC0100018224.hg.1	<i>FAM183A</i>	family with sequence similarity 183, member A	8.58E -04	1.61
TC0400006487.hg.1	<i>TMEM175</i>	transmembrane protein 175	5.56E -03	1.61
TC2100008533.hg.1	<i>PCBP3</i>	poly(rC) binding protein 3	1.59E -03	1.61
23064098	NA	NA	4.63E -03	1.61
TC0500013322.hg.1	<i>NAIP</i>	NLR family, apoptosis inhibitory protein	1.45E -03	1.61
TC0200008811.hg.1	<i>SH3RF3</i>	SH3 domain containing ring finger 3	8.31E -04	1.61
TC1100006495.hg.1	<i>TSPAN4</i>	tetraspanin 4	4.67E -03	1.61
TC1700011910.hg.1	<i>CYTH1</i>	cytohesin 1	3.38E -03	1.61
TC0300009773.hg.1	<i>FETUB</i>	fetuin B	8.30E -04	1.61
TC0100008066.hg.1	<i>PTPRF</i>	protein tyrosine phosphatase, receptor type, F	2.95E -03	1.61
AFFX-r2-Bs-dap-5_st	NA	NA	1.70E -03	1.60
HTA2-neg-47421950_st	NA	NA	7.68E -03	1.60
TC0500012659.hg.1	<i>FABP6</i>	Memczak2013 ANTISENSE, coding, INTERNAL, intronic best transcript NM_001040442	1.62E -03	1.60
TC0400007495.hg.1	<i>DCUN1D4</i>	DCN1, defective in cullin neddylation 1, domain containing 4	7.84E -03	1.60

TC1100007786.hg.1	<i>TMEM132A</i>	transmembrane protein 132A	8.64E -04	1.60
23076534	NA	NA	4.76E -03	1.60
TC1300008918.hg.1	<i>RCBTB1</i>	regulator of chromosome condensation (RCC1) and BTB (POZ) domain containing protein 1	3.53E -03	1.60
TC1700012027.hg.1	<i>ENTHD2</i>	ENTH domain containing 2	9.31E -03	1.60
TC1200010702.hg.1	<i>SMAGP</i>	small cell adhesion glycoprotein	1.43E -03	1.60
TC0X00010445.hg.1	<i>ESX1</i>	ESX homeobox 1	9.05E -04	1.60
TC0400008686.hg.1	<i>C4orf33</i>	chromosome 4 open reading frame 33	5.01E -03	1.60
TC1500008346.hg.1	<i>PRC1-AS1</i>	PRC1 antisense RNA 1	2.75E -03	1.60
TC0100007678.hg.1	<i>HDAC1</i>	histone deacetylase 1	1.02E -03	1.60
TC1100007943.hg.1	<i>PLCB3</i>	phospholipase C, beta 3 (phosphatidylinositol-specific)	1.98E -03	1.60
TC0500009423.hg.1	<i>NPM1</i>	Zhang2013 ALT_ACCEPTOR, ALT_DONOR, coding, INTERNAL, intronic best transcript NM_002520	1.83E -03	1.60
TC0700009680.hg.1	<i>TMEM176A</i>	transmembrane protein 176A	4.31E -03	1.60
TC0800007119.hg.1	<i>ESCO2</i>	establishment of sister chromatid cohesion N-acetyltransferase 2	4.99E -03	1.60
TC1200010156.hg.1	<i>CASC1</i>	cancer susceptibility candidate 1	1.04E -03	1.59
TC1900006684.hg.1	<i>SHD</i>	Src homology 2 domain containing transforming protein D	8.82E -03	1.59

APPENDIX

TC0100011316.hg.1	<i>NFASC</i>	neurofascin	6.75E -04	1.59
TC0900010925.hg.1	<i>ZNF782</i>	zinc finger protein 782	8.86E -03	1.59
TC0100016035.hg.1	<i>ETV3</i>	ets variant 3	3.54E -03	1.59
23076202	<i>NA</i>	NA	2.90E -03	1.59
TC0600011590.hg.1	<i>SPDEF</i>	SAM pointed domain containing ETS transcription factor	1.32E -03	1.59
TC1400009329.hg.1	<i>RTN1</i>	reticulon 1	5.72E -03	1.59
TC1700011083.hg.1	<i>SAMD14</i>	sterile alpha motif domain containing 14	7.29E -04	1.59
TC1100011052.hg.1	<i>FADS3</i>	fatty acid desaturase 3	7.82E -03	1.59
TC2000006627.hg.1	<i>CHGB</i>	chromogranin B	6.86E -03	1.59
23075583	<i>NA</i>	NA	1.34E -03	1.59
TC0100018081.hg.1	<i>ZNF670</i>	zinc finger protein 670	3.55E -03	1.59
TC0200008223.hg.1	<i>DNAH6</i>	dynein, axonemal, heavy chain 6	1.60E -03	1.59
TC0700011574.hg.1	<i>SPDYE16</i>	speedy/RINGO cell cycle regulator family member E16 [Source:HGNC Symbol;Acc:HGNC:51512]	4.79E -03	1.59
TC0100016122.hg.1	<i>IGSF8</i>	immunoglobulin superfamily, member 8	6.32E -03	1.59
TC2200008257.hg.1	<i>LRP5L</i>	LDL receptor related protein 5 like	4.65E -03	1.59
TC1700008014.hg.1	<i>ADAM11</i>	ADAM metallopeptidase domain 11	7.16E -03	1.59
TC2100007327.hg.1	<i>RRP1</i>	ribosomal RNA processing 1	4.18E -03	1.59

23069208	NA	NA	1.24E -03	1.58
TC1700011208.hg.1	<i>TRIM25</i>	tripartite motif containing 25	3.68E -03	1.58
HTA2-neg-47422105_st	NA	NA	3.87E -03	1.58
TC0200013008.hg.1	<i>CD207</i>	CD207 molecule, langerin	8.14E -03	1.58
TC1100008085.hg.1	<i>PELI3</i>	pellino E3 ubiquitin protein ligase family member 3	1.21E -03	1.58
HTA2-pos-PSR09020086.hg.1	NA	NA	8.78E -04	1.58
TC1800007969.hg.1	<i>L3MBTL4</i>	I(3)mbt-like 4 (Drosophila)	3.79E -03	1.58
TC1700007645.hg.1	<i>CTB-75G16.3</i>	---	1.10E -03	1.58
TC1300009012.hg.1	<i>THSD1</i>	thrombospondin type 1 domain containing 1	7.24E -03	1.58
TC0700012584.hg.1	<i>UBE2H</i>	ubiquitin conjugating enzyme E2H	5.24E -04	1.58
TC1900007090.hg.1	<i>BEST2</i>	bestrophin 2	2.75E -03	1.58
TC0600008622.hg.1	<i>SH3BGRL2</i>	SH3 domain binding glutamate-rich protein like 2	4.89E -04	1.58
TC1800008162.hg.1	<i>FAM210A</i>	family with sequence similarity 210, member A	4.13E -03	1.58
23070298	NA	NA	3.05E -03	1.58
TC0X00010877.hg.1	<i>FAM122B</i>	family with sequence similarity 122B	7.01E -04	1.58
TC0600011805.hg.1	<i>USP49</i>	ubiquitin specific peptidase 49	3.36E -03	1.58
TC0900008197.hg.1	<i>GALNT12</i>	polypeptide N-acetylgalactosaminyltransferase 12	9.49E -04	1.58

APPENDIX

TC0100018553.hg.1	<i>PLEKHA6</i>	pleckstrin homology domain containing, family A member 6	2.25E -03	1.58
TC1100012681.hg.1	<i>SIAE</i>	sialic acid acetylesterase	2.37E -03	1.58
TC1200012248.hg.1	<i>HCAR3</i>	hydroxycarboxylic acid receptor 3	1.53E -03	1.58
TC0600014251.hg.1	<i>ZBED9</i>	zinc finger, BED-type containing 9	9.69E -04	1.58
TC1500010134.hg.1	<i>CIB2</i>	calcium and integrin binding family member 2	1.89E -03	1.58
TC0900009776.hg.1	<i>MOB3B</i>	MOB kinase activator 3B	7.12E -03	1.58
TC1700009402.hg.1	<i>SMYD4</i>	SET and MYND domain containing 4	3.20E -03	1.58
23066358	NA	NA	2.49E -03	1.57
TC2000009748.hg.1	<i>CABLES2</i>	Cdk5 and Abl enzyme substrate 2	1.80E -03	1.57
TC1400007706.hg.1	<i>FOS</i>	FBJ murine osteosarcoma viral oncogene homolog	2.79E -03	1.57
TC1100011609.hg.1	<i>P4HA3</i>	prolyl 4-hydroxylase, alpha polypeptide III	4.74E -03	1.57
TC0900011432.hg.1	<i>RBM18</i>	RNA binding motif protein 18	5.52E -03	1.57
TC1100008010.hg.1	<i>CDC42EP2</i>	CDC42 effector protein (Rho GTPase binding) 2	3.40E -03	1.57
TC1700008661.hg.1	<i>PRKCA</i>	protein kinase C, alpha	1.98E -03	1.57
TC1200011599.hg.1	<i>LTA4H</i>	leukotriene A4 hydrolase	2.51E -03	1.57
TC1700009383.hg.1	<i>PITPNA</i>	Memczak2013 ALT_ACCEPTOR, ALT_DONOR, coding, INTERNAL, intronic best transcript NM_006224	5.55E -03	1.57

TC0200016746.hg.1	<i>TTC21B</i>	tetratricopeptide repeat domain 21B	4.51E -03	1.57
23075424	NA	NA	9.53E -03	1.57
23070118	NA	NA	2.35E -03	1.57
TC0700012712.hg.1	<i>LUZP6</i>	leucine zipper protein 6	1.21E -03	1.57
23076310	NA	NA	7.70E -03	1.57
23076464	NA	NA	7.70E -03	1.57
AFFX-r2-Ec-bioB-5_at	NA	NA	5.69E -04	1.57
TC0900007869.hg.1	<i>SEMA4D</i>	Memczak2013 ANTISENSE, coding, INTERNAL, UTR3 best transcript NM_006378	1.67E -03	1.57
TC0900007050.hg.1	<i>DNAI1</i>	Transcript Identified by AceView, Entrez Gene ID(s) 27019	2.07E -03	1.57
TC1600011286.hg.1	<i>CHMP1A</i>	charged multivesicular body protein 1A	9.92E -04	1.57
TC1100009068.hg.1	<i>NCAM1</i>	neural cell adhesion molecule 1	4.48E -04	1.57
TC1600010122.hg.1	<i>LINC00273</i>	long intergenic non-protein coding RNA 273	1.81E -03	1.57
TC0700011779.hg.1	<i>ERVW-1</i>	endogenous retrovirus group W, member 1	7.25E -03	1.57
23070246	NA	NA	8.37E -03	1.56
TC1100010990.hg.1	<i>MRPL16</i>	mitochondrial ribosomal protein L16	2.06E -03	1.56
TC0100016316.hg.1	<i>ADCY10</i>	adenylate cyclase 10 (soluble)	8.20E -04	1.56
TC1600008231.hg.1	<i>NFAT5</i>	nuclear factor of activated T-cells 5, tonicity-responsive	3.06E -03	1.56

APPENDIX

TC0500013140.hg.1	<i>AHRR</i>	aryl-hydrocarbon receptor repressor	4.82E -03	1.56
TC1600007967.hg.1	<i>MT1IP</i>	metallothionein 1l, pseudogene	3.13E -03	1.56
TC2000009180.hg.1	<i>OSER1</i>	oxidative stress responsive serine-rich 1	2.75E -03	1.56
TC0200008516.hg.1	<i>CNNM3</i>	Zhang2013 ALT_ACCEPTOR, ALT_DONOR, coding, INTERNAL, intronic, OVERLAPTX best transcript NM_017623	1.12E -03	1.56
TC0500008467.hg.1	<i>SRFBP1</i>	serum response factor binding protein 1	1.59E -03	1.56
TC0300009724.hg.1	<i>VPS8</i>	vacuolar protein sorting 8 homolog (S. cerevisiae)	5.12E -03	1.56
TC1900011908.hg.1	<i>PDE4C</i>	phosphodiesterase 4C, cAMP-specific	1.64E -03	1.56
TSUnmapped00000213.hg.1	<i>DGKD</i>	diacylglycerol kinase, delta 130kDa	5.15E -03	1.56
TC0700009398.hg.1	<i>TAS2R3</i>	taste receptor, type 2, member 3	5.01E -03	1.56
TC1900009743.hg.1	<i>TNPO2</i>	transportin 2	4.02E -03	1.56
TC1700008440.hg.1	<i>PPM1E</i>	protein phosphatase, Mg ²⁺ /Mn ²⁺ dependent, 1E	3.13E -03	1.56
TC1400009563.hg.1	<i>SLC10A1</i>	solute carrier family 10 (sodium/bile acid cotransporter), member 1	7.30E -03	1.56
TC0700011344.hg.1	<i>GUSB</i>	glucuronidase, beta	2.09E -03	1.56
TC0900009307.hg.1	<i>ARRDC1</i>	arrestin domain containing 1	3.40E -03	1.56
TC0100009658.hg.1	<i>SRGAP2C</i>	SLIT-ROBO Rho GTPase activating protein 2C	5.94E -04	1.56
TC1900011596.hg.1	<i>C19orf18</i>	chromosome 19 open reading frame 18	1.03E -03	1.56

TC0200013765.hg.1	<i>UXS1</i>	UDP-glucuronate decarboxylase 1	1.11E -03	1.56
TC0200014029.hg.1	<i>C2orf76</i>	chromosome 2 open reading frame 76	1.67E -03	1.56
TC0X00007558.hg.1	<i>NLGN3</i>	neuroligin 3	5.15E -03	1.56
TC1900010997.hg.1	<i>DACT3</i>	dishevelled-binding antagonist of beta-catenin 3	3.73E -03	1.56
TC1200009959.hg.1	<i>LRP6</i>	LDL receptor related protein 6	2.00E -03	1.56
23075524	NA	NA	1.06E -03	1.56
TC0100010341.hg.1	<i>FCER1G</i>	Fc fragment of IgE, high affinity I, receptor for; gamma polypeptide	2.49E -03	1.56
TC0200012009.hg.1	<i>DTNB</i>	dystrobrevin beta	4.27E -03	1.56
TC0900010587.hg.1	<i>C9orf64</i>	Transcript Identified by AceView, Entrez Gene ID(s) 84267	4.18E -03	1.55
TCUn_GL000218v100006433.hg.1	<i>LOC389834</i>	ankyrin repeat domain 57 pseudogene	5.24E -03	1.55
AFFX-BioB-M_at	NA	NA	5.46E -04	1.55
TC0500009863.hg.1	<i>LPCAT1</i>	lysophosphatidylcholine acyltransferase 1	2.56E -03	1.55
TC1600010778.hg.1	<i>HYDIN</i>	HYDIN, axonemal central pair apparatus protein	2.05E -03	1.55
23075525	NA	NA	2.57E -03	1.55
HTA2-neg-47422968_st	NA	NA	6.28E -03	1.55
AFFX-r2-Ec-bioB-M_at	NA	NA	8.83E -04	1.55
TC0300008375.hg.1	<i>ZDHHC23</i>	zinc finger, DHHC-type containing 23	2.31E -03	1.55

APPENDIX

TC0X00010661.hg.1	<i>RHOXF2B</i>	Rhox homeobox family, member 2B	8.06E -03	1.55
TC0X00008080.hg.1	<i>VSIG1</i>	V-set and immunoglobulin domain containing 1	2.85E -03	1.55
TC1000012117.hg.1	<i>CHST15</i>	carbohydrate (N-acetylgalactosamine 4-sulfate 6-O) sulfotransferase 15	2.33E -03	1.55
TC0500008684.hg.1	<i>TCF7</i>	transcription factor 7 (T-cell specific, HMG-box)	1.95E -03	1.55
TC1200008678.hg.1	<i>EID3</i>	EP300 interacting inhibitor of differentiation 3	7.50E -03	1.55
TC1900011573.hg.1	<i>ZNF416</i>	zinc finger protein 416	1.19E -03	1.55
TC0100007091.hg.1	<i>CROCC</i>	Zhang2013 ALT_ACCEPTOR, ALT_DONOR, coding, INTERNAL, intronic best transcript NM_014675	1.63E -03	1.55
TC1100007833.hg.1	<i>INCENP</i>	inner centromere protein	2.37E -03	1.55
TC0500007552.hg.1	<i>LOC100421561</i>	family with sequence similarity 133, member A pseudogene	7.93E -03	1.55
TC0700013435.hg.1	<i>CDHR3</i>	cadherin-related family member 3	2.35E -03	1.55
TC0100013837.hg.1	<i>RIMS3</i>	regulating synaptic membrane exocytosis 3	5.07E -03	1.55
TC1900011593.hg.1	<i>ZNF418</i>	zinc finger protein 418	3.17E -03	1.55
AFFX-BioB-5_at	NA	NA	9.17E -04	1.55
TC1700006877.hg.1	<i>ADPRM</i>	ADP-ribose/CDP-alcohol diphosphatase, manganese-dependent	2.54E -03	1.55
TC0300009280.hg.1	<i>KCNAB1</i>	Transcript Identified by AceView, Entrez Gene ID(s) 7881	2.82E -03	1.55

TC0900008959.hg.1	<i>FUBP3</i>	far upstream element (FUSE) binding protein 3	5.43E -04	1.54
ERCCmix2step23	NA	NA	9.50E -03	1.54
TC1600010172.hg.1	<i>RP11-93O14.2</i>	---	1.02E -03	1.54
TC2200008864.hg.1	<i>CYP2D6</i>	cytochrome P450, family 2, subfamily D, polypeptide 6	1.03E -03	1.54
TC0800007370.hg.1	<i>ADAM32</i>	ADAM metallopeptidase domain 32	5.80E -03	1.54
23075807	NA	NA	1.69E -03	1.54
TC1200011968.hg.1	<i>HECTD4</i>	HECT domain containing E3 ubiquitin protein ligase 4	4.70E -03	1.54
TC1600007262.hg.1	<i>TNRC6A</i>	trinucleotide repeat containing 6A	6.92E -03	1.54
TC2000008095.hg.1	<i>TPD52L2</i>	tumor protein D52-like 2	9.62E -03	1.54
HTA2-pos-PSR14009921.hg.1	NA	NA	2.83E -03	1.54
23075679	NA	NA	8.01E -03	1.54
23076144	NA	NA	8.01E -03	1.54
TC0700008584.hg.1	<i>AP1S1</i>	Transcript Identified by AceView, Entrez Gene ID(s) 1174	4.22E -03	1.54
TC0800011259.hg.1	<i>ANKRD46</i>	ankyrin repeat domain 46	7.10E -03	1.54
TC1000012586.hg.1	<i>SEC31B</i>	SEC31 homolog B, COPII coat complex component	2.67E -03	1.54
TC0700008011.hg.1	<i>NCF1</i>	neutrophil cytosolic factor 1	2.26E -03	1.54
TC1100010907.hg.1	<i>BTBD18</i>	BTB (POZ) domain containing 18	3.49E -03	1.54
TC1900010521.hg.1	<i>ZFP14</i>	ZFP14 zinc finger protein	5.55E -04	1.54

APPENDIX

TC0X00008394.hg.1	<i>BCORL1</i>	BCL6 corepressor-like 1	2.84E -03	1.54
TC0100010282.hg.1	<i>ATP1A4</i>	ATPase, Na+/K+ transporting, alpha 4 polypeptide	5.46E -04	1.54
TC0100018398.hg.1	<i>TNFRSF25</i>	tumor necrosis factor receptor superfamily, member 25	8.29E -03	1.54
TC1500010945.hg.1	<i>LINS1</i>	lines homolog 1	2.15E -03	1.54
TC0500010592.hg.1	<i>C6</i>	complement component 6	1.38E -03	1.54
TC0600009262.hg.1	<i>SLC35F1</i>	solute carrier family 35, member F1	7.79E -03	1.54
TC1700008846.hg.1	<i>KIF19</i>	kinesin family member 19	1.29E -03	1.53
TC1200010105.hg.1	<i>RECQL</i>	RecQ helicase-like	3.73E -03	1.53
TC1900006968.hg.1	<i>C19orf66</i>	chromosome 19 open reading frame 66	8.48E -03	1.53
TC2200009259.hg.1	<i>SMTN</i>	smoothelin	1.64E -03	1.53
TC0100015891.hg.1	<i>CRTC2</i>	CREB regulated transcription coactivator 2	4.21E -03	1.53
TC1900007328.hg.1	<i>SLC27A1</i>	solute carrier family 27 (fatty acid transporter), member 1	2.29E -03	1.53
TC1600011358.hg.1	<i>C16orf45</i>	chromosome 16 open reading frame 45	1.85E -03	1.53
TC1100008090.hg.1	<i>ACTN3</i>	actinin, alpha 3 (gene/pseudogene)	9.54E -04	1.53
23076398	NA	NA	1.12E -03	1.53
23070245	NA	NA	2.04E -03	1.53
TC0800009621.hg.1	<i>CTSB</i>	Jeck2013 ALT_DONOR, coding, INTERNAL, intronic best transcript NM_147780	5.48E -03	1.53

TC0200012417.hg.1	<i>ABCG5</i>	ATP binding cassette subfamily G member 5	8.74E -03	1.53
TC0200016446.hg.1	<i>ACYP2</i>	acylphosphatase 2, muscle type	3.21E -03	1.53
TC0300012190.hg.1	<i>KPNA1</i>	Transcript Identified by AceView, Entrez Gene ID(s) 3836	9.83E -03	1.53
TC0500008342.hg.1	<i>DCP2</i>	decapping mRNA 2	2.32E -03	1.53
TC0200011379.hg.1	<i>SNED1</i>	sushi, nidogen and EGF-like domains 1	5.35E -03	1.53
TC1600008329.hg.1	<i>HP</i>	haptoglobin	8.99E -03	1.53
TC0X00008276.hg.1	<i>ATP1B4</i>	ATPase, Na+/K+ transporting, beta 4 polypeptide	7.05E -04	1.53
TC0700013429.hg.1	<i>PILRA</i>	paired immunoglobulin-like type 2 receptor alpha	6.98E -03	1.53
TC0700011554.hg.1	<i>PMS2P3</i>	PMS1 homolog 2, mismatch repair system component pseudogene 3	2.85E -03	1.53
TC2100008459.hg.1	<i>FTCD</i>	formimidoyltransferase cyclodeaminase	8.00E -03	1.53
TC0300011183.hg.1	<i>NEK4</i>	NIMA-related kinase 4	6.41E -03	1.53
TC0500007586.hg.1	<i>RGS7BP</i>	regulator of G-protein signaling 7 binding protein	9.35E -03	1.53
TC1600006941.hg.1	<i>SNX29</i>	sorting nexin 29	5.23E -03	1.53
HTA2-pos-PSR02004963.hg.1	<i>NA</i>	NA	4.02E -03	1.53
TC0700009400.hg.1	<i>TAS2R5</i>	taste receptor, type 2, member 5	6.43E -03	1.53
TC1600011494.hg.1	<i>ARL6IP1</i>	ADP-ribosylation factor like GTPase 6 interacting protein 1	4.18E -03	1.53

APPENDIX

TC1900007688.hg.1	<i>CCNE1</i>	cyclin E1	5.89E -03	1.53
TC1600010680.hg.1	<i>SLC7A6OS</i>	solute carrier family 7, member 6 opposite strand	2.74E -03	1.53
TC1000012549.hg.1	<i>PARG</i>	poly (ADP-ribose) glycohydrolase	1.87E -03	1.53
TC0300013350.hg.1	<i>YEATS2</i>	Memczak2013 ANTISENSE, coding, INTERNAL, intronic best transcript NM_018023	1.28E -03	1.52
TC0700011961.hg.1	<i>GJC3</i>	gap junction protein gamma 3	1.38E -03	1.52
AFFX-r2-Ec-bioB-3_at	NA	NA	1.21E -03	1.52
TC0300014085.hg.1	<i>TBCCD1</i>	TBCC domain containing 1	6.94E -03	1.52
AFFX-BioC-3_at	NA	NA	1.36E -03	1.52
TC1000006796.hg.1	<i>SEC61A2</i>	Sec61 translocon alpha 2 subunit	9.58E -03	1.52
TC1200009136.hg.1	<i>CABP1</i>	calcium binding protein 1	3.97E -03	1.52
TC1700012283.hg.1	<i>LUC7L3</i>	LUC7-like 3 pre-mRNA splicing factor	3.86E -03	1.52
TC1900010632.hg.1	<i>SIRT2</i>	sirtuin 2	9.22E -03	1.52
TC1200012707.hg.1	<i>ALDH2</i>	aldehyde dehydrogenase 2 family (mitochondrial)	4.78E -03	1.52
TC0300006564.hg.1	<i>IL17RE</i>	interleukin 17 receptor E	7.02E -03	1.52
TC1800006635.hg.1	<i>TWSG1</i>	twisted gastrulation BMP signaling modulator 1	3.00E -03	1.52
TC0400007128.hg.1	<i>TBC1D19</i>	TBC1 domain family, member 19	4.82E -03	1.52
TC1900008600.hg.1	<i>GPR32</i>	G protein-coupled receptor 32	2.00E -03	1.52
TC0700009395.hg.1	<i>WEE2</i>	WEE1 homolog 2 (S. pombe)	6.94E -03	1.52

TC1200012561.hg.1	ZNF891	zinc finger protein 891	7.73E -03	1.52
TC0200009902.hg.1	NOSTRIN	nitric oxide synthase trafficking	6.78E -03	1.52
TC0X00011126.hg.1	GABRA3	gamma-aminobutyric acid (GABA) A receptor, alpha 3	9.19E -03	1.52
TC0100015572.hg.1	SRGAP2B	SLIT-ROBO Rho GTPase activating protein 2B	1.18E -03	1.52
23069198	NA	NA	6.97E -03	1.52
TC0300013670.hg.1	TNK2	tyrosine kinase, non-receptor, 2	1.06E -03	1.52
TC1900011889.hg.1	MAN2B1	mannosidase, alpha, class 2B, member 1	5.51E -03	1.52
TC1300008426.hg.1	USP12	Transcript Identified by AceView, Entrez Gene ID(s) 219333	2.12E -03	1.52
23071966	NA	NA	7.67E -03	1.52
TC1100013065.hg.1	KRTAP5-9	keratin associated protein 5-9	1.27E -03	1.52
TC2200007904.hg.1	ATP6V1E1	ATPase, H+ transporting, lysosomal 31kDa, V1 subunit E1	7.46E -04	1.52
TC0100018348.hg.1	CNIH3	cornichon family AMPA receptor auxiliary protein 3	5.63E -03	1.52
23075438	NA	NA	5.49E -03	1.52
TC1100012930.hg.1	B3GAT1	beta-1,3-glucuronyltransferase 1	6.47E -03	1.52
TC1700010731.hg.1	PSMC3IP	PSMC3 interacting protein	1.54E -03	1.52
TC1700012242.hg.1	LOC101060389	TBC1 domain family member-like	7.50E -03	1.52
TC0Y00006476.hg.1	CD99	Homo sapiens CD99 molecule (CD99), transcript variant 2, mRNA.	1.13E -03	1.52

APPENDIX

TC0200012068.hg.1	<i>SLC30A3</i>	solute carrier family 30 (zinc transporter), member 3	3.44E -03	1.52
HTA2-pos-2930600_st	NA	NA	7.24E -04	1.52
23075427	NA	NA	8.45E -03	1.52
AFFX-r2-Ec-bioC-5_at	NA	NA	1.25E -03	1.52
TC0100016053.hg.1	<i>CD5L</i>	CD5 molecule-like	2.84E -03	1.51
TC1700011448.hg.1	<i>POLG2</i>	polymerase (DNA directed), gamma 2, accessory subunit	2.66E -03	1.51
TC1900006730.hg.1	<i>KDM4B</i>	lysine (K)-specific demethylase 4B	2.87E -03	1.51
TC0600008870.hg.1	<i>FUT9</i>	fucosyltransferase 9 (alpha (1,3) fucosyltransferase)	4.79E -03	1.51
TC0Y00006858.hg.1	<i>VAMP7</i>	Homo sapiens vesicle-associated membrane protein 7 (VAMP7), transcript variant 2, mRNA.	2.67E -03	1.51
HTA2-pos-PSR01002166.hg.1	NA	NA	5.01E -03	1.51
TC1700006638.hg.1	<i>ARRB2</i>	arrestin, beta 2	7.20E -03	1.51
TC1300007045.hg.1	<i>GPALPP1</i>	GPALPP motifs containing 1	2.81E -03	1.51
TC0600013431.hg.1	<i>PLAGL1</i>	pleiomorphic adenoma gene-like 1	1.91E -03	1.51
TC0200006539.hg.1	<i>ALLC</i>	allantoicase	2.87E -03	1.51
TC1500009224.hg.1	<i>STRC</i>	stereocilin	4.60E -03	1.51
TC2000009907.hg.1	<i>EFCAB8</i>	EF-hand calcium binding domain 8	4.24E -03	1.51
TC2000007114.hg.1	<i>KIF3B</i>	kinesin family member 3B	3.14E -03	1.51

TC0500006822.hg.1	<i>OTULIN</i>	OTU deubiquitinase with linear linkage specificity	1.91E -03	1.51
TC0300008369.hg.1	<i>ATP6V1A</i>	ATPase, H ⁺ transporting, lysosomal 70kDa, V1 subunit A	8.71E -03	1.51
TC1900006999.hg.1	<i>DNM2</i>	Transcript Identified by AceView, Entrez Gene ID(s) 1785	1.08E -03	1.51
TC0200016413.hg.1	<i>FKBP1B</i>	FK506 binding protein 1B	1.84E -03	1.51
TC0900008463.hg.1	<i>HSDL2</i>	hydroxysteroid dehydrogenase like 2	7.29E -03	1.51
TC1100010741.hg.1	<i>CELF1</i>	CUGBP, Elav-like family member 1	1.37E -03	1.51
TC1500007980.hg.1	<i>CHRNA5</i>	cholinergic receptor, nicotinic alpha 5	6.50E -03	1.51
TC0900012258.hg.1	<i>MFSD14C</i>	major facilitator superfamily domain containing 14C	1.11E -03	1.51
TC1900007325.hg.1	<i>MVB12A</i>	multivesicular body subunit 12A	4.20E -03	1.51
TC0600009167.hg.1	<i>WISP3</i>	WNT1 inducible signaling pathway protein 3	6.60E -03	1.51
TC0600008722.hg.1	<i>ZNF292</i>	zinc finger protein 292	2.57E -03	1.51
TC0200010897.hg.1	<i>SGPP2</i>	sphingosine-1-phosphate phosphatase 2	8.14E -03	1.51
HTA2-neg-47420332_st	NA	NA	8.54E -03	1.51
TC0800007738.hg.1	<i>SDCBP</i>	syndecan binding protein	1.30E -03	1.51
TC0700010182.hg.1	<i>PMS2</i>	PMS1 homolog 2, mismatch repair system component	1.57E -03	1.51
TC1600007739.hg.1	<i>PHKB</i>	phosphorylase kinase, beta	6.26E -03	1.51
TC0600007616.hg.1	<i>HSPA1B</i>	heat shock 70kDa protein 1B	1.99E -03	1.51

APPENDIX

TC0400007456.hg.1	<i>ZAR1</i>	zygote arrest 1	2.35E -03	1.51
TC1900006804.hg.1	<i>TNFSF9</i>	tumor necrosis factor (ligand) superfamily, member 9	1.05E -03	1.51
TC1600009958.hg.1	<i>NPIP4</i>	nuclear pore complex interacting protein family, member B4	1.24E -03	1.51
TSUnmapped00000460.hg.1	<i>DGKD</i>	diacylglycerol kinase, delta 130kDa	6.01E -03	1.51
TC1900011931.hg.1	<i>SYNE4</i>	spectrin repeat containing, nuclear envelope family member 4	4.40E -03	1.51
TC0100007943.hg.1	<i>RLF</i>	rearranged L-myc fusion	2.05E -03	1.51
TC0300012980.hg.1	<i>SPTSSB</i>	serine palmitoyltransferase, small subunit B	9.29E -03	1.51
23074924	<i>NA</i>	NA	1.12E -03	1.51
TC1000008088.hg.1	<i>SAMD8</i>	sterile alpha motif domain containing 8	3.47E -03	1.50
TC1400010615.hg.1	<i>MNAT1</i>	MNAT CDK-activating kinase assembly factor 1	8.21E -04	1.50
TC1600009042.hg.1	<i>CLCN7</i>	chloride channel, voltage-sensitive 7	7.50E -03	1.50
TC1000007564.hg.1	<i>MAPK8</i>	mitogen-activated protein kinase 8	3.72E -03	1.50
TC0400010141.hg.1	<i>LDB2</i>	LIM domain binding 2	5.21E -03	1.50
TC1300007707.hg.1	<i>GPC5</i>	glypican 5	4.22E -03	1.50
TC1900007100.hg.1	<i>MAST1</i>	microtubule associated serine/threonine kinase 1	2.01E -03	1.50
TC0500007120.hg.1	<i>TTC23L</i>	tetratricopeptide repeat domain 23-like	4.23E -03	1.50
TC0600014006.hg.1	<i>WDR27</i>	WD repeat domain 27	3.41E -03	1.50

TC0500011754.hg.1	<i>TMED7-TICAM2</i>	TMED7-TICAM2 readthrough	8.21E-03	1.50
TC0200009071.hg.1	<i>CFAP221</i>	cilia and flagella associated protein 221	1.40E-03	1.50
23075740	NA	NA	2.79E-03	1.50
TC0100011534.hg.1	<i>FAM71A</i>	family with sequence similarity 71, member A	3.44E-03	1.50
TC0200016660.hg.1	<i>C2orf61</i>	chromosome 2 open reading frame 61	2.42E-03	1.50

Supplementary Table 4: BGB290 single treatment versus control: Differentially expressed genes

Probe ID	Symbol	Gene name	P value	Fold change
TC0600014190.hg.1	<i>ZC2HC1B</i>	zinc finger, C2HC-type containing 1B	4.28E-03	5.60
TC1200011845.hg.1	<i>SEPLG</i>	selectin P ligand	5.33E-03	5.09
23076543	NA	NA	5.03E-05	4.67
TC0700013472.hg.1	<i>MGAM</i>	maltase-glucoamylase	4.09E-05	4.04
TC0300014032.hg.1	<i>POPDC2</i>	popeye domain containing 2	7.87E-05	3.85
HTA2-pos-3295162_st	NA	NA	1.04E-04	3.80
TC1200008686.hg.1	<i>CHST11</i>	Transcript Identified by AceView, Entrez Gene ID(s) 50515	2.18E-03	3.68
TC0600009597.hg.1	<i>TNFAIP3</i>	tumor necrosis factor, alpha-induced protein 3	1.14E-03	3.40
TC0500012017.hg.1	<i>IRF1</i>	interferon regulatory factor 1	6.32E-03	3.13
TC1900006977.hg.1	<i>ICAM1</i>	intercellular adhesion molecule 1	8.16E-04	3.07

APPENDIX

HTA2-neg-47424041_st	NA	NA	9.05E-03	3.03
TC2100007599.hg.1	SAMSN1	SAM domain, SH3 domain and nuclear localization signals 1	7.08E-04	2.97
TC2100008297.hg.1	SIK1	salt-inducible kinase 1	7.78E-03	2.92
TC1200007053.hg.1	SPX	spexin hormone	3.18E-03	2.89
HTA2-neg-47422282_st	NA	NA	8.84E-03	2.88
TC0700013442.hg.1	LSMEM1	leucine-rich single-pass membrane protein 1	1.03E-03	2.86
HTA2-neg-47424062_st	NA	NA	1.73E-03	2.84
TC0500007077.hg.1	NPR3	natriuretic peptide receptor 3	5.08E-04	2.80
TC2000009964.hg.1	SDCBP2	syndecan binding protein (syntenin) 2	3.53E-04	2.73
TC0300012007.hg.1	CD200R1	CD200 receptor 1	2.66E-03	2.71
TC1000006911.hg.1	TMEM236	transmembrane protein 236	2.36E-03	2.70
TC0700009411.hg.1	MGAM2	maltase-glucoamylase 2 (putative)	3.78E-04	2.67
TC0700008495.hg.1	BUD31	Transcript Identified by AceView, Entrez Gene ID(s) 8896	4.62E-05	2.65
HTA2-pos-47421926_st	NA	NA	2.02E-03	2.62
TC0400008240.hg.1	DAPP1	dual adaptor of phosphotyrosine and 3-phosphoinositides	8.72E-03	2.58
HTA2-pos-47421925_st	NA	NA	1.05E-03	2.57

TC1300008813.hg.1	<i>KCTD4</i>	potassium channel tetramerization domain containing 4	1.99E-03	2.54
TC0800011566.hg.1	<i>RAD21</i>	Transcript Identified by AceView, Entrez Gene ID(s) 5885	4.45E-03	2.52
TC0900010737.hg.1	<i>DIRAS2</i>	DIRAS family, GTP-binding RAS-like 2	1.23E-03	2.51
HTA2-pos-2960249_st	NA	NA	9.75E-05	2.44
TC0700013424.hg.1	<i>GS1-259H13.2</i>	transmembrane protein 225-like	2.16E-03	2.37
TC0600013231.hg.1	<i>SGK1</i>	serum/glucocorticoid regulated kinase 1	2.73E-03	2.36
TC0400007360.hg.1	<i>DCAF4L1</i>	DDB1 and CUL4 associated factor 4-like 1	1.79E-03	2.35
TC1100008188.hg.1	<i>PPP6R3</i>	Memczak2013 ALT_ACCEPTOR, ALT_DONOR, coding, INTERNAL, intronic best transcript NM_001164162	2.79E-04	2.35
TC1300008048.hg.1	<i>TEX29</i>	testis expressed 29	1.50E-03	2.32
TC2000009945.hg.1	<i>FAM209A</i>	family with sequence similarity 209, member A	6.42E-05	2.24
TC0900008219.hg.1	<i>NR4A3</i>	nuclear receptor subfamily 4, group A, member 3	6.97E-03	2.22
HTA2-neg-47422433_st	NA	NA	3.59E-04	2.22
HTA2-pos-47421982_st	NA	NA	1.81E-03	2.20
TC1600006593.hg.1	<i>RAB26</i>	RAB26, member RAS oncogene family	8.76E-03	2.17
TC1900011817.hg.1	<i>ZNF773</i>	zinc finger protein 773	5.17E-05	2.14
HTA2-pos-2985881_st	NA	NA	1.12E-03	2.13

APPENDIX

TC0200014361.hg.1	<i>LYPD1</i>	LY6/PLAUR domain containing 1	5.06E-03	2.13
HTA2-neg-47422979_st	NA	NA	8.83E-03	2.13
TC0500011334.hg.1	<i>TMEM167A</i>	Transcript Identified by AceView, Entrez Gene ID(s) 153339	2.52E-03	2.11
TC0300007050.hg.1	<i>C3orf35</i>	chromosome 3 open reading frame 35	2.64E-04	2.10
TC0200015402.hg.1	<i>FAM126B</i>	family with sequence similarity 126, member B	1.10E-03	2.09
HTA2-neg-47423115_st	NA	NA	4.14E-05	2.06
TC1100007216.hg.1	<i>PRRG4</i>	proline rich Gla (G-carboxyglutamic acid) 4 (transmembrane)	8.31E-03	2.05
TC0600007263.hg.1	<i>HIST1H4A</i>	histone cluster 1, H4a	3.20E-03	2.05
TC1500010745.hg.1	<i>POLR2M</i>	polymerase (RNA) II (DNA directed) polypeptide M	5.61E-03	2.05
HTA2-pos-2960237_st	NA	NA	2.45E-03	2.04
TC1100010505.hg.1	<i>ABTB2</i>	ankyrin repeat and BTB (POZ) domain containing 2	6.09E-04	2.03
HTA2-neg-47423121_st	NA	NA	2.61E-03	2.01
HTA2-neg-47422060_st	NA	NA	2.04E-03	2.01
TC2000008211.hg.1	<i>UBOX5</i>	U-box domain containing 5	1.95E-03	2.01
TC2100007140.hg.1	<i>ETS2</i>	v-ets avian erythroblastosis virus E26 oncogene homolog 2	7.29E-03	2.00
TC0500012870.hg.1	<i>STC2</i>	stanniocalcin 2	1.20E-04	2.00
TC0700013587.hg.1	<i>SHFM1</i>	split hand/foot malformation (ectrodactyly) type 1	1.32E-03	1.99

TC1500009458.hg.1	<i>ARPP19</i>	cAMP-regulated phosphoprotein 19kDa	7.19E-04	1.98
TC0100008631.hg.1	<i>SGIP1</i>	SH3-domain GRB2-like (endophilin) interacting protein 1	7.52E-03	1.97
23076544	NA	NA	1.07E-03	1.97
HTA2-pos-2985880_st	NA	NA	4.20E-03	1.96
TC1100007729.hg.1	<i>DTX4</i>	deltex 4, E3 ubiquitin ligase	9.09E-04	1.96
TC1400008940.hg.1	<i>NFKBIA</i>	nuclear factor of kappa light polypeptide gene enhancer in B-cells inhibitor, alpha	2.22E-03	1.95
TC0600012064.hg.1	<i>GCM1</i>	glial cells missing homolog 1 (Drosophila)	6.78E-03	1.95
TC1700010560.hg.1	<i>PLXDC1</i>	plexin domain containing 1	1.89E-03	1.94
TC0500008541.hg.1	<i>TEX43</i>	testis expressed 43	7.95E-04	1.94
TC0700010899.hg.1	<i>POLR2J4</i>	polymerase (RNA) II (DNA directed) polypeptide J4, pseudogene	2.29E-03	1.93
TC1700006763.hg.1	<i>ATP1B2</i>	ATPase, Na+/K+ transporting, beta 2 polypeptide	9.42E-03	1.93
TC0500009984.hg.1	<i>FLJ33360</i>	FLJ33360 protein	4.69E-03	1.92
TC0900007877.hg.1	<i>GADD45G</i>	growth arrest and DNA-damage-inducible, gamma	5.52E-04	1.92
TC0300009916.hg.1	<i>HES1</i>	hes family bHLH transcription factor 1	1.91E-03	1.91
TC0200010586.hg.1	<i>CPO</i>	carboxypeptidase O	3.44E-03	1.91
TC0100009417.hg.1	<i>C1orf162</i>	chromosome 1 open reading frame 162	3.86E-04	1.90
TC0600012502.hg.1	<i>GJB7</i>	gap junction protein beta 7	4.44E-03	1.89

APPENDIX

TC0X00006585.hg.1	<i>SHROOM2</i>	shroom family member 2	5.43E-03	1.89
TSUnmapped00000354.hg.1	<i>EIF3F</i>	Eukaryotic translation initiation factor 3 subunit F [Source:UniProtKB/Swiss-Prot;Acc:O00303]	7.91E-03	1.89
TC0400008389.hg.1	<i>RRH</i>	retinal pigment epithelium-derived rhodopsin homolog	8.86E-04	1.88
TC0200014620.hg.1	<i>CACNB4</i>	calcium channel, voltage-dependent, beta 4 subunit	8.99E-04	1.88
TC0600010056.hg.1	<i>WTAP</i>	Wilms tumor 1 associated protein	3.81E-03	1.87
TC1800006733.hg.1	<i>PRELID3A</i>	PREL1 domain containing 3A	1.32E-03	1.85
TC0500009059.hg.1	<i>GRPEL2</i>	GrpE-like 2, mitochondrial (E. coli)	7.59E-05	1.85
TC0200012977.hg.1	<i>MXD1</i>	Memczak2013 ANTISENSE, coding, INTERNAL, intronic best transcript NM_001202514	8.19E-03	1.85
TC0400011421.hg.1	<i>LAMTOR3</i>	late endosomal/lysosomal adaptor, MAPK and MTOR activator 3	5.85E-03	1.85
HTA2-neg-47423502_st	NA	NA	2.51E-03	1.84
HTA2-neg-47421633_st	NA	NA	8.96E-04	1.84
TC1200009192.hg.1	<i>BCL7A</i>	B-cell CLL/lymphoma 7A	8.29E-03	1.84
TC0200013638.hg.1	<i>LONRF2</i>	LON peptidase N-terminal domain and ring finger 2	2.64E-03	1.84
TC0200016661.hg.1	<i>C2orf61</i>	chromosome 2 open reading frame 61	4.73E-03	1.84
TC0200007746.hg.1	<i>B3GNT2</i>	UDP-GlcNAc:betaGal beta-1,3-N-acetylglucosaminyltransferase 2	4.90E-03	1.83

HTA2-neg-47422334_st	NA	NA	5.45E-03	1.82
HTA2-neg-47424061_st	NA	NA	5.73E-03	1.82
TC0100010341.hg.1	<i>FCER1G</i>	Fc fragment of IgE, high affinity I, receptor for; gamma polypeptide	1.36E-04	1.82
TC0500007050.hg.1	<i>PDZD2</i>	PDZ domain containing 2	1.38E-03	1.81
TC0500007895.hg.1	<i>CMYA5</i>	cardiomyopathy associated 5	2.21E-03	1.81
TC1300009810.hg.1	<i>ANKRD10</i>	ankyrin repeat domain 10	3.94E-03	1.81
TC2000009886.hg.1	<i>PANK2</i>	pantothenate kinase 2	5.91E-04	1.80
TC0100015271.hg.1	<i>OVGP1</i>	oviductal glycoprotein 1	2.40E-03	1.80
TC1200012737.hg.1	<i>ZNF268</i>	zinc finger protein 268	1.43E-04	1.80
TC0200008904.hg.1	<i>FBLN7</i>	fibulin 7	6.57E-03	1.80
TC1000012117.hg.1	<i>CHST15</i>	carbohydrate (N-acetylgalactosamine 4-sulfate 6-O) sulfotransferase 15	4.12E-04	1.79
TC2000006791.hg.1	<i>PCSK2</i>	proprotein convertase subtilisin/kexin type 2	4.40E-03	1.79
TC2100007967.hg.1	<i>PAXBP1</i>	PAX3 and PAX7 binding protein 1	2.31E-04	1.78
TC0200008894.hg.1	<i>MERTK</i>	MER proto-oncogene, tyrosine kinase	4.14E-03	1.77
TC0700011458.hg.1	<i>CALN1</i>	calneuron 1	4.88E-03	1.77
TC0100018248.hg.1	<i>RNPC3</i>	RNA binding region (RNP1, RRM) containing 3	8.48E-04	1.76
TC2000007094.hg.1	<i>TTLL9</i>	tubulin tyrosine ligase-like family member 9	3.77E-03	1.76

APPENDIX

TC1100012389.hg.1	<i>CADM1</i>	cell adhesion molecule 1	2.14E-03	1.76
TC1400008415.hg.1	<i>ZFYVE21</i>	zinc finger, FYVE domain containing 21	8.02E-04	1.76
AFFX-DapX-5_st	NA	NA	4.53E-03	1.75
TC0800007529.hg.1	<i>SPIDR</i>	scaffolding protein involved in DNA repair	5.32E-03	1.75
TC0900008790.hg.1	<i>ZBTB43</i>	zinc finger and BTB domain containing 43	2.59E-03	1.75
TC0800011713.hg.1	<i>MTSS1</i>	metastasis suppressor 1	4.17E-03	1.75
TC0600006870.hg.1	<i>SNRNP48</i>	small nuclear ribonucleoprotein, U11/U12 48KDa subunit	2.81E-03	1.75
TC1300008938.hg.1	<i>DLEU2</i>	deleted in lymphocytic leukemia 2 (non-protein coding)	6.60E-03	1.74
TC2000006756.hg.1	<i>MACROD2</i>	MACRO domain containing 2	6.45E-03	1.74
TC0700006945.hg.1	<i>MPP6</i>	membrane protein, palmitoylated 6	2.65E-04	1.73
TC1400007145.hg.1	<i>FRMD6</i>	FERM domain containing 6	6.53E-03	1.73
HTA2-pos-PSR02023970.hg.1	NA	NA	1.10E-03	1.72
TC0500009488.hg.1	<i>CREBRF</i>	CREB3 regulatory factor	6.98E-03	1.72
TC2000010008.hg.1	<i>NFS1</i>	NFS1 cysteine desulfurase	3.54E-03	1.72
TC1900009588.hg.1	<i>ZNF121</i>	zinc finger protein 121	9.74E-04	1.72
TC0X00011275.hg.1	<i>TCEANC</i>	transcription elongation factor A (SII) N-terminal and central domain containing	3.61E-03	1.71

TC1100010531.hg.1	<i>SLC1A2</i>	solute carrier family 1 (glial high affinity glutamate transporter), member 2	3.53E-03	1.71
TC1400008622.hg.1	<i>OR5AU1</i>	olfactory receptor, family 5, subfamily AU, member 1	7.36E-03	1.71
TC1600007147.hg.1	<i>TMEM159</i>	transmembrane protein 159	6.65E-03	1.71
23071851	NA	NA	7.38E-03	1.71
23071994	NA	NA	7.38E-03	1.71
AFFX-DapX-M_st	NA	NA	5.66E-03	1.71
TC1500008986.hg.1	<i>LPCAT4</i>	lysophosphatidylcholine acyltransferase 4	9.88E-03	1.70
TC1000009612.hg.1	<i>KLF6</i>	Kruppel-like factor 6	3.16E-03	1.70
TC0900008793.hg.1	<i>ZBTB34</i>	zinc finger and BTB domain containing 34	1.02E-03	1.70
TC0500010635.hg.1	<i>HMGCS1</i>	3-hydroxy-3-methylglutaryl-CoA synthase 1 (soluble)	3.41E-03	1.70
TC0700011782.hg.1	<i>FAM133B</i>	family with sequence similarity 133, member B	8.36E-03	1.70
TC1200011965.hg.1	<i>NAA25</i>	N(alpha)-acetyltransferase 25, NatB auxiliary subunit	8.21E-04	1.70
TC1200008255.hg.1	<i>ZDHHC17</i>	zinc finger, DHHC-type containing 17	5.39E-03	1.70
HTA2-pos-PSR02023951.hg.1	NA	NA	2.51E-03	1.69
AFFX-r2-Bs-phe-M_st	NA	NA	2.05E-03	1.69
TC1500010886.hg.1	<i>CALML4</i>	calmodulin-like 4	1.80E-03	1.69
HTA2-neg-47420666_st	NA	NA	5.81E-03	1.69
TC0300006462.hg.1	<i>TRNT1</i>	tRNA nucleotidyl transferase, CCA-adding, 1	4.92E-04	1.69

APPENDIX

TC0200015424.hg.1	<i>ALS2CR12</i>	amyotrophic lateral sclerosis 2 chromosome region candidate 12	4.45E-03	1.69
TC1200007108.hg.1	<i>KRAS</i>	Memczak2013 ANTISENSE, coding, INTERNAL, intronic best transcript NM_033360	1.17E-03	1.69
TC1500010723.hg.1	<i>CHAC1</i>	ChaC glutathione-specific gamma-glutamylcyclotransferase 1	1.31E-03	1.69
TC0200014362.hg.1	<i>NCKAP5</i>	NCK-associated protein 5	1.66E-03	1.69
TC0800012447.hg.1	<i>AZIN1</i>	antizyme inhibitor 1	2.89E-03	1.69
TC0200009428.hg.1	<i>CCNT2</i>	cyclin T2	3.01E-03	1.68
TC0600007262.hg.1	<i>HIST1H3A</i>	histone cluster 1, H3a	7.11E-03	1.68
TC0400008331.hg.1	<i>NPNT</i>	nephronectin	3.15E-03	1.68
TC1600006533.hg.1	<i>UBE2I</i>	ubiquitin conjugating enzyme E2I	2.16E-03	1.68
TC1800008456.hg.1	<i>ZSCAN30</i>	zinc finger and SCAN domain containing 30	3.95E-03	1.67
TC0100007876.hg.1	<i>RRAGC</i>	Memczak2013 ANTISENSE, coding, INTERNAL, intronic best transcript NM_022157	4.99E-03	1.67
TC0700011876.hg.1	<i>ASNS</i>	asparagine synthetase (glutamine-hydrolyzing)	8.07E-03	1.67
TC1900010782.hg.1	<i>ATP1A3</i>	ATPase, Na+/K+ transporting, alpha 3 polypeptide	2.62E-03	1.67
TC1600010291.hg.1	<i>SALL1</i>	spalt-like transcription factor 1	8.52E-04	1.67
TC1500010157.hg.1	<i>ADAMTS7</i>	ADAM metallopeptidase with thrombospondin type 1 motif 7	3.84E-03	1.67
TC0600014151.hg.1	<i>SMIM8</i>	small integral membrane protein 8	5.20E-03	1.67

TC1900011596.hg.1	<i>C19orf18</i>	chromosome 19 open reading frame 18	3.76E-04	1.67
TC1700007918.hg.1	<i>AOC2</i>	amine oxidase, copper containing 2 (retina-specific)	4.38E-03	1.66
TC1200012668.hg.1	<i>TRHDE</i>	thyrotropin-releasing hormone degrading enzyme	3.11E-03	1.66
HTA2-neg-47422968_st	NA	NA	1.18E-03	1.66
TC1900009743.hg.1	<i>TNPO2</i>	transportin 2	1.28E-03	1.66
TC1900009867.hg.1	<i>AKAP8L</i>	A kinase (PRKA) anchor protein 8-like	1.03E-03	1.66
TC1500010788.hg.1	<i>CHD2</i>	chromodomain helicase DNA binding protein 2	3.95E-03	1.66
TC0100015976.hg.1	<i>KIAA0907</i>	KIAA0907	4.52E-03	1.66
TC1000012565.hg.1	<i>DNAJC9</i>	Dnaj (Hsp40) homolog, subfamily C, member 9	3.83E-03	1.66
TC1700011919.hg.1	<i>CEP295NL</i>	CEP295 N-terminal like	7.12E-03	1.66
HTA2-neg-47419608_st	NA	NA	4.81E-03	1.65
TC0400007495.hg.1	<i>DCUN1D4</i>	DCN1, defective in cullin neddylation 1, domain containing 4	3.33E-03	1.65
TSUnmapped00000105.hg.1	<i>ZNF501</i>	zinc finger protein 501 [Source:HGNC Symbol;Acc:HGNC:23717]	3.72E-03	1.65
TC0200010374.hg.1	<i>MARS2</i>	methionyl-tRNA synthetase 2, mitochondrial	5.47E-03	1.64
TC0200016601.hg.1	<i>GIGYF2</i>	GRB10 interacting GYF protein 2	5.43E-03	1.64
HTA2-neg-47423547_st	NA	NA	4.56E-03	1.64
TC1900011593.hg.1	<i>ZNF418</i>	zinc finger protein 418	3.77E-03	1.64

APPENDIX

TC1700007557.hg.1	<i>CCL2</i>	chemokine (C-C motif) ligand 2	5.43E-03	1.64
TC0600009262.hg.1	<i>SLC35F1</i>	solute carrier family 35, member F1	8.17E-04	1.64
TC0700013525.hg.1	<i>FAM126A</i>	family with sequence similarity 126, member A	6.00E-03	1.64
TC0300007044.hg.1	<i>GOLGA4</i>	golgin A4	1.09E-03	1.64
TC1200012775.hg.1	<i>ST8SIA1</i>	ST8 alpha-N-acetyl-neuraminide alpha-2,8-sialyltransferase 1	2.48E-03	1.63
HTA2-pos-47422722_st	NA	NA	1.37E-03	1.63
TC0700009240.hg.1	<i>AGBL3</i>	ATP/GTP binding protein-like 3	8.22E-03	1.63
TC0100010926.hg.1	<i>OCLM</i>	Transcript Identified by AceView, Entrez Gene ID(s) 10896	4.15E-03	1.63
TC1700009746.hg.1	<i>MYH3</i>	myosin, heavy chain 3, skeletal muscle, embryonic	4.40E-03	1.63
TC0500008467.hg.1	<i>SRFBP1</i>	serum response factor binding protein 1	1.92E-03	1.63
AFFX-r2-Bs-dap-M_st	NA	NA	7.13E-03	1.63
TC1500007975.hg.1	<i>IREB2</i>	iron responsive element binding protein 2	1.62E-03	1.63
TC2000009966.hg.1	<i>FKBP1A-SDCBP2</i>	FKBP1A-SDCBP2 readthrough (NMD candidate)	2.51E-03	1.63
TC1000007217.hg.1	<i>KIF5B</i>	Memczak2013 ANTISENSE, CDS, coding, INTERNAL, UTR3 best transcript NM_004521	8.03E-03	1.63
AFFX-r2-Bs-dap-3_st	NA	NA	8.00E-03	1.63
HTA2-pos-47422721_st	NA	NA	6.00E-03	1.63

TC0500009423.hg.1	<i>NPM1</i>	Zhang2013 ALT_ACCEPTOR, ALT_DONOR, coding, INTERNAL, intronic best transcript NM_002520	1.53E-03	1.63
TC0100009900.hg.1	<i>CIART</i>	circadian associated repressor of transcription	3.69E-03	1.62
TC1000008927.hg.1	<i>VTI1A</i>	vesicle transport through interaction with t-SNAREs 1A	3.07E-03	1.62
TC0100010925.hg.1	<i>OCLM</i>	oculomedin	3.80E-03	1.62
TC1600011351.hg.1	<i>CARHSP1</i>	Jeck2013 ANTISENSE, CDS, coding, INTERNAL, OVCODE, OVEXON best transcript NM_001042476	4.12E-03	1.61
23072532	NA	NA	9.39E-03	1.61
TC0500009012.hg.1	<i>TCERG1</i>	Transcript Identified by AceView, Entrez Gene ID(s) 10915	7.79E-03	1.61
TC1100012712.hg.1	<i>ACRV1</i>	acrosomal vesicle protein 1	9.97E-03	1.61
TC0100007690.hg.1	<i>RBBP4</i>	retinoblastoma binding protein 4	6.66E-04	1.61
TC2000006627.hg.1	<i>CHGB</i>	chromogranin B	1.59E-03	1.61
TC1900006578.hg.1	<i>SF3A2</i>	splicing factor 3a subunit 2	1.11E-03	1.61
HTA2-neg-47422985_st	NA	NA	8.52E-03	1.60
TC1900011814.hg.1	<i>ZNF17</i>	zinc finger protein 17	1.35E-03	1.60
TC0X00007562.hg.1	<i>ITGB1BP2</i>	integrin beta 1 binding protein (melusin) 2	2.13E-03	1.60
TC0600014276.hg.1	<i>HLA-DMB</i>	major histocompatibility complex, class II, DM beta	8.96E-03	1.60
TC0400008103.hg.1	<i>RP11-10L7.1</i>	---	5.40E-03	1.60

APPENDIX

TC0400008335.hg.1	<i>AIMP1</i>	aminoacyl tRNA synthetase complex-interacting multifunctional protein 1	1.79E-03	1.59
TC0200015876.hg.1	<i>SERPINE2</i>	serpin peptidase inhibitor, clade E (nexin, plasminogen activator inhibitor type 1), member 2	1.37E-03	1.59
TC1400010632.hg.1	<i>GPATCH2L</i>	G-patch domain containing 2 like	1.39E-03	1.59
TC1600010711.hg.1	<i>CHTF8</i>	chromosome transmission fidelity factor 8	3.84E-03	1.59
TC0500012030.hg.1	<i>GDF9</i>	growth differentiation factor 9	8.06E-03	1.59
TC0400010141.hg.1	<i>LDB2</i>	LIM domain binding 2	4.88E-03	1.59
TC1100007293.hg.1	<i>LDLRAD3</i>	low density lipoprotein receptor class A domain containing 3	9.11E-03	1.59
TC1800009215.hg.1	<i>ANKRD12</i>	ankyrin repeat domain 12	6.13E-03	1.58
TC1300009714.hg.1	<i>ARGLU1</i>	arginine and glutamate rich 1	1.85E-03	1.58
TC1000008806.hg.1	<i>CFAP58</i>	cilia and flagella associated protein 58	3.15E-03	1.58
TC0300009280.hg.1	<i>KCNAB1</i>	Transcript Identified by AceView, Entrez Gene ID(s) 7881	7.09E-03	1.58
TC0500010920.hg.1	<i>SREK1IP1</i>	SREK1-interacting protein 1	1.64E-03	1.58
HTA2-pos-PSR02004962.hg.1	NA	NA	3.20E-03	1.58
TC1500009466.hg.1	<i>ONECUT1</i>	one cut homeobox 1	7.20E-03	1.58
HTA2-pos-3183407_st	NA	NA	7.19E-03	1.57
TC2100007534.hg.1	<i>TEKT4P2</i>	tektin 4 pseudogene 2	5.36E-03	1.57

TC0400009221.hg.1	<i>MSMO1</i>	methylsterol monooxygenase 1	1.83E-03	1.57
TC0700009827.hg.1	<i>RBM33</i>	RNA binding motif protein 33	1.16E-03	1.57
AFFX-DapX-3_st	NA	NA	7.66E-03	1.57
TC1200009881.hg.1	<i>CLEC2B</i>	C-type lectin domain family 2, member B	1.64E-03	1.57
TC1700008769.hg.1	<i>KCNJ2</i>	potassium channel, inwardly rectifying subfamily J, member 2	5.66E-03	1.57
TC0100009112.hg.1	<i>LOC729970</i>	hCG2028352-like	6.88E-03	1.56
HTA2-pos-PSR01002164.hg.1	NA	NA	4.10E-03	1.56
TC1900011816.hg.1	<i>ZNF419</i>	zinc finger protein 419	9.41E-04	1.56
TC1700012483.hg.1	<i>MAFG</i>	v-maf avian musculoaponeurotic fibrosarcoma oncogene homolog G	5.22E-03	1.56
HTA2-pos-PSR10021746.hg.1	NA	NA	2.63E-03	1.56
TC1800008891.hg.1	<i>BCL2</i>	B-cell CLL/lymphoma 2	7.63E-03	1.56
TC0100009383.hg.1	<i>RBM15</i>	RNA binding motif protein 15	3.10E-03	1.56
TC0900010177.hg.1	<i>CNTNAP3B</i>	Salzman2013 ANNOTATED, CDS, coding, INTERNAL, OVCODE, OVEXON best transcript NM_001201380	9.32E-03	1.55
AFFX-PheX-M_st	NA	NA	1.30E-03	1.55
TC1100010990.hg.1	<i>MRPL16</i>	mitochondrial ribosomal protein L16	3.80E-03	1.55
TC0600014366.hg.1	<i>PDE10A</i>	phosphodiesterase 10A	7.59E-03	1.55

APPENDIX

TC0600008379.hg.1	<i>MTRNR2L9</i>	MT-RNR2-like 9	4.53E-03	1.55
TC0100008066.hg.1	<i>PTPRF</i>	protein tyrosine phosphatase, receptor type, F	5.67E-03	1.55
TC1300006690.hg.1	<i>POLR1D</i>	polymerase (RNA) I polypeptide D	4.94E-03	1.55
TC1600011560.hg.1	<i>MTSS1L</i>	metastasis suppressor 1-like	3.83E-03	1.55
TSUnmapped00000057.hg.1	<i>SURF4</i>	surfeit 4	3.64E-03	1.54
TC1800009306.hg.1	<i>RNF152</i>	ring finger protein 152	3.77E-03	1.54
HTA2-pos-PSR02004963.hg.1	NA	NA	3.91E-03	1.54
TC0200008734.hg.1	<i>C2orf49</i>	chromosome 2 open reading frame 49	1.58E-03	1.54
TC0X00011306.hg.1	<i>NHSL2</i>	NHS-like 2	9.23E-03	1.54
TC1200009997.hg.1	<i>GRIN2B</i>	glutamate receptor, ionotropic, N-methyl D-aspartate 2B	6.80E-03	1.53
TC0500012519.hg.1	<i>SPARC</i>	secreted protein, acidic, cysteine-rich (osteonectin)	2.93E-03	1.53
TC0300006714.hg.1	<i>EAF1</i>	ELL associated factor 1	5.28E-03	1.53
TC0200010745.hg.1	<i>IGFBP2</i>	insulin like growth factor binding protein 2	7.32E-03	1.53
HTA2-pos-PSR02023963.hg.1	NA	NA	3.21E-03	1.53
TC1900011734.hg.1	<i>MIA</i>	melanoma inhibitory activity	2.21E-03	1.53
TC1100012930.hg.1	<i>B3GAT1</i>	beta-1,3-glucuronyltransferase 1	1.41E-03	1.53
TC0600012540.hg.1	<i>GABRR2</i>	gamma-aminobutyric acid (GABA) A receptor, rho 2	4.21E-03	1.53
TC1900011573.hg.1	<i>ZNF416</i>	zinc finger protein 416	3.80E-03	1.53

TC1000006464.hg.1	<i>GTPBP4</i>	GTP binding protein 4	5.66E-03	1.53
TC0400011180.hg.1	<i>SCD5</i>	stearoyl-CoA desaturase 5	4.21E-03	1.53
TC2000009247.hg.1	<i>SPATA25</i>	spermatogenesis associated 25	8.33E-03	1.52
HTA2-neg-47424009_st	NA	NA	7.88E-03	1.52
TC0400010242.hg.1	<i>PPARGC1A</i>	peroxisome proliferator-activated receptor gamma, coactivator 1 alpha	6.07E-03	1.52
TC0500010540.hg.1	<i>LIFR</i>	leukemia inhibitory factor receptor alpha	4.26E-03	1.52
TC1800008550.hg.1	<i>SYT4</i>	synaptotagmin IV	2.91E-03	1.52
TC0400011014.hg.1	<i>CXCL5</i>	chemokine (C-X-C motif) ligand 5	9.08E-03	1.52
TC0700009222.hg.1	<i>LRGUK</i>	leucine-rich repeats and guanylate kinase domain containing	3.09E-03	1.52
TC2100008533.hg.1	<i>PCBP3</i>	poly(rC) binding protein 3	2.29E-03	1.52
TC0600011868.hg.1	<i>SRF</i>	Jeck2013 ANTISENSE, CDS, coding, INTERNAL, intronic, OVCODE, OVEXON best transcript NM_003131	9.18E-03	1.52
TC1100013229.hg.1	<i>FXYD6</i>	FXYD domain containing ion transport regulator 6	6.27E-03	1.52
TC0900012222.hg.1	<i>APTX</i>	aprataxin	2.12E-03	1.52
TC2000006872.hg.1	<i>INSM1</i>	insulinoma-associated 1	5.83E-03	1.52
TC0X00009356.hg.1	<i>TMEM47</i>	transmembrane protein 47	5.78E-03	1.51
TC1200012667.hg.1	<i>TPH2</i>	tryptophan hydroxylase 2	9.51E-03	1.51

APPENDIX

TC2100007082.hg.1	DYRK1A	dual specificity tyrosine-(Y)-phosphorylation regulated kinase 1A	6.93E-03	1.51
HTA2-pos-JUC01000985.hg.1	NA	NA	4.16E-03	1.51
HTA2-pos-JUC13008384.hg.1	NA	NA	4.16E-03	1.51
HTA2-pos-JUC19003067.hg.1	NA	NA	4.16E-03	1.51
TC1100011182.hg.1	PYGM	phosphorylase, glycogen, muscle	2.91E-03	1.51
TC0200009806.hg.1	TANK	TRAF family member-associated NFKB activator	1.89E-03	1.51
TC1800007969.hg.1	L3MBTL4	I(3)mbt-like 4 (Drosophila)	3.64E-03	1.51
TC0500008540.hg.1	PHAX	phosphorylated adaptor for RNA export	5.34E-03	1.51
TC1500010890.hg.1	HEXA	hexosaminidase A (alpha polypeptide)	8.70E-03	1.51
TC0600014236.hg.1	TXNDC5	thioredoxin domain containing 5 (endoplasmic reticulum)	4.18E-03	1.51
TC1000010515.hg.1	NCOA4	nuclear receptor coactivator 4	3.85E-03	1.51
AFFX-PheX-3_st	NA	NA	2.06E-03	1.50

Supplementary Table 5: Romidepsin single treatment versus control

Probe ID	Symbol	Gene name	P value	Fold change
TC1400006697.hg.1	DHRS2	dehydrogenase/reductase (SDR family) member 2	2.20E-07	19.43
TC1900008057.hg.1	ZFP36	ZFP36 ring finger protein	7.70E-05	9.50
TC0700008582.hg.1	SERPINE1	serpin peptidase inhibitor, clade E (nexin, plasminogen activator inhibitor type 1), member 1	2.71E-04	8.90

TC0800009891.hg.1	<i>STC1</i>	stanniocalcin 1	1.76E -06	7.69
TC0500006744.hg.1	<i>ROPN1L</i>	rhophilin associated tail protein 1-like	1.69E -05	7.10
TC1100010054.hg.1	<i>NRIP3</i>	nuclear receptor interacting protein 3	9.02E -05	6.36
TC1700006763.hg.1	<i>ATP1B2</i>	ATPase, Na+/K+ transporting, beta 2 polypeptide	3.35E -07	6.20
TC0700007977.hg.1	<i>FZD9</i>	frizzled class receptor 9	6.76E -07	6.14
TC1900006537.hg.1	<i>REEP6</i>	receptor accessory protein 6	7.51E -06	5.75
TC1600007931.hg.1	<i>LPCAT2</i>	lysophosphatidylcholine acyltransferase 2	2.65E -06	5.63
HTA2-pos-2978683_st	NA	NA	1.84E -04	5.59
TC0300009412.hg.1	<i>SERPINI1</i>	serpin peptidase inhibitor, clade I (neuroserpin), member 1	6.92E -06	5.51
TC1900009240.hg.1	<i>GNG7</i>	guanine nucleotide binding protein (G protein), gamma 7	4.76E -04	5.30
TC0600006873.hg.1	<i>BMP6</i>	bone morphogenetic protein 6	6.40E -06	5.23
TSUnmapped00000485.hg. .1	<i>RPS6KA1</i>	ribosomal protein S6 kinase, 90kDa, polypeptide 1	9.84E -08	5.10
TC1700008635.hg.1	<i>RGS9</i>	regulator of G-protein signaling 9	6.22E -04	5.06
TC1000007895.hg.1	<i>TSPAN15</i>	tetraspanin 15	1.59E -05	5.06
TC0100007705.hg.1	<i>AZIN2</i>	antizyme inhibitor 2	6.05E -04	5.01
TC0200015869.hg.1	<i>AP1S3</i>	adaptor-related protein complex 1 sigma 3 subunit	3.18E -04	5.01
TC0800011620.hg.1	<i>ENPP2</i>	ectonucleotide pyrophosphatase/phosphodiesterase 2	7.80E -04	4.94
TC1600009677.hg.1	<i>CRYM</i>	crystallin mu	2.06E -05	4.76

APPENDIX

TC1000010768.hg.1	<i>EGR2</i>	early growth response 2	2.63E -04	4.76
TC1700009318.hg.1	<i>FAM101B</i>	family with sequence similarity 101, member B	9.04E -06	4.75
TC1700008673.hg.1	<i>CACNG5</i>	calcium channel, voltage-dependent, gamma subunit 5	1.05E -03	4.69
TC0X00008747.hg.1	<i>GABRQ</i>	gamma-aminobutyric acid (GABA) A receptor, theta	3.41E -06	4.64
TC1500009606.hg.1	<i>MYO1E</i>	Transcript Identified by AceView, Entrez Gene ID(s) 4643	2.72E -04	4.51
TC2000007202.hg.1	<i>ACSS2</i>	acyl-CoA synthetase short-chain family member 2	3.34E -05	4.45
TC0100017018.hg.1	<i>ETNK2</i>	ethanolamine kinase 2	7.31E -06	4.40
TC0500008785.hg.1	<i>EGR1</i>	early growth response 1	1.15E -06	4.39
TC1500007972.hg.1	<i>CRABP1</i>	cellular retinoic acid binding protein 1	1.87E -04	4.33
TC0800010926.hg.1	<i>PAG1</i>	phosphoprotein membrane anchor with glycosphingolipid microdomains 1	2.49E -07	4.29
TC0700007105.hg.1	<i>ADCYAP1R1</i>	adenylate cyclase activating polypeptide 1 (pituitary) receptor type I	7.67E -03	4.23
TC0200008894.hg.1	<i>MERTK</i>	MER proto-oncogene, tyrosine kinase	3.81E -06	4.22
TC1900010016.hg.1	<i>ISYNA1</i>	inositol-3-phosphate synthase 1	2.81E -05	4.18
TC0800012076.hg.1	<i>ARC</i>	activity-regulated cytoskeleton-associated protein	5.99E -03	4.14
TC0400012078.hg.1	<i>NR3C2</i>	nuclear receptor subfamily 3, group C, member 2	5.37E -04	4.12
TC0100010609.hg.1	<i>DNM3</i>	dynamin 3	6.04E -06	4.11
TC1400007443.hg.1	<i>HSPA2</i>	heat shock 70kDa protein 2	1.33E -04	4.11

TC1200010598.hg.1	<i>RND1</i>	Rho family GTPase 1	5.21E -04	4.10
TC1000012433.hg.1	<i>SPAG6</i>	sperm associated antigen 6	1.16E -06	4.07
TC0100018464.hg.1	<i>PPM1J</i>	protein phosphatase, Mg ²⁺ /Mn ²⁺ -dependent, 1J	1.72E -06	3.96
TC1600011060.hg.1	<i>COTL1</i>	coactosin-like F-actin binding protein 1	1.06E -06	3.94
TC0100018307.hg.1	<i>ACKR1</i>	atypical chemokine receptor 1 (Duffy blood group)	6.99E -07	3.91
TC0300009696.hg.1	<i>VWA5B2</i>	von Willebrand factor A domain containing 5B2	4.20E -06	3.89
TC0700009472.hg.1	<i>EPHB6</i>	EPH receptor B6	6.21E -04	3.89
TC1600010239.hg.1	<i>CBLN1</i>	cerebellin 1 precursor	1.01E -03	3.87
TC1100009075.hg.1	<i>NCAM1</i>	Transcript Identified by AceView, Entrez Gene ID(s) 4684	4.08E -03	3.85
TC1800008281.hg.1	<i>TMEM241</i>	transmembrane protein 241	7.57E -07	3.84
TC0300009033.hg.1	<i>PLS1</i>	plastin 1	9.89E -05	3.78
TC0800010138.hg.1	<i>RAB11FIP1</i>	RAB11 family interacting protein 1 (class I)	4.77E -05	3.78
TC0200013021.hg.1	<i>PAIP2B</i>	poly(A) binding protein interacting protein 2B	2.45E -06	3.76
TC1900008287.hg.1	<i>PVRL2</i>	poliovirus receptor-related 2 (herpesvirus entry mediator B)	2.26E -06	3.68
TC1100013045.hg.1	<i>SIPA1</i>	signal-induced proliferation-associated 1	3.28E -05	3.67
TC1200011207.hg.1	<i>CPM</i>	carboxypeptidase M	9.44E -04	3.66
TC0X00009025.hg.1	<i>ANOS1</i>	anosmin 1	7.82E -05	3.66
TC1600007147.hg.1	<i>TMEM159</i>	transmembrane protein 159	6.32E -07	3.65

APPENDIX

TC0800010224.hg.1	<i>ZMAT4</i>	zinc finger, matrin-type 4	6.88E -04	3.64
TC0800011861.hg.1	<i>LRRC6</i>	leucine rich repeat containing 6	1.02E -05	3.64
TC2100008508.hg.1	<i>CHAF1B</i>	chromatin assembly factor 1, subunit B (p60)	4.71E -04	3.63
TC0X00010382.hg.1	<i>BEX5</i>	brain expressed X-linked 5	1.54E -03	3.61
TC1900010375.hg.1	<i>RHPN2</i>	rhophilin, Rho GTPase binding protein 2	2.44E -05	3.58
TC0100018519.hg.1	<i>F11R</i>	F11 receptor	2.83E -04	3.57
TSUnmapped00000108.hg.1	<i>RPS6KA1</i>	ribosomal protein S6 kinase, 90kDa, polypeptide 1	2.18E -06	3.56
TC0400011973.hg.1	<i>CLGN</i>	calmegin	1.54E -06	3.54
TC0900012173.hg.1	<i>GARNL3</i>	GTPase activating Rap/RanGAP domain-like 3	1.37E -06	3.53
TC1200009800.hg.1	<i>SLC2A3</i>	solute carrier family 2 (facilitated glucose transporter), member 3	4.16E -04	3.50
23076546	NA	NA	5.93E -04	3.46
TC0300008086.hg.1	<i>ARL6</i>	ADP-ribosylation factor like GTPase 6	1.99E -05	3.46
TC0X00009576.hg.1	<i>SYN1</i>	synapsin I	1.06E -05	3.45
TC0400012288.hg.1	<i>FSTL5</i>	follistatin-like 5	1.23E -03	3.45
TC0200006831.hg.1	<i>VSNL1</i>	visinin like 1	2.05E -03	3.44
TC1600007448.hg.1	<i>CORO1A</i>	coronin, actin binding protein, 1A	7.49E -06	3.44
TC1200009796.hg.1	<i>SLC2A14</i>	solute carrier family 2 (facilitated glucose transporter), member 14	4.13E -04	3.43
TC0100007469.hg.1	<i>RPS6KA1</i>	ribosomal protein S6 kinase, 90kDa, polypeptide 1	3.19E -06	3.42

TC0300014084.hg.1	<i>CRYGS</i>	crystallin gamma S	2.51E -05	3.41
TC0800007051.hg.1	<i>NEFM</i>	neurofilament, medium polypeptide	8.73E -05	3.41
TC1900007173.hg.1	<i>ADGRE5</i>	adhesion G protein-coupled receptor E5	2.36E -04	3.40
TC0100010855.hg.1	<i>NPL</i>	N-acetylneuraminate pyruvate lyase (dihydrodipicolinate synthase)	5.47E -05	3.40
TC0200006671.hg.1	<i>GRHL1</i>	grainyhead-like transcription factor 1	7.22E -05	3.38
TC0400010519.hg.1	<i>APBB2</i>	amyloid beta (A4) precursor protein-binding, family B, member 2	3.47E -05	3.38
TC1200007804.hg.1	<i>METTL7B</i>	methyltransferase like 7B	5.77E -03	3.35
TC0100007584.hg.1	<i>PTPRU</i>	protein tyrosine phosphatase, receptor type, U	3.00E -06	3.34
TC0400009958.hg.1	<i>ABLIM2</i>	actin binding LIM protein family, member 2	9.88E -06	3.32
TC1100012722.hg.1	<i>CDON</i>	cell adhesion associated, oncogene regulated	5.92E -04	3.30
TC0X00006799.hg.1	<i>SAT1</i>	spermidine/spermine N1-acetyltransferase 1	6.37E -04	3.30
TC1400010071.hg.1	<i>CLMN</i>	calmin (calponin-like, transmembrane)	6.30E -07	3.30
TC0600014220.hg.1	<i>SERPINB9</i>	serpin peptidase inhibitor, clade B (ovalbumin), member 9	2.17E -04	3.29
TC1500010942.hg.1	<i>LYSMD4</i>	LysM, putative peptidoglycan-binding, domain containing 4	2.65E -05	3.27
TC0200014703.hg.1	<i>CCDC148</i>	coiled-coil domain containing 148	1.32E -06	3.26
TC0300006477.hg.1	<i>ITPR1</i>	inositol 1,4,5-trisphosphate receptor, type 1	3.33E -04	3.26
TC1900006603.hg.1	<i>ZNF556</i>	zinc finger protein 556	1.03E -05	3.25

APPENDIX

TC0200009078.hg.1	<i>EPB41L5</i>	erythrocyte membrane protein band 4.1 like 5	5.78E -05	3.23
TC1200008667.hg.1	<i>HSP90B1</i>	Transcript Identified by AceView, Entrez Gene ID(s) 7184	6.37E -06	3.23
TC0100015401.hg.1	<i>IGSF3</i>	immunoglobulin superfamily, member 3	2.07E -05	3.23
TC0100010674.hg.1	<i>GPR52</i>	G protein-coupled receptor 52	2.36E -04	3.21
TC0400009088.hg.1	<i>GUCY1B3</i>	guanylate cyclase 1, soluble, beta 3	2.01E -05	3.17
TC0200007399.hg.1	<i>PLEKHH2</i>	pleckstrin homology domain containing, family H (with MyTH4 domain) member 2	3.21E -06	3.17
TC1300010007.hg.1	<i>TMEM255B</i>	transmembrane protein 255B	2.84E -05	3.17
TC0300009310.hg.1	<i>MLF1</i>	myeloid leukemia factor 1	3.10E -06	3.17
TC0600013165.hg.1	<i>EPB41L2</i>	erythrocyte membrane protein band 4.1-like 2	9.56E -07	3.17
TC1100010123.hg.1	<i>DKK3</i>	dickkopf WNT signaling pathway inhibitor 3	3.26E -04	3.17
TC0300013520.hg.1	<i>CLDN1</i>	claudin 1	5.83E -05	3.16
TC0100018306.hg.1	<i>CADM3</i>	cell adhesion molecule 3	5.34E -07	3.15
TC0600014055.hg.1	<i>NQO2</i>	NAD(P)H dehydrogenase, quinone 2	1.05E -03	3.12
TC0100008779.hg.1	<i>ST6GALNAC3</i>	ST6 (alpha-N-acetyl-neuraminyl-2,3-beta-galactosyl-1,3)-N-acetylgalactosaminide alpha-2,6-sialyltransferase 3	1.64E -05	3.11
TC0100017844.hg.1	<i>NID1</i>	nidogen 1	5.53E -04	3.11
TC1300007752.hg.1	<i>CLDN10</i>	claudin 10	7.80E -05	3.10
TC0200007458.hg.1	<i>EPAS1</i>	endothelial PAS domain protein 1	1.72E -04	3.09

TC0200015266.hg.1	<i>TMEFF2</i>	transmembrane protein with EGF-like and two follistatin-like domains 2	1.59E -06	3.08
TSUnmapped00000390.hg.1	<i>RPS6KA1</i>	ribosomal protein S6 kinase, 90kDa, polypeptide 1	8.41E -06	3.05
TC0500013261.hg.1	<i>GALNT10</i>	polypeptide N-acetylgalactosaminyltransferase 10	2.71E -03	3.04
TC0500013280.hg.1	<i>ZDHHC11B</i>	zinc finger, DHHC-type containing 11B	1.54E -04	3.02
TC0400012821.hg.1	<i>C4orf22</i>	chromosome 4 open reading frame 22	2.67E -04	3.02
TC0100018403.hg.1	<i>ERRFI1</i>	ERBB receptor feedback inhibitor 1	2.37E -04	3.01
TC0100014191.hg.1	<i>RAB3B</i>	RAB3B, member RAS oncogene family	3.49E -04	3.01
TC0100010720.hg.1	<i>BRINP2</i>	bone morphogenetic protein/retinoic acid inducible neural-specific 2	1.75E -05	3.00
TC1600008607.hg.1	<i>PLCG2</i>	phospholipase C, gamma 2 (phosphatidylinositol-specific)	5.11E -03	3.00
TC0500013089.hg.1	<i>GFPT2</i>	glutamine-fructose-6-phosphate transaminase 2	9.61E -04	2.99
TC0300012392.hg.1	<i>EFCAB12</i>	EF-hand calcium binding domain 12	1.03E -03	2.97
TC1000008715.hg.1	<i>ELOVL3</i>	ELOVL fatty acid elongase 3	5.02E -05	2.96
TC0100016121.hg.1	<i>KCNJ10</i>	potassium channel, inwardly rectifying subfamily J, member 10	1.82E -05	2.95
TC0800010685.hg.1	<i>MYBL1</i>	v-myb avian myeloblastosis viral oncogene homolog-like 1	5.57E -05	2.95
TC1700008262.hg.1	<i>CACNA1G</i>	calcium channel, voltage-dependent, T type, alpha 1G subunit	2.96E -06	2.94
TC010009101.hg.1	<i>ABCD3</i>	Transcript Identified by AceView, Entrez Gene ID(s) 5825	2.61E -04	2.94

APPENDIX

TC1300008824.hg.1	<i>SLC25A30</i>	solute carrier family 25, member 30	5.59E -04	2.92
TC0300009855.hg.1	<i>IL1RAP</i>	interleukin 1 receptor accessory protein	7.02E -05	2.91
TC0900011938.hg.1	<i>C9orf116</i>	chromosome 9 open reading frame 116	8.56E -05	2.91
TC1200011993.hg.1	<i>SLC8B1</i>	solute carrier family 8 (sodium/lithium/calcium exchanger), member B1	4.44E -05	2.90
TC0200011040.hg.1	<i>ITM2C</i>	integral membrane protein 2C	1.01E -04	2.90
TC2200007952.hg.1	<i>CLTCL1</i>	clathrin, heavy chain-like 1	3.40E -06	2.89
TC0100015707.hg.1	<i>HIST2H4A</i>	histone cluster 2, H4a	2.37E -06	2.89
TC0700006795.hg.1	<i>AHR</i>	aryl hydrocarbon receptor	6.51E -03	2.88
TC0100009870.hg.1	<i>HIST2H4B</i>	histone cluster 2, H4b	2.61E -06	2.86
TC0X00009637.hg.1	<i>PIM2</i>	Pim-2 proto-oncogene, serine/threonine kinase	6.69E -05	2.85
TC1900010593.hg.1	<i>DPF1</i>	D4, zinc and double PHD fingers family 1	3.02E -05	2.85
TC0400006685.hg.1	<i>WFS1</i>	Wolfram syndrome 1 (wolframin)	3.02E -04	2.85
TC0400012640.hg.1	<i>CCDC110</i>	coiled-coil domain containing 110	2.23E -04	2.85
TC0500013282.hg.1	<i>ZDHHC11</i>	zinc finger, DHHC-type containing 11	5.11E -05	2.84
TC0X00006715.hg.1	<i>SCML1</i>	sex comb on midleg-like 1 (Drosophila)	4.32E -04	2.84
TC1500007977.hg.1	<i>HYKK</i>	hydroxylysine kinase	9.66E -05	2.82
TC2000009218.hg.1	<i>SDC4</i>	syndecan 4	4.76E -04	2.82
TC0700013224.hg.1	<i>LMBR1</i>	Transcript Identified by AceView, Entrez Gene ID(s) 64327	6.14E -05	2.81

TC1200010559.hg.1	<i>VDR</i>	vitamin D (1,25- dihydroxyvitamin D3) receptor	8.32E -04	2.81
TC0800011597.hg.1	<i>EXT1</i>	Jeck2013 ALT_ACCEPTOR, ALT_DONOR, coding, INTERNAL, intronic best transcript NM_000127	1.40E -04	2.81
TC0600009819.hg.1	<i>ULBP2</i>	UL16 binding protein 2	1.13E -04	2.80
TC0100006787.hg.1	<i>PIK3CD</i>	phosphatidylinositol-4,5- bisphosphate 3-kinase, catalytic subunit delta	4.88E -05	2.80
TC0200007048.hg.1	<i>MAPRE3</i>	microtubule-associated protein, RP/EB family, member 3	4.12E -06	2.80
TC1900010782.hg.1	<i>ATP1A3</i>	ATPase, Na+/K+ transporting, alpha 3 polypeptide	7.60E -06	2.78
TC1000008891.hg.1	<i>DUSP5</i>	dual specificity phosphatase 5	2.51E -04	2.78
TC1900007040.hg.1	<i>CNN1</i>	calponin 1, basic, smooth muscle	1.51E -05	2.78
TC0900007006.hg.1	<i>PRSS3</i>	protease, serine, 3	4.85E -03	2.77
TC0100016973.hg.1	<i>CYB5R1</i>	cytochrome b5 reductase 1	4.83E -04	2.77
TC1900009155.hg.1	<i>GAMT</i>	guanidinoacetate N- methyltransferase	2.63E -05	2.76
TC0400010618.hg.1	<i>TEC</i>	tec protein tyrosine kinase	1.73E -05	2.76
TC0600014151.hg.1	<i>SMIM8</i>	small integral membrane protein 8	5.52E -04	2.73
TC1900007426.hg.1	<i>NCAN</i>	neurocan	1.02E -03	2.73
TC0700010899.hg.1	<i>POLR2J4</i>	polymerase (RNA) II (DNA directed) polypeptide J4, pseudogene	2.57E -05	2.73
TC0300013719.hg.1	<i>CEP19</i>	centrosomal protein 19kDa	1.88E -04	2.73

APPENDIX

23076588	<i>NA</i>	NA	4.21E -04	2.71
TC0800009212.hg.1	<i>MAPK15</i>	mitogen-activated protein kinase 15	4.21E -04	2.71
TC0100013076.hg.1	<i>PADI2</i>	peptidyl arginine deiminase, type II	4.04E -05	2.70
TC0200009662.hg.1	<i>TNFAIP6</i>	tumor necrosis factor, alpha-induced protein 6	9.48E -03	2.70
TC0600007262.hg.1	<i>HIST1H3A</i>	histone cluster 1, H3a	9.23E -04	2.69
TSUnmapped00000572.hg. .1	<i>RPS6KA1</i>	ribosomal protein S6 kinase, 90kDa, polypeptide 1	6.93E -06	2.69
TC0200016571.hg.1	<i>OSBPL6</i>	oxysterol binding protein-like 6	4.83E -05	2.68
TC1300006919.hg.1	<i>FREM2</i>	FRAS1 related extracellular matrix protein 2	4.95E -06	2.68
TC1600009246.hg.1	<i>ROGDI</i>	rogdi homolog	5.23E -06	2.67
TC0100011378.hg.1	<i>RASSF5</i>	Ras association (RalGDS/AF-6) domain family member 5	1.76E -04	2.67
TC0200013602.hg.1	<i>TSGA10</i>	testis specific 10	1.16E -04	2.67
TC0700008261.hg.1	<i>RUND3B</i>	RUN domain containing 3B	3.09E -05	2.67
TC1200012111.hg.1	<i>TAOK3</i>	TAO kinase 3	1.05E -03	2.67
TC1500010941.hg.1	<i>LYSMD4</i>	LysM, putative peptidoglycan-binding, domain containing 4	1.57E -03	2.67
TC1700011436.hg.1	<i>ERN1</i>	endoplasmic reticulum to nucleus signaling 1	7.18E -04	2.66
TC0200009829.hg.1	<i>GCA</i>	grancalcin, EF-hand calcium binding protein	1.08E -05	2.65
TC0X00006723.hg.1	<i>CDKL5</i>	cyclin-dependent kinase-like 5	2.16E -03	2.65
TC1200010612.hg.1	<i>RHEBL1</i>	Ras homolog enriched in brain like 1	6.48E -04	2.65

TC1000007176.hg.1	<i>MAP3K8</i>	mitogen-activated protein kinase kinase kinase 8	8.54E -04	2.65
TC1500008120.hg.1	<i>SH3GL3</i>	SH3-domain GRB2-like 3	1.39E -04	2.64
TC0300007973.hg.1	<i>CADM2</i>	cell adhesion molecule 2	1.71E -04	2.64
TC0600014362.hg.1	<i>TFB1M</i>	transcription factor B1, mitochondrial	3.11E -03	2.64
TC1100011282.hg.1	<i>CD248</i>	CD248 molecule, endosialin	6.78E -05	2.64
TC0400008725.hg.1	<i>PCDH10</i>	protocadherin 10	4.84E -03	2.64
TC0900011370.hg.1	<i>BRINP1</i>	bone morphogenetic protein/retinoic acid inducible neural-specific 1	4.60E -04	2.63
TC1900007688.hg.1	<i>CCNE1</i>	cyclin E1	1.86E -05	2.63
TC0100015102.hg.1	<i>COL11A1</i>	collagen, type XI, alpha 1	2.97E -04	2.63
TC0200013298.hg.1	<i>ST3GAL5</i>	ST3 beta-galactoside alpha-2,3-sialyltransferase 5	1.88E -04	2.62
TC1100008541.hg.1	<i>AAMDC</i>	adipogenesis associated, Mth938 domain containing	5.06E -05	2.62
TC0100018418.hg.1	<i>IFFO2</i>	intermediate filament family orphan 2	3.40E -05	2.61
TC0600011133.hg.1	<i>HIST1H2BE</i>	Memczak2013 ANTISENSE, CDS, coding, upstream_start, UTR3, UTR5 best transcript NM_003523	3.55E -03	2.60
TC0600007610.hg.1	<i>MSH5</i>	mutS homolog 5	1.94E -03	2.60
TC2200007318.hg.1	<i>H1F0</i>	H1 histone family, member 0	7.34E -05	2.59
TC1100007394.hg.1	<i>CD82</i>	CD82 molecule	3.89E -04	2.59
TC1200007359.hg.1	<i>CNTN1</i>	contactin 1	7.69E -04	2.59

APPENDIX

TC1600006525.hg.1	<i>CACNA1H</i>	calcium channel, voltage-dependent, T type, alpha 1H subunit	3.24E -04	2.59
TC0100015803.hg.1	<i>TDRKH</i>	tudor and KH domain containing	5.20E -04	2.58
TC0100014127.hg.1	<i>SPATA6</i>	spermatogenesis associated 6	1.96E -04	2.58
TC1200007809.hg.1	<i>GDF11</i>	growth differentiation factor 11	2.14E -05	2.58
TC1500010744.hg.1	<i>GCOM1</i>	GRINL1A complex locus 1	1.14E -05	2.57
TC0300008853.hg.1	<i>TMEM108</i>	transmembrane protein 108	2.42E -05	2.57
TC1200010413.hg.1	<i>ABCD2</i>	ATP binding cassette subfamily D member 2	3.38E -04	2.57
TC0200011837.hg.1	<i>FAM49A</i>	family with sequence similarity 49, member A	3.33E -04	2.57
TC1900007127.hg.1	<i>IER2</i>	immediate early response 2	2.80E -06	2.57
TSUnmapped00000109.hg.1	<i>ATG16L1</i>	autophagy related 16-like 1	2.53E -04	2.57
TC2000009023.hg.1	<i>SAMHD1</i>	SAM domain and HD domain 1	4.64E -05	2.56
TC0100018466.hg.1	<i>DENND2C</i>	DENN/MADD domain containing 2C	7.74E -03	2.56
TC1400009184.hg.1	<i>TXNDC16</i>	thioredoxin domain containing 16	7.92E -06	2.56
TC1600008737.hg.1	<i>FLJ30679</i>	uncharacterized protein FLJ30679	5.84E -03	2.56
TC0400008106.hg.1	<i>HERC5</i>	HECT and RLD domain containing E3 ubiquitin protein ligase 5	2.41E -03	2.56
TC1900009670.hg.1	<i>DOCK6</i>	dedicator of cytokinesis 6	7.54E -05	2.55
TC1700011060.hg.1	<i>FAM117A</i>	family with sequence similarity 117, member A	4.15E -05	2.54
TC2100006585.hg.1	<i>RBM11</i>	RNA binding motif protein 11	2.16E -05	2.54

TC2200007987.hg.1	<i>CLDN5</i>	claudin 5	1.51E -04	2.54
TC0600012815.hg.1	<i>PPIL6</i>	peptidylprolyl isomerase (cyclophilin)-like 6	1.20E -04	2.53
TC1900006507.hg.1	<i>CNN2</i>	calponin 2	9.01E -05	2.53
TC0600014371.hg.1	<i>RNASET2</i>	ribonuclease T2	3.07E -04	2.53
23075523	NA	NA	1.93E -03	2.53
23075806	NA	NA	1.93E -03	2.53
23076508	NA	NA	1.93E -03	2.53
TC0100016649.hg.1	<i>NMNAT2</i>	nicotinamide nucleotide adenylyltransferase 2	2.45E -03	2.53
TC2000008242.hg.1	<i>RNF24</i>	ring finger protein 24	1.39E -04	2.53
TC0500007549.hg.1	<i>ZSWIM6</i>	zinc finger, SWIM-type containing 6	4.30E -04	2.52
TC1900009369.hg.1	<i>PLIN3</i>	perilipin 3	4.72E -04	2.52
TC0200008870.hg.1	<i>BCL2L11</i>	BCL2-like 11 (apoptosis facilitator)	4.96E -04	2.51
TC1100006899.hg.1	<i>ARNTL</i>	aryl hydrocarbon receptor nuclear translocator-like	1.12E -03	2.50
TC0800007311.hg.1	<i>ADGRA2</i>	adhesion G protein-coupled receptor A2	7.02E -06	2.49
TSUnmapped00000435.hg .1	<i>RPS6KA1</i>	ribosomal protein S6 kinase, 90kDa, polypeptide 1	7.48E -05	2.49
HTA2-neg-47419722_st	NA	NA	4.96E -04	2.49
TC1100011192.hg.1	<i>ATG2A</i>	autophagy related 2A	6.83E -04	2.49
23075724	NA	NA	6.16E -03	2.48

APPENDIX

TC0100015925.hg.1	<i>KCNN3</i>	potassium channel, calcium activated intermediate/small conductance subfamily N alpha, member 3	1.24E -03	2.48
TC1600010603.hg.1	<i>RRAD</i>	Ras-related associated with diabetes	4.08E -03	2.48
TC0700009680.hg.1	<i>TMEM176A</i>	transmembrane protein 176A	2.27E -04	2.48
TC0200007954.hg.1	<i>PCYOX1</i>	prenylcysteine oxidase 1	5.04E -05	2.48
TC1900008328.hg.1	<i>PPM1N</i>	protein phosphatase, Mg ²⁺ /Mn ²⁺ dependent, 1N (putative)	1.89E -03	2.48
TC0900008197.hg.1	<i>GALNT12</i>	polypeptide N-acetylgalactosaminyltransferase 12	1.04E -05	2.47
TC1100009242.hg.1	<i>ABCG4</i>	ATP binding cassette subfamily G member 4	8.66E -05	2.47
TC0600011943.hg.1	<i>ENPP5</i>	ectonucleotide pyrophosphatase/phosphodiesterase 5 (putative)	5.24E -04	2.47
TC1900011892.hg.1	<i>RTBDN</i>	retbindin	2.70E -04	2.47
TC1100012019.hg.1	<i>SESN3</i>	sestrin 3	4.19E -03	2.47
TC0100013205.hg.1	<i>ECE1</i>	endothelin converting enzyme 1	5.39E -05	2.47
TC1500008029.hg.1	<i>FAH</i>	fumarylacetoacetate hydrolase (fumarylacetoacetate)	5.26E -04	2.46
TC2000008268.hg.1	<i>SLC23A2</i>	solute carrier family 23 (ascorbic acid transporter), member 2	2.45E -04	2.46
TC2100006659.hg.1	<i>CXADR</i>	coxsackie virus and adenovirus receptor	9.67E -05	2.46
23075965	NA	NA	1.64E -03	2.46
TC0600007012.hg.1	<i>CD83</i>	CD83 molecule	5.16E -04	2.46

TC1500010909.hg.1	<i>STARD5</i>	StAR-related lipid transfer domain containing 5	1.23E -05	2.46
TC0200007053.hg.1	<i>KHK</i>	ketohexokinase	1.41E -05	2.45
TC1900008826.hg.1	<i>CACNG7</i>	calcium channel, voltage-dependent, gamma subunit 7	1.56E -04	2.45
TC1900010360.hg.1	<i>ANKRD27</i>	ankyrin repeat domain 27 (VPS9 domain)	8.41E -04	2.45
TC1000012536.hg.1	<i>MPP7</i>	membrane protein, palmitoylated 7	9.84E -05	2.45
TC0300009916.hg.1	<i>HES1</i>	hes family bHLH transcription factor 1	3.34E -04	2.44
TC0800009194.hg.1	<i>RHPN1</i>	rhophilin, Rho GTPase binding protein 1	3.02E -04	2.43
TC0600013709.hg.1	<i>SERAC1</i>	serine active site containing 1	6.74E -04	2.43
TC0200010745.hg.1	<i>IGFBP2</i>	insulin like growth factor binding protein 2	5.48E -04	2.43
TC1100013054.hg.1	<i>RAD9A</i>	RAD9 checkpoint clamp component A	2.15E -04	2.43
TC0200013595.hg.1	<i>MGAT4A</i>	mannosyl (alpha-1,3)-glycoprotein beta-1,4-N-acetylglucosaminyltransferase, isozyme A	4.58E -04	2.43
TC2200007150.hg.1	<i>TIMP3</i>	TIMP metallopeptidase inhibitor 3	7.98E -04	2.43
TC2000010026.hg.1	<i>TMEM189</i>	transmembrane protein 189	6.34E -04	2.43
TC0800010506.hg.1	<i>PLAG1</i>	pleiomorphic adenoma gene 1	3.57E -03	2.42
TC0600008166.hg.1	<i>SLC25A27</i>	solute carrier family 25, member 27	3.78E -04	2.42
TC1800007066.hg.1	<i>MAPRE2</i>	microtubule-associated protein, RP/EB family, member 2	9.14E -04	2.42
TC0100009215.hg.1	<i>CDC14A</i>	cell division cycle 14A	1.75E -05	2.42

APPENDIX

23076189	<i>NA</i>	NA	8.05E -03	2.41
TC0100009959.hg.1	<i>TUFT1</i>	tuftelin 1	1.93E -03	2.41
TC1900007103.hg.1	<i>GCDH</i>	glutaryl-CoA dehydrogenase	1.76E -04	2.41
TC1300007707.hg.1	<i>GPC5</i>	glypican 5	1.70E -04	2.41
TC0X00010643.hg.1	44080	septin 6	1.16E -04	2.40
TC0200012412.hg.1	<i>C1GALT1C1L</i>	C1GALT1-specific chaperone 1 like	2.68E -05	2.40
TC0900008243.hg.1	<i>PLPPR1</i>	phospholipid phosphatase related 1	2.05E -03	2.39
TC0600013193.hg.1	<i>STX7</i>	syntaxin 7	2.40E -05	2.39
TC0700010504.hg.1	<i>OSBPL3</i>	oxysterol binding protein-like 3	1.02E -04	2.39
TC0300014085.hg.1	<i>TBCCD1</i>	TBCC domain containing 1	2.27E -05	2.38
TC0100006571.hg.1	<i>SKI</i>	Memczak2013 ALT_ACCEPTOR, ALT_DONOR, coding, INTERNAL, intronic best transcript NM_003036	5.47E -05	2.38
TC0300006961.hg.1	<i>CMTM8</i>	CKLF-like MARVEL transmembrane domain containing 8	5.30E -05	2.38
TC1700010358.hg.1	<i>MYO1D</i>	myosin ID	1.40E -04	2.38
TC1600010452.hg.1	<i>DOK4</i>	docking protein 4	7.19E -05	2.38
TC0200015815.hg.1	<i>EPHA4</i>	EPH receptor A4	3.21E -03	2.38
TC1900011844.hg.1	<i>MFSD12</i>	major facilitator superfamily domain containing 12	2.66E -03	2.37
TC0700008252.hg.1	<i>CROT</i>	carnitine O-octanoyltransferase	3.50E -03	2.37

TC0200011972.hg.1	<i>C2orf44</i>	chromosome 2 open reading frame 44	1.57E -03	2.37
TC1600008661.hg.1	<i>CRISPLD2</i>	cysteine-rich secretory protein LCCL domain containing 2	1.58E -03	2.37
TC0600011234.hg.1	<i>HIST1H4L</i>	histone cluster 1, H4I	1.94E -03	2.37
TC1300009026.hg.1	<i>PCDH8</i>	protocadherin 8	3.03E -04	2.37
TC1100009374.hg.1	<i>VWA5A</i>	von Willebrand factor A domain containing 5A	9.83E -03	2.36
TC2000007177.hg.1	<i>RALY</i>	Jeck2013 ALT_DONOR, coding, INTERNAL, intronic best transcript NM_016732	2.39E -04	2.36
TC0700013047.hg.1	<i>TMEM176B</i>	transmembrane protein 176B	6.07E -05	2.36
TC0500012023.hg.1	<i>KIF3A</i>	kinesin family member 3A	1.16E -04	2.36
TC0900010933.hg.1	<i>CTSV</i>	cathepsin V	2.70E -03	2.36
TC1900006605.hg.1	<i>ZNF57</i>	zinc finger protein 57	1.18E -04	2.36
TC0600012379.hg.1	<i>ELOVL4</i>	ELOVL fatty acid elongase 4	3.75E -03	2.36
TC0500012842.hg.1	<i>DUSP1</i>	dual specificity phosphatase 1	3.52E -04	2.35
TC0200012140.hg.1	<i>ALK</i>	anaplastic lymphoma receptor tyrosine kinase	7.32E -05	2.35
TC0300011525.hg.1	<i>RYBP</i>	RING1 and YY1 binding protein	2.94E -04	2.35
TC0900010969.hg.1	<i>CORO2A</i>	coronin, actin binding protein, 2A	4.32E -05	2.35
TC1500010776.hg.1	<i>IDH3A</i>	isocitrate dehydrogenase 3 (NAD+) alpha	3.43E -04	2.35
TC0200015242.hg.1	<i>STAT1</i>	signal transducer and activator of transcription 1	1.39E -05	2.34
TC1000007061.hg.1	<i>GPR158</i>	G protein-coupled receptor 158	2.51E -03	2.34

APPENDIX

TC0100008052.hg.1	<i>CFAP57</i>	cilia and flagella associated protein 57	2.31E -03	2.34
TC1700008661.hg.1	<i>PRKCA</i>	protein kinase C, alpha	8.04E -05	2.34
TC1400010708.hg.1	<i>TTC5</i>	tetratricopeptide repeat domain 5	1.31E -03	2.33
TC1400008116.hg.1	<i>GSKIP</i>	GSK3B interacting protein	6.76E -04	2.33
TC1300009004.hg.1	<i>ATP7B</i>	ATPase, Cu++ transporting, beta polypeptide	1.30E -04	2.33
TC1500010841.hg.1	<i>CHRFAM7A</i>	CHRNA7 (cholinergic receptor, nicotinic, alpha 7, exons 5-10) and FAM7A (family with sequence similarity 7A, exons A-E) fusion	1.64E -05	2.33
TC1700009954.hg.1	<i>TOM1L2</i>	target of myb1 like 2 membrane trafficking protein	1.28E -03	2.33
TC1900006588.hg.1	<i>GADD45B</i>	growth arrest and DNA-damage-inducible, beta	3.41E -03	2.33
TC0800011595.hg.1	<i>EXT1</i>	Jeck2013 ALT_ACCEPTOR, ALT_DONOR, coding, INTERNAL, intronic best transcript NM_000127	7.56E -03	2.33
TC0600009144.hg.1	<i>KIAA1919</i>	KIAA1919	3.00E -04	2.33
TC1300009712.hg.1	<i>EFNB2</i>	ephrin-B2	4.40E -03	2.32
TC0100015155.hg.1	<i>VAV3</i>	vav 3 guanine nucleotide exchange factor	1.76E -04	2.32
TC0100017310.hg.1	<i>ESRRG</i>	estrogen-related receptor gamma	1.76E -04	2.31
TC1100011190.hg.1	<i>EHD1</i>	EH domain containing 1	8.27E -04	2.31
TC0100010874.hg.1	<i>RGL1</i>	ral guanine nucleotide dissociation stimulator-like 1	7.61E -03	2.31
TC2200009257.hg.1	<i>TCN2</i>	transcobalamin II	5.18E -03	2.31

TC1400008452.hg.1	<i>ADSSL1</i>	adenylosuccinate synthase like 1	8.14E -03	2.31
TC1200009300.hg.1	<i>BRI3BP</i>	BRI3 binding protein	9.52E -04	2.31
TC1100011652.hg.1	<i>GDPD5</i>	glycerophosphodiester phosphodiesterase domain containing 5	1.98E -05	2.30
TC1700009402.hg.1	<i>SMYD4</i>	SET and MYND domain containing 4	1.59E -04	2.30
TC0X00008910.hg.1	<i>ASMTL</i>	acetylserotonin O-methyltransferase-like	2.40E -05	2.30
TC0Y00006884.hg.1	<i>ASMTL</i>	acetylserotonin O-methyltransferase-like	2.40E -05	2.30
23067838	NA	NA	4.96E -03	2.30
TC1400008058.hg.1	<i>PPP4R4</i>	protein phosphatase 4, regulatory subunit 4	4.96E -03	2.30
TC0X00008468.hg.1	<i>CCDC160</i>	coiled-coil domain containing 160	4.84E -04	2.30
TC0100013028.hg.1	<i>EPHA2</i>	EPH receptor A2	3.58E -04	2.29
TC2200007068.hg.1	<i>SLC35E4</i>	solute carrier family 35, member E4	3.37E -04	2.29
TC1900011150.hg.1	<i>NOSIP</i>	nitric oxide synthase interacting protein	4.20E -04	2.29
TC0200012009.hg.1	<i>DTNB</i>	dystrobrevin beta	8.50E -05	2.29
TC0100011325.hg.1	<i>TMCC2</i>	transmembrane and coiled-coil domain family 2	1.60E -05	2.29
TC0700012163.hg.1	<i>EFCAB10</i>	EF-hand calcium binding domain 10	1.23E -04	2.29
TC0400007280.hg.1	<i>WDR19</i>	WD repeat domain 19	9.27E -05	2.28
TC0800009094.hg.1	<i>DENND3</i>	DENN/MADD domain containing 3	1.10E -04	2.28
TC0100017241.hg.1	<i>TMEM206</i>	transmembrane protein 206	1.16E -04	2.28

APPENDIX

TC2100007999.hg.1	<i>DNAJC28</i>	DnaJ (Hsp40) homolog, subfamily C, member 28	4.91E -04	2.27
TC1100008627.hg.1	<i>ANKRD42</i>	ankyrin repeat domain 42	4.34E -03	2.27
TC1100006820.hg.1	<i>SWAP70</i>	SWAP switching B-cell complex 70kDa subunit	4.81E -05	2.27
TC0600013147.hg.1	<i>ARHGAP18</i>	Rho GTPase activating protein 18	6.74E -05	2.27
TC0400008424.hg.1	<i>C4orf32</i>	chromosome 4 open reading frame 32	7.86E -04	2.27
TC0300007596.hg.1	<i>FLNB</i>	filamin B, beta	7.87E -05	2.27
TC0600009622.hg.1	<i>CCDC28A</i>	coiled-coil domain containing 28A	8.94E -04	2.27
TC1900009603.hg.1	<i>OLFM2</i>	olfactomedin 2	1.43E -04	2.26
TC0600007274.hg.1	<i>HIST1H2BD</i>	histone cluster 1, H2bd	6.37E -05	2.26
23075524	<i>NA</i>	NA	1.44E -05	2.26
TC0200007535.hg.1	<i>PPP1R21</i>	protein phosphatase 1, regulatory subunit 21	1.24E -04	2.26
TC1100009521.hg.1	<i>APLP2</i>	amyloid beta (A4) precursor-like protein 2	5.01E -04	2.26
23076191	<i>NA</i>	NA	7.84E -03	2.25
TC0200016582.hg.1	<i>NABP1</i>	nucleic acid binding protein 1	4.60E -05	2.25
TC0X00009387.hg.1	<i>RPGR</i>	retinitis pigmentosa GTPase regulator	3.15E -03	2.25
23076268	<i>NA</i>	NA	9.50E -06	2.25
TC0200010615.hg.1	<i>CCNYL1</i>	cyclin Y like 1	5.34E -04	2.25
TC0300011540.hg.1	<i>SHQ1</i>	SHQ1, H/ACA ribonucleoprotein assembly factor	3.16E -03	2.25

TC1200007653.hg.1	<i>NR4A1</i>	nuclear receptor subfamily 4, group A, member 1	2.04E -03	2.25
TC1000011567.hg.1	<i>CRTAC1</i>	cartilage acidic protein 1	4.13E -04	2.25
TC0600010797.hg.1	<i>MAK</i>	male germ cell-associated kinase	5.30E -05	2.25
TC1400010012.hg.1	<i>LGMN</i>	legumain	4.93E -04	2.24
TC1100011367.hg.1	<i>UNC93B1</i>	unc-93 homolog B1 (C. elegans)	5.23E -03	2.24
TC1700011439.hg.1	<i>TEX2</i>	testis expressed 2	1.43E -04	2.24
TC1000008056.hg.1	<i>VCL</i>	vinculin	4.90E -03	2.24
TC0500009824.hg.1	<i>ZDHHC11</i>	Transcript Identified by AceView, Entrez Gene ID(s) 79844	5.13E -03	2.24
TC0500008356.hg.1	<i>KCNN2</i>	potassium channel, calcium activated intermediate/small conductance subfamily N alpha, member 2	9.29E -04	2.24
TC1900009806.hg.1	<i>PRKACA</i>	protein kinase, cAMP-dependent, catalytic, alpha	2.58E -04	2.24
TC0200013046.hg.1	<i>EXOC6B</i>	exocyst complex component 6B	1.15E -05	2.23
TC0800011312.hg.1	<i>RRM2B</i>	ribonucleotide reductase M2 B (TP53 inducible)	6.59E -04	2.23
TC1300009583.hg.1	<i>DOCK9</i>	dedicator of cytokinesis 9	6.70E -03	2.23
TC1700010198.hg.1	<i>UNC119</i>	unc-119 lipid binding chaperone	1.74E -05	2.23
23074629	NA	NA	3.83E -04	2.23
TC0400009376.hg.1	<i>WDR17</i>	WD repeat domain 17	3.82E -04	2.23
TC0400010558.hg.1	<i>ATP8A1</i>	ATPase, aminophospholipid transporter (APLT), class I, type 8A, member 1	8.83E -03	2.23

APPENDIX

TC0200010907.hg.1	<i>ACSL3</i>	acyl-CoA synthetase long-chain family member 3	1.07E -04	2.23
TC0100018210.hg.1	<i>SH3D21</i>	SH3 domain containing 21	3.56E -04	2.23
TC0500013200.hg.1	<i>RFESD</i>	Rieske (Fe-S) domain containing	3.74E -03	2.23
TC0X00006593.hg.1	<i>CLCN4</i>	chloride channel, voltage-sensitive 4	5.72E -05	2.22
TC1200008574.hg.1	<i>APAF1</i>	apoptotic peptidase activating factor 1	1.29E -04	2.22
TC1900006819.hg.1	<i>TRIP10</i>	thyroid hormone receptor interactor 10	2.06E -04	2.22
TC0500012282.hg.1	<i>HDAC3</i>	histone deacetylase 3	1.25E -04	2.22
TC0700009079.hg.1	<i>TSPAN33</i>	tetraspanin 33	4.83E -05	2.21
TC1000009092.hg.1	<i>INPP5F</i>	inositol polyphosphate-5-phosphatase F	1.53E -03	2.21
TC1900011139.hg.1	<i>SLC17A7</i>	solute carrier family 17 (vesicular glutamate transporter), member 7	2.02E -03	2.21
HTA2-pos-2985890_st	NA	NA	3.54E -04	2.21
23076478	NA	NA	4.81E -03	2.21
TC0800007416.hg.1	<i>GINS4</i>	GINS complex subunit 4 (Sld5 homolog)	5.24E -05	2.21
TC1100007943.hg.1	<i>PLCB3</i>	phospholipase C, beta 3 (phosphatidylinositol-specific)	4.25E -05	2.21
23075555	NA	NA	4.86E -03	2.20
23075693	NA	NA	4.86E -03	2.20
23075866	NA	NA	4.86E -03	2.20
23076012	NA	NA	4.86E -03	2.20

23076157	NA	NA	4.86E -03	2.20
23076325	NA	NA	4.86E -03	2.20
TC1900011866.hg.1	<i>RAB3D</i>	RAB3D, member RAS oncogene family	2.39E -04	2.20
TC0600014152.hg.1	<i>LINC01590</i>	long intergenic non-protein coding RNA 1590	5.92E -04	2.20
TC0300008375.hg.1	<i>ZDHHC23</i>	zinc finger, DHHC-type containing 23	2.50E -04	2.20
TC0300013763.hg.1	<i>RUBCN</i>	RUN domain and cysteine-rich domain containing, Beclin 1-interacting protein	1.64E -04	2.20
TC1100007026.hg.1	<i>ZDHHC13</i>	zinc finger, DHHC-type containing 13	2.45E -03	2.20
TC1600008712.hg.1	<i>IRF8</i>	interferon regulatory factor 8	4.52E -03	2.19
TC0800007269.hg.1	<i>UNC5D</i>	unc-5 netrin receptor D	9.18E -04	2.19
TC0300014082.hg.1	<i>ETV5</i>	ets variant 5	6.18E -04	2.19
HTA2-pos-2985912_st	NA	NA	5.33E -03	2.18
TC0400008686.hg.1	<i>C4orf33</i>	chromosome 4 open reading frame 33	1.68E -03	2.18
TC0600013537.hg.1	<i>RAET1G</i>	retinoic acid early transcript 1G	3.95E -05	2.18
23066337	NA	NA	6.39E -04	2.18
TC0100017500.hg.1	<i>TMEM63A</i>	transmembrane protein 63A	2.44E -03	2.18
TC0100007295.hg.1	<i>EPHB2</i>	EPH receptor B2	2.24E -03	2.17
TC0500011758.hg.1	<i>CDO1</i>	cysteine dioxygenase type 1	2.51E -04	2.17

APPENDIX

TC0200016530.hg.1	<i>PLEKHB2</i>	pleckstrin homology domain containing, family B (ejectins) member 2	4.90E -04	2.17
TC1400010629.hg.1	<i>FLVCR2</i>	feline leukemia virus subgroup C cellular receptor family, member 2	3.89E -03	2.17
TC0700008552.hg.1	<i>AGFG2</i>	ArfGAP with FG repeats 2	4.12E -04	2.17
TC0500010731.hg.1	<i>ARL15</i>	ADP-ribosylation factor like GTPase 15	1.86E -04	2.16
TC0700013223.hg.1	<i>LMBR1</i>	Transcript Identified by AceView, Entrez Gene ID(s) 64327	8.54E -03	2.16
TC1100009707.hg.1	<i>POLR2L</i>	polymerase (RNA) II (DNA directed) polypeptide L, 7.6kDa	9.40E -05	2.16
23075726	<i>NA</i>	NA	5.60E -03	2.16
TC0900007047.hg.1	<i>DNAI1</i>	dynein, axonemal, intermediate chain 1	1.92E -04	2.16
TC0300010821.hg.1	<i>ULK4</i>	unc-51 like kinase 4	3.07E -04	2.16
TC0700011784.hg.1	<i>FAM133B</i>	Transcript Identified by AceView, Entrez Gene ID(s) 257415	8.17E -04	2.16
TC1300009674.hg.1	<i>KDELC1</i>	KDEL (Lys-Asp-Glu-Leu) containing 1	3.48E -04	2.15
TC0500006816.hg.1	<i>FAM105A</i>	family with sequence similarity 105, member A	7.76E -05	2.15
TC0100017849.hg.1	<i>ERO1B</i>	endoplasmic reticulum oxidoreductase beta	1.37E -04	2.15
TC0X00007251.hg.1	<i>CCNB3</i>	cyclin B3	3.41E -03	2.15
TC0100014009.hg.1	<i>TESK2</i>	testis-specific kinase 2	2.22E -04	2.15
TSUnmapped00000262.hg .1	<i>MLXIP</i>	MLX interacting protein	2.80E -04	2.14
TC0600007060.hg.1	<i>MYLIP</i>	myosin regulatory light chain interacting protein	5.21E -03	2.14
TC0900007604.hg.1	<i>OSTF1</i>	osteoclast stimulating factor 1	1.21E -04	2.14

TC0100007678.hg.1	<i>HDAC1</i>	histone deacetylase 1	4.12E -05	2.14
TC0600011463.hg.1	<i>NEU1</i>	sialidase 1 (lysosomal sialidase)	4.11E -03	2.14
TC0700013394.hg.1	<i>CCDC146</i>	coiled-coil domain containing 146	6.09E -03	2.14
TC0X00008836.hg.1	<i>PLXNA3</i>	plexin A3	8.25E -05	2.14
TC0200016494.hg.1	<i>CNNM4</i>	cyclin and CBS domain divalent metal cation transport mediator 4	6.99E -03	2.14
23075635	NA	NA	5.16E -05	2.14
TC0700006781.hg.1	<i>BZW2</i>	basic leucine zipper and W2 domains 2	2.92E -03	2.14
TC2200009352.hg.1	<i>LOC400927</i>	TPTE and PTEN homologous inositol lipid phosphatase pseudogene	3.17E -03	2.13
TC0700011463.hg.1	<i>TYW1B</i>	tRNA-yW synthesizing protein 1 homolog B (<i>S. cerevisiae</i>)	4.08E -04	2.13
TC1700012025.hg.1	<i>CEP131</i>	centrosomal protein 131kDa	3.09E -04	2.13
TC1100008085.hg.1	<i>PEL13</i>	pellino E3 ubiquitin protein ligase family member 3	5.43E -05	2.13
TC0700011556.hg.1	<i>HIP1</i>	huntingtin interacting protein 1	3.45E -04	2.13
TC0200012936.hg.1	<i>FBXO48</i>	F-box protein 48	5.96E -03	2.13
TC1700009042.hg.1	<i>AFMID</i>	arylformamidase	1.01E -03	2.13
TC0100012089.hg.1	<i>GPR137B</i>	G protein-coupled receptor 137B	1.02E -03	2.13
TC0800010379.hg.1	<i>EFCAB1</i>	EF-hand calcium binding domain 1	1.10E -03	2.13
TC1200010415.hg.1	<i>SLC2A13</i>	solute carrier family 2 (facilitated glucose transporter), member 13	1.15E -04	2.13
HTA2-pos-47421984_st	NA	NA	1.98E -03	2.12

APPENDIX

23076565	NA	NA	3.30E -04	2.12
23076624	NA	NA	3.36E -03	2.12
TC1600011574.hg.1	GINS2	GINS complex subunit 2 (Psf2 homolog)	1.61E -03	2.12
TC2000008885.hg.1	SNTA1	syntrophin, alpha 1	3.58E -05	2.12
TC0600007613.hg.1	HSPA1A	heat shock 70kDa protein 1A	3.20E -05	2.12
TC1000009169.hg.1	ACADS2	acyl-CoA dehydrogenase, short/branched chain	2.49E -04	2.12
TC1100006492.hg.1	PNPLA2	patatin-like phospholipase domain containing 2	5.64E -04	2.12
TC0900010849.hg.1	BARX1	BARX homeobox 1	2.87E -04	2.11
TC1300007491.hg.1	KLF5	Kruppel-like factor 5 (intestinal)	2.35E -04	2.11
TC2000007704.hg.1	PARD6B	par-6 family cell polarity regulator beta	1.06E -04	2.11
TC0100015771.hg.1	SEMA6C	sema domain, transmembrane domain (TM), and cytoplasmic domain, (semaphorin) 6C	4.02E -05	2.11
TC1600008675.hg.1	KIAA0513	KIAA0513	1.46E -03	2.11
TC1500007980.hg.1	CHRNA5	cholinergic receptor, nicotinic alpha 5	3.30E -04	2.11
TC0200009626.hg.1	LYPD6	LY6/PLAUR domain containing 6	1.48E -04	2.10
TC1600007811.hg.1	PAPD5	PAP associated domain containing 5	8.05E -04	2.10
TC0700013603.hg.1	RASA4	RAS p21 protein activator 4	1.51E -03	2.10
TC2000009748.hg.1	CABLES2	Cdk5 and Abl enzyme substrate 2	1.92E -05	2.09
TC1100006495.hg.1	TSPAN4	tetraspanin 4	1.44E -04	2.09

TC1200009122.hg.1	<i>SIRT4</i>	sirtuin 4	2.46E -04	2.09
TC1900007363.hg.1	<i>MAST3</i>	microtubule associated serine/threonine kinase 3	4.60E -04	2.09
TC0300009724.hg.1	<i>VPS8</i>	vacuolar protein sorting 8 homolog (S. cerevisiae)	9.03E -05	2.09
TC1700009150.hg.1	<i>BAIAP2</i>	BAI1-associated protein 2	3.59E -04	2.09
TC0600014154.hg.1	<i>SLC35A1</i>	solute carrier family 35 (CMP-sialic acid transporter), member A1	3.78E -04	2.09
TC1200009768.hg.1	<i>LPCAT3</i>	lysophosphatidylcholine acyltransferase 3	1.29E -03	2.09
TC0300007466.hg.1	<i>ALAS1</i>	5-aminolevulinate synthase 1	1.57E -03	2.09
TC0200011419.hg.1	<i>ATG4B</i>	autophagy related 4B, cysteine peptidase	1.28E -04	2.09
TC1900010998.hg.1	<i>PRKD2</i>	protein kinase D2	4.77E -04	2.09
TC0200015958.hg.1	<i>DNER</i>	delta/notch like EGF repeat containing	6.61E -04	2.08
TC0900011501.hg.1	<i>NR6A1</i>	nuclear receptor subfamily 6, group A, member 1	5.36E -03	2.08
TC0100010775.hg.1	<i>SOAT1</i>	sterol O-acyltransferase 1	2.28E -04	2.08
TC1200006946.hg.1	<i>H2AFJ</i>	H2A histone family, member J	1.19E -03	2.08
TC0400012882.hg.1	<i>ZNF732</i>	zinc finger protein 732	4.69E -04	2.08
TC0700011519.hg.1	<i>STAG3L2</i>	stromal antigen 3-like 2 (pseudogene)	3.00E -05	2.08
TC1900009824.hg.1	<i>DNAJB1</i>	DnaJ (Hsp40) homolog, subfamily B, member 1	1.51E -03	2.08
TC0100018285.hg.1	<i>NBPF19</i>	neuroblastoma breakpoint family, member 19	1.50E -04	2.08
TC0700013509.hg.1	<i>DAGLB</i>	diacylglycerol lipase, beta	1.83E -03	2.08

APPENDIX

TC0400006540.hg.1	<i>FGFR3</i>	fibroblast growth factor receptor 3	1.73E -04	2.07
TC0600007400.hg.1	<i>ZSCAN16</i>	zinc finger and SCAN domain containing 16	3.14E -05	2.07
TC0300007720.hg.1	<i>KBTBD8</i>	kelch repeat and BTB (POZ) domain containing 8	1.05E -03	2.07
TC1200006520.hg.1	<i>TSPAN9</i>	tetraspanin 9	4.70E -03	2.07
TC1900011653.hg.1	<i>MCOLN1</i>	mucolipin 1	2.63E -04	2.07
TC2000008910.hg.1	<i>EIF2S2</i>	Zhang2013 ALT_ACCEPTOR, ALT_DONOR, coding, INTERNAL, intronic best transcript NM_003908	1.79E -03	2.07
TC0200016624.hg.1	<i>KIDINS220</i>	kinase D-interacting substrate 220kDa	3.84E -04	2.07
TC1700008668.hg.1	<i>PRKCA</i>	Jeck2013 ALT_ACCEPTOR, ALT_DONOR, coding, INTERNAL, intronic best transcript NM_002737	2.29E -03	2.07
TC1100009445.hg.1	<i>FAM118B</i>	family with sequence similarity 118, member B	2.36E -03	2.07
TC0700011924.hg.1	<i>TMEM130</i>	transmembrane protein 130	4.78E -03	2.07
TC0100009442.hg.1	<i>WNT2B</i>	wingless-type MMTV integration site family, member 2B	4.71E -04	2.07
TC0700013323.hg.1	<i>SUN1</i>	Sad1 and UNC84 domain containing 1	3.33E -04	2.07
HTA2-pos-47421925_st	NA	NA	3.86E -03	2.07
TC1100012020.hg.1	<i>SESN3</i>	Transcript Identified by AceView, Entrez Gene ID(s) 143686	8.09E -04	2.06
TC0700010189.hg.1	<i>CYTH3</i>	cytohesin 3	2.12E -04	2.06
TC0200015226.hg.1	<i>HIBCH</i>	Transcript Identified by AceView, Entrez Gene ID(s) 26275	1.68E -03	2.06

23075672	NA	NA	6.85E -04	2.06
23075844	NA	NA	6.85E -04	2.06
23075993	NA	NA	6.85E -04	2.06
23076303	NA	NA	6.85E -04	2.06
23076462	NA	NA	6.85E -04	2.06
TC0900008851.hg.1	<i>DNM1</i>	dynamin 1	5.19E -04	2.06
TC1600009620.hg.1	<i>SMG1</i>	SMG1 phosphatidylinositol 3-kinase-related kinase	7.01E -04	2.05
TC1200011991.hg.1	<i>IQCD</i>	IQ motif containing D	4.18E -05	2.05
TC2000008367.hg.1	<i>PAK7</i>	p21 protein (Cdc42/Rac)-activated kinase 7	1.17E -04	2.05
TC1900011861.hg.1	<i>S1PR2</i>	sphingosine-1-phosphate receptor 2	1.25E -03	2.05
TC0700008072.hg.1	<i>RHBDD2</i>	rhomboid domain containing 2	1.10E -03	2.05
HTA2-pos-47421981_st	NA	NA	8.35E -04	2.05
TC0100017445.hg.1	<i>TLR5</i>	toll-like receptor 5	7.04E -05	2.05
TC1900007025.hg.1	<i>PLPPR2</i>	phospholipid phosphatase related 2	1.28E -03	2.04
TC1200010341.hg.1	<i>PKP2</i>	plakophilin 2	2.13E -03	2.04
TC0200014991.hg.1	<i>GPR155</i>	G protein-coupled receptor 155	3.47E -04	2.04
TC1100010397.hg.1	<i>CCDC34</i>	coiled-coil domain containing 34	4.75E -04	2.04
TC1900011891.hg.1	<i>HOOK2</i>	hook microtubule-tethering protein 2	6.04E -05	2.04

APPENDIX

TC0300009459.hg.1	<i>GPR160</i>	G protein-coupled receptor 160	2.41E -04	2.04
TC1900006985.hg.1	<i>PDE4A</i>	phosphodiesterase 4A, cAMP-specific	2.68E -05	2.04
TC1800006891.hg.1	<i>C18orf8</i>	chromosome 18 open reading frame 8	1.22E -04	2.04
TC1700007262.hg.1	<i>MAP2K3</i>	mitogen-activated protein kinase kinase 3	9.91E -03	2.04
23075807	NA	NA	5.82E -05	2.04
TC1200008686.hg.1	<i>CHST11</i>	Transcript Identified by AceView, Entrez Gene ID(s) 50515	7.98E -03	2.04
TSUnmapped00000495.hg.1	<i>ZDHHC3</i>	zinc finger, DHHC-type containing 3	9.34E -04	2.04
TC1600008011.hg.1	<i>KATNB1</i>	katanin p80 (WD repeat containing) subunit B 1	3.93E -05	2.04
TC1200011470.hg.1	<i>DUSP6</i>	dual specificity phosphatase 6	6.62E -05	2.04
HTA2-pos-2985916_st	NA	NA	9.47E -03	2.03
TC1700010252.hg.1	<i>CORO6</i>	coronin 6	6.83E -03	2.03
TC1100013053.hg.1	<i>RAD9A</i>	RAD9 checkpoint clamp component A	2.94E -04	2.03
TC0900008148.hg.1	<i>TDRD7</i>	tudor domain containing 7	2.26E -03	2.03
TC0500007552.hg.1	<i>LOC10042156</i> 1	family with sequence similarity 133, member A pseudogene	1.41E -03	2.03
TC0600014148.hg.1	<i>CYB5R4</i>	cytochrome b5 reductase 4	1.20E -03	2.03
TC1300008253.hg.1	<i>CRYL1</i>	crystallin lambda 1	1.63E -03	2.03
TC0100007909.hg.1	<i>BMP8A</i>	bone morphogenetic protein 8a	8.93E -05	2.03
TC1100007063.hg.1	<i>ANO5</i>	anoctamin 5	7.39E -03	2.02

TC0300011264.hg.1	<i>IL17RD</i>	interleukin 17 receptor D	4.87E -03	2.02
TC0700013526.hg.1	<i>FAM126A</i>	family with sequence similarity 126, member A	1.76E -04	2.02
TC1900011845.hg.1	<i>MFSD12</i>	major facilitator superfamily domain containing 12	1.61E -03	2.02
TC0600012428.hg.1	<i>UBE3D</i>	ubiquitin protein ligase E3D	8.14E -05	2.02
TC0900008425.hg.1	<i>ZNF483</i>	zinc finger protein 483	6.43E -03	2.02
TC0700007352.hg.1	<i>BLVRA</i>	biliverdin reductase A	2.40E -03	2.02
TC1900009823.hg.1	<i>GIPC1</i>	GIPC PDZ domain containing family, member 1	3.23E -03	2.02
TC1100012528.hg.1	<i>THY1</i>	Thy-1 cell surface antigen	2.09E -04	2.02
TC0700006783.hg.1	<i>TSPAN13</i>	tetraspanin 13	8.01E -03	2.02
TC0900011163.hg.1	<i>PTPN3</i>	protein tyrosine phosphatase, non-receptor type 3	1.24E -04	2.02
TC1100011372.hg.1	<i>CHKA</i>	choline kinase alpha	3.06E -03	2.02
23066331	<i>NA</i>	NA	9.70E -03	2.02
TC1300009165.hg.1	<i>PCDH9</i>	protocadherin 9	3.18E -04	2.02
TC1500007640.hg.1	<i>IQCH</i>	IQ motif containing H	2.11E -03	2.02
TC0100013578.hg.1	<i>ADGRB2</i>	adhesion G protein-coupled receptor B2	1.12E -03	2.02
TC0300013636.hg.1	<i>ACAP2</i>	Transcript Identified by AceView, Entrez Gene ID(s) 23527	3.89E -03	2.01
TC0100010543.hg.1	<i>ATP1B1</i>	ATPase, Na+/K+ transporting, beta 1 polypeptide	1.72E -03	2.01
TC1100012389.hg.1	<i>CADM1</i>	cell adhesion molecule 1	2.07E -04	2.01

APPENDIX

TC1200008373.hg.1	<i>TMTC3</i>	transmembrane and tetratricopeptide repeat containing 3	6.27E -03	2.01
TC1900008113.hg.1	<i>LTBP4</i>	latent transforming growth factor beta binding protein 4	1.36E -03	2.01
TC0800011579.hg.1	<i>EXT1</i>	exostosin glycosyltransferase 1	4.28E -04	2.01
TC0700008745.hg.1	<i>PRKAR2B</i>	protein kinase, cAMP-dependent, regulatory, type II, beta	9.09E -03	2.01
TC0100010806.hg.1	<i>XPR1</i>	xenotropic and polytropic retrovirus receptor 1	5.34E -03	2.01
TC1500009597.hg.1	<i>MYO1E</i>	myosin IE	4.68E -04	2.01
TC0500008121.hg.1	<i>ARSK</i>	arylsulfatase family, member K	6.20E -04	2.01
TC0300013547.hg.1	<i>FGF12</i>	fibroblast growth factor 12	1.25E -03	2.01
TC0400007128.hg.1	<i>TBC1D19</i>	TBC1 domain family, member 19	6.07E -05	2.00
TC0500011596.hg.1	<i>SLCO4C1</i>	solute carrier organic anion transporter family, member 4C1	3.73E -03	2.00
TC1600006610.hg.1	<i>CCNF</i>	cyclin F	2.05E -03	2.00
TC0100016120.hg.1	<i>PIGM</i>	phosphatidylinositol glycan anchor biosynthesis class M	9.69E -05	2.00
TC1600009074.hg.1	<i>MSRB1</i>	methionine sulfoxide reductase B1	2.72E -03	2.00
TC0100007954.hg.1	<i>SMAP2</i>	small ArfGAP2	6.18E -03	2.00
TC0800008916.hg.1	<i>EFR3A</i>	EFR3 homolog A	7.97E -04	2.00
TC0200007746.hg.1	<i>B3GNT2</i>	UDP-GlcNAc:betaGal beta-1,3-N-acetylglucosaminyltransferase 2	7.22E -05	2.00
TC0500013425.hg.1	<i>C5orf45</i>	chromosome 5 open reading frame 45	1.01E -04	2.00
TC1700012315.hg.1	<i>SLC25A10</i>	solute carrier family 25 (mitochondrial carrier;	2.46E -03	1.99

		dicarboxylate transporter), member 10		
TC0100018208.hg.1	<i>ZBTB8B</i>	zinc finger and BTB domain containing 8B	7.89E -04	1.99
TC0100009373.hg.1	<i>SLC6A17</i>	solute carrier family 6 (neutral amino acid transporter), member 17	9.29E -03	1.99
HTA2-neg-47421950_st	NA	NA	7.14E -03	1.99
TC1000007703.hg.1	<i>BICC1</i>	BicC family RNA binding protein 1	7.78E -04	1.99
TC0X00007116.hg.1	<i>RP2</i>	retinitis pigmentosa 2 (X-linked recessive)	8.30E -05	1.99
TC2100008459.hg.1	<i>FTCD</i>	formimidoyltransferase cyclodeaminase	7.92E -03	1.99
TC1100007220.hg.1	<i>DEPDC7</i>	DEP domain containing 7	7.68E -04	1.99
TC1700008440.hg.1	<i>PPM1E</i>	protein phosphatase, Mg ²⁺ /Mn ²⁺ dependent, 1E	1.74E -04	1.99
TC0800008663.hg.1	<i>MAL2</i>	mal, T-cell differentiation protein 2 (gene/pseudogene)	1.20E -04	1.98
TC0200016637.hg.1	<i>SMC6</i>	structural maintenance of chromosomes 6	7.13E -03	1.98
TC0100017059.hg.1	<i>RBBP5</i>	retinoblastoma binding protein 5	2.22E -03	1.98
TC1700006911.hg.1	<i>ARHGAP44</i>	Rho GTPase activating protein 44	6.21E -03	1.98
TC1200008795.hg.1	<i>ACACB</i>	acetyl-CoA carboxylase beta	3.98E -03	1.98
TC0800008150.hg.1	<i>CPNE3</i>	copine III	2.71E -05	1.98
23076506	NA	NA	6.38E -03	1.98
TC1200012680.hg.1	<i>ACSS3</i>	acyl-CoA synthetase short-chain family member 3	9.18E -04	1.98

APPENDIX

TC0900009324.hg.1	<i>CACNA1B</i>	calcium channel, voltage-dependent, N type, alpha 1B subunit	5.56E -04	1.98
TC1200011599.hg.1	<i>LTA4H</i>	leukotriene A4 hydrolase	3.85E -04	1.98
TC0800007439.hg.1	<i>POLB</i>	polymerase (DNA directed), beta	1.79E -04	1.98
TC1400009175.hg.1	<i>NID2</i>	nidogen 2 (osteonidogen)	2.49E -03	1.98
TC1300007312.hg.1	<i>PCDH17</i>	protocadherin 17	5.12E -04	1.98
TC1900009201.hg.1	<i>MKNK2</i>	MAP kinase interacting serine/threonine kinase 2	7.47E -04	1.98
TC0200014790.hg.1	<i>GRB14</i>	growth factor receptor bound protein 14	5.48E -04	1.97
TC0800012323.hg.1	<i>CA13</i>	carbonic anhydrase XIII	8.93E -04	1.97
TC0200010275.hg.1	<i>GLS</i>	glutaminase	1.88E -03	1.97
TC0800012405.hg.1	<i>FUT10</i>	fucosyltransferase 10 (alpha (1,3)fucosyltransferase)	1.93E -03	1.97
TC0700011050.hg.1	<i>FIGNL1</i>	fidgetin-like 1	2.28E -04	1.97
TC1900007382.hg.1	<i>PGPEP1</i>	pyroglutamyl-peptidase I	2.97E -04	1.97
TC0600014150.hg.1	<i>SMIM8</i>	small integral membrane protein 8	1.08E -03	1.97
TC1900011981.hg.1	<i>ERCC2</i>	excision repair cross-complementation group 2	2.26E -04	1.97
TC0200006983.hg.1	<i>EFR3B</i>	EFR3 homolog B	6.39E -03	1.96
TC0500012160.hg.1	<i>NME5</i>	NME/NM23 family member 5	4.96E -04	1.96
TC0400010733.hg.1	<i>KDR</i>	kinase insert domain receptor	5.51E -03	1.96
TC0600007103.hg.1	<i>KDM1B</i>	lysine (K)-specific demethylase 1B	8.28E -05	1.96

TC1500010755.hg.1	<i>ANKDD1A</i>	ankyrin repeat and death domain containing 1A	5.63E -05	1.96
TC0500009521.hg.1	<i>CPEB4</i>	cytoplasmic polyadenylation element binding protein 4	6.45E -04	1.96
TC1900011874.hg.1	<i>ZNF878</i>	zinc finger protein 878	3.69E -04	1.96
TC1500008470.hg.1	<i>ARRDC4</i>	arrestin domain containing 4	7.79E -04	1.96
TC1400009198.hg.1	<i>DDHD1</i>	DDHD domain containing 1	3.54E -03	1.96
TC0200009071.hg.1	<i>CFAP221</i>	cilia and flagella associated protein 221	3.56E -04	1.96
HTA2-pos-47421982_st	NA	NA	2.10E -03	1.96
TC1200006905.hg.1	<i>FAM234B</i>	family with sequence similarity 234, member B	5.14E -04	1.96
TC0900011340.hg.1	<i>ASTN2</i>	astrotactin 2	6.21E -03	1.96
TC0700013575.hg.1	<i>STAG3L3</i>	stromal antigen 3-like 3 (pseudogene)	3.45E -05	1.96
TC2000007695.hg.1	<i>PTPN1</i>	protein tyrosine phosphatase, non-receptor type 1	1.32E -03	1.96
TC0100015701.hg.1	<i>HIST2H3A</i>	histone cluster 2, H3a	2.84E -03	1.96
TC0300012765.hg.1	<i>HLTF</i>	Transcript Identified by AceView, Entrez Gene ID(s) 6596	2.61E -03	1.96
TC0100009181.hg.1	<i>PLPPR4</i>	phospholipid phosphatase related 4	8.78E -03	1.96
TSUnmapped00000050.hg.1	<i>MLXIP</i>	MLX interacting protein	2.68E -03	1.95
TC2000007670.hg.1	<i>SNAI1</i>	snail family zinc finger 1	1.88E -04	1.95
TC2200008449.hg.1	<i>DUSP18</i>	dual specificity phosphatase 18	1.46E -03	1.95
TC0200006715.hg.1	<i>PQLC3</i>	PQ loop repeat containing 3	2.71E -03	1.95

APPENDIX

TC1700011448.hg.1	<i>POLG2</i>	polymerase (DNA directed), gamma 2, accessory subunit	2.32E -04	1.95
TC0700013327.hg.1	<i>CHST12</i>	carbohydrate (chondroitin 4) sulfotransferase 12	8.89E -04	1.95
TC2100007241.hg.1	<i>ABCG1</i>	ATP binding cassette subfamily G member 1	5.03E -04	1.95
TC0300008715.hg.1	<i>EEFSEC</i>	eukaryotic elongation factor, selenocysteine-tRNA-specific	2.16E -04	1.95
TC1100011052.hg.1	<i>FADS3</i>	fatty acid desaturase 3	7.12E -04	1.95
TSUnmapped00000128.hg.1	<i>ZNF852</i>	zinc finger protein 852	2.75E -03	1.95
TC0700013388.hg.1	<i>STAG3L1</i>	stromal antigen 3-like 1 (pseudogene)	3.26E -05	1.95
TC1100007812.hg.1	<i>LRRC10B</i>	leucine rich repeat containing 10B	1.03E -04	1.95
TC0600009143.hg.1	<i>SLC16A10</i>	solute carrier family 16 (aromatic amino acid transporter), member 10	5.01E -04	1.94
TC1500007615.hg.1	<i>MAP2K1</i>	Transcript Identified by AceView, Entrez Gene ID(s) 5604	2.56E -03	1.94
TC1600010987.hg.1	<i>CMIP</i>	Memczak2013 ANTISENSE, coding, INTERNAL, intronic best transcript NM_198390	5.28E -05	1.94
TC0900011523.hg.1	<i>HSPA5</i>	heat shock 70kDa protein 5 (glucose-regulated protein, 78kDa)	8.38E -04	1.94
TC1700012212.hg.1	<i>CCDC144NL-AS1</i>	CCDC144NL antisense RNA 1	8.49E -03	1.94
TC1100010418.hg.1	<i>KIF18A</i>	kinesin family member 18A	8.09E -03	1.94
TC0500010780.hg.1	<i>SLC38A9</i>	Transcript Identified by AceView, Entrez Gene ID(s) 153129	4.57E -03	1.94
TC1600007240.hg.1	<i>PRKCB</i>	protein kinase C, beta	4.72E -03	1.94
TC0200007296.hg.1	<i>GALM</i>	galactose mutarotase (aldose 1-epimerase)	1.27E -04	1.94

TC1200010156.hg.1	CASC1	cancer susceptibility candidate 1	1.97E -04	1.94
TC0800010163.hg.1	<i>FGFR1</i>	fibroblast growth factor receptor 1	4.10E -04	1.94
TC0X00009117.hg.1	<i>FANCB</i>	Fanconi anemia complementation group B	1.52E -04	1.94
TC0700011780.hg.1	<i>PEX1</i>	peroxisomal biogenesis factor 1	2.68E -04	1.94
TC1400009787.hg.1	<i>SPTLC2</i>	serine palmitoyltransferase, long chain base subunit 2	4.15E -03	1.93
TC0100013417.hg.1	<i>SLC9A1</i>	solute carrier family 9, subfamily A (NHE1, cation proton antiporter 1), member 1	3.24E -03	1.93
TC1100006576.hg.1	<i>CD81</i>	CD81 molecule	2.67E -04	1.93
23075476	NA	NA	8.27E -04	1.93
TC1700008441.hg.1	<i>PPM1E</i>	Transcript Identified by AceView, Entrez Gene ID(s) 22843	5.08E -03	1.93
TC0600011127.hg.1	<i>HIST1H1C</i>	histone cluster 1, H1c	1.77E -03	1.93
TC0900008933.hg.1	<i>TOR1B</i>	torsin family 1, member B (torsin B)	3.83E -04	1.93
TC1100007390.hg.1	<i>EXT2</i>	exostosin glycosyltransferase 2	1.22E -03	1.93
TC0800007328.hg.1	<i>BAG4</i>	BCL2-associated athanogene 4	5.77E -03	1.93
TC0400011043.hg.1	<i>CDKL2</i>	cyclin-dependent kinase-like 2 (CDC2-related kinase)	6.18E -03	1.93
TC0200009402.hg.1	<i>MGAT5</i>	mannosyl (alpha-1,6)-glycoprotein beta-1,6-N-acetyl-glucosaminyltransferase	1.11E -03	1.93
TC0100014365.hg.1	<i>CYP2J2</i>	cytochrome P450, family 2, subfamily J, polypeptide 2	8.91E -04	1.93
TC0100018261.hg.1	<i>GSTM4</i>	glutathione S-transferase mu 4	4.10E -03	1.93

APPENDIX

TC0100011463.hg.1	<i>SYT14</i>	synaptotagmin XIV	6.69E -03	1.93
TC1900007356.hg.1	<i>KCNN1</i>	potassium channel, calcium activated intermediate/small conductance subfamily N alpha, member 1	4.77E -04	1.92
TC1400007307.hg.1	<i>ARID4A</i>	AT rich interactive domain 4A (RBP1-like)	3.50E -04	1.92
TC0700008617.hg.1	<i>SH2B2</i>	SH2B adaptor protein 2	4.50E -03	1.92
TC0100007634.hg.1	<i>ZCCHC17</i>	zinc finger, CCHC domain containing 17	3.23E -03	1.92
TC0100018479.hg.1	<i>NOTCH2NL</i>	notch 2 N-terminal like	2.60E -04	1.92
TC1800006715.hg.1	<i>IMPA2</i>	inositol(myo)-1(or 4)-monophosphatase 2	2.15E -04	1.92
TC1200007236.hg.1	<i>METTL20</i>	methyltransferase like 20	4.57E -03	1.92
TC0100018437.hg.1	<i>MKNK1</i>	MAP kinase interacting serine/threonine kinase 1	1.26E -04	1.92
TC1200012700.hg.1	<i>C12orf75</i>	chromosome 12 open reading frame 75	4.32E -03	1.92
TC0800012351.hg.1	<i>WDYHV1</i>	WDYHV motif containing 1	1.91E -04	1.92
TC0500010203.hg.1	<i>MYO10</i>	myosin X	2.52E -04	1.92
TC0X00010532.hg.1	<i>AMOT</i>	angiomotin	1.03E -03	1.92
TC1400010759.hg.1	<i>ATP6V1D</i>	ATPase, H ⁺ transporting, lysosomal 34kDa, V1 subunit D	6.91E -04	1.92
TC0300006520.hg.1	<i>LMCD1</i>	LIM and cysteine-rich domains 1	6.19E -04	1.92
TC0100018417.hg.1	<i>ALDH4A1</i>	aldehyde dehydrogenase 4 family, member A1	3.08E -04	1.92
TC1100012535.hg.1	<i>PVRL1</i>	poliovirus receptor-related 1 (herpesvirus entry mediator C)	1.60E -03	1.92

TC1700008228.hg.1	<i>ITGA3</i>	integrin alpha 3	6.51E -03	1.92
TC0100017716.hg.1	<i>FAM89A</i>	family with sequence similarity 89, member A	5.05E -05	1.92
TC0900011286.hg.1	<i>DFNB31</i>	deafness, autosomal recessive 31	3.20E -04	1.92
TC0200015776.hg.1	<i>RESP18</i>	regulated endocrine-specific protein 18	4.84E -03	1.92
TC0600013727.hg.1	<i>EZR</i>	ezrin	4.74E -03	1.92
TC1900010391.hg.1	<i>PEPD</i>	peptidase D	3.50E -04	1.92
TC1600007957.hg.1	<i>MT2A</i>	metallothionein 2A	1.18E -03	1.92
TC1900009433.hg.1	<i>TUBB4A</i>	tubulin, beta 4A class IVa	3.65E -04	1.91
TC0500007136.hg.1	<i>SPEF2</i>	sperm flagellar 2	8.73E -04	1.91
TC0100009656.hg.1	<i>FCGR1B</i>	Fc fragment of IgG, high affinity Ib, receptor (CD64)	4.89E -03	1.91
TC0700006977.hg.1	<i>NFE2L3</i>	nuclear factor, erythroid 2-like 3	5.01E -03	1.91
TC0900009307.hg.1	<i>ARRDC1</i>	arrestin domain containing 1	3.94E -04	1.91
TC0X00007707.hg.1	<i>ATP7A</i>	ATPase, Cu++ transporting, alpha polypeptide	2.87E -03	1.91
TC1400007201.hg.1	<i>CDKN3</i>	cyclin-dependent kinase inhibitor 3	1.46E -04	1.91
TC1600008020.hg.1	<i>USB1</i>	U6 snRNA biogenesis 1	2.01E -04	1.91
TC1100012052.hg.1	<i>CCDC82</i>	coiled-coil domain containing 82	3.91E -04	1.91
TC1500010753.hg.1	<i>TLN2</i>	talin 2	5.67E -04	1.91
TC0300007432.hg.1	<i>MAPKAPK3</i>	mitogen-activated protein kinase-activated protein kinase 3	1.14E -04	1.91

APPENDIX

TC0100015246.hg.1	KCNA3	potassium channel, voltage gated shaker related subfamily A, member 3	2.44E -03	1.91
TC1700007949.hg.1	ARL4D	ADP-ribosylation factor like GTPase 4D	5.27E -03	1.91
TC1600006893.hg.1	CLEC16A	C-type lectin domain family 16, member A	3.72E -04	1.91
TC0900011260.hg.1	ALAD	aminolevulinic acid dehydratase	6.15E -05	1.91
TC0100014218.hg.1	SCP2	Jeck2013 ANTISENSE, coding, INTERNAL, OVEON, UTR3 best transcript NM_001007098	2.24E -04	1.90
TC0800012306.hg.1	MTFR1	mitochondrial fission regulator 1	1.86E -03	1.90
TC0600012452.hg.1	CEP162	centrosomal protein 162kDa	9.77E -05	1.90
TC2100008533.hg.1	PCBP3	poly(rC) binding protein 3	4.90E -04	1.90
TC1200009452.hg.1	MMP17	matrix metallopeptidase 17 (membrane-inserted)	9.46E -04	1.90
TC0400010784.hg.1	NOA1	nitric oxide associated 1	4.97E -03	1.90
TC0600013604.hg.1	RGS17	regulator of G-protein signaling 17	2.14E -04	1.90
TC0100017058.hg.1	TMEM81	transmembrane protein 81	4.54E -03	1.90
TC0100007365.hg.1	NIPAL3	NIPA-like domain containing 3	8.47E -04	1.90
TC0300009353.hg.1	PPM1L	protein phosphatase, Mg ²⁺ /Mn ²⁺ dependent, 1L	3.31E -03	1.90
TC1600009944.hg.1	KCTD13	potassium channel tetramerization domain containing 13	3.20E -04	1.90
TC1200008906.hg.1	TRAFD1	TRAF-type zinc finger domain containing 1	3.58E -03	1.90
TC1000010499.hg.1	ZFAND4	zinc finger, AN1-type domain 4	4.17E -04	1.90

TC0400008331.hg.1	<i>NPNT</i>	nephronectin	4.58E -03	1.90
TC0300013025.hg.1	<i>BCHE</i>	butyrylcholinesterase	2.24E -03	1.90
TC0100018302.hg.1	<i>EFNA4</i>	ephrin-A4	6.83E -04	1.89
TC0100009877.hg.1	<i>HIST2H3A</i>	histone cluster 2, H3a	3.64E -03	1.89
TC0200011013.hg.1	<i>FBXO36</i>	F-box protein 36	1.97E -03	1.89
TC1600009351.hg.1	<i>GRIN2A</i>	Transcript Identified by AceView, Entrez Gene ID(s) 2903	1.65E -04	1.89
TSUnmapped00000488.hg. .1	<i>ZDHHC3</i>	zinc finger, DHHC-type containing 3	1.31E -03	1.89
TC0100015180.hg.1	<i>WDR47</i>	WD repeat domain 47	2.22E -03	1.89
TC0100011269.hg.1	<i>LINC00260</i>	long intergenic non-protein coding RNA 260	5.62E -04	1.89
TC0400011579.hg.1	<i>PLA2G12A</i>	phospholipase A2, group XIIA	8.41E -04	1.89
TC1700011181.hg.1	<i>MMD</i>	monocyte to macrophage differentiation-associated	1.23E -03	1.89
TC0100016659.hg.1	<i>APOBEC4</i>	apolipoprotein B mRNA editing enzyme, catalytic polypeptide-like 4 (putative)	5.63E -04	1.89
TC0600012040.hg.1	<i>TRAM2</i>	translocation associated membrane protein 2	7.31E -04	1.89
TC0300012319.hg.1	<i>goyborbu</i>	Transcript Identified by AceView	1.30E -03	1.88
TC1100012906.hg.1	<i>IGSF9B</i>	immunoglobulin superfamily, member 9B	1.44E -04	1.88
TC0100009097.hg.1	<i>ABCD3</i>	ATP binding cassette subfamily D member 3	2.34E -03	1.88
TC0500013186.hg.1	<i>PTCD2</i>	pentatricopeptide repeat domain 2	2.33E -03	1.88
TC1100008091.hg.1	<i>CCS</i>	copper chaperone for superoxide dismutase	7.87E -03	1.88

APPENDIX

TC0X00011278.hg.1	<i>PRRG1</i>	proline rich Gla (G-carboxyglutamic acid) 1	1.13E -03	1.88
TC1900012045.hg.1	<i>RDH13</i>	retinol dehydrogenase 13 (all-trans/9-cis)	6.82E -04	1.88
TC0X00007053.hg.1	<i>MAOA</i>	monoamine oxidase A	1.44E -04	1.88
TC1800008862.hg.1	<i>PIGN</i>	phosphatidylinositol glycan anchor biosynthesis class N	2.53E -03	1.88
TC0900006762.hg.1	<i>ACER2</i>	alkaline ceramidase 2	5.58E -04	1.88
TC0300010038.hg.1	<i>SENP5</i>	Transcript Identified by AceView, Entrez Gene ID(s) 205564	4.99E -03	1.88
TC1700011277.hg.1	<i>TRIM37</i>	Transcript Identified by AceView, Entrez Gene ID(s) 4591	8.95E -03	1.88
TC0900010925.hg.1	<i>ZNF782</i>	zinc finger protein 782	8.02E -04	1.88
TC0600014194.hg.1	<i>TIAM2</i>	T-cell lymphoma invasion and metastasis 2	5.12E -03	1.88
TC1600009642.hg.1	<i>GDE1</i>	glycerophosphodiester phosphodiesterase 1	6.99E -03	1.87
TC1900009297.hg.1	<i>TBXA2R</i>	thromboxane A2 receptor	6.77E -04	1.87
TC0200015556.hg.1	<i>FZD5</i>	frizzled class receptor 5	3.03E -03	1.87
TC1100011867.hg.1	<i>FZD4</i>	frizzled class receptor 4	4.90E -04	1.87
TC0X00008235.hg.1	<i>LONRF3</i>	LON peptidase N-terminal domain and ring finger 3	6.60E -03	1.87
TC0200011402.hg.1	<i>FARP2</i>	FERM, ARH/RhoGEF and pleckstrin domain protein 2	6.91E -04	1.87
TC0300008979.hg.1	<i>CLSTN2</i>	calsyntenin 2	1.52E -03	1.87
TC1500007695.hg.1	<i>PAQR5</i>	progesterin and adipoQ receptor family member V	1.29E -04	1.87
TC0100006861.hg.1	<i>FBXO44</i>	F-box protein 44	8.33E -04	1.87

TC0X00008394.hg.1	<i>BCORL1</i>	BCL6 corepressor-like 1	5.95E -05	1.87
TC1100012526.hg.1	<i>USP2</i>	ubiquitin specific peptidase 2	1.28E -03	1.87
HTA2-pos-47421983_st	NA	NA	9.79E -04	1.87
TC0400009001.hg.1	<i>FAM160A1</i>	family with sequence similarity 160, member A1	5.37E -03	1.87
TC0700010352.hg.1	<i>ANKMY2</i>	ankyrin repeat and MYND domain containing 2	7.81E -03	1.86
TC0700010582.hg.1	<i>HIBADH</i>	Salzman2013 ALT_ACCEPTOR, ALT_DONOR, coding, INTERNAL, intronic best transcript NM_152740	6.59E -04	1.86
TC2000009014.hg.1	<i>NDRG3</i>	NDRG family member 3	4.66E -04	1.86
TC0X00007507.hg.1	<i>EFNB1</i>	ephrin-B1	3.45E -03	1.86
TC0800009853.hg.1	<i>BIN3</i>	bridging integrator 3	2.83E -04	1.86
TC0900008109.hg.1	<i>HABP4</i>	hyaluronan binding protein 4	1.41E -04	1.86
TC0100013281.hg.1	<i>ASAP3</i>	ArfGAP with SH3 domain, ankyrin repeat and PH domain 3	1.44E -03	1.86
TC1200010839.hg.1	<i>ITGA5</i>	integrin alpha 5	5.29E -04	1.86
TC2000006688.hg.1	<i>SNAP25</i>	synaptosome associated protein 25kDa	3.73E -03	1.86
TC1700008372.hg.1	<i>SCPEP1</i>	serine carboxypeptidase 1	2.86E -03	1.86
TC1500010846.hg.1	<i>GOLGA8K</i>	golgin A8 family, member K	3.46E -04	1.86
TC0100009418.hg.1	<i>RAP1A</i>	RAP1A, member of RAS oncogene family	7.42E -04	1.86
TC1000008005.hg.1	<i>MCU</i>	mitochondrial calcium uniporter	1.85E -03	1.86

APPENDIX

TC1100010175.hg.1	<i>RRAS2</i>	related RAS viral (r-ras) oncogene homolog 2	7.78E -03	1.86
TC0500009046.hg.1	<i>ADRB2</i>	adrenoceptor beta 2, surface	2.53E -03	1.86
TC0900008865.hg.1	<i>CERCAM</i>	cerebral endothelial cell adhesion molecule	4.84E -03	1.86
TC2000010027.hg.1	<i>TMEM189-UBE2V1</i>	TMEM189-UBE2V1 readthrough	2.70E -03	1.85
TC0200009687.hg.1	<i>ARL6IP6</i>	ADP-ribosylation factor like GTPase 6 interacting protein 6	4.49E -04	1.85
TC0200014851.hg.1	<i>LRP2</i>	LDL receptor related protein 2	5.25E -03	1.85
23071946	NA	NA	1.38E -04	1.85
TC0400011749.hg.1	<i>BBS7</i>	Bardet-Biedl syndrome 7	1.67E -03	1.85
TC0100018481.hg.1	<i>NOTCH2NL</i>	notch 2 N-terminal like	4.19E -04	1.85
TC1600011292.hg.1	<i>FANCA</i>	Fanconi anemia complementation group A	7.03E -03	1.85
TC0600008571.hg.1	<i>MYO6</i>	Transcript Identified by AceView, Entrez Gene ID(s) 4646	2.90E -03	1.84
HTA2-pos-3513255_st	NA	NA	8.30E -04	1.84
TC0100015211.hg.1	<i>GSTM3</i>	glutathione S-transferase mu 3 (brain)	2.78E -03	1.84
TC1100011643.hg.1	<i>ARRB1</i>	arrestin, beta 1	2.53E -03	1.84
TC0300012764.hg.1	<i>HLTF</i>	helicase-like transcription factor	9.11E -03	1.84
TC1300008834.hg.1	<i>SIAH3</i>	siah E3 ubiquitin protein ligase family member 3	2.54E -04	1.84
TC0600010960.hg.1	<i>TPMT</i>	thiopurine S-methyltransferase	7.89E -03	1.84
HTA2-pos-PSR12013086.hg.1	NA	NA	7.93E -03	1.84

TC1600008943.hg.1	<i>TMEM8A</i>	transmembrane protein 8A	2.65E -04	1.84
TC0300009713.hg.1	<i>EPHB3</i>	EPH receptor B3	2.78E -03	1.84
TC0500013088.hg.1	<i>MAPK9</i>	mitogen-activated protein kinase 9	1.08E -03	1.84
TC0600011809.hg.1	<i>CCND3</i>	cyclin D3	1.12E -03	1.84
TC2000008267.hg.1	<i>RASSF2</i>	Ras association (RalGDS/AF-6) domain family member 2	2.35E -04	1.84
TC2200007909.hg.1	<i>MICAL3</i>	microtubule associated monooxygenase, calponin and LIM domain containing 3	1.91E -04	1.84
23071925	NA	NA	1.65E -04	1.84
TC0200015314.hg.1	<i>STK17B</i>	serine/threonine kinase 17b	4.72E -03	1.84
HTA2-pos-3371082_st	NA	NA	7.01E -03	1.84
TC0800010045.hg.1	<i>TEX15</i>	testis expressed 15	9.68E -03	1.84
TC1300006643.hg.1	<i>ATP8A2</i>	ATPase, aminophospholipid transporter, class I, type 8A, member 2	2.58E -04	1.83
TC0700012731.hg.1	<i>DGKI</i>	diacylglycerol kinase, iota	8.11E -04	1.83
TC1900010025.hg.1	<i>CRLF1</i>	cytokine receptor-like factor 1	5.14E -04	1.83
TC0400007016.hg.1	<i>SLC2</i>	slit guidance ligand 2	3.28E -03	1.83
TC0300011628.hg.1	<i>ROBO1</i>	roundabout guidance receptor 1	2.94E -04	1.83
TC0700007137.hg.1	<i>BBS9</i>	Bardet-Biedl syndrome 9	8.93E -03	1.83
TC1000009908.hg.1	<i>RSU1</i>	Ras suppressor protein 1	5.86E -04	1.83

APPENDIX

TC1900009302.hg.1	<i>PIP5K1C</i>	phosphatidylinositol-4-phosphate 5-kinase, type I, gamma	6.56E -04	1.83
TC0900007113.hg.1	<i>RECK</i>	reversion-inducing-cysteine-rich protein with kazal motifs	2.59E -03	1.83
TC1100011101.hg.1	<i>NXF1</i>	nuclear RNA export factor 1	2.11E -03	1.83
HTA2-pos-PSR02023982.hg.1	NA	NA	8.77E -04	1.83
TC1600011465.hg.1	<i>ERVK13-1</i>	endogenous retrovirus group K13, member 1	1.08E -03	1.83
TC0100010159.hg.1	<i>SLC25A44</i>	solute carrier family 25, member 44	2.31E -03	1.83
TC0100006675.hg.1	<i>KCNAB2</i>	potassium channel, voltage gated subfamily A regulatory beta subunit 2	2.45E -03	1.82
TC2100006714.hg.1	<i>NCAM2</i>	neural cell adhesion molecule 2	3.03E -04	1.82
TC2100007420.hg.1	<i>COL18A1</i>	collagen, type XVIII, alpha 1	6.89E -04	1.82
TC1700006767.hg.1	<i>WRAP53</i>	WD repeat containing, antisense to <i>TP53</i>	1.14E -03	1.82
TC1900010005.hg.1	<i>RAB3A</i>	RAB3A, member RAS oncogene family	1.72E -03	1.82
TC0700008295.hg.1	<i>CFAP69</i>	cilia and flagella associated protein 69	8.32E -04	1.82
HTA2-pos-2978678_st	NA	NA	1.35E -03	1.82
TC1100010105.hg.1	<i>GALNT18</i>	polypeptide N-acetylgalactosaminyltransferase 18	7.38E -04	1.82
HTA2-pos-PSR02023992.hg.1	NA	NA	3.79E -03	1.82
TC0200011054.hg.1	<i>ARMC9</i>	armadillo repeat containing 9	5.11E -03	1.82
TC0100015483.hg.1	<i>NOTCH2</i>	notch 2	4.04E -04	1.82

TC1800009026.hg.1	<i>FBXO15</i>	F-box protein 15	6.86E -03	1.82
TC2200006907.hg.1	<i>SGSM1</i>	small G protein signaling modulator 1	3.55E -03	1.82
TC0700011500.hg.1	<i>STX1A</i>	syntaxin 1A (brain)	8.03E -04	1.82
TC0100013804.hg.1	<i>BMP8B</i>	bone morphogenetic protein 8b	2.50E -03	1.82
TC1100009302.hg.1	<i>TECTA</i>	tectorin alpha	8.57E -04	1.82
TC0500012285.hg.1	<i>FCHSD1</i>	FCH and double SH3 domains 1	3.66E -03	1.82
TC0200007929.hg.1	<i>GMCL1</i>	germ cell-less, spermatogenesis associated 1	9.87E -03	1.81
TC1200006570.hg.1	<i>KCNA1</i>	potassium channel, voltage gated shaker related subfamily A, member 1	6.96E -03	1.81
HTA2-pos-2978682_st	NA	NA	7.71E -04	1.81
TC1700008254.hg.1	<i>ACSF2</i>	acyl-CoA synthetase family member 2	8.92E -03	1.81
TC1400010261.hg.1	<i>MOK</i>	MOK protein kinase	9.63E -04	1.81
TC0200007353.hg.1	<i>EML4</i>	echinoderm microtubule associated protein like 4	6.15E -04	1.81
TC1500010157.hg.1	<i>ADAMTS7</i>	ADAM metallopeptidase with thrombospondin type 1 motif 7	9.56E -05	1.81
TC2000007476.hg.1	<i>STK4</i>	serine/threonine kinase 4	4.58E -04	1.81
HTA2-pos-2985914_st	NA	NA	2.73E -03	1.81
TC0100018303.hg.1	<i>EFNA3</i>	ephrin-A3	1.05E -04	1.81
HTA2-neg-47421381_st	NA	NA	7.62E -03	1.81
TC1400010620.hg.1	<i>SNAPC1</i>	small nuclear RNA activating complex polypeptide 1	2.38E -03	1.81

APPENDIX

TC0X00010130.hg.1	<i>MAGT1</i>	magnesium transporter 1	1.72E -04	1.81
TC1100010718.hg.1	<i>LRP4</i>	LDL receptor related protein 4	4.22E -04	1.81
TC1100011609.hg.1	<i>P4HA3</i>	prolyl 4-hydroxylase, alpha polypeptide III	7.97E -04	1.81
TC2100008536.hg.1	<i>PCBP3</i>	poly(rC) binding protein 3	1.53E -03	1.81
TC1500010908.hg.1	<i>STARD5</i>	STAR-related lipid transfer domain containing 5	4.86E -04	1.81
TC0800008467.hg.1	<i>ATP6V1C1</i>	ATPase, H ⁺ transporting, lysosomal 42kDa, V1 subunit C1	8.28E -03	1.81
TC0200015434.hg.1	<i>ALS2</i>	ALS2, alsin Rho guanine nucleotide exchange factor	6.35E -04	1.80
TC0600008156.hg.1	<i>ENPP4</i>	ectonucleotide pyrophosphatase/phosphodiesterase 4 (putative)	2.52E -03	1.80
TC0400008329.hg.1	<i>GSTCD</i>	glutathione S-transferase, C-terminal domain containing	6.43E -04	1.80
23072018	NA	NA	2.68E -04	1.80
23072048	NA	NA	2.68E -04	1.80
TC0100006805.hg.1	<i>RBP7</i>	retinol binding protein 7, cellular	5.01E -03	1.80
TC0600006870.hg.1	<i>SNRNP48</i>	small nuclear ribonucleoprotein, U11/U12 48KDa subunit	1.11E -03	1.80
TC0100018434.hg.1	<i>MYCBP</i>	MYC binding protein	1.33E -03	1.80
TC0300007386.hg.1	<i>APEH</i>	acylaminoacyl-peptide hydrolase	7.39E -03	1.80
TC1200010812.hg.1	<i>CALCOCO1</i>	calcium binding and coiled-coil domain 1	3.83E -03	1.80
TC1200011099.hg.1	<i>GNS</i>	glucosamine (N-acetyl)-6-sulfatase	6.33E -04	1.80
TC2100006976.hg.1	<i>ITSN1</i>	intersectin 1	9.49E -04	1.80

TC1400010754.hg.1	<i>C14orf37</i>	chromosome 14 open reading frame 37	9.61E -05	1.80
TC1600008169.hg.1	<i>PARD6A</i>	par-6 family cell polarity regulator alpha	3.52E -04	1.80
TSUnmapped00000726.hg. .1	<i>ZDHHC3</i>	zinc finger, DHHC-type containing 3	1.57E -03	1.80
TC2100007964.hg.1	<i>SYNJ1</i>	synaptojanin 1	3.03E -03	1.79
TC0900012276.hg.1	<i>SCAI</i>	suppressor of cancer cell invasion	4.69E -04	1.79
TC0200015773.hg.1	<i>PTPRN</i>	protein tyrosine phosphatase, receptor type, N	3.12E -03	1.79
TC0500008278.hg.1	<i>FER</i>	fer (fps/fes related) tyrosine kinase	5.24E -04	1.79
TC1200006472.hg.1	<i>ADIPOR2</i>	adiponectin receptor 2	2.63E -03	1.79
TC1200009031.hg.1	<i>RNFT2</i>	ring finger protein, transmembrane 2	5.99E -04	1.79
TC0600007374.hg.1	<i>HIST1H2AI</i>	histone cluster 1, H2ai	9.98E -03	1.79
TC1800008578.hg.1	<i>EPG5</i>	ectopic P-granules autophagy protein 5 homolog (C. elegans)	7.16E -04	1.79
TC0X00010877.hg.1	<i>FAM122B</i>	family with sequence similarity 122B	1.93E -03	1.79
TC0400012781.hg.1	<i>STIM2</i>	stromal interaction molecule 2	2.19E -03	1.79
TC0500007050.hg.1	<i>PDZD2</i>	PDZ domain containing 2	6.41E -04	1.79
TC1600008498.hg.1	<i>VAT1L</i>	vesicle amine transport 1-like	7.09E -03	1.78
TC2000008230.hg.1	<i>C20orf27</i>	chromosome 20 open reading frame 27	6.77E -03	1.78
TC1600009199.hg.1	<i>SLX4</i>	SLX4 structure-specific endonuclease subunit	1.55E -03	1.78
TC1700010879.hg.1	<i>MAP3K14</i>	mitogen-activated protein kinase kinase kinase 14	7.01E -03	1.78

APPENDIX

TC0800007065.hg.1	<i>CDCA2</i>	cell division cycle associated 2	1.18E -03	1.78
TC0100012675.hg.1	<i>ACOT7</i>	acyl-CoA thioesterase 7	6.26E -03	1.78
TC0800010382.hg.1	<i>SNAI2</i>	snail family zinc finger 2	8.55E -04	1.78
TC0300008046.hg.1	<i>ARL13B</i>	ADP-ribosylation factor like GTPase 13B	3.40E -04	1.78
TC1400007950.hg.1	<i>CALM1</i>	calmodulin 1 (phosphorylase kinase, delta)	2.66E -04	1.78
TC0200009895.hg.1	<i>CERS6</i>	ceramide synthase 6	1.35E -03	1.78
TC1500007067.hg.1	<i>CKMT1A</i>	creatine kinase, mitochondrial 1A	2.96E -04	1.78
TC0900008795.hg.1	<i>RALGPS1</i>	Ral GEF with PH domain and SH3 binding motif 1	8.77E -04	1.78
TC1500009238.hg.1	<i>FRMD5</i>	FERM domain containing 5	2.49E -03	1.78
TC0100013072.hg.1	<i>ATP13A2</i>	ATPase type 13A2	2.86E -04	1.78
TC0200015616.hg.1	<i>ERBB4</i>	erb-b2 receptor tyrosine kinase 4	8.36E -04	1.78
TC0300008369.hg.1	<i>ATP6V1A</i>	ATPase, H ⁺ transporting, lysosomal 70kDa, V1 subunit A	1.26E -03	1.78
TC1200007137.hg.1	<i>FGFR1OP2</i>	FGFR1 oncogene partner 2	5.55E -03	1.78
TC0300013932.hg.1	<i>SRGAP3</i>	SLIT-ROBO Rho GTPase activating protein 3	1.12E -03	1.77
TC1500009984.hg.1	<i>NPTN</i>	neuroplastin	4.70E -04	1.77
TC1200009981.hg.1	<i>HEBP1</i>	heme binding protein 1	1.83E -03	1.77
TC0100013634.hg.1	<i>TMEM54</i>	transmembrane protein 54	3.18E -03	1.77
TC0100013763.hg.1	<i>POU3F1</i>	POU class 3 homeobox 1	3.26E -04	1.77

TC1900009266.hg.1	<i>ZNF77</i>	zinc finger protein 77	5.83E -03	1.77
TC1000006704.hg.1	<i>TAF3</i>	TATA box binding protein associated factor 3	1.52E -03	1.77
TC1000007925.hg.1	<i>EIF4EBP2</i>	eukaryotic translation initiation factor 4E binding protein 2	8.27E -04	1.77
TC1700009378.hg.1	<i>PITPNA</i>	phosphatidylinositol transfer protein, alpha	4.93E -04	1.77
TC0900011259.hg.1	<i>HDHD3</i>	haloacid dehalogenase-like hydrolase domain containing 3	9.43E -03	1.77
TC0300010908.hg.1	<i>ZDHHC3</i>	zinc finger, DHHC-type containing 3	2.62E -03	1.77
TC1400007706.hg.1	<i>FOS</i>	FBJ murine osteosarcoma viral oncogene homolog	4.68E -03	1.77
TC1800009203.hg.1	<i>PQLC1</i>	PQ loop repeat containing 1	3.06E -04	1.77
TC0900009673.hg.1	<i>MLLT3</i>	myeloid/lymphoid or mixed-lineage leukemia; translocated to, 3	4.89E -03	1.77
TC1100006906.hg.1	<i>FAR1</i>	fatty acyl CoA reductase 1	9.49E -04	1.77
TC0600013010.hg.1	<i>MAN1A1</i>	mannosidase, alpha, class 1A, member 1	1.84E -03	1.77
TC0800011679.hg.1	<i>ATAD2</i>	ATPase family, AAA domain containing 2	5.20E -03	1.77
TC0600010040.hg.1	<i>FNDC1</i>	fibronectin type III domain containing 1	8.83E -04	1.77
TC0600008127.hg.1	<i>SLC29A1</i>	solute carrier family 29 (equilibrative nucleoside transporter), member 1	3.01E -03	1.77
TSUnmapped00000569.hg.1	<i>ZDHHC3</i>	zinc finger, DHHC-type containing 3	8.04E -03	1.77
TC0100015194.hg.1	<i>SORT1</i>	sortilin 1	1.45E -03	1.77
TC0X00008674.hg.1	<i>AFF2</i>	AF4/FMR2 family, member 2	7.15E -03	1.77
TC0200014717.hg.1	<i>WDSUB1</i>	WD repeat, sterile alpha motif and U-box domain containing 1	4.23E -03	1.77

APPENDIX

TC0100013302.hg.1	<i>GALE</i>	UDP-galactose-4-epimerase	8.37E -03	1.77
TC0600011138.hg.1	<i>HIST1H1D</i>	histone cluster 1, H1d	1.46E -03	1.77
TSUnmapped00000178.hg. .1	<i>SLC16A1</i>	solute carrier family 16 (monocarboxylate transporter), member 1	5.71E -03	1.77
TC0600009343.hg.1	<i>NKAIN2</i>	Na+/K+ transporting ATPase interacting 2	2.78E -03	1.76
TC0900010971.hg.1	<i>TBC1D2</i>	TBC1 domain family, member 2	3.58E -03	1.76
TC1700012089.hg.1	<i>DCXR</i>	dicarbonyl/L-xylulose reductase	1.85E -03	1.76
TC0X00007936.hg.1	<i>CENPI</i>	centromere protein I	2.28E -03	1.76
TC0600007799.hg.1	<i>FANCE</i>	Fanconi anemia complementation group E	2.89E -03	1.76
TC0100009408.hg.1	<i>PIFO</i>	primary cilia formation	1.60E -03	1.76
TC1000009248.hg.1	<i>FANK1</i>	fibronectin type III and ankyrin repeat domains 1	8.61E -04	1.76
TC1300009012.hg.1	<i>THSD1</i>	thrombospondin type 1 domain containing 1	2.25E -03	1.76
TC1700007677.hg.1	<i>DUSP14</i>	dual specificity phosphatase 14	3.66E -03	1.76
HTA2-neg-47420655_st	NA	NA	1.47E -03	1.76
TC0100016350.hg.1	<i>CCDC181</i>	coiled-coil domain containing 181	8.29E -03	1.76
TC0600009697.hg.1	<i>PHACTR2</i>	Jeck2013 ALT_ACCEPTOR, ALT_DONOR, coding, INTERNAL, intronic best transcript NM_001100164	8.78E -03	1.76
TC1900007063.hg.1	<i>ZNF788</i>	zinc finger family member 788	3.60E -03	1.76
TC0300007610.hg.1	<i>PXK</i>	PX domain containing serine/threonine kinase	1.17E -04	1.76

TC0500011260.hg.1	<i>SERINC5</i>	serine incorporator 5	1.96E -04	1.76
TC0900008803.hg.1	<i>SLC2A8</i>	solute carrier family 2 (facilitated glucose transporter), member 8	8.36E -04	1.76
TC0500008602.hg.1	<i>LYRM7</i>	LYR motif containing 7	6.13E -04	1.76
TC0500011702.hg.1	<i>STARD4</i>	StAR-related lipid transfer domain containing 4	8.21E -04	1.76
TC0200012489.hg.1	<i>PIGF</i>	phosphatidylinositol glycan anchor biosynthesis class F	2.40E -04	1.76
23071874	NA	NA	3.49E -04	1.75
TC1200010968.hg.1	<i>DDIT3</i>	DNA-damage-inducible transcript 3	9.99E -04	1.75
TC0800009854.hg.1	<i>BIN3-IT1</i>	BIN3 intronic transcript 1	3.74E -03	1.75
TC2200006827.hg.1	<i>GNAZ</i>	guanine nucleotide binding protein (G protein), alpha z polypeptide	4.13E -03	1.75
TSUnmapped00000068.hg.1	<i>ZNF780A</i>	zinc finger protein 780A	9.88E -03	1.75
TC1400009214.hg.1	<i>BMP4</i>	bone morphogenetic protein 4	7.06E -04	1.75
TC1200011908.hg.1	<i>GPN3</i>	GPN-loop GTPase 3	1.80E -03	1.75
TC0600008632.hg.1	<i>BCKDHB</i>	branched chain keto acid dehydrogenase E1, beta polypeptide	6.59E -04	1.75
TC0900011655.hg.1	<i>ZER1</i>	zyg-11 related, cell cycle regulator	5.79E -03	1.75
TC0100016567.hg.1	<i>TOR1AIP2</i>	torsin A interacting protein 2	1.46E -03	1.75
TC1900006586.hg.1	<i>TMPRSS9</i>	transmembrane protease, serine 9	9.55E -03	1.75
TC0900009776.hg.1	<i>MOB3B</i>	MOB kinase activator 3B	5.63E -03	1.75
TC1400007500.hg.1	<i>ARG2</i>	arginase 2	3.42E -03	1.75

APPENDIX

TC1600010000.hg.1	<i>STX1B</i>	syntaxin 1B	3.89E -03	1.75
TC0900010808.hg.1	<i>BICD2</i>	bicaudal D homolog 2 (Drosophila)	2.33E -03	1.75
TC0600009800.hg.1	<i>GINM1</i>	glycoprotein integral membrane 1	3.90E -04	1.75
TC1200008275.hg.1	<i>SYT1</i>	synaptotagmin I	2.46E -03	1.75
TC0600009102.hg.1	<i>FIG4</i>	FIG4 phosphoinositide 5-phosphatase	3.69E -04	1.75
TC0700012099.hg.1	<i>RASA4</i>	Salzman2013 ALT_ACCEPTOR, ALT_DONOR, coding, INTERNAL, intronic best transcript NM_006989	3.28E -03	1.75
TC0200014204.hg.1	<i>HS6ST1</i>	heparan sulfate 6-O-sulfotransferase 1	3.83E -04	1.75
TC1700006702.hg.1	<i>TXNDC17</i>	thioredoxin domain containing 17	1.36E -03	1.75
TC0800012447.hg.1	<i>AZIN1</i>	antizyme inhibitor 1	1.36E -03	1.74
TC0X00011211.hg.1	<i>G6PD</i>	glucose-6-phosphate dehydrogenase	7.10E -03	1.74
TC1500010845.hg.1	<i>OTUD7A</i>	OTU deubiquitinase 7A	1.42E -03	1.74
TC2000006571.hg.1	<i>SMOX</i>	spermine oxidase	1.43E -03	1.74
TC0500009161.hg.1	<i>SAP30L</i>	SAP30-like	5.92E -03	1.74
TC0300009856.hg.1	<i>IL1RAP</i>	interleukin 1 receptor accessory protein	5.36E -03	1.74
TC1700011208.hg.1	<i>TRIM25</i>	tripartite motif containing 25	1.11E -03	1.74
TC1500010128.hg.1	<i>TBC1D2B</i>	TBC1 domain family, member 2B	4.03E -03	1.74
HTA2-neg-47423726_st	NA	NA	3.37E -03	1.74

TC0700013525.hg.1	<i>FAM126A</i>	family with sequence similarity 126, member A	6.89E -03	1.74
TSUnmapped00000085.hg.1	<i>CCDC84</i>	coiled-coil domain containing 84	3.27E -03	1.74
TC1900008259.hg.1	<i>ZNF233</i>	zinc finger protein 233	1.29E -03	1.74
TC0X00009057.hg.1	<i>MID1</i>	midline 1	4.24E -04	1.74
TC1500010160.hg.1	<i>CTSH</i>	cathepsin H	2.66E -03	1.74
23071987	NA	NA	2.65E -04	1.74
TC0900011379.hg.1	<i>MEGF9</i>	multiple EGF-like-domains 9	6.83E -04	1.74
TC1200010011.hg.1	<i>HIST4H4</i>	histone cluster 4, H4	6.26E -03	1.74
TC1400010331.hg.1	<i>XRCC3</i>	X-ray repair complementing defective repair in Chinese hamster cells 3	1.30E -03	1.74
TC0800007351.hg.1	<i>TACC1</i>	transforming, acidic coiled-coil containing protein 1	8.48E -04	1.74
23071967	NA	NA	2.02E -04	1.74
TC0900012277.hg.1	<i>AK1</i>	adenylate kinase 1	9.06E -04	1.74
TC0700010581.hg.1	<i>HIBADH</i>	3-hydroxyisobutyrate dehydrogenase	3.24E -03	1.74
TC1200008814.hg.1	<i>ANKRD13A</i>	ankyrin repeat domain 13A	2.28E -04	1.74
TC0100009241.hg.1	<i>S1PR1</i>	sphingosine-1-phosphate receptor 1	7.88E -04	1.74
23075636	NA	NA	3.05E -03	1.74
23076269	NA	NA	3.05E -03	1.74

APPENDIX

TC1900006848.hg.1	<i>CAMSAP3</i>	calmodulin regulated spectrin-associated protein family, member 3	5.66E -03	1.74
TC2000009960.hg.1	<i>SRXN1</i>	sulfiredoxin 1	6.66E -03	1.73
TC1600010593.hg.1	<i>CMTM4</i>	CKLF-like MARVEL transmembrane domain containing 4	4.89E -04	1.73
TC1100010491.hg.1	<i>FBXO3</i>	F-box protein 3	4.43E -03	1.73
TC1400010615.hg.1	<i>MNAT1</i>	MNAT CDK-activating kinase assembly factor 1	7.80E -04	1.73
TC1400009705.hg.1	<i>PGF</i>	placental growth factor	4.77E -04	1.73
TC1200007835.hg.1	<i>COQ10A</i>	coenzyme Q10A	1.20E -03	1.73
TC0200011107.hg.1	<i>EFHD1</i>	EF-hand domain family member D1	3.68E -03	1.73
HTA2-pos-PSR02023981.hg.1	NA	NA	7.91E -03	1.73
TC1300008443.hg.1	<i>LNX2</i>	ligand of numb-protein X 2	5.08E -03	1.73
TC0100009958.hg.1	<i>CGN</i>	cingulin	8.82E -03	1.73
TC1900007366.hg.1	<i>MPV17L2</i>	MPV17 mitochondrial membrane protein-like 2	1.40E -03	1.73
TC1000008743.hg.1	<i>SUFU</i>	Transcript Identified by AceView, Entrez Gene ID(s) 51684	9.10E -04	1.73
TC1000011660.hg.1	<i>MGEA5</i>	Salzman2013 ALT_ACCEPTOR, ALT_DONOR, coding, INTERNAL, intronic best transcript NM_012215	8.00E -03	1.73
23075808	NA	NA	2.01E -03	1.73
TC1400010716.hg.1	<i>HOMEZ</i>	homeobox and leucine zipper encoding	1.64E -03	1.73

TC2200006678.hg.1	<i>SNAP29</i>	synaptosome associated protein 29kDa	2.91E -03	1.72
TC0700008495.hg.1	<i>BUD31</i>	Transcript Identified by AceView, Entrez Gene ID(s) 8896	3.94E -03	1.72
TC0700008292.hg.1	<i>STEAP1</i>	six transmembrane epithelial antigen of the prostate 1	9.99E -03	1.72
TC1200007594.hg.1	<i>ASIC1</i>	acid sensing ion channel 1	3.16E -03	1.72
HTA2-pos-3529035_st	NA	NA	4.43E -03	1.72
HTA2-pos-PSR19012462.hg.1	NA	NA	2.66E -03	1.72
TC0100018480.hg.1	<i>NBPF14</i>	neuroblastoma breakpoint family, member 14	2.06E -04	1.72
TC0200013765.hg.1	<i>UXS1</i>	UDP-glucuronate decarboxylase 1	9.23E -04	1.72
TC1700012307.hg.1	<i>TSEN54</i>	TSEN54 tRNA splicing endonuclease subunit	3.02E -04	1.72
TC0300011550.hg.1	<i>PDZRN3</i>	PDZ domain containing ring finger 3	4.64E -03	1.72
TC0500012294.hg.1	<i>PCDH1</i>	protocadherin 1	8.99E -04	1.72
TC1700011910.hg.1	<i>CYTH1</i>	cytohesin 1	1.35E -03	1.72
TC1900006602.hg.1	<i>ZNF555</i>	zinc finger protein 555	9.45E -04	1.72
23071900	NA	NA	3.56E -04	1.72
TC0200011720.hg.1	<i>ODC1</i>	ornithine decarboxylase 1	4.88E -03	1.72
TC1600011315.hg.1	<i>FAM234A</i>	family with sequence similarity 234, member A	8.91E -04	1.72
TC0700006512.hg.1	<i>INTS1</i>	Memczak2013 ANTISENSE, CDS, coding, INTERNAL best transcript NM_001080453	2.77E -03	1.72
TC1700007189.hg.1	<i>ALDH3A2</i>	aldehyde dehydrogenase 3 family, member A2	2.17E -03	1.72

APPENDIX

TC0100016122.hg.1	<i>IGSF8</i>	immunoglobulin superfamily, member 8	1.22E -03	1.72
TC0X00006816.hg.1	<i>PDK3</i>	pyruvate dehydrogenase kinase, isozyme 3	1.66E -03	1.72
TC1500008983.hg.1	<i>SLC12A6</i>	solute carrier family 12 (potassium/chloride transporter), member 6	7.36E -03	1.72
TC1600009989.hg.1	<i>CCDC189</i>	coiled-coil domain containing 189	3.15E -03	1.72
TC1100008010.hg.1	<i>CDC42EP2</i>	CDC42 effector protein (Rho GTPase binding) 2	9.86E -04	1.72
TC1900009584.hg.1	<i>ZNF560</i>	zinc finger protein 560	6.08E -03	1.72
TC1000010982.hg.1	<i>ASCC1</i>	Transcript Identified by AceView, Entrez Gene ID(s) 51008	3.45E -03	1.72
TC1600010685.hg.1	<i>SMPD3</i>	sphingomyelin phosphodiesterase 3, neutral membrane (neutral sphingomyelinase II)	4.72E -03	1.72
TC1200011573.hg.1	<i>NR2C1</i>	nuclear receptor subfamily 2, group C, member 1	8.76E -03	1.72
TC1000007132.hg.1	<i>BAMBI</i>	BMP and activin membrane-bound inhibitor	2.02E -03	1.72
TC0100006954.hg.1	<i>KAZN</i>	kazrin, periplakin interacting protein	9.43E -03	1.71
23075955	<i>NA</i>	NA	3.86E -03	1.71
TC1400009829.hg.1	<i>CEP128</i>	centrosomal protein 128kDa	7.84E -03	1.71
TC0300013853.hg.1	<i>ST3GAL6</i>	ST3 beta-galactoside alpha-2,3-sialyltransferase 6	3.59E -03	1.71
TC0200006738.hg.1	<i>LPIN1</i>	Transcript Identified by AceView, Entrez Gene ID(s) 23175	5.26E -03	1.71
TC0300009131.hg.1	<i>HPS3</i>	Hermansky-Pudlak syndrome 3	2.02E -03	1.71
TC1900011867.hg.1	<i>TMEM205</i>	transmembrane protein 205	7.15E -04	1.71

TC0900009489.hg.1	<i>GLDC</i>	glycine dehydrogenase (decarboxylating)	5.19E -03	1.71
TC0200007419.hg.1	<i>CAMKMT</i>	calmodulin-lysine N-methyltransferase	3.81E -03	1.71
TC1100008899.hg.1	<i>CEP126</i>	centrosomal protein 126kDa	3.03E -03	1.71
TC0600008255.hg.1	<i>EFHC1</i>	EF-hand domain (C-terminal) containing 1	2.73E -03	1.71
TC1900010067.hg.1	<i>PBX4</i>	pre-B-cell leukemia homeobox 4	5.71E -04	1.71
TC0700009020.hg.1	<i>SND1</i>	staphylococcal nuclease and tudor domain containing 1	7.46E -04	1.71
TC2200007109.hg.1	<i>DEPDC5</i>	DEP domain containing 5	4.24E -04	1.71
TC0800012176.hg.1	<i>PLEC</i>	plectin	2.76E -03	1.71
TC0500012826.hg.1	<i>SH3PXD2B</i>	SH3 and PX domains 2B	1.84E -03	1.71
TC0500008054.hg.1	<i>POLR3G</i>	polymerase (RNA) III (DNA directed) polypeptide G (32kD)	7.86E -03	1.71
TC1700009417.hg.1	<i>SMG6</i>	SMG6 nonsense mediated mRNA decay factor	1.29E -03	1.71
TC1700008769.hg.1	<i>KCNJ2</i>	potassium channel, inwardly rectifying subfamily J, member 2	1.34E -03	1.71
TC0700007398.hg.1	<i>ZMIZ2</i>	zinc finger, MIZ-type containing 2	1.18E -03	1.71
TC1100012966.hg.1	<i>MICAL2</i>	microtubule associated monooxygenase, calponin and LIM domain containing 2	1.35E -03	1.71
TC1600006760.hg.1	<i>UBN1</i>	ubinuclein 1	5.22E -03	1.71
TC0100018233.hg.1	<i>FPGT</i>	fucose-1-phosphate guanylyltransferase	3.01E -03	1.70
TC0500011408.hg.1	<i>TMEM161B</i>	transmembrane protein 161B	1.34E -03	1.70
TC1500007034.hg.1	<i>SNAP23</i>	synaptosome associated protein 23kDa	5.23E -03	1.70

APPENDIX

TC0100009324.hg.1	<i>FAM102B</i>	family with sequence similarity 102, member B	9.34E -03	1.70
TC1400010630.hg.1	<i>TTLL5</i>	tubulin tyrosine ligase-like family member 5	5.04E -03	1.70
TC1700009333.hg.1	<i>NXN</i>	nucleoredoxin	1.05E -03	1.70
TC0100017617.hg.1	<i>HIST3H2A</i>	histone cluster 3, H2a	7.49E -04	1.70
HTA2-neg-47419773_st	NA	NA	2.37E -03	1.70
TSUnmapped00000732.hg.1	<i>SLC37A4</i>	solute carrier family 37 (glucose-6-phosphate transporter), member 4 [Source:HGNC Symbol;Acc:HGNC:4061]	8.24E -03	1.70
TC0200015876.hg.1	<i>SERPINE2</i>	serpin peptidase inhibitor, clade E (nexin, plasminogen activator inhibitor type 1), member 2	4.49E -04	1.70
HTA2-neg-47420711_st	NA	NA	9.17E -03	1.70
TC0400012381.hg.1	<i>NEK1</i>	NIMA-related kinase 1	5.81E -03	1.70
TC0100013837.hg.1	<i>RIMS3</i>	regulating synaptic membrane exocytosis 3	9.68E -04	1.70
TC0200010624.hg.1	<i>PIKFYVE</i>	phosphoinositide kinase, FYVE finger containing	4.39E -03	1.70
TC0100009969.hg.1	<i>RIIAD1</i>	regulatory subunit of type II PKA R-subunit (RIIa) domain containing 1	1.45E -03	1.70
TC0700011066.hg.1	<i>COBL</i>	cordon-bleu WH2 repeat protein	4.42E -04	1.70
TC0100010798.hg.1	<i>QSOX1</i>	quiescin Q6 sulfhydryl oxidase 1	1.70E -03	1.70
TC1200006670.hg.1	<i>CLSTN3</i>	calsyntenin 3	2.48E -03	1.70
TC1700011815.hg.1	<i>MXRA7</i>	matrix-remodelling associated 7	9.72E -03	1.70

TC0900008887.hg.1	<i>TBC1D13</i>	TBC1 domain family, member 13	2.09E -03	1.70
TC0900006937.hg.1	<i>ACO1</i>	aconitase 1, soluble	6.80E -04	1.70
TC1900006859.hg.1	<i>EVI5L</i>	ecotropic viral integration site 5-like	2.77E -04	1.69
TC0200016587.hg.1	<i>PLCL1</i>	phospholipase C-like 1	3.19E -03	1.69
TC0700008367.hg.1	<i>PEG10</i>	paternally expressed 10	8.46E -03	1.69
TC0300008948.hg.1	<i>ESYT3</i>	extended synaptotagmin-like protein 3	4.56E -04	1.69
TC0900011461.hg.1	<i>STRBP</i>	spermatid perinuclear RNA binding protein	1.06E -03	1.69
TC1900011172.hg.1	<i>VRK3</i>	vaccinia related kinase 3	8.07E -04	1.69
TC0400009856.hg.1	<i>LYAR</i>	Ly1 antibody reactive	5.00E -03	1.69
TC1500010886.hg.1	<i>CALML4</i>	calmodulin-like 4	1.79E -03	1.69
TC0900008684.hg.1	<i>GPR21</i>	G protein-coupled receptor 21	8.89E -04	1.69
TC1200012622.hg.1	<i>SLC48A1</i>	solute carrier family 48 (heme transporter), member 1	2.67E -04	1.69
TSUnmapped00000530.hg.1	<i>ATG16L1</i>	autophagy related 16-like 1	6.13E -03	1.69
TC2200009324.hg.1	<i>DRICH1</i>	aspartate-rich 1	2.40E -03	1.69
TC1700009274.hg.1	<i>FN3KRP</i>	fructosamine 3 kinase related protein	3.26E -03	1.69
TC1200011968.hg.1	<i>HECTD4</i>	HECT domain containing E3 ubiquitin protein ligase 4	4.21E -03	1.69
TC0400009132.hg.1	<i>ETFDH</i>	electron-transferring-flavoprotein dehydrogenase	6.71E -04	1.68
TC0200007028.hg.1	<i>GAREM2</i>	GRB2 associated regulator of MAPK1 2	2.30E -03	1.68

APPENDIX

TC2000008130.hg.1	<i>TBC1D20</i>	TBC1 domain family, member 20	5.97E -03	1.68
TC2100006980.hg.1	<i>ITSN1</i>	Transcript Identified by AceView, Entrez Gene ID(s) 6453	1.36E -03	1.68
TC0800008197.hg.1	<i>OTUD6B</i>	OTU domain containing 6B	1.46E -03	1.68
TC0100011245.hg.1	<i>ADORA1</i>	adenosine A1 receptor	4.27E -04	1.68
TC0300011939.hg.1	<i>IFT57</i>	intraflagellar transport 57	3.35E -03	1.68
TC1100009245.hg.1	<i>CBL</i>	Cbl proto-oncogene, E3 ubiquitin protein ligase	3.52E -03	1.68
TC2000009780.hg.1	<i>TCFL5</i>	transcription factor-like 5 (basic helix-loop-helix)	5.09E -03	1.68
TC0600007616.hg.1	<i>HSPA1B</i>	heat shock 70kDa protein 1B	5.60E -04	1.68
TC1100010661.hg.1	<i>CHST1</i>	carbohydrate (keratan sulfate Gal- 6) sulfotransferase 1	1.38E -03	1.68
TC0100011552.hg.1	<i>VASH2</i>	vasohibin 2	2.21E -03	1.68
TC0600008670.hg.1	<i>PRSS35</i>	protease, serine 35	2.23E -04	1.68
TC0600008569.hg.1	<i>MYO6</i>	myosin VI	6.41E -03	1.68
TC0100012846.hg.1	<i>DFFA</i>	DNA fragmentation factor, 45kDa, alpha polypeptide	1.50E -03	1.68
TC1200010865.hg.1	<i>ITGA7</i>	integrin alpha 7	6.24E -03	1.68
TC0400011518.hg.1	<i>INTS12</i>	integrator complex subunit 12	2.46E -03	1.68
TC0600013228.hg.1	<i>SLC2A12</i>	solute carrier family 2 (facilitated glucose transporter), member 12	6.97E -03	1.68
TC0100016631.hg.1	<i>RGS16</i>	regulator of G-protein signaling 16	9.97E -04	1.68
TC0200016746.hg.1	<i>TTC21B</i>	tetratricopeptide repeat domain 21B	4.60E -03	1.68

TC0300014050.hg.1	<i>NPHP3</i>	nephronophthisis 3 (adolescent)	7.19E -03	1.68
TC2000007132.hg.1	<i>DNMT3B</i>	DNA (cytosine-5-)-methyltransferase 3 beta	4.19E -03	1.68
TC0200009091.hg.1	<i>RALB</i>	v-ral simian leukemia viral oncogene homolog B	6.37E -03	1.68
TC0100009333.hg.1	<i>GPSM2</i>	G-protein signaling modulator 2	4.08E -03	1.68
TC1000010993.hg.1	<i>MICU1</i>	mitochondrial calcium uptake 1	1.59E -03	1.68
TC0100007240.hg.1	<i>NBPF3</i>	neuroblastoma breakpoint family, member 3	2.05E -03	1.68
TC0500009580.hg.1	<i>SIMC1</i>	SUMO-interacting motifs containing 1	2.09E -03	1.67
TC1900007447.hg.1	<i>ZNF101</i>	zinc finger protein 101	6.00E -03	1.67
TC0200010511.hg.1	<i>NBEAL1</i>	neurobeachin like 1	2.69E -03	1.67
TC1600011409.hg.1	<i>PDP2</i>	pyruvate dehydrogenase phosphatase catalytic subunit 2	5.98E -04	1.67
TC1700011956.hg.1	<i>TBC1D16</i>	TBC1 domain family, member 16	2.73E -04	1.67
TC0400011203.hg.1	<i>HPSE</i>	heparanase	7.91E -04	1.67
TC0300010223.hg.1	<i>PRRT3</i>	proline-rich transmembrane protein 3	3.54E -04	1.67
TC0300007445.hg.1	<i>GRM2</i>	glutamate receptor, metabotropic 2	1.22E -03	1.67
TC1700008014.hg.1	<i>ADAM11</i>	ADAM metallopeptidase domain 11	1.30E -03	1.67
TC1100010410.hg.1	<i>BDNF</i>	brain-derived neurotrophic factor	5.88E -03	1.67
TC0X00009215.hg.1	<i>EIF1AX</i>	eukaryotic translation initiation factor 1A, X-linked	6.46E -03	1.67
TC1500008772.hg.1	<i>GABRB3</i>	gamma-aminobutyric acid (GABA) A receptor, beta 3	6.86E -03	1.67

APPENDIX

TC0900011013.hg.1	<i>ERP44</i>	endoplasmic reticulum protein 44	4.17E -03	1.67
TC1400006521.hg.1	<i>PNP</i>	purine nucleoside phosphorylase	7.39E -04	1.67
TC1500010915.hg.1	<i>GOLGA6L5P</i>	golgin A6 family-like 5, pseudogene	6.02E -03	1.67
TC0900010580.hg.1	<i>GKAP1</i>	G kinase anchoring protein 1	2.59E -03	1.67
TC1100012811.hg.1	<i>NFRKB</i>	nuclear factor related to kappaB binding protein	5.44E -04	1.67
TC0200012809.hg.1	<i>PELI1</i>	pellino E3 ubiquitin protein ligase 1	2.81E -03	1.67
TC0100010735.hg.1	<i>RASAL2</i>	RAS protein activator like 2	1.13E -03	1.67
TC2000009890.hg.1	<i>ANKEF1</i>	ankyrin repeat and EF-hand domain containing 1	6.25E -03	1.67
TC1700012184.hg.1	<i>CHRNB1</i>	cholinergic receptor, nicotinic beta 1	7.66E -03	1.67
23074909	<i>NA</i>	NA	5.03E -03	1.67
TC2000008023.hg.1	<i>SLCO4A1</i>	solute carrier organic anion transporter family, member 4A1	4.87E -03	1.67
TC0100012002.hg.1	<i>KIAA1804</i>	mixed lineage kinase 4	9.75E -04	1.67
TC1500007004.hg.1	<i>RTF1</i>	RTF1 homolog, Paf1/RNA polymerase II complex component	6.93E -03	1.67
TC1700009256.hg.1	<i>NARF</i>	nuclear prelamin A recognition factor	1.46E -03	1.67
TC0100014457.hg.1	<i>JAK1</i>	Janus kinase 1	9.52E -04	1.67
TC0600007375.hg.1	<i>HIST1H3H</i>	histone cluster 1, H3h	9.84E -03	1.67
TC0300011183.hg.1	<i>NEK4</i>	NIMA-related kinase 4	6.57E -04	1.67
TC1700008539.hg.1	<i>MRC2</i>	mannose receptor, C type 2	7.04E -04	1.67

HTA2-pos-PSR03025032.hg.1	NA	NA	3.42E -03	1.67
TC1600011168.hg.1	<i>ZCCHC14</i>	zinc finger, CCHC domain containing 14	2.81E -03	1.66
TC0900011120.hg.1	<i>KLF4</i>	Kruppel-like factor 4 (gut)	1.20E -03	1.66
TC0100018478.hg.1	<i>NBPF10</i>	neuroblastoma breakpoint family, member 10	7.75E -04	1.66
TC160006941.hg.1	<i>SNX29</i>	sorting nexin 29	2.58E -03	1.66
TC010007691.hg.1	<i>KIAA1522</i>	KIAA1522	5.39E -04	1.66
TC1500008521.hg.1	<i>MEF2A</i>	myocyte enhancer factor 2A	6.81E -04	1.66
TC0X00010351.hg.1	<i>TAF7L</i>	TATA box binding protein associated factor 7 like	5.21E -03	1.66
TC2200007910.hg.1	<i>MICAL3</i>	Transcript Identified by AceView, Entrez Gene ID(s) 57553	1.76E -03	1.66
TC0800007738.hg.1	<i>SDCBP</i>	syndecan binding protein	1.03E -03	1.66
TC1200008726.hg.1	<i>TCP11L2</i>	t-complex 11, testis-specific-like 2	1.50E -03	1.66
TC1100009618.hg.1	<i>GLB1L2</i>	galactosidase beta 1 like 2	6.26E -03	1.66
TC0300010557.hg.1	<i>NEK10</i>	NIMA-related kinase 10	9.57E -03	1.66
TC0600010066.hg.1	<i>IGF2R</i>	insulin-like growth factor 2 receptor	7.12E -04	1.66
TC0600011635.hg.1	<i>FKBP5</i>	FK506 binding protein 5	1.00E -02	1.66
TC1600008189.hg.1	<i>PLA2G15</i>	phospholipase A2, group XV	4.27E -03	1.66
TC0900008463.hg.1	<i>HSDL2</i>	hydroxysteroid dehydrogenase like 2	3.49E -03	1.66
TC1300006774.hg.1	<i>MEDAG</i>	mesenteric estrogen-dependent adipogenesis	9.53E -04	1.66

APPENDIX

TC0300006618.hg.1	SYN2	synapsin II	2.27E -03	1.66
TC0700013604.hg.1	UPK3BL	uroplakin 3B-like	8.38E -04	1.66
TC0200008223.hg.1	DNAH6	dynein, axonemal, heavy chain 6	6.51E -03	1.65
TC0300007406.hg.1	SEMA3F	sema domain, immunoglobulin domain (Ig), short basic domain, secreted, (semaphorin) 3F	3.63E -03	1.65
TC1900009808.hg.1	ADGRL1	adhesion G protein-coupled receptor L1	2.83E -03	1.65
TC1500010712.hg.1	GOLGA8N	golgin A8 family, member N	3.21E -03	1.65
TC1600011047.hg.1	HSDL1	hydroxysteroid dehydrogenase like 1	1.14E -03	1.65
TC1200011846.hg.1	CORO1C	coronin, actin binding protein, 1C	6.26E -03	1.65
TC0100017073.hg.1	SLC45A3	solute carrier family 45, member 3	8.67E -04	1.65
HTA2-neg-47422238_st	NA	NA	7.05E -03	1.65
TC1600010864.hg.1	WDR59	WD repeat domain 59	1.66E -03	1.65
TC0100018367.hg.1	CHRM3	cholinergic receptor, muscarinic 3	7.33E -03	1.65
TC1500007851.hg.1	ARID3B	AT rich interactive domain 3B (BRIGHT-like)	2.75E -03	1.65
TC1900007328.hg.1	SLC27A1	solute carrier family 27 (fatty acid transporter), member 1	3.01E -03	1.65
TC1200011574.hg.1	FGD6	FYVE, RhoGEF and PH domain containing 6	2.53E -03	1.65
TC0200014728.hg.1	LY75-CD302	LY75-CD302 readthrough	3.69E -03	1.65
TC0100011219.hg.1	PPP1R12B	protein phosphatase 1, regulatory subunit 12B	5.16E -04	1.65
TC0100009048.hg.1	RPL5	Memczak2013 ALT_ACCEPTOR, ALT_DONOR, coding, INTERNAL,	4.11E -03	1.65

		intronic best transcript NM_000969		
TC1200011321.hg.1	<i>OSBPL8</i>	oxysterol binding protein-like 8	8.33E -04	1.65
TC1500006643.hg.1	<i>GABRA5</i>	gamma-aminobutyric acid (GABA) A receptor, alpha 5	6.32E -03	1.65
23071983	<i>NA</i>	NA	4.10E -03	1.64
TC1500010236.hg.1	<i>GOLGA6L10</i>	golgin A6 family-like 10	2.94E -03	1.64
TC0100013000.hg.1	<i>CASP9</i>	caspase 9	6.82E -03	1.64
TC0500009268.hg.1	<i>TTC1</i>	tetratricopeptide repeat domain 1	5.83E -03	1.64
TC1600007955.hg.1	<i>MT3</i>	metallothionein 3	4.21E -03	1.64
HTA2-pos- PSR02023963.hg.1	<i>NA</i>	NA	9.49E -04	1.64
TC0600006659.hg.1	<i>BPHL</i>	biphenyl hydrolase-like (serine hydrolase)	1.98E -03	1.64
TC0300006994.hg.1	<i>FBXL2</i>	F-box and leucine-rich repeat protein 2	3.32E -03	1.64
TC2100006951.hg.1	<i>OL/G1</i>	oligodendrocyte transcription factor 1	9.05E -04	1.64
TC0800009921.hg.1	<i>KCTD9</i>	potassium channel tetramerization domain containing 9	1.05E -03	1.64
TC1700008452.hg.1	<i>GDPD1</i>	glycerophosphodiester phosphodiesterase domain containing 1	2.04E -03	1.64
TC0600012536.hg.1	<i>SRSF12</i>	serine/arginine-rich splicing factor 12	8.31E -03	1.64
TC1700008033.hg.1	<i>HEXIM1</i>	hexamethylene bis-acetamide inducible 1	2.61E -03	1.64
TC0500006479.hg.1	<i>NKD2</i>	naked cuticle homolog 2 (<i>Drosophila</i>)	3.43E -03	1.64
TC2200006630.hg.1	<i>TANGO2</i>	transport and golgi organization 2 homolog	4.92E -04	1.64

APPENDIX

TC1400008462.hg.1	<i>C14orf79</i>	chromosome 14 open reading frame 79	8.11E -03	1.64
TC1700008467.hg.1	<i>VMP1</i>	vacuole membrane protein 1	8.69E -04	1.63
TC1600007317.hg.1	<i>KIAA0556</i>	KIAA0556	9.19E -04	1.63
TC0100016917.hg.1	<i>CSRP1</i>	cysteine and glycine-rich protein 1	5.96E -03	1.63
TC0500009609.hg.1	<i>FGFR4</i>	fibroblast growth factor receptor 4	1.31E -03	1.63
TC0X00010670.hg.1	<i>TMEM255A</i>	transmembrane protein 255A	8.51E -03	1.63
TC1700008455.hg.1	<i>YPEL2</i>	yippee like 2	8.42E -04	1.63
TC0700013602.hg.1	<i>POLR2J3</i>	polymerase (RNA) II (DNA directed) polypeptide J3	7.20E -04	1.63
TC1700006638.hg.1	<i>ARRB2</i>	arrestin, beta 2	9.51E -03	1.63
TC0500011150.hg.1	<i>GFM2</i>	G elongation factor, mitochondrial 2	7.22E -03	1.63
TC1400009697.hg.1	<i>NPC2</i>	Niemann-Pick disease, type C2	6.12E -03	1.63
TC2000006464.hg.1	<i>FAM110A</i>	family with sequence similarity 110, member A	6.09E -04	1.63
TC1500010723.hg.1	<i>CHAC1</i>	ChaC glutathione-specific gamma-glutamylcyclotransferase 1	7.58E -03	1.63
TC0100012490.hg.1	<i>C1orf233</i>	chromosome 1 open reading frame 233	5.95E -04	1.63
TC0200007590.hg.1	<i>CHAC2</i>	ChaC, cation transport regulator homolog 2 (E. coli)	2.78E -03	1.63
TC0900012179.hg.1	<i>SPTAN1</i>	spectrin, alpha, non-erythrocytic 1	1.76E -03	1.63
TC1900007100.hg.1	<i>MAST1</i>	microtubule associated serine/threonine kinase 1	9.42E -03	1.63
TC0300010744.hg.1	<i>ACAA1</i>	acetyl-CoA acyltransferase 1	6.68E -03	1.63

TC1000009880.hg.1	<i>NMT2</i>	N-myristoyltransferase 2	3.33E -04	1.63
TC0200010837.hg.1	<i>ANKZF1</i>	ankyrin repeat and zinc finger domain containing 1	9.71E -03	1.63
TC1700011919.hg.1	<i>CEP295NL</i>	CEP295 N-terminal like	5.41E -03	1.63
HTA2-neg-47424241_st	<i>NA</i>	NA	7.96E -03	1.63
TC0400011180.hg.1	<i>SCD5</i>	stearoyl-CoA desaturase 5	2.65E -03	1.63
TC0500007792.hg.1	<i>HEXB</i>	hexosaminidase B (beta polypeptide)	4.11E -03	1.63
TC1000009894.hg.1	<i>FAM188A</i>	family with sequence similarity 188, member A	5.43E -03	1.63
TC1900011724.hg.1	<i>ZNF540</i>	zinc finger protein 540	2.10E -03	1.63
TC1900007049.hg.1	<i>ZNF440</i>	zinc finger protein 440	5.44E -03	1.63
TC0900007547.hg.1	<i>C9orf85</i>	chromosome 9 open reading frame 85	8.91E -03	1.62
TC0100012889.hg.1	<i>MAD2L2</i>	MAD2 mitotic arrest deficient-like 2 (yeast)	3.33E -03	1.62
TC0400008041.hg.1	<i>PTPN13</i>	protein tyrosine phosphatase, non-receptor type 13 (APO-1/CD95 (Fas)-associated phosphatase)	7.63E -03	1.62
TC0800006447.hg.1	<i>FBXO25</i>	F-box protein 25	1.25E -03	1.62
TC1600010778.hg.1	<i>HYDIN</i>	HYDIN, axonemal central pair apparatus protein	5.80E -04	1.62
TC0800009726.hg.1	<i>MTMR7</i>	myotubularin related protein 7	7.41E -04	1.62
TC2000007435.hg.1	<i>IFT52</i>	intraflagellar transport 52	1.04E -03	1.62
TC0100008897.hg.1	<i>WDR63</i>	WD repeat domain 63	3.78E -03	1.62
TC0500008342.hg.1	<i>DCP2</i>	decapping mRNA 2	7.88E -04	1.62

APPENDIX

TC0700013219.hg.1	<i>LMBR1</i>	limb development membrane protein 1	1.20E -03	1.62
TC1800007385.hg.1	<i>WDR7</i>	WD repeat domain 7	7.90E -04	1.62
TC0700013337.hg.1	<i>UMAD1</i>	UBAP1-MVB12-associated (UMA) domain containing 1	4.62E -03	1.62
TC0900011613.hg.1	<i>FAM102A</i>	family with sequence similarity 102, member A	8.47E -03	1.62
TC1200012859.hg.1	<i>RHOF</i>	ras homolog family member F (in filopodia)	4.18E -03	1.62
TC1100012269.hg.1	<i>ARHGAP20</i>	Rho GTPase activating protein 20	3.53E -03	1.62
TC1000010699.hg.1	<i>IPMK</i>	inositol polyphosphate multikinase	4.48E -03	1.62
TC1600011494.hg.1	<i>ARL6IP1</i>	ADP-ribosylation factor like GTPase 6 interacting protein 1	1.49E -03	1.62
TC2000008530.hg.1	<i>DZANK1</i>	double zinc ribbon and ankyrin repeat domains 1	8.79E -04	1.62
TC1600010633.hg.1	<i>ATP6V0D1</i>	ATPase, H ⁺ transporting, lysosomal 38kDa, V0 subunit d1	2.30E -03	1.62
TC1500006645.hg.1	<i>GABRG3</i>	gamma-aminobutyric acid (GABA) A receptor, gamma 3	3.50E -03	1.62
TC0100017079.hg.1	<i>SLC41A1</i>	solute carrier family 41 (magnesium transporter), member 1	7.48E -03	1.62
23071942	<i>NA</i>	NA	5.21E -03	1.62
TC1800006905.hg.1	<i>CABYR</i>	calcium binding tyrosine-(Y)- phosphorylation regulated	3.95E -03	1.62
TC0900008482.hg.1	<i>SLC31A2</i>	solute carrier family 31 (copper transporter), member 2	2.32E -03	1.62
TC1200007510.hg.1	<i>CCDC184</i>	coiled-coil domain containing 184	6.10E -04	1.62
TC1100012509.hg.1	<i>SLC37A4</i>	solute carrier family 37 (glucose-6-phosphate transporter), member 4	5.34E -03	1.61
TC0900012294.hg.1	<i>TPRN</i>	taperin	3.54E -03	1.61

TC1300006503.hg.1	<i>IFT88</i>	intraflagellar transport 88	2.46E -03	1.61
TC2000009447.hg.1	<i>DPM1</i>	dolichyl-phosphate mannosyltransferase polypeptide 1, catalytic subunit	6.33E -04	1.61
TC0900011404.hg.1	<i>STOM</i>	stomatin	7.25E -04	1.61
TC0500012948.hg.1	<i>SNCB</i>	synuclein beta	1.07E -03	1.61
TC1900011766.hg.1	<i>MARK4</i>	MAP/microtubule affinity-regulating kinase 4	1.04E -03	1.61
TC0100006650.hg.1	<i>AJAP1</i>	adherens junctions associated protein 1	9.10E -03	1.61
TC1000011487.hg.1	<i>SORBS1</i>	sorbin and SH3 domain containing 1	3.43E -03	1.61
TC1100009068.hg.1	<i>NCAM1</i>	neural cell adhesion molecule 1	1.03E -03	1.61
TC1700010684.hg.1	<i>HAP1</i>	huntingtin-associated protein 1	6.54E -03	1.61
TC1500008511.hg.1	<i>LRRC28</i>	leucine rich repeat containing 28	4.56E -03	1.61
TC2100008560.hg.1	<i>DONSON</i>	downstream neighbor of SON	7.50E -04	1.61
TC1500007659.hg.1	<i>PIAS1</i>	protein inhibitor of activated STAT 1	1.75E -03	1.61
TC0700013429.hg.1	<i>PILRA</i>	paired immunoglobulin-like type 2 receptor alpha	3.20E -03	1.61
TC2100008534.hg.1	<i>PCBP3</i>	poly(rC) binding protein 3	2.77E -03	1.61
TC0100011316.hg.1	<i>NFASC</i>	neurofascin	6.58E -04	1.61
TC1100013065.hg.1	<i>KRTAP5-9</i>	keratin associated protein 5-9	5.53E -03	1.61
TC0100016113.hg.1	<i>IGSF9</i>	immunoglobulin superfamily, member 9	3.25E -03	1.61
TC0700010162.hg.1	<i>FBXL18</i>	F-box and leucine-rich repeat protein 18	5.49E -04	1.61

APPENDIX

TC0100013049.hg.1	<i>NBPF1</i>	neuroblastoma breakpoint family, member 1	1.67E -03	1.61
TC0300013855.hg.1	<i>NFKBIZ</i>	nuclear factor of kappa light polypeptide gene enhancer in B-cells inhibitor, zeta	8.32E -03	1.60
TC2200006552.hg.1	<i>TMEM191B</i>	transmembrane protein 191B	9.81E -03	1.60
TC1900007342.hg.1	<i>FCHO1</i>	FCH domain only 1	2.52E -03	1.60
TC0100006857.hg.1	<i>PTCHD2</i>	patched domain containing 2	8.02E -03	1.60
TC1400010171.hg.1	<i>CCDC85C</i>	coiled-coil domain containing 85C	1.17E -03	1.60
TC0900010390.hg.1	<i>ABHD17B</i>	abhydrolase domain containing 17B	8.45E -03	1.60
TC0700012296.hg.1	<i>C7orf60</i>	chromosome 7 open reading frame 60	3.47E -03	1.60
TC1500007005.hg.1	<i>ITPKA</i>	inositol-trisphosphate 3-kinase A	7.25E -04	1.60
TC1500009951.hg.1	<i>GRAMD2</i>	GRAM domain containing 2	2.45E -03	1.60
TC0200007032.hg.1	<i>HADHB</i>	hydroxyacyl-CoA dehydrogenase/3-ketoacyl-CoA thiolase/enoyl-CoA hydratase (trifunctional protein), beta subunit	1.07E -03	1.60
TC0400008834.hg.1	<i>SCOC</i>	short coiled-coil protein	6.52E -03	1.60
TC0X00008795.hg.1	<i>ABCD1</i>	ATP binding cassette subfamily D member 1	2.61E -03	1.60
TC0100013889.hg.1	<i>ZMYND12</i>	zinc finger, MYND-type containing 12	9.57E -03	1.60
TC0800007119.hg.1	<i>ESCO2</i>	establishment of sister chromatid cohesion N-acetyltransferase 2	2.73E -03	1.60
TC0200016166.hg.1	<i>IQCA1</i>	IQ motif containing with AAA domain 1	5.32E -03	1.60
HTA2-neg-47420640_st	<i>NA</i>	NA	3.51E -03	1.60

TC1900007087.hg.1	<i>WDR83</i>	WD repeat domain 83	1.03E -03	1.60
TC1700012482.hg.1	<i>SIRT7</i>	sirtuin 7	4.05E -03	1.60
HTA2-neg-47419576_st	NA	NA	5.10E -03	1.60
TC1600008454.hg.1	<i>GABARAPL2</i>	GABA(A) receptor-associated protein like 2	5.16E -04	1.59
TC0100013995.hg.1	<i>EIF2B3</i>	eukaryotic translation initiation factor 2B, subunit 3 gamma, 58kDa	8.51E -03	1.59
TC1900006994.hg.1	<i>DNM2</i>	dynamin 2	1.65E -03	1.59
TC1100008082.hg.1	<i>NPAS4</i>	neuronal PAS domain protein 4	4.51E -03	1.59
TC1900007419.hg.1	<i>SLC25A42</i>	solute carrier family 25, member 42	9.59E -03	1.59
TC2000007572.hg.1	<i>NCOA3</i>	nuclear receptor coactivator 3	7.86E -03	1.59
HTA2-neg-47422675_st	NA	NA	8.52E -03	1.59
TC1200007864.hg.1	<i>NXPH4</i>	neurexophilin 4	9.20E -03	1.59
TC0100018286.hg.1	<i>NBPF19</i>	neuroblastoma breakpoint family, member 19	8.50E -04	1.59
TC1500006994.hg.1	<i>CHP1</i>	calcineurin-like EF-hand protein 1	5.81E -03	1.59
TC0600008663.hg.1	<i>DOPEY1</i>	dopey family member 1	3.90E -03	1.59
TC1500009781.hg.1	<i>UBAP1L</i>	ubiquitin associated protein 1 like	3.35E -03	1.59
TC1000006796.hg.1	<i>SEC61A2</i>	Sec61 translocon alpha 2 subunit	1.93E -03	1.59
TC1900008416.hg.1	<i>INAFM1</i>	InaF-motif containing 1	4.89E -03	1.59
TC0400010626.hg.1	<i>FRYL</i>	FRY like transcription coactivator	4.55E -03	1.59

APPENDIX

TC1800008952.hg.1	<i>DSEL</i>	dermatan sulfate epimerase-like	5.40E -03	1.59
TC0200008534.hg.1	<i>ANKRD36</i>	ankyrin repeat domain 36	3.05E -03	1.59
TC1900010701.hg.1	<i>C19orf47</i>	chromosome 19 open reading frame 47	5.99E -03	1.59
TC0700012086.hg.1	<i>POLR2J</i>	polymerase (RNA) II (DNA directed) polypeptide J, 13.3kDa	7.39E -04	1.59
HTA2-pos-PSR02018287.hg.1	NA	NA	2.53E -03	1.59
TC1000007698.hg.1	<i>CISD1</i>	CDGSH iron sulfur domain 1	6.84E -03	1.59
TC0100014175.hg.1	<i>EPS15</i>	epidermal growth factor receptor pathway substrate 15	3.40E -03	1.59
TC1100009241.hg.1	<i>HINFP</i>	histone H4 transcription factor	3.62E -03	1.59
TC1100013061.hg.1	<i>NADSYN1</i>	NAD synthetase 1	5.39E -03	1.59
TC0900008793.hg.1	<i>ZBTB34</i>	zinc finger and BTB domain containing 34	1.50E -03	1.59
TC0300010889.hg.1	<i>ZNF445</i>	zinc finger protein 445	8.74E -03	1.59
TC1700006735.hg.1	<i>SLC2A4</i>	solute carrier family 2 (facilitated glucose transporter), member 4	3.06E -03	1.59
TC0200016626.hg.1	<i>MBOAT2</i>	membrane bound O-acyltransferase domain containing 2	2.10E -03	1.58
TC1900011029.hg.1	<i>MEIS3</i>	Meis homeobox 3	3.37E -03	1.58
TC1500007546.hg.1	<i>SNX22</i>	sorting nexin 22	9.23E -04	1.58
TC0800008032.hg.1	<i>ZC2HC1A</i>	zinc finger, C2HC-type containing 1A	5.56E -03	1.58
TC1100009858.hg.1	<i>CHRNA10</i>	cholinergic receptor, nicotinic alpha 10	2.88E -03	1.58
23075426	NA	NA	6.35E -03	1.58

TC1800006650.hg.1	<i>RAB31</i>	RAB31, member RAS oncogene family	4.46E -03	1.58
TC0100018224.hg.1	<i>FAM183A</i>	family with sequence similarity 183, member A	9.35E -03	1.58
TC0100017693.hg.1	<i>PGBD5</i>	piggyBac transposable element derived 5	9.35E -04	1.58
TC2200008831.hg.1	<i>PMM1</i>	phosphomannomutase 1	4.65E -03	1.58
TC1200012707.hg.1	<i>ALDH2</i>	aldehyde dehydrogenase 2 family (mitochondrial)	2.35E -03	1.58
TC0200016039.hg.1	<i>PDE6D</i>	phosphodiesterase 6D, cGMP-specific, rod, delta	2.84E -03	1.58
TC1600010500.hg.1	<i>GOT2</i>	glutamic-oxaloacetic transaminase 2, mitochondrial	8.41E -03	1.58
TC0100007963.hg.1	<i>EXO5</i>	exonuclease 5	5.14E -03	1.58
TC0900011705.hg.1	<i>ASB6</i>	ankyrin repeat and SOCS box containing 6	2.60E -03	1.58
TSUnmapped00000027.hg.1	<i>MLXIP</i>	MLX interacting protein	6.93E -03	1.58
TC0X00007310.hg.1	<i>TSPYL2</i>	TSPY-like 2	1.26E -03	1.58
TC1000012050.hg.1	<i>FGFR2</i>	fibroblast growth factor receptor 2	2.99E -03	1.58
TC1000007564.hg.1	<i>MAPK8</i>	mitogen-activated protein kinase 8	1.27E -03	1.57
TC1900011806.hg.1	<i>ZNF582-AS1</i>	ZNF582 antisense RNA 1 (head to head)	2.65E -03	1.57
TC1500008514.hg.1	<i>LRRC28</i>	Transcript Identified by AceView, Entrez Gene ID(s) 123355	2.91E -03	1.57
TC0300011815.hg.1	<i>DCBLD2</i>	discoidin, CUB and LCCL domain containing 2	1.54E -03	1.57
TSUnmapped00000166.hg.1	<i>LRP6</i>	LDL receptor related protein 6	3.85E -03	1.57
TC1000012549.hg.1	<i>PARG</i>	poly (ADP-ribose) glycohydrolase	8.61E -03	1.57

APPENDIX

TC0200008569.hg.1	<i>INPP4A</i>	inositol polyphosphate-4-phosphatase type I A	1.70E -03	1.57
TC2000009886.hg.1	<i>PANK2</i>	pantothenate kinase 2	1.16E -03	1.57
TC1500010319.hg.1	<i>KLHL25</i>	kelch-like family member 25	3.54E -03	1.57
TC0600014101.hg.1	<i>MICA</i>	MHC class I polypeptide-related sequence A	9.39E -03	1.57
TC1400007566.hg.1	<i>SMOC1</i>	SPARC related modular calcium binding 1	8.41E -04	1.57
TC1000009873.hg.1	<i>DCLRE1C</i>	DNA cross-link repair 1C	2.74E -03	1.57
TC0600010331.hg.1	<i>FAM120B</i>	family with sequence similarity 120B	5.39E -03	1.57
TC0500013336.hg.1	<i>SSBP2</i>	single-stranded DNA binding protein 2	3.29E -03	1.57
TC1000012577.hg.1	<i>LIPA</i>	lipase A, lysosomal acid, cholesterol esterase	2.35E -03	1.57
HTA2-pos-PSR05025584.hg.1	<i>NA</i>	NA	5.09E -03	1.57
23071963	<i>NA</i>	NA	6.13E -03	1.57
TC1500010796.hg.1	<i>SYNM</i>	synemin, intermediate filament protein	9.47E -03	1.57
TC1900010050.hg.1	<i>SUGP1</i>	SURP and G-patch domain containing 1	6.20E -03	1.57
TC0800009619.hg.1	<i>CTSB</i>	cathepsin B	1.76E -03	1.57
TC0200015402.hg.1	<i>FAM126B</i>	family with sequence similarity 126, member B	5.61E -03	1.57
TC0600008957.hg.1	<i>BVES-AS1</i>	BVES antisense RNA 1	1.67E -03	1.57
TC0200012252.hg.1	<i>STRN</i>	striatin, calmodulin binding protein	3.55E -03	1.57
TC1900009304.hg.1	<i>PIP5K1C</i>	Zhang2013 ALT_ACCEPTOR, ALT_DONOR, coding, INTERNAL,	2.38E -03	1.57

		intronic best transcript NM_012398		
TC0200014192.hg.1	<i>SAP130</i>	Sin3A associated protein 130kDa	2.32E -03	1.57
TC0X00009256.hg.1	<i>KLHL15</i>	kelch-like family member 15	1.89E -03	1.57
TC0800007870.hg.1	<i>CSPP1</i>	centrosome and spindle pole associated protein 1	1.19E -03	1.57
TC0500012153.hg.1	<i>FAM13B</i>	family with sequence similarity 13, member B	9.65E -03	1.57
TC0100011698.hg.1	<i>DISP1</i>	dispatched homolog 1 (Drosophila)	2.37E -03	1.57
TC1100013040.hg.1	<i>TM7SF2</i>	transmembrane 7 superfamily member 2	1.43E -03	1.56
TC0100014627.hg.1	<i>ST6GALNAC3</i>	Memczak2013 ANTISENSE, coding, INTERNAL, intronic best transcript NM_152996	1.83E -03	1.56
TC0700013598.hg.1	<i>LRCH4</i>	leucine-rich repeats and calponin homology (CH) domain containing 4	1.21E -03	1.56
TC0100006865.hg.1	<i>AGTRAP</i>	angiotensin II receptor-associated protein	3.72E -03	1.56
TC0700008450.hg.1	<i>LMTK2</i>	lemur tyrosine kinase 2	4.39E -03	1.56
23071896	NA	NA	6.95E -03	1.56
TC0200011125.hg.1	<i>ATG16L1</i>	autophagy related 16-like 1	3.53E -03	1.56
TC1700010565.hg.1	<i>FBXL20</i>	F-box and leucine-rich repeat protein 20	1.29E -03	1.56
TC0600009980.hg.1	<i>ZDHHC14</i>	zinc finger, DHHC-type containing 14	5.54E -03	1.56
TC2000007666.hg.1	<i>RNF114</i>	ring finger protein 114	3.65E -03	1.56
TC1400008415.hg.1	<i>ZFYVE21</i>	zinc finger, FYVE domain containing 21	1.69E -03	1.56

APPENDIX

TC0400012992.hg.1	<i>MFAP3L</i>	microfibrillar associated protein 3 like	8.84E -03	1.56
TC2200008907.hg.1	<i>SCUBE1</i>	signal peptide, CUB domain, EGF-like 1	7.52E -03	1.56
TC0100018249.hg.1	<i>AMY2B</i>	amylase, alpha 2B (pancreatic)	7.38E -03	1.56
TC0100018242.hg.1	<i>HS2ST1</i>	heparan sulfate 2-O-sulfotransferase 1	4.42E -03	1.56
TC1700008984.hg.1	<i>SEC14L1</i>	SEC14-like lipid binding 1	1.17E -03	1.56
TC1600009958.hg.1	<i>NPIPBP4</i>	nuclear pore complex interacting protein family, member B4	2.57E -03	1.56
TC0100012465.hg.1	<i>CPSF3L</i>	cleavage and polyadenylation specific factor 3-like	2.67E -03	1.56
TC1100010274.hg.1	<i>SPTY2D1</i>	SPT2 chromatin protein domain containing 1	3.61E -03	1.56
TC0300009468.hg.1	<i>PRKCI</i>	protein kinase C, iota	1.34E -03	1.55
23075525	<i>NA</i>	NA	2.94E -03	1.55
TC1800007518.hg.1	<i>ZCCHC2</i>	zinc finger, CCHC domain containing 2	7.52E -03	1.55
TC0X00007012.hg.1	<i>ATP6AP2</i>	ATPase, H ⁺ transporting, lysosomal accessory protein 2	9.88E -03	1.55
TC0100014528.hg.1	<i>DIRAS3</i>	DIRAS family, GTP-binding RAS-like 3	7.72E -03	1.55
TC1700012183.hg.1	<i>FGF11</i>	fibroblast growth factor 11	8.03E -03	1.55
TC1500009200.hg.1	<i>TTBK2</i>	tau tubulin kinase 2	8.21E -03	1.55
TC1000009152.hg.1	<i>HTRA1</i>	HtrA serine peptidase 1	6.76E -03	1.55
TC0300008904.hg.1	<i>PPP2R3A</i>	protein phosphatase 2, regulatory subunit B, alpha	3.65E -03	1.55
TC1000011948.hg.1	<i>PDZD8</i>	PDZ domain containing 8	3.87E -03	1.55

HTA2-neg-47422968_st	NA	NA	6.81E -03	1.55
TC0X00007190.hg.1	PORCN	porcupine homolog (Drosophila)	2.68E -03	1.55
TC2000010008.hg.1	NFS1	NFS1 cysteine desulfurase	3.21E -03	1.55
HTA2-pos- PSR02018288.hg.1	NA	NA	2.01E -03	1.55
TC1100013206.hg.1	STARD10	StAR-related lipid transfer domain containing 10	5.15E -03	1.55
HTA2-pos- PSR02018286.hg.1	NA	NA	3.50E -03	1.55
TC1200006604.hg.1	CD9	CD9 molecule	8.02E -03	1.55
TC1600011445.hg.1	SPG7	spastic paraplegia 7 (pure and complicated autosomal recessive)	5.36E -03	1.55
TC1200008147.hg.1	CCT2	chaperonin containing TCP1, subunit 2 (beta)	2.53E -03	1.55
TC0300009282.hg.1	TIPARP	TCDD-inducible poly(ADP-ribose) polymerase	3.81E -03	1.55
TC1200010252.hg.1	TMTC1	transmembrane and tetratricopeptide repeat containing 1	2.18E -03	1.55
TC0800006866.hg.1	VPS37A	vacuolar protein sorting 37 homolog A (S. cerevisiae)	5.53E -03	1.55
TC1200007567.hg.1	KCNH3	potassium channel, voltage gated eag related subfamily H, member 3	3.81E -03	1.55
TC0800011881.hg.1	NDRG1	N-myc downstream regulated 1	2.49E -03	1.55
TC1700008846.hg.1	KIF19	kinesin family member 19	7.11E -03	1.55
TC0X00008521.hg.1	SLC9A6	solute carrier family 9, subfamily A (NHE6, cation proton antiporter 6), member 6	5.07E -03	1.54
TC0300013877.hg.1	EPHB1	EPH receptor B1	2.58E -03	1.54

APPENDIX

TC1600009533.hg.1	<i>MYH11</i>	myosin, heavy chain 11, smooth muscle	4.56E -03	1.54
TC1500010687.hg.1	<i>OR4M2</i>	olfactory receptor, family 4, subfamily M, member 2	5.81E -03	1.54
TC1500006726.hg.1	<i>ULK4P1</i>	ULK4 pseudogene 1	2.22E -03	1.54
TC1000006639.hg.1	<i>FBXO18</i>	F-box protein, helicase, 18	2.60E -03	1.54
TC1200012256.hg.1	<i>ABCB9</i>	ATP binding cassette subfamily B member 9	2.49E -03	1.54
TC1100007030.hg.1	<i>NAV2</i>	neuron navigator 2	3.81E -03	1.54
TC2100007039.hg.1	<i>DOPEY2</i>	dopey family member 2	8.93E -03	1.54
TC1500008309.hg.1	<i>ZNF774</i>	zinc finger protein 774	2.31E -03	1.54
TC1100011629.hg.1	<i>XRRA1</i>	X-ray radiation resistance associated 1	9.65E -03	1.54
23074628	<i>NA</i>	NA	3.39E -03	1.54
TC1000012162.hg.1	<i>UROS</i>	uroporphyrinogen III synthase	7.55E -03	1.54
TC0900008156.hg.1	<i>NCBP1</i>	nuclear cap binding protein subunit 1	9.88E -04	1.54
TC1100010077.hg.1	<i>SBF2</i>	SET binding factor 2	2.02E -03	1.54
TC2200008856.hg.1	<i>NAGA</i>	N-acetylgalactosaminidase, alpha-	7.83E -03	1.54
TC0900010607.hg.1	<i>AGTPBP1</i>	ATP/GTP binding protein 1	4.99E -03	1.54
TC1300007861.hg.1	<i>PCCA</i>	propionyl-CoA carboxylase alpha subunit	2.25E -03	1.54
23075826	<i>NA</i>	NA	1.86E -03	1.54
TC0200015082.hg.1	<i>FKBP7</i>	FK506 binding protein 7	9.95E -03	1.54

TC1200012663.hg.1	<i>RAB3IP</i>	RAB3A interacting protein	2.38E -03	1.54
TC0100009646.hg.1	<i>NBPF26</i>	neuroblastoma breakpoint family, member 26	1.79E -03	1.54
TC1700010828.hg.1	<i>FAM171A2</i>	family with sequence similarity 171, member A2	7.79E -03	1.54
TC1600011346.hg.1	<i>SEC14L5</i>	SEC14-like lipid binding 5	1.76E -03	1.54
TC0700013502.hg.1	<i>SNX8</i>	sorting nexin 8	2.53E -03	1.54
TC1900011007.hg.1	<i>AP2S1</i>	adaptor-related protein complex 2 sigma 1 subunit	4.90E -03	1.54
23076566	<i>NA</i>	NA	3.24E -03	1.54
TC0300009004.hg.1	<i>RASA2</i>	RAS p21 protein activator 2	2.83E -03	1.54
TC1900007988.hg.1	<i>SIPA1L3</i>	signal-induced proliferation- associated 1 like 3	3.36E -03	1.54
TC0200012068.hg.1	<i>SLC30A3</i>	solute carrier family 30 (zinc transporter), member 3	3.68E -03	1.53
TC0X00006697.hg.1	<i>SYAP1</i>	synapse associated protein 1	2.53E -03	1.53
TC2100007996.hg.1	<i>TMEM50B</i>	transmembrane protein 50B	3.61E -03	1.53
TC0900009076.hg.1	<i>STKLD1</i>	serine/threonine kinase-like domain containing 1	4.34E -03	1.53
TC0400012857.hg.1	<i>RAPGEF2</i>	Rap guanine nucleotide exchange factor 2	1.61E -03	1.53
TC0100006983.hg.1	<i>CTRC</i>	chymotrypsin C (caldecrin)	5.93E -03	1.53
TC0500012523.hg.1	<i>ATOX1</i>	antioxidant 1 copper chaperone	1.82E -03	1.53
TC1500010906.hg.1	<i>RP11- 351M8.2</i>	---	4.34E -03	1.53
TC0400010242.hg.1	<i>PPARGC1A</i>	peroxisome proliferator-activated receptor gamma, coactivator 1 alpha	3.67E -03	1.53

APPENDIX

TC0700012584.hg.1	<i>UBE2H</i>	ubiquitin conjugating enzyme E2H	7.36E -03	1.53
TC1100007865.hg.1	<i>METTL12</i>	methyltransferase like 12	6.29E -03	1.53
TC2000009604.hg.1	<i>PMEPA1</i>	prostate transmembrane protein, androgen induced 1	6.67E -03	1.53
TC1700008331.hg.1	<i>HLF</i>	hepatic leukemia factor	4.80E -03	1.53
TC0700009560.hg.1	<i>CNTNAP2</i>	contactin associated protein-like 2	1.33E -03	1.53
TC1600007210.hg.1	<i>HS3ST2</i>	heparan sulfate (glucosamine) 3-O-sulfotransferase 2	9.64E -03	1.53
TC1300007774.hg.1	<i>MBNL2</i>	muscleblind-like splicing regulator 2	8.89E -03	1.53
TC1400010169.hg.1	<i>SETD3</i>	SET domain containing 3	6.56E -03	1.53
TC1600011399.hg.1	<i>MT1X</i>	metallothionein 1X	3.79E -03	1.53
TC1700010248.hg.1	<i>GIT1</i>	G protein-coupled receptor kinase interacting ArfGAP 1	2.54E -03	1.53
TC1900010997.hg.1	<i>DACT3</i>	dishevelled-binding antagonist of beta-catenin 3	3.95E -03	1.53
TC0300009701.hg.1	<i>PSMD2</i>	proteasome 26S subunit, non-ATPase 2	1.25E -03	1.53
TC0500013350.hg.1	<i>RAPGEF6</i>	Rap guanine nucleotide exchange factor 6	2.29E -03	1.53
TC1700010811.hg.1	<i>HDAC5</i>	histone deacetylase 5	4.84E -03	1.53
TC0400012792.hg.1	<i>NIPAL1</i>	NIPA-like domain containing 1	7.09E -03	1.53
TC1000007007.hg.1	<i>ARMC3</i>	armadillo repeat containing 3	2.70E -03	1.53
TC1000011556.hg.1	<i>AVPI1</i>	arginine vasopressin-induced 1	5.50E -03	1.53
TC1100007906.hg.1	<i>RTN3</i>	reticulon 3	1.22E -03	1.52

TC0800007431.hg.1	<i>AP3M2</i>	adaptor-related protein complex 3, mu 2 subunit	2.87E -03	1.52
TC1700007787.hg.1	<i>WIPF2</i>	WAS/WASL interacting protein family, member 2	2.23E -03	1.52
TC0600010853.hg.1	<i>GFOD1</i>	glucose-fructose oxidoreductase domain containing 1	1.72E -03	1.52
TC1300007158.hg.1	<i>MLNR</i>	motilin receptor	3.48E -03	1.52
TC1900008245.hg.1	<i>ZNF221</i>	zinc finger protein 221	7.05E -03	1.52
TC0300010739.hg.1	<i>PLCD1</i>	phospholipase C, delta 1	5.95E -03	1.52
TC0500007868.hg.1	<i>SCAMP1</i>	secretory carrier membrane protein 1	5.19E -03	1.52
TC0200011130.hg.1	<i>DGKD</i>	diacylglycerol kinase, delta 130kDa	1.29E -03	1.52
23075655	NA	NA	4.15E -03	1.52
TC1100008502.hg.1	<i>LOC100506127</i>	putative uncharacterized protein FLJ37770-like	4.42E -03	1.52
TC1200008924.hg.1	<i>DTX1</i>	deltex 1, E3 ubiquitin ligase	5.17E -03	1.52
TC0100018235.hg.1	<i>FPGT-TNNI3K</i>	FPGT-TNNI3K readthrough	3.27E -03	1.52
TC0500009061.hg.1	<i>PCYOX1L</i>	prenylcysteine oxidase 1 like	5.20E -03	1.52
HTA2-neg-47419616_st	NA	NA	7.38E -03	1.52
TC1900011690.hg.1	<i>ZNF493</i>	zinc finger protein 493	8.34E -03	1.52
TC1000009865.hg.1	<i>FAM107B</i>	Memczak2013 ALT_ACCEPTOR, ALT_DONOR, coding, INTERNAL, intronic best transcript NM_031453	1.76E -03	1.52
TC1900009628.hg.1	<i>CDC37</i>	cell division cycle 37	6.04E -03	1.52

APPENDIX

TC0600009683.hg.1	<i>AIG1</i>	androgen-induced 1	9.90E -03	1.52
TC1200009959.hg.1	<i>LRP6</i>	LDL receptor related protein 6	6.14E -03	1.52
TC1600008869.hg.1	<i>ZNF778</i>	zinc finger protein 778	9.42E -03	1.51
TC0200008263.hg.1	<i>USP39</i>	ubiquitin specific peptidase 39	3.14E -03	1.51
TC0200013863.hg.1	<i>NPHP1</i>	nephronophthisis 1 (juvenile)	7.14E -03	1.51
TC1300008338.hg.1	<i>MIPEP</i>	mitochondrial intermediate peptidase	9.55E -03	1.51
TC1000012117.hg.1	<i>CHST15</i>	carbohydrate (N-acetylgalactosamine 4-sulfate 6-O) sulfotransferase 15	7.87E -03	1.51
TC0500013320.hg.1	<i>GTF2H2</i>	general transcription factor IIH subunit 2	9.78E -03	1.51
TC0X00006590.hg.1	<i>WWC3</i>	WWC family member 3	6.69E -03	1.51
TC1500009753.hg.1	<i>OAZ2</i>	ornithine decarboxylase antizyme 2	3.76E -03	1.51
TC0200016606.hg.1	<i>SCLY</i>	selenocysteine lyase	3.86E -03	1.51
TC0700012427.hg.1	<i>FAM3C</i>	family with sequence similarity 3, member C	1.70E -03	1.51
TC2200007278.hg.1	<i>KCTD17</i>	potassium channel tetramerization domain containing 17	7.94E -03	1.51
TC1600006619.hg.1	<i>PDPK1</i>	3-phosphoinositide dependent protein kinase 1	9.36E -03	1.51
TC0800009237.hg.1	<i>GPAA1</i>	glycosylphosphatidylinositol anchor attachment 1	6.70E -03	1.51
TC0600011725.hg.1	<i>GLO1</i>	glyoxalase I	2.49E -03	1.51
TC0100007493.hg.1	<i>TRNP1</i>	TMF1-regulated nuclear protein 1	1.64E -03	1.51
TC0200016562.hg.1	<i>PHOSPHO2</i>	phosphatase, orphan 2	3.28E -03	1.51

TC0100010267.hg.1	<i>DUSP23</i>	dual specificity phosphatase 23	1.40E -03	1.51
HTA2-pos-3374492_st	NA	NA	7.37E -03	1.51
TC1200010292.hg.1	<i>AMN1</i>	antagonist of mitotic exit network 1 homolog	8.15E -03	1.51
TSUnmapped00000399.hg. .1	<i>ZNF852</i>	zinc finger protein 852	1.87E -03	1.51
TC1900011194.hg.1	<i>KCNC3</i>	potassium channel, voltage gated Shaw related subfamily C, member 3	7.42E -03	1.51
TC0400007938.hg.1	<i>BMP2K</i>	BMP2 inducible kinase	1.59E -03	1.51
TC1700008844.hg.1	<i>TTYH2</i>	tweety family member 2	6.76E -03	1.51
TC0300008242.hg.1	<i>ALCAM</i>	activated leukocyte cell adhesion molecule	7.60E -03	1.51
TC1900008555.hg.1	<i>AP2A1</i>	adaptor-related protein complex 2, alpha 1 subunit	7.95E -03	1.51
TC0600007038.hg.1	<i>JARID2</i>	jumonji, AT rich interactive domain 2	1.90E -03	1.51
TC1400007172.hg.1	<i>STYX</i>	serine/threonine/tyrosine interacting protein	4.41E -03	1.50
HTA2-pos- PSR05025585.hg.1	NA	NA	7.29E -03	1.50
TC0300013635.hg.1	<i>ACAP2</i>	ArfGAP with coiled-coil, ankyrin repeat and PH domains 2	3.22E -03	1.50
TC0500009622.hg.1	<i>GRK6</i>	G protein-coupled receptor kinase 6	6.70E -03	1.50
TC0X00011413.hg.1	<i>L1CAM</i>	L1 cell adhesion molecule	2.23E -03	1.50
TC0800008371.hg.1	<i>SPAG1</i>	sperm associated antigen 1	5.38E -03	1.50
TC1100007876.hg.1	<i>TMEM179B</i>	transmembrane protein 179B	4.04E -03	1.50
TC1200007686.hg.1	<i>KRT18</i>	keratin 18, type I	1.30E -03	1.50

APPENDIX

TC0600013531.hg.1	<i>NUP43</i>	nucleoporin 43kDa	2.42E -03	1.50
TC1700012308.hg.1	<i>LLGL2</i>	lethal giant larvae homolog 2 (Drosophila)	9.14E -03	1.50
TC0700010887.hg.1	<i>COA1</i>	cytochrome c oxidase assembly factor 1 homolog	9.58E -03	1.50

8. Acknowledgements

I would like to acknowledge the following people who played their part in the success of the study:

Aurelie Ernst for her supervision during my PhD and for all the helpful discussions about the project.

Peter Licher for all the helpful suggestions about the project throughout my PhD and for his guidance and support as a member of my thesis advisory committee and as head of Division of Molecular Genetics.

Thomas Höfer for being my primary evaluator and a member of my thesis advisory committee.

Sascha Dietrich for being a member of my thesis advisory committee. His input on the screen set-up and analysis of the data was of great importance for the success of the project.

Joe Lewis, Marc Zapatka, Marcel Kool and Till Milde for great collaborations which played a beyond measure important role in the completion of the project in three years.

Murat Iskar and John KL Wong for their bioinformatics support and their input in the interpretation of the data.

Michaela Hergt, Michael Hain and Frauke Devens for their excellent technical support during the whole project.

Norman Mack for his support with the orthotopic injections.

Martina Seiffert, Bernhard Radlwimmer, Violaine Goidts, Daniel Mertens and Stefan Pfister for all their helpful comments and discussions throughout my PhD especially in B060 seminars.

Tolga Lokumcu, Michael Persicke, Jasmin Mangei, Mona Göttmann, Marie Bordas, Venu Thalikonda, Himanshi Soni, Emma Phillips, Rithu Kumar, Andreas Kienzle, Thorsten Kolb, Theresa Schmid, Silya and Michiel Bolkestein for all the great times, whether during lunch, coffee breaks, retreats, parties, hikes or in badminton courts.

All the other members of B06x and B420 for providing such a great working atmosphere.

And finally, my family especially my parents for making me who I am today and my wife for the emotional support throughout this journey.